UNIVERSITY OF SOUTHAMPTON

ENANTIOSELECTIVE RECEPTORS FOR RACEMATE SEPARATION OF AMINO ACIDS' DERIVATIVES

by

Sara Rossi

Doctor of Philosophy

Faculty of Science

Department of Chemistry

September 2003

UNIVERSITY OF SOUTHAMPTON

ABSTRACT

FACULTY OF SCIENCE
CHEMISTRY

Doctor of Philosophy

ENANTIOSELECTIVE RECEPTORS FOR RACEMATE SEPARATION OF AMINO ACIDS' DERIVATIVES

By Sara Rossi

This thesis entails the synthesis of a series of thiourea-based macrocyclic receptors and their ability to selectively bind amino acid derivatives. Efforts focused on the synthesis of receptors specifically designed to bind to glutamate.

Chapter two discusses the synthesis of a bisthiourea-based macrocyclic receptor and its ability to selectively bind to *N*-Boc protected glutamate. Other derivatives were considered, such as aspartate, to fully investigate its binding properties. Traditional NMR titration studies and isothermal calorimetry were employed as tools to study the complexation process in different solvents. Synthetic variations were prepared, which are discussed in chapter three.

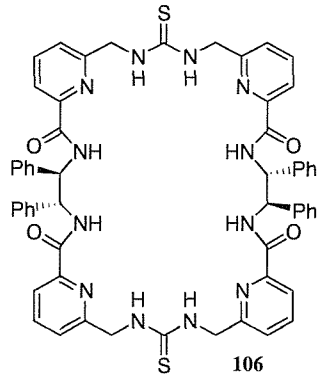

106

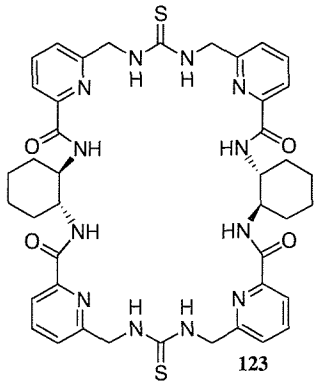

123

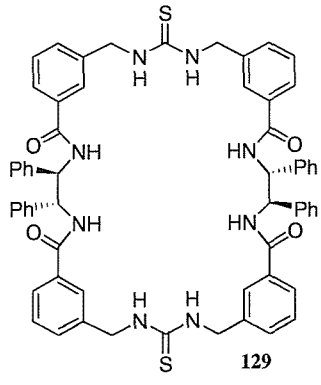

129

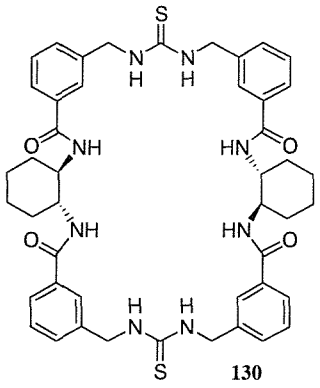

130

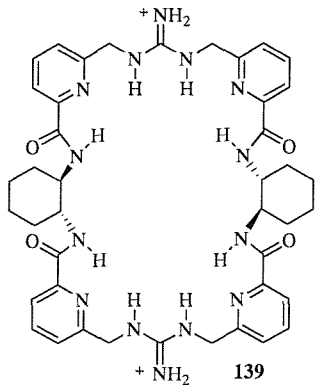

139

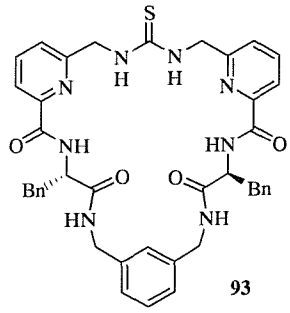

93

Table of contents

1 INTRODUCTION 1

1.1 THE ADVENT OF SUPRAMOLECULAR CHEMISTRY 3
1.2 MOLECULAR RECOGNITION 3
1.3 STABILISATION OF A COMPLEX 4
1.3.1 Hydrogen Bond
1.3.2 Electrostatic Interactions
1.3.3 π-Stacking Interactions
1.3.4 Van der Waals Interactions
1.3.5 Solvent
1.4 FACTORS INFLUENCING THE THERMODYNAMICS DURING THE FORMATION OF A COMPLEX 10
1.4.1 Conformational Reorganisation
1.4.2 Co-operativity effects
1.4.3 *Solvent*
1.5 SYNTHETIC RECEPTORS FOR CARBOXYLATES AND CARBOXYLIC ACIDS 15
1.5.1 Polyaza and Crown Ether Receptors for Carboxylates
1.5.2 Thiourea and Urea Receptors for Carboxylates
1.5.3 Amidopyridine Receptors for Carboxylic Acids
1.5.4 Guanidinium Receptors for Carboxylates
1.5.5 Organometallic Receptors for Carboxylates and Carboxylic Acids
1.5.6 Miscellaneous Receptors for Carboxylates
1.6 APPLICATION OF ISOTHERMAL CALORIMETRY TO SUPRAMOLECULAR CHEMISTRY 37
1.6.1 Introduction
1.6.2 Molecular Recognition of Carboxylates and Carboxylic Acids
1.7 AIMS OF THE PROJECT 45

2 A NOVEL BISTHIOUREA MACROCYCLE 46

2.1 INTRODUCTION 47
2.2 MONOTHIOUREA MACROCYCLIC RECEPTOR FOR CARBOXYLATES 53
*2.2.1 Synthesis of Thiourea Receptor **93***
2.3 BISTHIOUREA RECEPTOR FOR DICARBOXYLATES 58
*2.3.1 Synthesis of Bisthiourea Receptor **106***
*2.3.2 Conformational Properties of Receptor **106***
*2.3.3 Binding Studies of Receptor **106***
2.3.4 *Conclusions*

3 SECOND GENERATION RECEPTORS 85

3.1 INTRODUCTION 86

3.2 BISTHIOUREA RECEPTOR **123** 86

3.2.1 Receptor Design

*3.2.2 Synthesis of Bisthiourea Receptor **123***

*3.2.3 Conformational Properties of Receptor **123***

*3.2.4 Binding Studies of Receptor **123***

3.2.5 Conclusions

3.3 BENZO BISTHIOUREA ANALOGUES **129** AND **130** 98

3.3.1 Receptor Design

*3.3.2 Synthesis of Benzo Bisthiourea Receptor **129***

*3.3.3 Synthesis of Benzo Bisthiourea Receptor **130***

*3.3.4 Conformational Properties of Benzo Bisthiourea Receptors **129** and **130***

*3.3.5 Binding Studies of Receptors **129** and **130** – Investigation of the Preorganisation Hypothesis*

3.3.6 Conclusions

3.4 GUANIDINIUM BISTHIOUREA MACROCYCLIC ANALOGUE 107

*3.4.1 Attempted Synthesis of Guanidinium Bisthiourea Receptor **139***

*3.4.2 Binding Studies of Receptor **141***

3.5 CONCLUSIONS AND OUTLOOKS 109

4 EXPERIMENTAL PART 112

4.1 GENERAL EXPERIMENTAL AND INSTRUMENTATION 113

4.2 EXPERIMENTAL FOR CHAPTER 2 115

4.3 EXPERIMENTAL FOR CHAPTER 3 129

4.4 EXPERIMENTAL FOR APPENDIX 1 140

4.5 EXPERIMENTAL FOR GUESTS 144

4.6 EXPERIMENTAL FOR BINDING STUDIES 147

4.7 EXPERIMENTAL FOR CALORIMETRIC STUDIES 166

REFERENCES 202

APPENDICES 208

1 THIOUREA U-CLEFT RECEPTOR FOR CARBOXYLATES 209

2 SOFTWARE FOR THE DETERMINATION OF ASSOCIATION CONSTANTS FROM NMR BINDING STUDIES 215

3 EQUATION USED FOR FITTING ITC BINDING STUDIES 217

4 CRYSTALLOGRAPHIC DATA 224

Preface

The research described in this thesis was carried out under the supervision of Professor Jeremy D. Kilburn at the University of Southampton between November 1999 and October 2002. No part of this thesis has been previously submitted at this or any other university.

To dad

Acknowledgments

I wish to thank Prof. Kilburn for his help and support throughout my PhD (sorry for being sometimes too "mediterranean").

I am deeply indebted to my family for their support, encouragement and understanding.

I wish also to thank all the people who made these three years highly enjoyable: the Kilburn group, past and present for the pleasant days in the lab and the many people I met, among whom Lene, Elaine, Andy, Paul, Holly, Colin and Paul.

Thanks to Matt for his support and patience, to Rossella for her help and friendship, to Andrea for his jokes (even for the pretty bad ones) and to Sandra for all the cigarettes breaks.

Abbreviations

Boc	*tert*-butyloxycarbonyl
Bn	Benzyl
CBS	Carboxylate binding site
COSY	Correlated spectroscopy
CPK	Corey, Pauling and Kultan
DABCO	1,4-Diazabicyclo-[2.2.2]octane
DCC	*N,N'*-Dicyclohexylcarbodiimide
DCM	Dichloromethane
DIC	Diisopropylcarbodiimide
DIPEA	*N,N'*-Diisopropylethyleneamine
DMAP	4-Dimethylaminopyridine
DME	1,2-Dimethoxyethane
DMF	*N,N'*-Dimethylformamide
DMSO	Dimethylsulfoxide
DPPA	Diphenylphosphoryl azide
EDC	1-(3-Dimethylaminopropyl)-3-ethylcarbodiimide hydrochloride
ES^+ MS	Positive electrospray mass spectrometry
ES^- MS	Negative electrospray mass spectrometry
FAB	Fast atom bombardment
FT-IR	Fourier transform infrared
HOBt	1-Hydroxybenzotriazole
HRMS	High resolution mass spectrometry
m.p.	Melting point
n.O.e	Nuclear Overhauser effect
NMR	Nuclear magnetic resonance
NOESY	Nuclear Overhauser effect spectroscopy
obsc.	Obscured
ppm	parts per million
pyr	pyridyl
quant.	Quantitative
Tf	Triflate

TFA	Trifluoroacetic acid
THF	Tetrahydrofuran
TLC	Thin layer chromatography
TMS	Trimethylsilyl
Ts	Tosyl

Amino Acids

Ala	Alanine
Asp	Aspartic acid
Gln	Glutamine
Glu	Glutamic acid
Gly	Glycine
His	Histidine
Ile	Isoleucine
Leu	Leucine
Phe	Phenylalanine
Ser	Serine
Thr	Threonine
Trp	Tryptophan
Tyr	Tyrosine
Val	Valine

1 Introduction

1.1 The advent of Supramolecular Chemistry

In 1828, Fredrich Wöhler demonstrated the first natural product synthesis by assembling urea.[1] Since then, chemistry has evolved into a mature science that has seen an increasing mastery of the covalent bond, allowing elegant synthesis of more and more complex natural and unnatural products. In 1894, Emil Fischer introduced the idea of geometric complementarity and therefore selectivity through his famous and evocative concept of the *lock and key*[2], Alfred Werner introduced the idea of co-ordination chemistry[3] and Paul Ehrlich recognised that molecules do not act if they do not bind.[4] Building on these and later developments Jean–Marie Lehn introduced the concept of supramolecular chemistry in 1978.[5] In 1987, along with D. J. Cram and C. J. Pedersen, he received the Nobel Prize for chemistry for laying the foundations of this fertile area of study.[6]

Supramolecular chemistry is defined as the study of the intermolecular bond. It involves the study of new molecular systems in which the most important feature is that the components are held together reversibly by intermolecular forces, not by covalent bonds.[7] Supermolecules are composed of a molecular receptor and substrate.

Once a receptor-substrate complex is formed several processes may occur including: binding and selection of a substrate (recognition) and transformation of bound species into products (catalysis).[8]

1.2 Molecular Recognition

Molecular recognition lies at the heart of biochemistry, and involves the investigation of the selective interactions between biomolecules that control or initiate specific physical functions. Vital biochemical processes such as protein assembly, information processing and molecular transport all inherently require selective molecular recognition and complexation to be successful. The degree of exquisite control and efficiency exhibited by natural systems is a challenging goal for the host-guest chemist to emulate, and has led to much interest in the design of a diverse range of synthetic receptors. The interest in artificial hosts is not only due to their direct relevance to the corresponding biological systems, but also because of their potential to lead to new therapeutics, biosensors[9] and catalysts[10,11]. Research into all areas of host guest chemistry has led to the development of a plethora of novel hosts for important biological substrates such as nucleotides[12,13,14], carbohydrates[15,16], amino acids and derivatives[17,18]. All utilise the same fundamental principle: there must exist a complementary relationship between a

receptor and its substrate for effective recognition. Firstly, the receptor must contain a cleft or cavity whose size and shape must closely fit the form of the substrate. Secondly, the binding groups lining the interior of this cavity must have a chemical complementarity to the guest both sterically and electronically. This principle is schematically represented in Figure 1-1.

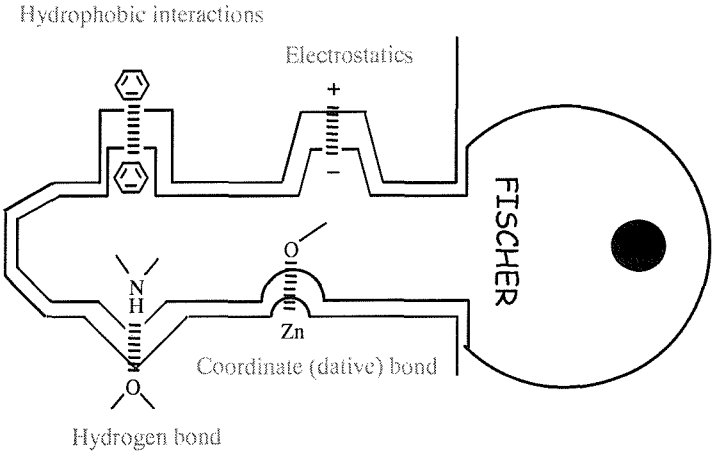

Figure 1-1 Representation of the complementary structural features between a receptor and its substrate ("Lock and Key" principle)[2]

Perhaps the most important example of complementarity is base pairing in the DNA double helix, in which two antiparallel strands are held together by complementary hydrogen bonds between pairs of bases. Ideally, a receptor would be perfectly pre-organised to have as its sole conformation, the structural complement of the substrate to be bound. As the number of low energy conformations of a receptor increases, binding becomes less discriminating and diverges from maximum selectivity. The host then has the opportunity to adopt whatever state is most appropriate to bind any substrate it may encounter. The host-guest chemist thus strives to reduce the conformational flexibility of a receptor by introducing as much preorganisation as possible in an effort to achieve selective molecular recognition.

1.3 Stabilisation of a complex

Herein are described a number of non-covalent interactions that can be utilised for the design and synthesis of supramolecules. The power of supramolecular chemistry lies in the combination of such weak interactions, allowing strong and selective recognition of a specific guest to be achieved. The bond energy of a typical single covalent bond ranges from 350 kJ mol^{-1} up to 942 kJ mol^{-1} for the very stable

triple bond in N_2. The strengths of non-covalent interactions are much weaker, from around 2 kJ mol^{-1} for dispersion forces, from 20 kJ mol^{-1} for a hydrogen bond up to 250 kJ mol^{-1} for an ion-ion interaction.

1.3.1 Hydrogen bond

The hydrogen bond is a particularly important phenomenon in recognition processes, especially in biological systems. The bond between a hydrogen atom and an electronegative element, such as nitrogen, is highly polarised. If this bond is directed towards another electronegative atom bearing a lone pair of electrons, such as oxygen, a weak bond is formed and is termed a hydrogen bond. The distance between the hydrogen atom and the non-covalently bound electronegative atom is a little less than a typical Van der Waals contact distance. An analysis of NH---OC bonds gave a range of bond lengths from 2.0 to 1.7Å, however significantly larger distances of 2.9Å have been reported.[19] The range of strengths of hydrogen bonds is wide and may reach a value of 190 kJ mol^{-1} for an ionic hydrogen bond. A well designed hydrogen bonding receptor should possess hydrogen bonding groups complementary to the desired guest, which must be preorganised and rigidly held so that they will interact with the guest molecule and not collapse down onto each other. Hamilton gives a striking example of hydrogen bonding used in a host-guest system.[20] He developed a receptor for barbiturate with six hydrogen bonding groups directed towards the centre of its cavity, Figure 1-2. These groups are all ideally positioned for binding to the barbituric acid framework and the complex shown has a binding constant of approximately 10^5 $mol^{-1}dm^3$. Hamilton demonstrated the importance of hydrogen bonding in this complex by investigating a series of guests strategically modified to prevent the exploitation of all of the potential hydrogen bonding sites. As the number of hydrogen bonds formed between host and guest decreased a corresponding drop in the value of the binding constant was observed.

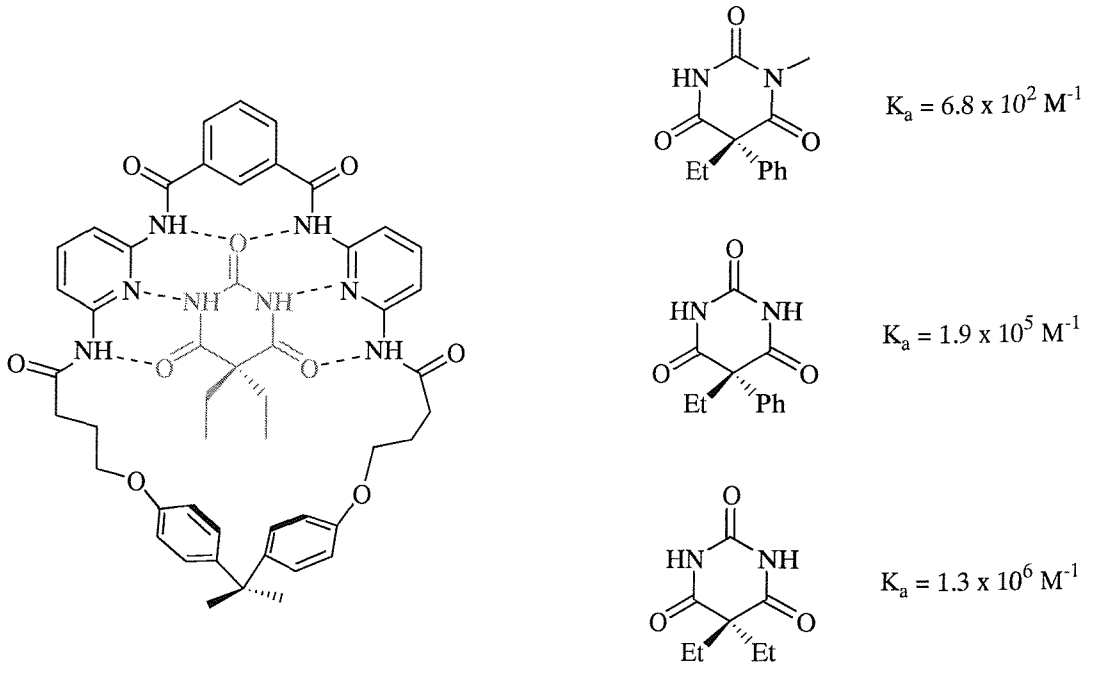

Figure 1-2 Hamilton's barbiturate receptor

As hydrogen bonds have a considerable electrostatic character, diagonal interactions are also important in determining binding strengths. These secondary interactions are important and can be attractive, hence strengthening the binding, or repulsive, leading to a weakening of the binding. The strength of these interactions can be up to as much as one third of that of the primary hydrogen bonds.[21,22]

In systems where several hydrogen bond donors and acceptors lie in close proximity to one another, the possibility of forming secondary hydrogen bond interactions arises, Figure 1-3.[23] This example shows also how multiple hydrogen bonds can be used to confer a high level of selectivity in the binding of a host to its substrate. The outer two complexes have a high level of symmetry allowing association to occur either way around; in the middle complex however, there is no symmetry, and so the two components may only associate as shown. Recently, it has been recognised that besides conventional NH□ □ O and OH□ □ O hydrogen bonds, CH□ □ O interactions can play an important role as weak, but significant, secondary interactions.[24] Normally, C□ □ O separations are typically ≥ 3 Å, with a binding energy ≤ 2-3 Å.[25] In a recent work, Schmuck *et al.* demonstrated that CH□ □ O interactions can serve as a full isofunctional replacement for more conventional NH□ □ O hydrogen bonds in supramolecular arrangements. A value for CH□ □ O of 2.9 Å was observed, Figure 1-4.[26]

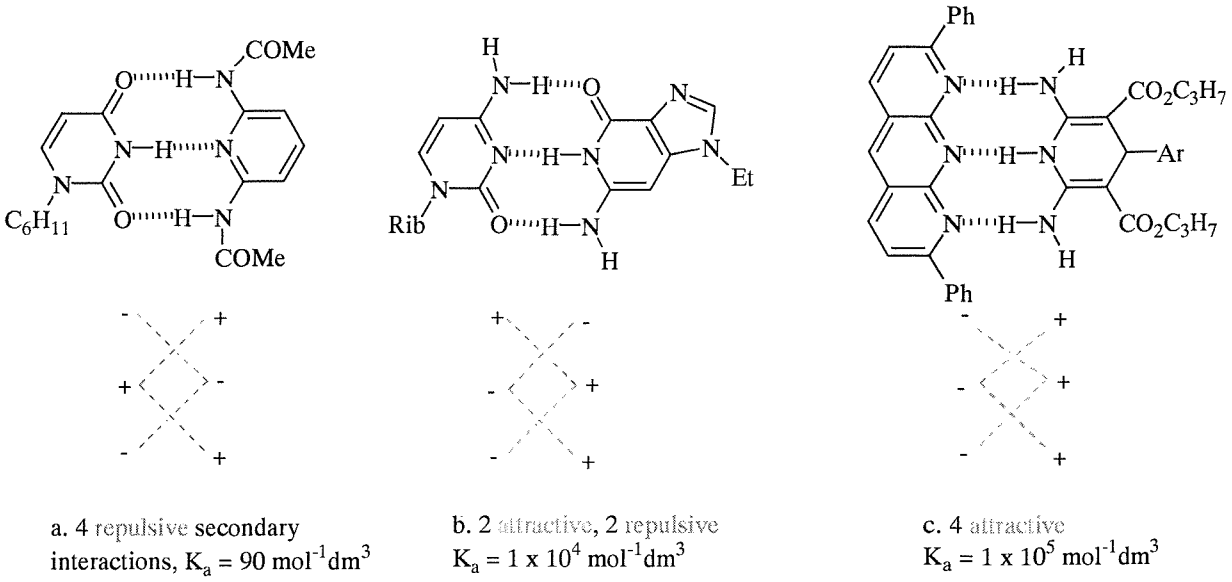

a. 4 repulsive secondary interactions, K_a = 90 $mol^{-1}dm^3$

b. 2 attractive, 2 repulsive $K_a = 1 \times 10^4$ $mol^{-1}dm^3$

c. 4 attractive $K_a = 1 \times 10^5$ $mol^{-1}dm^3$

Figure 1-3 Secondary interactions arising from multiple hydrogen bonds

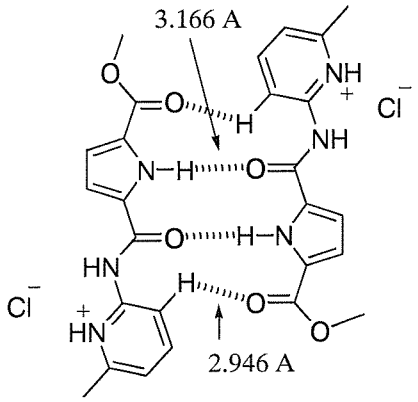

Figure 1-4 Secondary interactions arising from CH□ □ O hydrogen bonds

1.3.2 Electrostatic interactions

Electrostatic forces play a central role in molecular recognition, both in biological and synthetic systems, as they allow strong binding. As the potential between two ions is a function of their separation and charge, in a host-guest complex designed around the utility of electrostatics, it is desirable that the system contains several ionised regions and that charged sites approach closely. The use of electrostatic

interactions is exemplified by polyaza receptors. Kimura[27,28] and Lehn[29,30,31] both produced a series of macrocyclic ammonium salts to bind anions and in particular carboxylates, these are discussed in §1.5.1.

1.3.3 π-Stacking Interactions

p-p interactions are known as the forces present between the p–electrons of different species, most commonly between the p–electrons of aromatic substituents. Aromatic species are characterised by a negatively polarised region above and below the plane of the aromatic ring and a positively polarised region located on the hydrogen atoms.[32] Three types of p-p interactions can be invisaged, Figure 1-5.

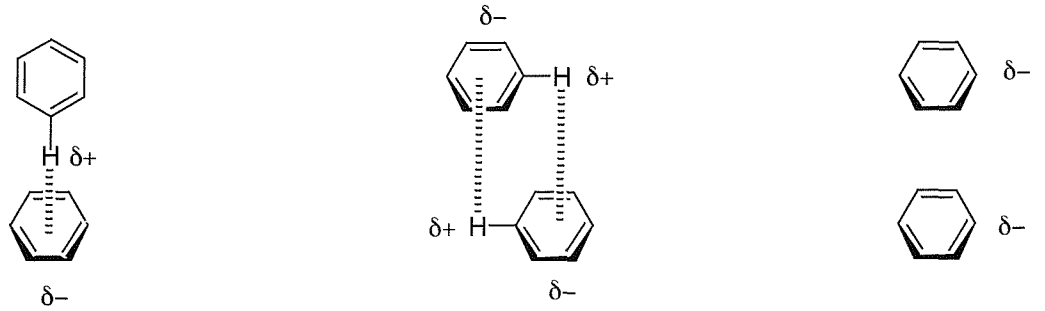

Figure 1-5 p-p interaction modes

The positively polarised aromatic hydrogen atoms are directed towards the regions of high electron density, namely the π-electron cloud, of another ring. This gives rise to the off-set stacking geometries observed. For benzene rings, the "edge-to-face" geometry with an interplanar angle of 90° has been calculated to be a global energy minimum more stable than the "face to face" geometry by approximately 6.3 $kJmol^{-1}$.[33,34] Face to face stacking is not favoured as this result in regions of negative charge being in close proximity. Prediction of such aromatic interactions in host-guest systems is complicated, as the interactions are often between heterocyclic species. The magnitude of the π-π stacking interaction was investigated by Wilcox[35] using a molecular torsion balance to measure an intramolecular 'edge-to-face' π-π interaction: this value was reported as 1 $kJmol^{-1}$. More recently, Hunter[36] has employed a double mutant approach to estimate the value of an 'edge-to-face' π-π interaction to be -1.4 kJ mol^{-1} although Schneider has questioned the validity of this measurement.[37] Hunter specifically designed a receptor in which the aromatic groups act together with the hydrogen bonds to polarise and activate a non-covalently bound molecule of benzoquinone, Figure 1-6.[38] A

change in the electrochemical properties of the guest was observed and measured by cyclic voltammetry.

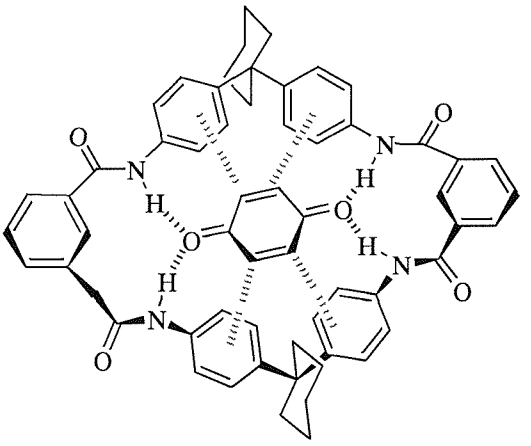

Figure 1-6 Hunter's benzoquinone receptor

1.3.4 Van der Waals interactions

Van der Waals interactions are short range, exerting their influence over only a few molecular diameters. They arise from induced dipole-dipole interactions, and consequently their energies are heavily dependent on the polarisability of the substance in question. Atoms with unshared pairs are generally more polarisable than those with only binding pairs. The attraction is also dependent upon the area of contact of the two molecules: the greater the area the larger the attractive forces. The attractive force increases as the distance between the atoms reduces until the point when the electron clouds begin to overlap at the Van der Waals contact distance, at this point the force becomes repulsive. Although these forces are weak, making individual energies low, the interactions are additive and can make significant contributions to binding when summed over the entire system.

1.3.5 Solvent

The solvent's influence over the complexation event is extremely important and two-fold:[39,40]

- *Hydrogen bonding competition:* The solvation of the host in a polar protic solvent will encourage H-bonding between the host (and the guest) and the solvent. In the presence of a guest there is competition for the H-bonding sites of the host, resulting in an enthalpic trade-off whereby the guest needs to form more H-bonds with the host than those solvent molecules that it displaces.

- *Solvophobic effects:* If a molecule is not well solvated, for example a hydrophobic molecule in water, the solvent forms an ordered structure around it. When the molecule is complexed, solvent molecules are released into the bulk solution, thereby increasing the entropy of the system. In an aqueous medium these are given the specific title of hydrophobic effects. When a non-polar organic solvent is used as a medium for a host-guest system, the same principles as for hydrophobic effects apply; however, the values of the different thermodynamic terms involved in the binding event, such as desolvation of the guest, may vary considerably. In non-polar solvents such as chloroform, desolvation may represent a less severe barrier towards complexation, due to the reorganisation of the local environment between solvent and guest, than is the case with water. Association is favoured by solvents which either weakly solvate the uncomplexed components of the system or strongly solvate the molecular complex. Diederich[41] used the binding of aromatic guest molecules to water-soluble cyclophanes with hydrophobic cavities to demonstrate the relationship between binding strength and solvent polarity, which in turn is dependent upon the solvent's dipole moment, cohesion and polarisability. He found that the binding constants decreased for this system when moving from polar protic solvents through to non-polar solvents, which is directly due to solvation.

1.4 Factors influencing the thermodynamics during the formation of a complex

The measure of how successful a synthetic receptor is at binding a specific guest is measured as the strength of binding or binding efficiency, and is represented by the equilibrium constant, K_a:

$$K_a = \frac{[Host - Guest]}{[Host][Guest]}$$

A high value of the equilibrium constant indicates a strong tendency towards complex formation. The equilibrium constant is related to the Gibb's free energy of the system by the following equation:

$$K_a = e^{(-\Delta G/RT)}$$

where R is the gas constant, T is the temperature in Kelvin and ΔG is the free energy change. During a successful complexation event the system will experience a decrease in Gibb's free energy. This energy change is governed by both an enthalpic and an entropic term.

$$\Delta G = \Delta H - T\Delta S$$

ΔH refers to the change in enthalpy of the system and ΔS corresponds to the change in entropy.

Factors contributing to the enthalpic term include electrostatic interactions, hydrogen bonding, Van der Waals, aromatic interactions and solvent competition. The entropic term accounts for the conformational reorganisation during association and alterations in translational and rotational degrees of freedom of the host and guest molecules. After complexation the degrees of freedom of the host and the guest are reduced. The gross motion of the free host and guest molecules can be broken down into three translational and three rotational components along the *x*, *y* and *z* axes, therefore six degrees of freedom each, twelve in total. Following complexation the host and guest molecules move as one, i.e. they have a total of six degrees of freedom, and therefore the system is more ordered. Bond rotation becomes more restricted for host and guest on complexation, incurring a further entropy loss. De-solvation effects also contribute to the entropy.

1.4.1 Conformational reorganisation

An example of reorganisation occurring during complexation is represented by the crystal structures of the complexed and uncomplexed forms of 18-crown-6 host, Figure 1-7.[42] In the uncomplexed form two of the ethylene bridges are turned inwards filling the potential cavity. The potassium ion re-organises the structure during complexation enabling it to bind within the cavity incurring an entropic and enthalpic penalty.

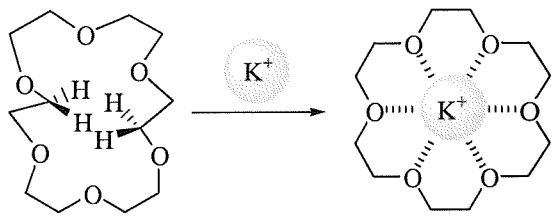

Figure 1-7 Complexation and reorganisation of K^+ by 18-crown-6 host

1.4.2 Cooperativity effects

Williams noted that when many weak non-covalent interactions act together to generate an organised structure, the net release of free energy is often higher than the one expected from the properties of the individual intermolecular interactions.[43] This phenomenon is referred to as cooperativity. Cooperative effects have been found on clusters of polar solvents such as methanol and ethanol.[44] They can be

mediated by conformational changes or restrictions of conformational, translational, or rotational mobility. This effect manifests itself in different ways. If different interaction sites are present on the same molecule the binding of the covalently linked molecule **AB** is more favourable than the complexation of the separate components, **A** and **B**, Figure 1-8. This process is generally entropically-driven but enthalpic effects may also make a contribution.[45]

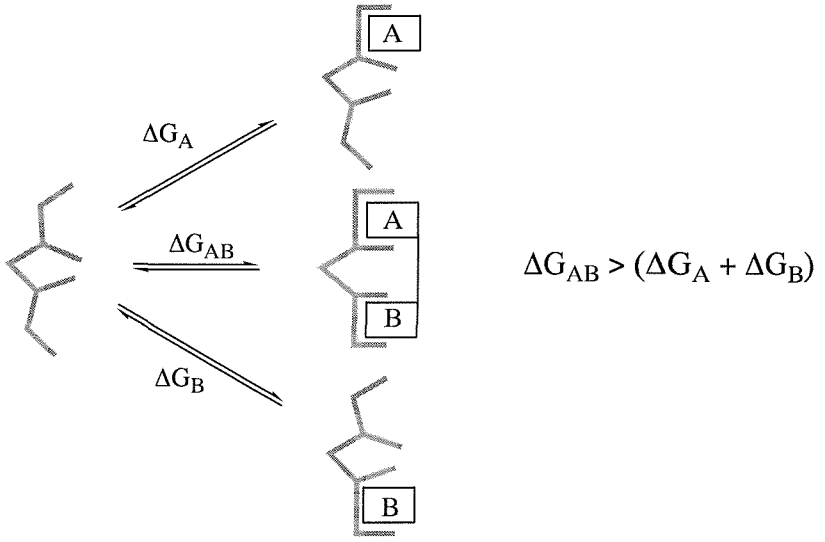

Figure 1-8 Cooperativity interactions between different interaction sites on the same molecule

Cooperativity can involve interaction sites on two or more different molecules. This may be due to a change in the conformation of the receptor induced by the binding of the first substrate, Figure 1-9a, or by a direct interaction between the two substrates in the ternary complex, Figure 1-9b.[46,47]

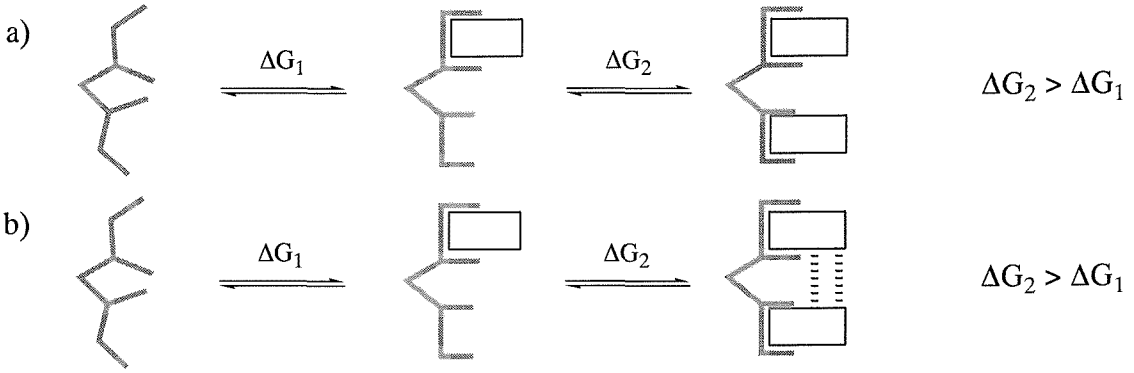

Figure 1-9 Cooperativity interactions between two recognition sites on different molecules in an intermolecular complex

In polar systems containing intermolecular electrostatic interactions strong enough to induce a polarisation, an additional contribution to the total electrostatic interaction energy arises. The size of this interaction is greater than that which might be expected by considering the charge distribution of the single molecules. Such effects are believed to play an important part in protein folding, as the formation of one amide–amide hydrogen bond increases the NH and CO bond dipoles, so a second hydrogen bond on the other face of the amide is energetically more favourable, Figure 1-10.

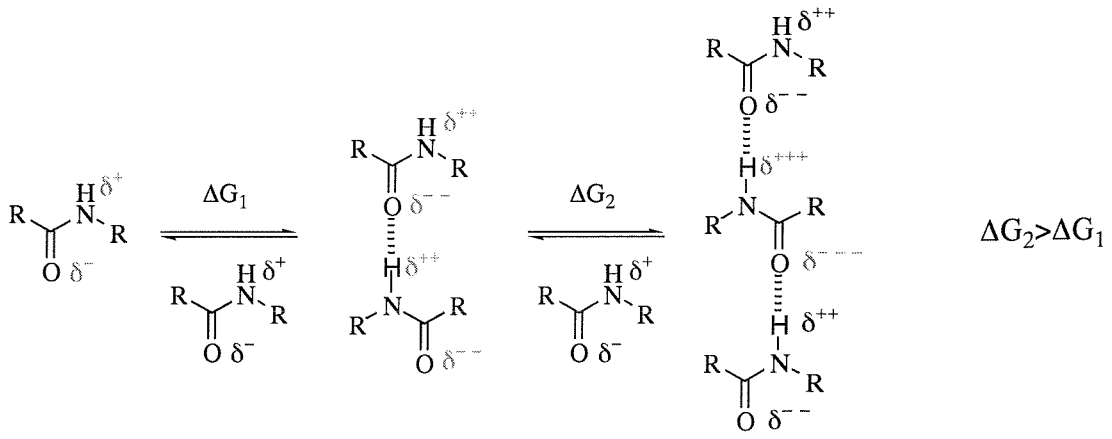

Figure 1-10 Cooperative binding interactions caused by induction

The importance of the cooperativity arising from induction has been demonstrated by Hunter using molecular zipper molecules, Figure 1-11.[48] Williams has also reported evidence of cooperativity in the binding of two molecules of vancomycin to two molecules of *N*-Ac-D-Ala-D-Ala.[49] In both cases, the authors showed that inductive cooperativity makes a significant energetic contribution to the free energy of hydrogen-bonding interactions between neutral molecules in organic solvents. More recently, the cooperativity effects in the protonation of aliphatic polyamines have been investigated.[50] The authors noted that the cooperativity potential depended on the distance between the sites and could be attributed to electrostatic interactions. In particular the binding of a proton to one site yielded a weaker electrostatic attraction between the second site and the next proton.

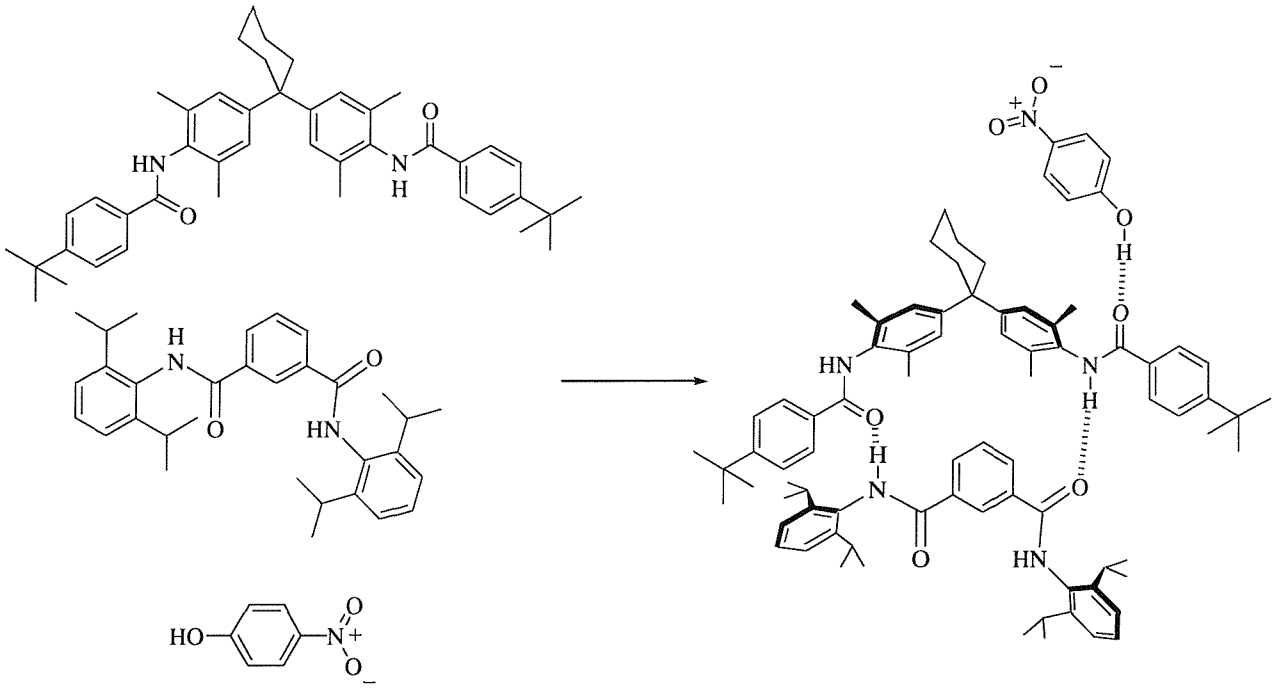

Figure 1-11 Representation of the most stable complex formed in presence of the ternary mixture.

1.4.3 Solvent

Again, the role of the solvent is critical when considering the thermodynamic stability of the host-guest complex formed. For hosts and guests with non-polar cavities, solvation in polar solvents, for example aqueous media, is enthalpically unfavourable, since the solvent molecules surrounding the solutes can form fewer hydrogen bonds than would be possible in the bulk solution. There is also an entropic contribution: the solvent molecules surrounding the host and guest are organised in a highly ordered clathrate structure, which maximises the hydrogen bonding within the system.[51] When this cage-like formation is disrupted the molecules of solvent returning to the bulk solution adopt a less ordered state, inferring a positive entropic contribution. When non-polar hosts and guests are dissolved in non-polar solvents, such as chloroform, the interactions between the host, guest and solvent - usually dipole interactions and Van der Waals forces - are commonly of similar magnitude, hence the enthalpic drive for complexation is low.[52] Similarly, for polar host and guest molecules in polar solvents, the uncomplexed components are well solvated therefore the interactions between the host, guest and solvent are similar in nature and the tendency towards complexation is weak. As with all thermodynamic processes the free energy change must be negative to be favourable. For successful complexation the

contribution from binding interactions must offset the energy penalty incurred to organise the host and guest during complexation. In order to understand fully the interaction between a receptor and a substrate, it is necessary to characterise the underlying thermodynamics of the binding process. Thanks to recent developments in instrumentation and a burgeoning range of applications, isothermal calorimetry (ITC) is becoming increasingly important as a tool for probing the thermodynamics of such processes, as we will see in §1.6.

When designing a viable synthetic receptor it is, for the reasons outlined above, expedient to maximise the functional group complementarity between the host and the guest and seek to reduce the conformational flexibility of the host, thereby reducing the reorganisation required upon association. The incorporation of numerous binding sites into host molecules is also important for enantioselective recognition.[53] De Mendoza's receptor for aromatic amino acids exemplifies such concepts, Figure 1-12.[54] The aromatic amino acid associates to the receptor *via* a guanidinium-carboxylate interaction; the ammonium moiety is bound to the crown ether and the naphthalene ring provides a planar surface to facilitate π-π stacking interactions, §1.5.4.

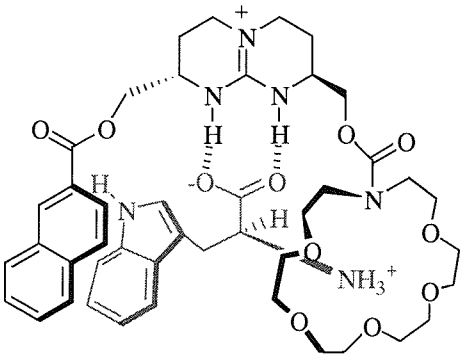

Figure 1-12 de Mendoza's receptor

1.5 Synthetic Receptors for Carboxylates and Carboxylic Acids

There are several systems able to bind to carboxylic acids and carboxylates. The following review is divided into sections relating to the site within the receptor to which the carboxylate or carboxylic acid group is bound (*i.e.* the carboxylate or carboxylic acid binding site or CBS).

1.5.1 Polyaza and crown ether receptors for carboxylates

Lehn and Kimura were among the first to exploit the interaction between a carboxylate anion and a protonated amine. Kimura found that pentamines **1-3** and hexamine **4** (as their polyammonium salts) functioned as carboxylate receptors, Figure 1-13. At neutral pH all the receptors were fully protonated and proved to bind small bicarboxylates in a 1:1 fashion.[55]

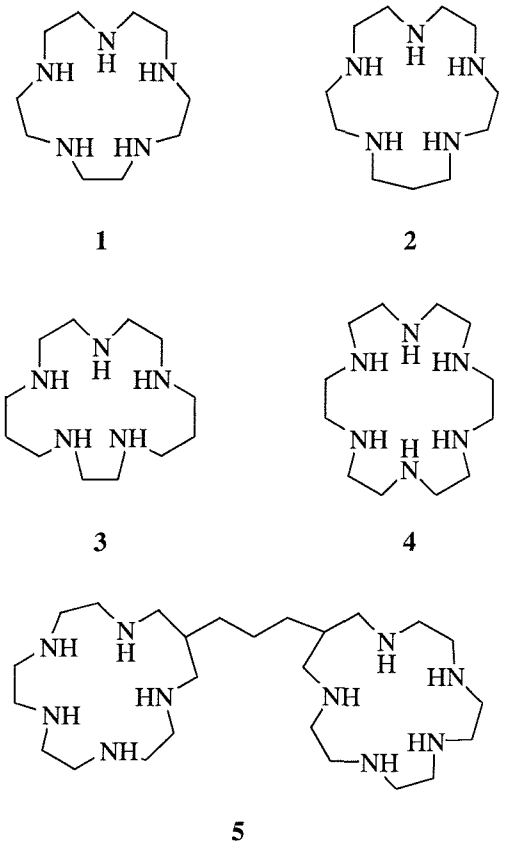

Guest	1	2	3	4	5
Citrate	55	250	100	24	480
Succinate	-	120	92	18	-
Malonate	-	66	25	33	-
Malate	-	50	26	15	-
Maleate	-	76	-	29	-
Fumarate	-	-	-	-	-

Figure 1-13 Kimura's polyaza receptors and association constants with a range of carboxylates in water (- negligible binding)

By comparing association constants for **1-4** with a range of carboxylates the effect of the macrocycle ring size could be probed. The smallest 15-membered ring **1** was the poorest anion acceptor, presumably due to steric hindrance marring the hydrogen-bonding sites for the ion-pair formation. The 16- and 17-membered macrocycles **2** and **3** were found to bind to dicarboxylates with similar orders of magnitude. The tricarboxylic citrate anions bound to receptors **2-4** more tightly than any of the dicarboxylate anions,

indicating that electrostatic interactions were fundamental to the ion-pair complexation. Bispolyazacrown **5** formed a sandwich complex with citrate.[56]

Lehn synthesised larger polyaza macrocycles **6**, **7** and **8**, Figure 1-14, which as their polyammonium salts were found to bind a range of carboxylate anions.[57]

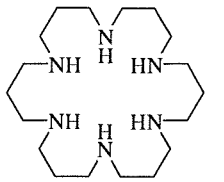

6

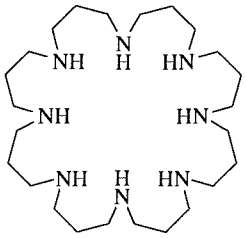

7

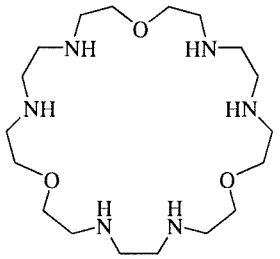

8

Guest	6-6H$^+$	7-8H$^+$	8-6H$^+$
Oxalate	6.3 x 10^3	6.3 x 10^3	50 x 10^3
Malonate	2.0 x 10^3	5.0 x 10^3	6.3 x 10^3
Succinate	2.5 x 10^2	7.9 x 10^3	6.3 x 10^2
Tartrate	3.2 x 10^2	-	7.9 x 10^2
Maleate	5.0 x 10^3	12.5 x 10^3	10.0 x 10^3
Fumarate	1.6 x 10^2	7.9 x 10^2	4.0 x 10^2
Citrate	50 x 10^3	40 x 10^6	630 x 10^3
1,3,5-benzene-tricarboxylate	3.2 x 10^3	1.3 x 10^6	6.3 x 10^3

Figure 1-14 Lehn's polyaza macrocycles and association constants with a range of dicarboxylates (- not performed)

All three fully protonated compounds **6**-6H$^+$, 7-8H$^+$ and **8**-6H$^+$ formed strong complexes with both inorganic and organic polyanions in aqueous solution. Complexation of monoanions was not detected. Electrostatic interactions were found to play a major role in both the strength and selectivity of anion binding. Thus, the anions most strongly complexed were usually the smallest and most highly charged ones: oxalate > malonate > succinate > and maleate > fumarate. Large polyanions such as citrate and 1,3,5-benzenetricarboxylate formed very strong complexes with the large and highly charged 7-8H$^+$.

More recently, an acridine based receptor, **9**, has been described by Lehn, Figure 1-15.[58] Two planar subunits were included, positioned at a distance suitable for the intercalation of flat substrate molecules. The macrocycle proved to bind flat aromatic substances, as well as nucleotides and nucleosides, by

means of π-stacking and electrostatic interactions, in particular, it was shown to bind *trans*-azobenzene dicarboxylate more strongly than the corresponding *cis* isomer in D_2O.

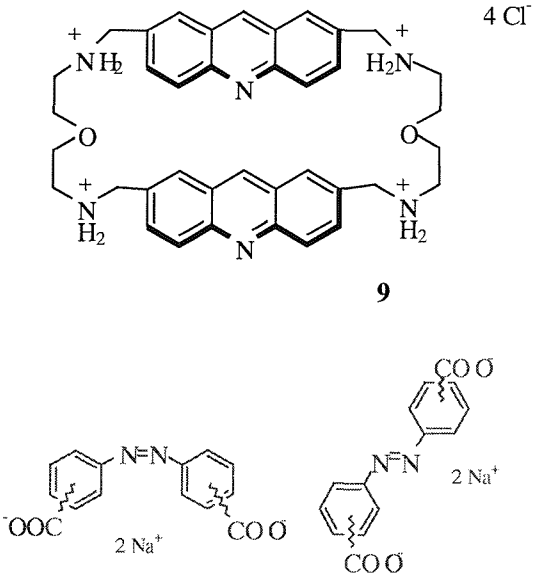

Guest	Log K_s
trans-3,3'-azobenzene dicarboxylate	5.4
cis-3,3'-azobenzene dicarboxylate	4.0
trans-2,2'-azobenzene dicarboxylate	3.1
cis-2,2'-azobenzene dicarboxylate	2.7

Figure 1-15 Lehn's acridine receptor and stability constants for azobenzene dicarboxylates

A 1:1 stoichiometry was observed for all the complexes and an intercalative or sandwich type of binding was suggested. The results showed marked positional (3,3'>2,2') and configurational (*trans*>*cis*) selectivity in the binding of the four substrates by receptor **9**. It was also found that binding led to acceleration in *cis* to *trans* isomerisation. The very strong and preferential binding of the receptor revealed the marked electrostatic and structural complementarity between host and guest.

Diederich *et al.* have produced polyammonium cyclophane receptors, Figure 1-16, which partially mimic the vancomycin carboxylate binding site complexing aromatic and aliphatic carboxylates as well as *N*-protected α-amino acids and dipeptides.[59]

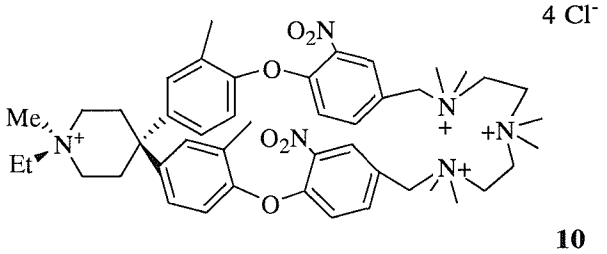

10

Figure 1-16 Diederich's cyclophane receptor

The cyclophane structure was inserted to provide a degree of preorganisation for the carboxylate binding site. However, titration binding experiments indicated that it did not provide a cavity for inclusion of the guests and instead binding occurs exclusively on the external surface. The driving force for binding is the ion-pairing interactions between the adjacent quaternary ammonium ions of the host and the carboxylate anion. Although the sodium salts of Ac-D-Ala, Ac-D-Val and Ac-D-Ala-D-Ala were bound with association constants of 74 dm^3mol^{-1}; 36 dm^3mol^{-1} and 51 dm^3mol^{-1} respectively, the unprotected zwitterionic α-amino acids were found not to bind.

Kilburn has synthesised a novel macrocycle **11**, featuring a crown ether ring, amide functionality and a rigid biaryl unit as a receptor for small peptides, Figure 1-17.[60]

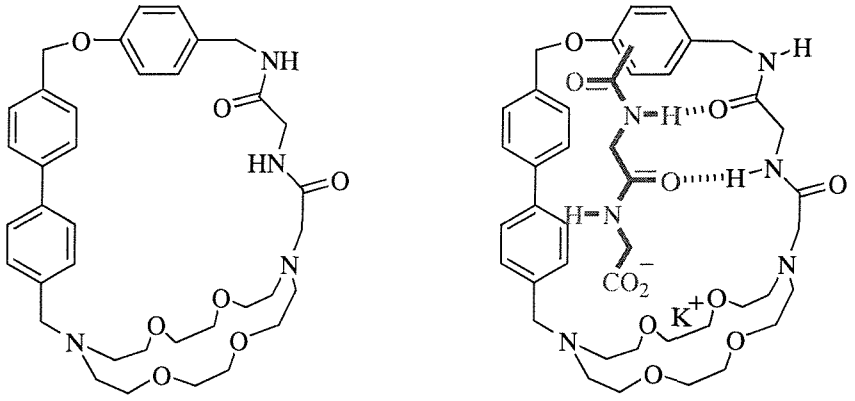

11 **12**

Figure 1-17 Kilburn's peptide receptor

FAB mass spectrometry was used to investigate the host-guest complex. In the absence of any guest, no signal corresponding to macrocycle **11** was observed, however, in the presence of the potassium salts of *N*-Ac-glycine or *N*-Ac-ß-alanine, peaks corresponding to the macrocycle were observed. In addition, in the case of *N*-Ac-ß-alanine, peaks corresponding to complex **12** were observed. Under identical conditions, in the presence of *N*-Boc-glycine and *N*-Boc-ß-alanine, no peaks corresponding to the macrocycle, or its complexes, could be detected. These results suggested that the *N*-acetyl substrates are bound within the macrocycle while the bulkier *N*-Boc substrates are not.

Pietraszkiewicz developed a relatively straightforward crown ether receptor for the selective transport of amino acids through liquid membranes, Figure 1-18.[61] To an 18-crown-6 ring was incorporated a naphthalene unit as a lipophilic group and to provide secondary π-π interactions with aromatic amino acids. Methyl D-mannopyranose was also inserted as a chiral auxiliary. Transport and extraction

experiments were performed with the free amino acids and their sodium and potassium salts of Ph-Gly, Ph-Ala and Trp.

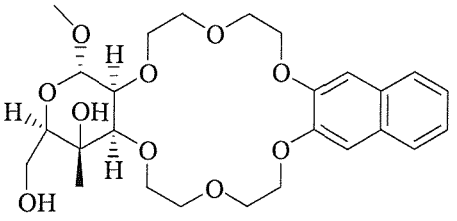

13

Figure 1-18 Pietraszkiewicz's receptor

A more pronounced enantioselectivity of pure amino acids was noted, attributed to a stronger complex formation compared to the salts of the amino acids. The presence of the mannopyranose unit seemed to enhance the complexation due to additional hydrogen bonding between the carboxylic group and the two free hydroxyl groups. A favourable π-stacking interaction between the naphthalene moiety and the aromatic part of the amino acid was the reason for the high transport rates for tryptophan. The transport experiments did not reveal a general trend in which enantiomer was preferred but the extraction experiments showed that L-enantiomers were better extracted than the corresponding D-forms, even if, as in the case of tryptophan the situation was reversed.

Sessler investigated the use of sapphirins as receptors for carboxylates. Sapphirins are pentapyrrolic expanded porphyrins known to act as efficient anion receptors (mainly phosphate and fluoride) under a wide range of conditions. The large pentaaza core of sapphiryn is monoprotonated at neutral pH and the NH protons of this same centre can act as effective hydrogen bond donors. An example of a sapphyrin-based polytopic receptor, **14**, is shown in Figure 1-19.[62] Here, two protonated sapphyrins serve as essential carboxylate-binding blocks, while the diaminopropane spacer allows the conformational mobility needed to accommodate a range of substrates. In all cases dicarboxylate protons' signals shifted upfield as result of chelation by the sapphyrin dimmer, due to the receptor via the formation of a complex in which the bound guests are held between the two protonated sapphyrin units. The receptor showed little affinity for monocarboxylate substrates like trifluoroacetate ($K_a \leq 20\ M^{-1}$).

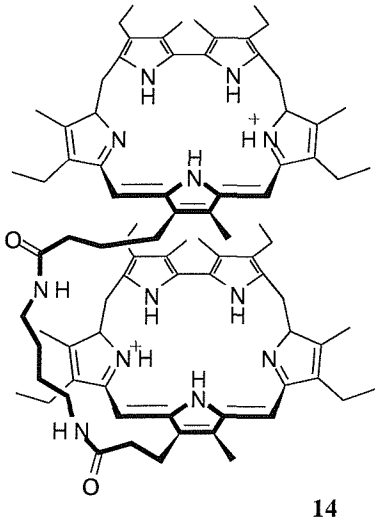

14

Guest	14	
	$K_a M^{-1}$	*Selectivity*
Phtalate	$K_1 = 310$, $K_2 = 280$	1.2
Isophtalate	2400	9.4
5-nitroisophtalate	5300	20.4
Terephtalate	4600	17.7
Nitroterephtalate	9100	35.0
Benzoate	K_1, $K_2 = 1380$	5.6
Oxalate	260	-
Malonate	450	1.7

*Figure 1-19 Sessler's sapphyrin-based receptor and binding constants of receptor **14** and various dicarboxylates in methanol. Selectivity is as compared to worst bound substrate, oxalate*

1.5.2 Thiourea and Urea Receptors for Carboxylates

Ureas and thioureas provide a strong binding site for carboxylates via a bidentate hydrogen motif, Figure 1-20.

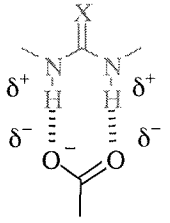

X = O $pK_a = 26.9$

X = S $pK_a = 21.0$

Figure 1-20 Hydrogen bond bidentate motif

Hamilton examined the binding of dicarboxylates by bis-urea receptors.[63] He developed a simple bis-urea in which four hydrogen bond donors are positioned to interact with two carboxylate oxygens, Figure 1-21. Titration of **15** in CD_3CN with tetrabutylammonium acetate gave large downfield shifts of the urea NH signals (>1.8 ppm), consistent with the formation of a hydrogen bonding complexation and a binding constant of 2.24×10^3 M^{-1}. The participation of both ureas was confirmed by a Job's plot, which showed a maximum at mole ratio 0.5, consistent with a 1:1 binding stoichiometry, and by the ten-fold weaker binding by **16**.

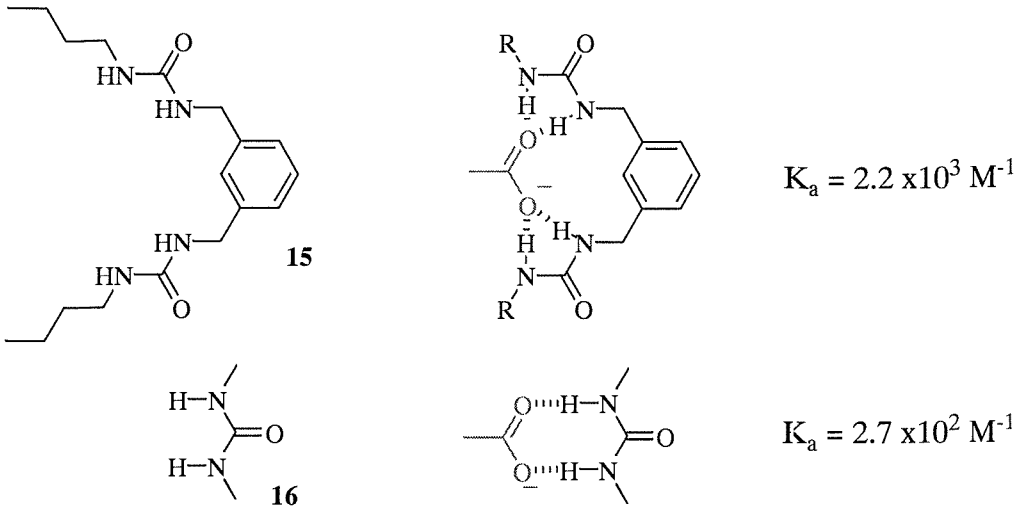

Figure 1-21 Hamilton's bis-urea

Hamilton studied the behaviour of ureas and thioureas in polar solvents such as DMSO.[64] Addition of tetramethylammonium acetate to a DMSO-d_6 solution of 1,3-dimethylurea gave large downfield shifts of the urea NH resonance (>1 ppm), which were consistent with the formation of a bidentate hydrogen-bonded complex as in Figure 1-20 and gave an association constant of 45 M^{-1}. The switch to thiourea resulted in a ten fold increase in stability with an association constant of 340 M^{-1}, due to its higher acidity (pK_a = 21.0, as compared to pK_a = 26.9 for an urea).

Umezawa investigated the use of urea and thiourea moieties to bind carboxylates.[65] Urea **17** and thiourea **18** were prepared, and their ability to bind acetate examined, Figure 1-22.

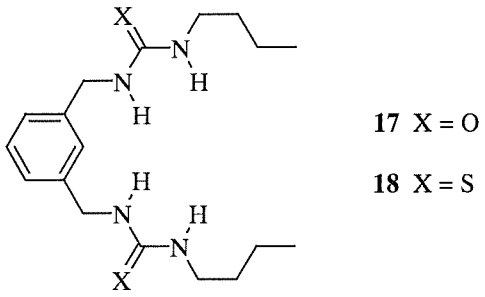

Figure 1-22 Umezawa's thiourea and urea receptor

In DMSO-d_6, receptor **17** gave an association constant of 43 M^{-1}, while **18** produced a higher binding constant of 470 M^{-1}. Job plot analysis clearly indicated a 1:1 complex stoichiometry and large changes in chemical shifts were observed for the thiourea NH protons. Moreover, urea **17** was insoluble in

solvents of low polarity, whereas thiourea **18** was well solvated in $CDCl_3$ and showed no evidence of self-association.

Kilburn synthesised a bowl shaped receptor, **19**, for amino acid derivatives.[66] A biarylmethane unit formed the rigidifying part of the rim of the macrobicycle and chirality was introduced *via* two lysine derivatives, Figure 1-23. The receptor was found to bind to a range of *N*-acetyl amino acid derivatives with little selectivity, ranging from $K_a = 5.8 \times 10^3$ dm^3 mol^{-1} for *N*-Ac-L-histidine to 130×10^3 dm^3 mol^{-1} for *N*-Ac-L-lysine. However, NMR experiments revealed that the D-amino acid guests were bound on the external face of the macrocycle cavity whereas the L-amino acid derivatives were bound within the cavity *via* a strong carboxylate-thiourea interaction, Figure 1-23. The L-amino acid guests internalised in the macrocycle were also shown to adopt a *cis* configuration around the *N*-acetyl amide bond.

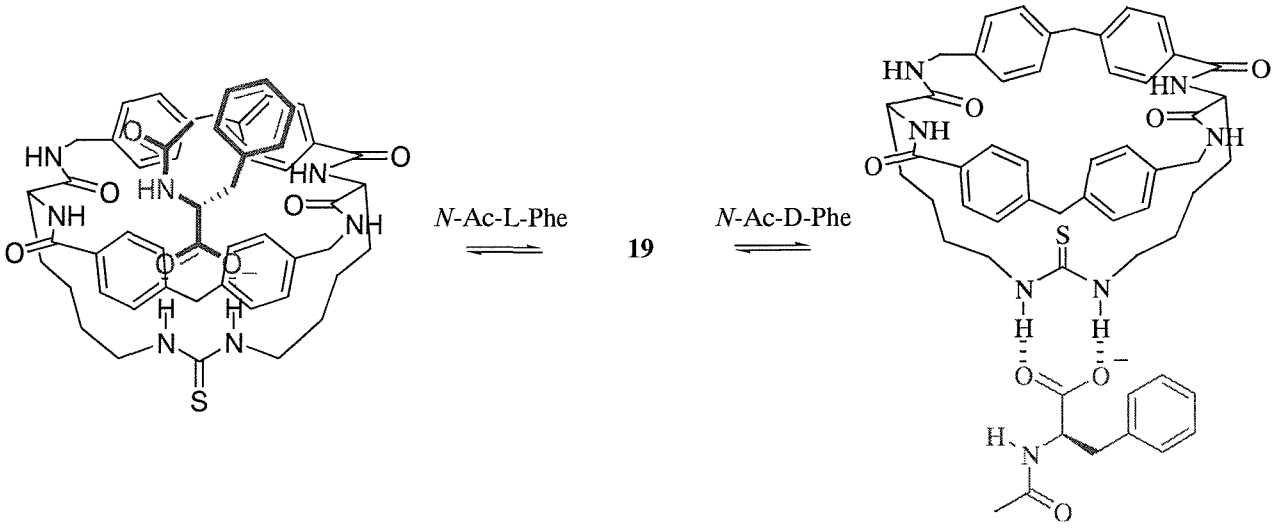

Figure 1-23 Kilburn's thiourea macrobicyclic receptor

1.5.3 Amidopyridine Receptors for Carboxylic Acids

The amidopyridine structural motif has been exploited in a number of carboxylic acid receptors, due to its ability to form two complementary hydrogen bonds from the carboxylic acid hydrogen and carbonyl to the pyridine nitrogen and the amide hydrogen as shown in Figure 1-24.

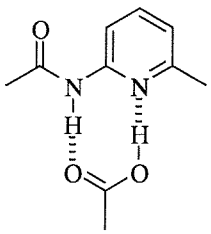

Figure 1-24 Amidopyridine hydrogen bond motif

Kilburn *et al.* developed variations on the macrobicyclic structure **19** by inserting a diamidopyridine unit as the carboxylic acid binding site.[67] The modified receptor featured the carboxylate binding site at the base of a deepened cavity with amide functionality, again used to provide a site for additional hydrogen bonding. A phenylalanine unit was incorporated to increase the chiral information within the receptor framework and to enhance the solubility of the host in non-polar solvents, Figure 1-25a.[68] The diamidopyridine receptor was found to be a strong, selective receptor for peptides with a carboxylic acid terminus, the strongest interaction with Cbz-β-Ala-D-Ala-OH (K_a = 12200 dm^3mol^{-1}).

a)

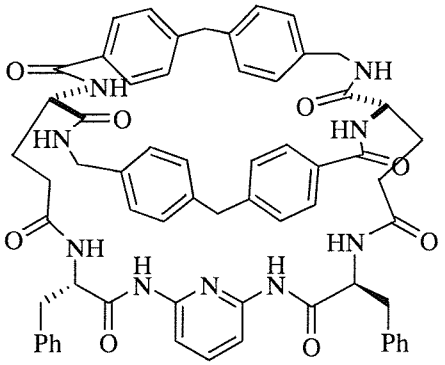

20

b)

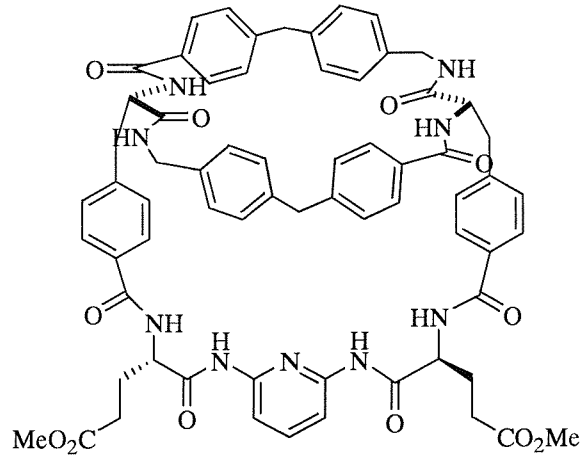

21

Figure 1-25 Kilburn's diamidopyridine receptors for peptides

A further modification was made to the diamidopyridine receptor to reduce its flexibility and produce a more preorganised host, Figure 1-25b.[69] The new receptor was found not only to strongly bind the dipeptide Cbz-L-Ala-L-AlaOH, K_a = 3.3 x 10^4 dm^3 mol^{-1}, but also to do so selectively. A result such as this is of particular interest due to the relevance to binding L-Lys-D-Ala-D-AlaOH, the bacterial cell wall precursor peptide.

Calixarenes have been attractive choices as scaffolds for ditopic molecular recognition. Recently, the synthesis of a bis-amidopyridine calix[4]arene, **22,** has been studied and its binding properties towards various dicarboxylic acids in DMSO / $CDCl_3$ reported, Figure 1-26.[70]

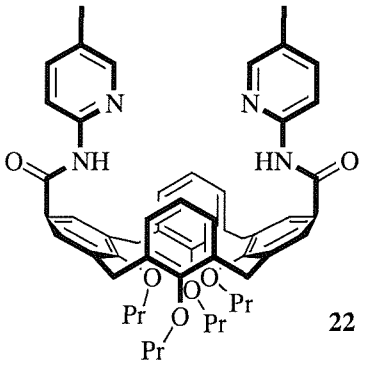

22

Figure 1-26 Bis(amidopyridine)-linked calyx[4]arene

Upon addition of the guests, downfield shifts in the ^1H NMR spectra corresponding to the two amido NH protons of receptor **22** were observed, consistent with the formation of amidopyridine–carboxylic acid hydrogen bonds, Table 1-1.

*Table 1-1 Binding constants of host **22** with various dicarboxylic acids (- = not determined)*

Guest	**K_a M^{-1}**	
	0.5% DMSO / $CDCl_3$	3% DMSO / $CDCl_3$
HOOC-$(CH_2)_n$-COOH		
n = 3	78	13
n = 4	80	-
n = 5	133	20
n = 6	392	39
n = 8	1530	-
n = 10	3000	-
n = 12	-	-
Isophtalic acid	*not soluble*	19
5-nitro-isophtalic acid	*not soluble*	23
1,3-phenylene diacetic acid	*not soluble*	15

Dicarboxylic acids up to n = 8 showed a 1:1 (host:guest) binding stoichiometry, as determined by Job plots. For dodecanedioic acid, a small amount of 1:2 stoichiometry was observed, whereas for n = 12 a 1:2 complex was formed. The results reflect a large alkyl spacer length (n = 3 – 10) dependence on the binding strength, with glutaric acid giving the smallest binding constant in the series. Binding constant values increased with increasing length of the alkyl spacer group, up to a maximum with n = 10. Two schematic representations of 1:1 complexes can be envisaged, Figure 1-27. A ditopic binding interaction with a small dicarboxylic acid, such as glutaric acid, would involve the two amidopyridine groups facing one another to minimise the steric hindrance between the guest and the phenyl groups and the strain in the short alkyl chain, Figure 1-27*a*. As the guest becomes larger the amidopyridine groups can rotate away from one another to accommodate the guest without steric hindrance from the ring or strain in the spacer group, located largely outside the calixarene cavity, Figure 1-27b. The X-ray crystal structure of the receptor showed three conformers in which the six amidopyridine units lie almost coplanar to their attached phenyl groups, similarly with their respective pyridine units.

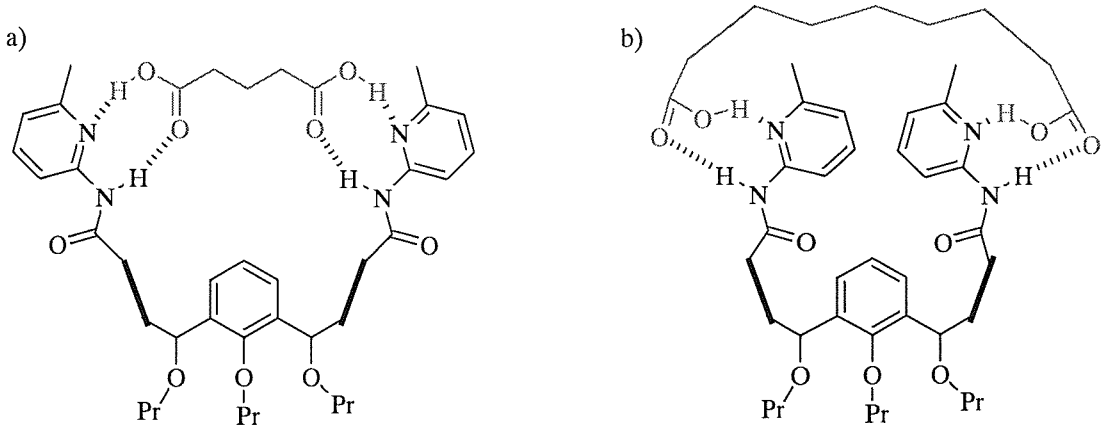

*Figure 1-27 Cooperative binding by **22** of different length of dicarboxylic acids: a) n=3, b) n=8*

It is probable that the binding strength is maximised when the disruption of such planarity is minimised, as is the case with larger guests. Presumably for very large guests, $n \geq 10$, this conformation becomes less favourable due to steric crowding in the alkyl chain, and more complex binding equilibria result. Aromatic diacids were also considered. Consideration of the similar K_a values for aliphatic and aromatic guests suggested that no π-π stacking between any of the aromatic guests and the phenyl groups of the calixarenes occurred.

1.5.4 Guanidinium Receptors for Carboxylates

One of the main advantages of the guanidinium group as a carboxylate binding moiety is its ability to remain protonated over a much wider pH range than the ammonium equivalent, thanks to its high pK_a (pK_a =13.5). The group forms characteristic pairs of zwitterionic hydrogen bonds (Figure 1-28), particularly strong due to their charge and structural organisation, as evidenced from the crystal structures of many guanidinium salts.

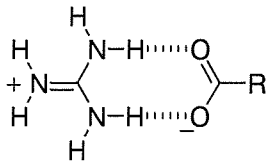

Figure 1-28 Bidentate guanidinium hydrogen-bonding pattern to carboxylates

A collaboration between Lehn and de Mendoza produced the chiral receptor **23** containing a rigid bicyclic guanidine and two naphthoyl units, Figure 1-29.[71] Sodium *p*-nitrobenzoate was successfully extracted from water into an organic solution. The ^{1}H NMR spectrum of the host-guest complex revealed significant shifts for most signals of both host and guest. The NH guanidinium protons showed a 1.78 ppm downfield shift in the complex relative to the free host. Most aromatic protons of the host and guest shifted upfield. This data strongly supported the formation of a complex involving double recognition of the guest by the guanidinium cation (zwitterionic hydrogen-bonds with the carboxylate function) and the naphthoyl side arms (p-p stacking with the *p*-nitrophenyl moiety).

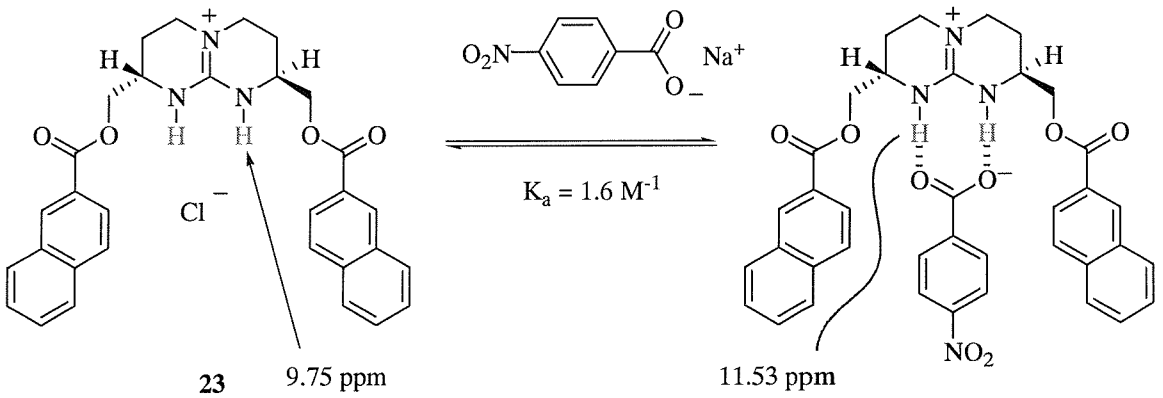

Figure 1-29 Lehn and Mendoza's chiral receptor containing a rigid bicyclic guanidine

De Mendoza designed a new receptor featuring a guanidinium as the binding site for carboxylate, a crown ether to bind ammonium and an aromatic planar surface (the naphthalene ring) for selective p-

stacking interactions with the side chains of aromatic amino acids, Figure 1-30.[54] The affinity of **24** toward amino acids was determined by liquid-liquid single extraction experiments, in which an aqueous solution of L-Trp, L-Phe, or L-Val was extracted into a CH_2Cl_2 solution containing **24**.

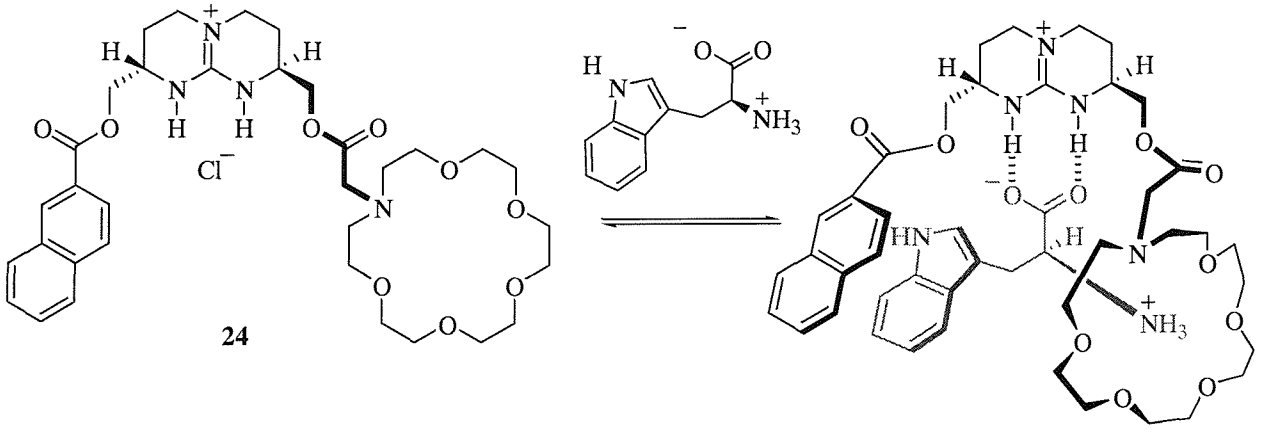

24

Figure 1-30 Mendoza's receptor incorporating a crown ether moiety

The extraction efficiencies (*i.e.* the fraction of receptor molecules occupied by the substrate in the organic phase) as determined by NMR integration, were around 40% for L-Trp and L-Phe. L-Val, without any aromatic side chain, was not detected. A competition experiment with a mixture of all three amino acids resulted in 100:97:6 Phe:Trp:Val ratios. The corresponding D-enantiomers were not extracted, as observed in the NMR spectrum. A more precise account of the selectivity was achieved by HPLC analysis of diastereomeric dipeptides, prepared from extracts of racemic samples of Phe or Trp and a suitable optically pure L-Leu derivative. The amount of D-isomer in the extracts was lower than 0.5% for D-Trp (determined as L-Leu-D-Trp) and 2% or less for D-Phe (as L-Leu-D-Phe). This high degree of chiral recognition is explained by the presence of three simultaneous non-covalent interactions of the substrate with the flexible and foldable receptor.

Drawing on a similar ensemble of building blocks, Schmidtchen synthesised a polytopic host, **25**, comprising a chiral bicyclic guanidinium unit attached to a triaza-crown ether. In addition a bulky silyl ether was inserted to convey the necessary lipophilicity, Figure 1-31.[72]

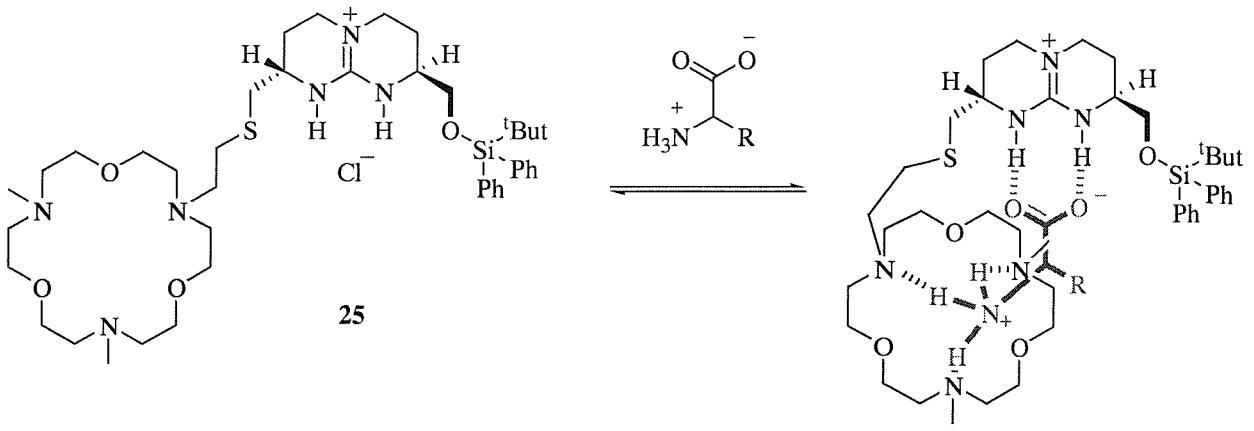

25

Figure 1-31 Schmidtchen's modified receptor

Host **25** proved to be able to extract highly hydrophilic zwitterionic amino acids to an organic phase. The order of decreasing extractability was: Phe > Leu > Trp > Gly >> Ser. The receptor extracted the highly hydrophilic glycine to the same extent as the more hydrophobic Phe, Leu and Trp, indicating a common mode of interaction in which both anchor moieties of the host cooperate in substrate binding. Less bulky amino acids were better extracted. The receptor also showed some enantioselectivity. Using D,L-phenyl alanine as a probe, it was found receptor **25** favoured the L enantiomer, with an *ee* of 40% in the extraction into chloroform.

Schmuck prepared some acyclic guanidinium receptors, **26** and **27**, Figure 1-32.[73] These guanidinocarbonylpyrroles bound carboxylates by ion pairing in combination with multiple hydrogen bonds. Guanidinium **46** incorporated a pyrrole NH to act as an additional hydrogen-bonding donor to carboxylate guests.

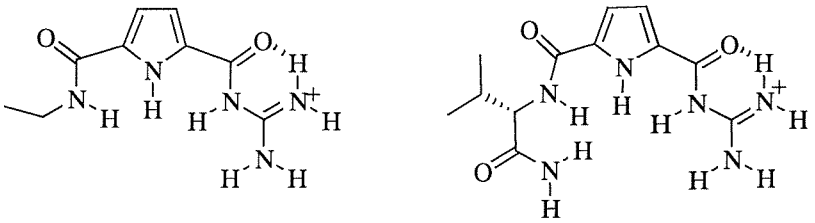

26 **27**

Figure 1-32 Schmuck's 2-(guanidinocarbonyl)pyrrole receptors (as picrate salts)

Receptor **26** was found to bind *N*-Ac-a-amino acid carboxylates in 40% H_2O/DMSO with association constants ranging from 360 to 1700 M^{-1}, depending on the structure of the amino acid side chain. Chiral receptor **27** bound carboxylates with association constants in the range of 350 to 5275 M^{-1}. The

association constants for the enantiomers with **27** differed by a factor of 1.2 for phenylalanine and tryptophan and 1.6 for alanine. In the case of alanine and tryptophan, the L-enantiomer was bound better than the D-enantiomer. With phenylalanine and tryptophan the aromatic system and the guanidiniocarbonyl pyrrole moiety of the receptor were found to be p-stacked. However, any side chain of amino acids bulkier than alanine methyl group caused unfavourable steric interactions with the isopropyl group of the receptor and decreased the binding energy for both enantiomers relative to the binding of alanine. In the case of phenylalanine the association constants were lower than with the ethyl-substituted receptor **26** (K_a = 1700 M^{-1}). The steric repulsion was more severe in the case of the L-enantiomer as the D-enantiomer can adopt a complex conformation that orientates the isopropyl group further away from the *N*-acetyl group. In the complexes with tryptophan the association constants were slightly larger than with **26** (K_a = 810 M^{-1}), probably because of the more extensive hydrophobic interactions or p-stacking.

Davis *et al.* prepared a series of receptors, **27** – **33**, bearing guanidinium, carbamate and other functional groups from cholic acid, Figure 1-33.[74]

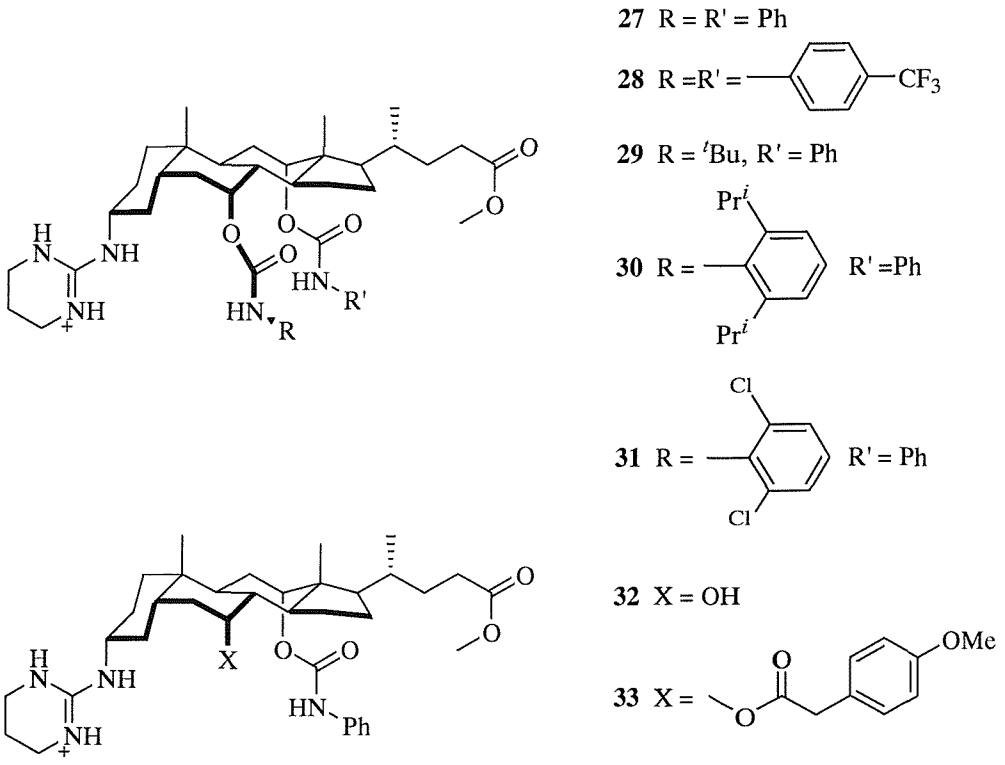

Figure 1-33 Davis' steroidal guanidinium receptors

Receptors **27** – **33** proved capable of extracting a range of *N*-acyl α-amino acids from aqueous phosphate buffer, pH = 7.4, into chloroform. NMR analysis of the extracts revealed substantial interactions between substrates and receptors. Receptors **27** and **28** extracted several amino acids with remarkably consistent L:D ratios of 7:1, Table 1-2.

Table 1-2 Extraction of N*-acyl-α-amino acids by "symmetrical" biscarbamate receptors 27 and 28*

Host	Guest	Extraction efficiency (%)	Enantioselectivity (L:D)
27	*N*-Ac-DL-alanine	52	7:1
27	*N*-Ac-DL-phenylalanine	87	7:1
27	*N*-Ac-DL-valine	71	7:1
27	*N*-Ac-DL-tryptophan	83	7:1
27	*N*-Ac-DL-asparagine	~0	-
27	*N*-*t*-Boc- DL-valine	98	1:1
27	*N*-*t*-Boc- DL-serine	92	3:1
27	*N*-*t*-Boc- DL-histidine	66	3.5:1
28	*N*-Ac-DL-alanine	41	10:1
28	*N*-Ac-DL-valine	63	9:1
28	*N*-Ac-DL-phenylalanine	90	9:1
28	*N*-Ac-DL-tryptophan	83	9:1
28	*N*-Ac-DL-methionine	74	7:1

Receptors **32** and **33** possess asymmetric binding sites and did not show any enantioselectivity with *N*-acyl-α-amino acid derivatives. Receptors **29–31** present an increased asymmetry due to differing carbamoyl substituents and showed some good enantioselectivity. In particular receptor **31** showed a small but significant increase in enantioselectivities and extraction ability for *N*-acetyl-α-amino acids, most obviously for N-Ac-DL-alanine (76% compared to 52% for host **27**).

Anslyn developed a chemosensor (synthetic sensor coupled with a signalling element) for citrate in beverages, Figure 1-34.[75] Bisguanidinium **34** consists of two guanidinium groups for hydrogen bonding and charge pairing with citrate. The steric gearing imparted by the ethyl groups on the 2-, 4-, and 6-

positions ensures that the guanidinium moieties are preorganised on the same face of the benzene ring. Phenantroline acts as signalling element, to which the metal is chelated. The binding events between receptor **34** and citrate were investigated by fluorescence spectroscopy.

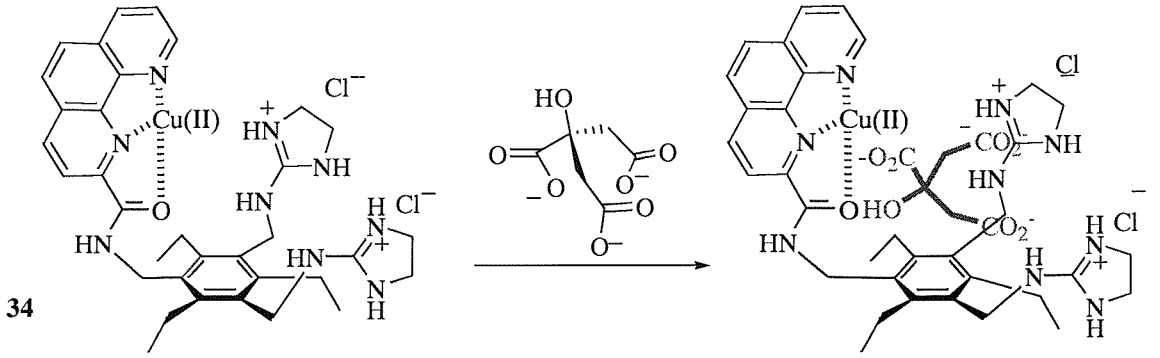

Figure 1-34 Chemosensor for citrate in beverages

A series of binding equilibria were found to be simultaneously present in solution, defining a cyclic equilibrium expression, Figure 1-35.

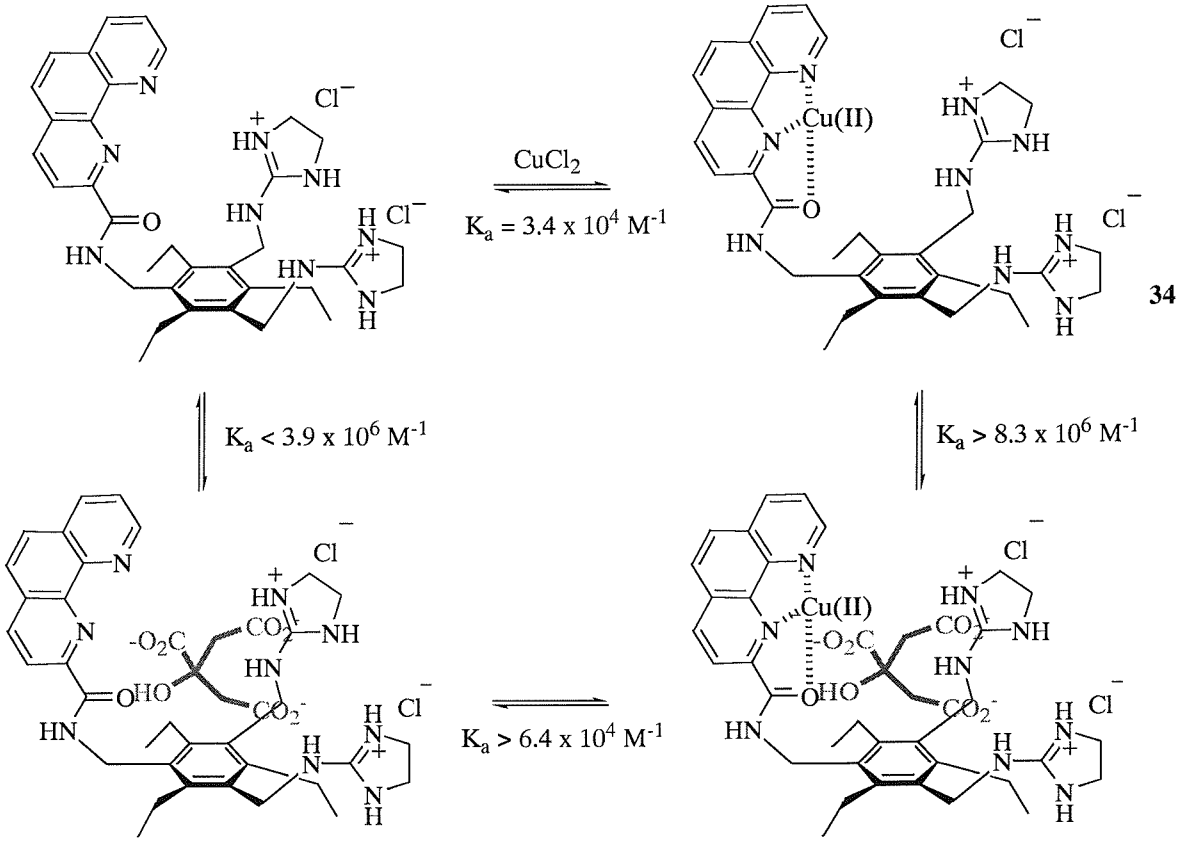

Figure 1-35 Cyclic equilibria present in solution

The binding association for each process were estimated by the increase in fluorescence intensities during titration experiments. It was noted that the presence of Cu(II) resulted in at least a 2.0 fold increase in the binding of citrate, due to a cooperative binding of $CuCl_2$ and citrate. The receptor proved to be effective at millimolar levels.

1.5.5 Organometallic Receptors for Carboxylates and Carboxylic acids

Since the geometrical control applied to the hydrogen bonding sites often requires several synthetic steps, the spontaneous assembling of smaller constituents to form receptors has been investigated. Based on the observation that transition metals have an ability to gather and orientate fragments, the self-assembly of half receptors around metallic templates has been used to develop a variety of receptors for neutral, anionic or cationic guests.

Weiss developed his receptor by assembling two catecholate ligands around molybdenum, **35**, Figure 1-36.[76] The two hydrogen bonding sites proved to be rigidly preorganised around the MoO_2 template. Evidence for a C_2 symmetry was obtained from ^1H and ^{13}C NMR.

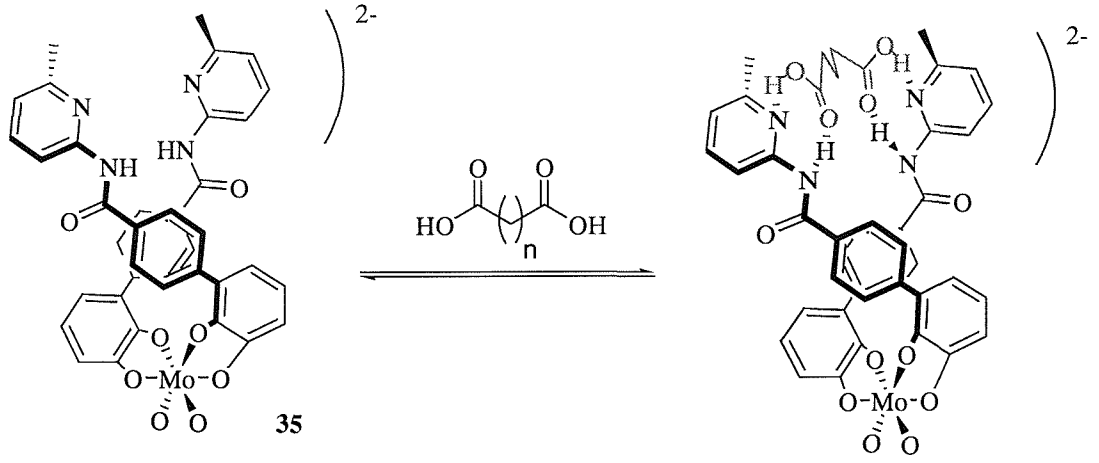

Figure 1-36 Weiss' dicarboxylic acid receptor incorporating a dioxomolybdenum core

UV-visible titrations of dicarboxylic acids were performed, due to the significant changes in the electronic absorption spectrum of the receptor assembled around the transition metal, Table 1-3. Despite the relative rigidity of the receptor's framework, only a slight preference for C_4 and C_5 dicarboxylic acids was noticeable, probably due to the free rotation of the CO-phenyl bond which enables the receptor to adapt to the length of the diacid carbon chain.

Table 1-3 Binding constants for the titration of C_n dicarboxylic acids from succinic to pimelic acid

Solvent	C4	C5	C6	C7
CH_3CN	$2.3x10^3$	$4.2x10^3$	$1.2x10^3$	$0.6x10^2$
CH_3CN	$5.7x10^3$	$3.7x10^3$	$1.8x10^3$	$1.1x10^3$
CH_2Cl_2	Not soluble	$8.9x10^3$	$4.7x10^3$	$5.1x10^3$

Hong *et al.* recently developed a water-soluble chiral receptor, **36**, exploiting the self-assembly of bis(4-pyridyl)-substituted (1*R*,2*R*)-diaminocyclohexane by Pd(II).[77] The binding of **36** to different aromatic carboxylates in water was investigated using ^1H NMR titrations. Association of *N*-Ac aromatic amino acids proved to be very weak.

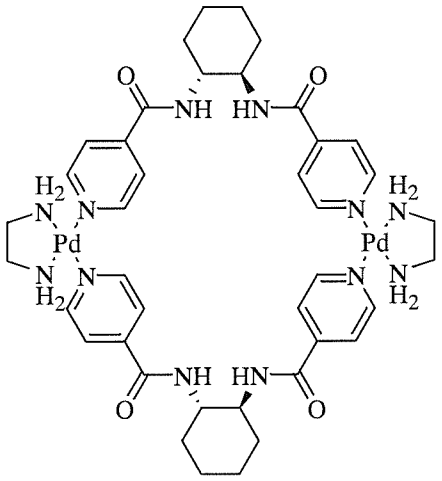

36

Figure 1-37 Weiss' self-assembled receptor

A 10-fold increase in selectivity was noted when naphthalene derivatives with two tethered carboxylate groups were investigated, both in water and in basic aqueous medium (pD = 8.5), Table 1-4. Job's plots indicated the formation of 1:1 host-guest complex with the naphthalene carboxylates. Larger binding constants were obtained when additional hydrophobic groups were introduced to the naphthalene dicarboxylate guests. The receptor exhibits poor enantioselectivity as the hydrophobic cavity is too rigid to be able to differentiate the subtle differences in the chiral shape of the guests. Temperature-dependent ^1H NMR titrations were performed: the complexation proved to be driven by entropically favourable desolvation of the ionic groups of both binding partners upon salt bridge formation. CPK modelling

suggested that the naphthalene unit positions itself in the middle of the symmetric host cavity with the two carboxylate groups interacting with Pd^{2+}, confirmed by upfield shifts of the ^1H NMR signal upon complexation of both H_α and H_β of the pyridine units of **36** and the aromatic protons of the guest.

*Table 1-4 Binding constants between various aromatic dicarboxylates and **36***

Guest	Ka (D_2O)	Ka (pD = 8.5)
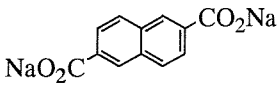	30	
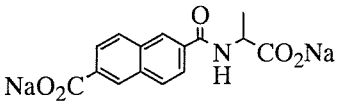	*rac* 160 L 280	*rac* 100 L 146 D 134
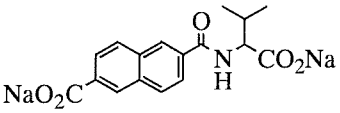	*rac* 280 L 260	L 120 D 155
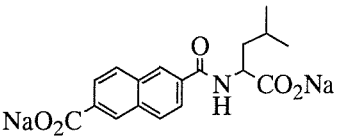	*rac* 450 L 430	L 210 D 125
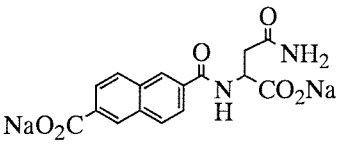	-	L 174
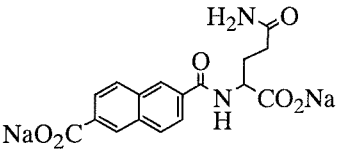	-	L 152
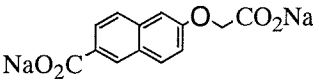	-	132

Metallocene-based receptors have been used on a number of occasions as redox-active receptors for organic molecules[78]. Beer developed a receptor, **37**, in which two amide units on the upper rim of the calix[4]arene were rigidly held by a cobaltocene moiety, Figure 1-38.[79]

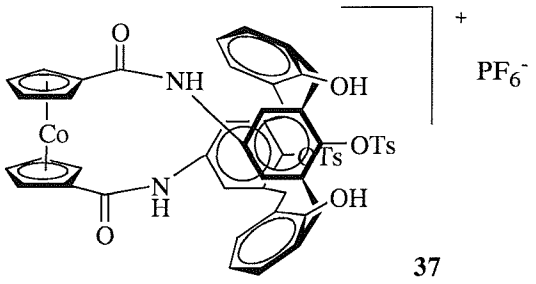

37

Figure 1-38 Beer's metallocene-based calixarene

To assess the role of the metal during the complexation process, tetrabutylammonium acetate was added to a solution of the host in acetonitrile. Cyclic voltammetry studies revealed a cathodic shift of –155 mV in the reversible Co(III) / Co(II) redox couple, which indicated that the anion was effectively stabilizing the positive charge on the cobaltocenium moiety and making the complex harder to reduce.

1.5.6 Miscellaneous Receptors for Carboxylates

Still produced water-soluble 2-armed receptors incorporating a water-soluble dye for screening of the receptor against peptide libraries, **38-40**, Figure 1-39.

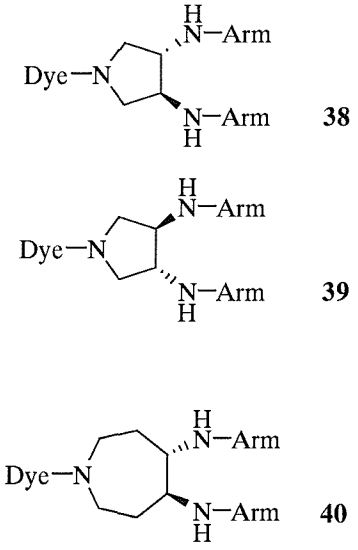

38

39

40

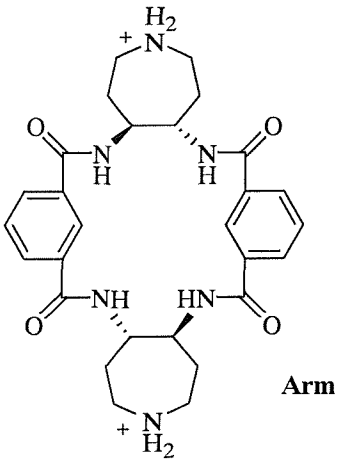

Arm

Figure 1-39 Still's water-soluble two-armed receptors

The selectivity of the new receptors was tested by equilibrating a dye-labelled receptor at low concentration with a combinatorial library of tripeptides on polymeric beads. The library was divided into two groups: the protected library, with *N*-terminal acetylation and all side chain protecting groups

intact and the deprotected library, with *N*-terminal amino group free and all side chain protecting groups removed. The receptors showed a high preference for binding peptides containing carboxamide-bearing amino acids, frequently L-Gln, followed by D-Leu. In particular, receptor **38** preferred peptides with an *N*-terminal Asn or Gln. Receptors **38** and **40** showed visible binding also with the deprotected tripeptide library. The majority of the beads carried various stereorandom aspartic and glutamic acid sequences, undoubtedly bound to the hosts by non-specific ionic associations. Interestingly, receptor **40** also bound the different sequence D-Asp-D-Leu(or Phe)-D-Asp in 6% of the coloured beads.

1.6 Application of Isothermal Calorimetry to Supramolecular Chemistry

1.6.1 Introduction

Thanks to recent advances in instrumentation sensitivity, isothermal calorimetry (ITC) is becoming increasingly important as a tool for probing the thermodynamics of a process. By directly measuring the heat evolved or absorbed as a function of time ITC can determine, in one stroke, all the thermodynamic parameters involved in a chemical process. In a single experiment the binding constant (K_a), the stoichiometry (n) and the enthalpy (ΔH) of the process investigated are determined. From the association constant the free energy and entropy of binding are determined. Recently supramolecular chemistry has started to apply the ITC tool to gain an insight into the thermodynamic parameters involved in the complexation of a guest by a synthetic receptor (or host). A brief overview of some of the uses ITC has found within supramolecular chemistry and specifically carboxylate recognition is presented here.[80]

1.6.2 Molecular Recognition of Carboxylates and Carboxylic acids

Hamilton *et al.* applied ITC to investigate the association between a series of simple guanidinium derivatives with tetrabutylammonium (TBA) acetate in DMSO, **40**–**47**, Figure 1-40.[81]

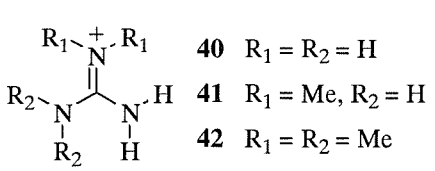

40 $R_1 = R_2 = H$
41 $R_1 = Me, R_2 = H$
42 $R_1 = R_2 = Me$

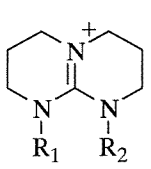

43 $R_1 = R_2 = H$
44 $R_1 = Me, R_2 = H$
45 $R_1 = R_2 = Me$

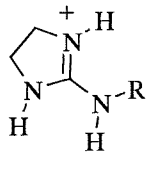

46 R = H
47 R = Bn

Figure 1-40 Hamilton's guanidinium receptors for acetate

Acyclic, monocyclic and bicyclic guanidinium salts were studied. In the acyclic systems **40-42**, sequential removal of hydrogen bond donors resulted in a drastic decrease in the association constant ($K_{1:1}$ = 7.9x10^3 M^{-1}, $K_{1:1}$ = 3.4x10^3 M^{-1}, $K_{1:1}$ = 1.1x10^2 M^{-1}). Similarly, sequential methylation of the corresponding bicyclic guanidiniums **43-45** resulted in a loss of binding affinity for TBA acetate ($K_{1:1}$ = 5.6x10^3 M^{-1}, **43**). Monocyclic guanidiniums **46** and **47** displayed a high affinity for acetate ($K_{1:1}$ = 8.7x10^3 M^{-1}, $K_{1:1}$ = 7.2x10^3 M^{-1} respectively). All the association constants were confirmed by traditional ^{1}H NMR titrations. Even though in most cases the receptors formed a 1:1 complex with the guest, two receptors (**40** and **46**) proved to complex an additional equivalent of TBA acetate to form a weak 2:1 complex, thanks to the availability of extra hydrogen bond donors. In all cases, both the association enthalpy and entropy were favourable, indicating that the complexation process was driven both by hydrogen bond formation and by the liberation of bound solvent molecules.

Building on this work, Hamilton moved to more complicated host-guest systems.[82] Although the role of the solvent in hydrophobic binding processes has previously been documented[83], no examples of solvent effects on host-guest systems reliant on hydrogen bonding were found in literature. This work focused on the changes in association and thermodynamics caused by increasingly competitive solvents, from DMSO to methanol and water. A series of synthetic receptors providing the same number and orientation of hydrogen donors, but varying greatly in binding strength, were prepared, **48–51**, Figure 1-41.

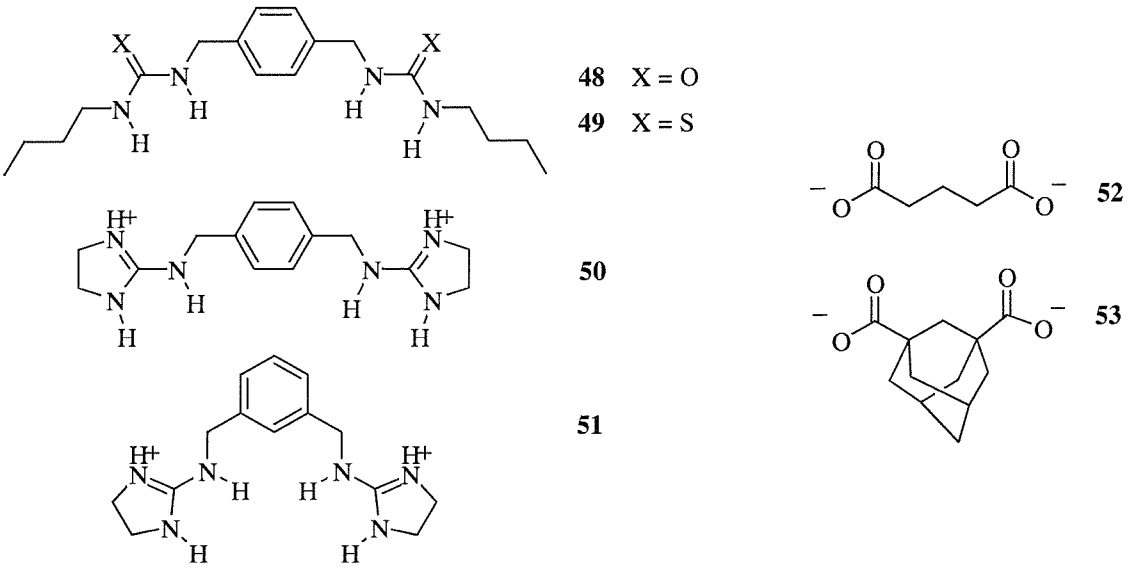

Figure 1-41 Hamilton's receptors for dicarboxylates

Three binding moieties, ureas, thioureas and guanidiniums, with increasing bond donor acidity (pK_a = 26.9, pK_a = 21.0 and pK_a = 13.5 respectively) and correspondingly increasing association strength, were selected. All the receptors bound two dicarboxylate guests, **52** and **53**, by forming a 1:1 complex. The association was measured by ITC and confirmed by NMR titration. The thermodynamic data for complexation by bis-urea and bis-thiourea receptors proved to be different from those of bis-guanidiniums. Association of bis-urea and bis-thiourea with dicarboxylates was characterised by negative enthalpies and near zero entropies. Bis-guanidinium systems instead showed positive enthalpies and large positive entropic contributions. In DMSO the complexation is enthalpically driven. Switching to methanol and methanol/water mixtures, the association becomes endothermic, with favourable entropy. ITC was used to show the change from the association being promoted mainly by hydrogen bond formation to an association driven by liberation of bound solvent molecules.

Kilburn and Bradley developed a tweezer receptor designed to bind to tripeptides.[84] The structure featured a guanidinium moiety to bind *via* a strong interaction to the carboxylate terminus of the guest peptide and peptidic arms, to form potential hydrophobic and β-sheet like hydrogen bonding interactions with the peptide substrate.

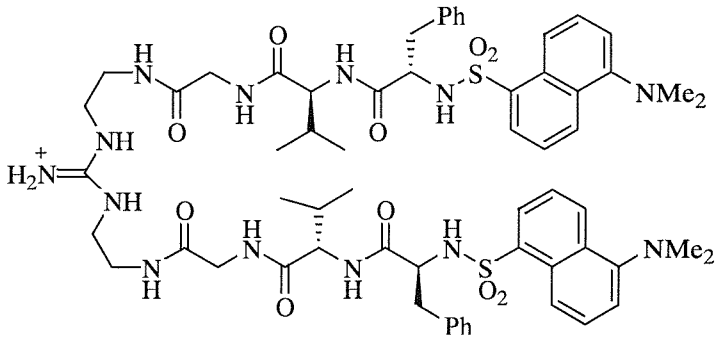

54

Figure 1-42 Kilburn and Bradley's tweezer receptor

Screening of the tweezer receptor against a 1000-member library of tripeptides attached to TentaGel resin *via* the amino terminus in water followed by appropriate sequencing of bound library members revealed a 95% selectivity for Val at the carboxyl terminus of the tripeptide and a 40% selectivity for Glu (O^tBu) at the amino terminus. The limited solubility of receptor **54** in predominantly aqueous solutions precluded an NMR investigation of its binding properties. ITC of **54** with tripeptide Z-Glu (O^tBu)-Ser (O^tBu)-Val-OH gave a K_a of $4x10^5$ $mol^{-1}dm^3$ in sodium borate buffer containing 17% DMSO.

Inoue *et al.* carried out some extensive studies on the thermodynamics involved in the complexation of various guests by cyclodextrins.[85] More than 100 acyclic and cyclic guests have been investigated exhibiting a wide variety of variation in terms of chain length, branching, flexibility, charge and oxygen atoms. The different guests included not only amino acids and carboxylic acids but also esters, amines and alcohols. In many cases the hydrophobic and Van der Waals interactions were the principal intermolecular weak forces responsible for the formation of stable supramolecular complexes. As a general rule it was also found that chiral guests with less symmetrical, non-polar penetrating groups or with a larger distance between chiral centre and the most hydrophilic part were more likely to exhibit chiral recognition. Following these promising results Inoue extended his interest to the association of a great variety of chiral and achiral guests with a modified β-cyclodextrin, am-β-CD, bearing an amino group in position 6, Figure 1-43.[86] It is well known that the most probable binding mode of native and modified cyclodextrins (CDs) with various guests involves the insertion of the less hydrophilic part of the guest molecule into the CD cavity. Meanwhile the more hydrophilic, often charged, group stays just outside the rim of the cavity. By introducing an oppositely charged group into the host, i.e. forcing an attractive Coulombic interaction, its binding affinity for a charged guest should increase.

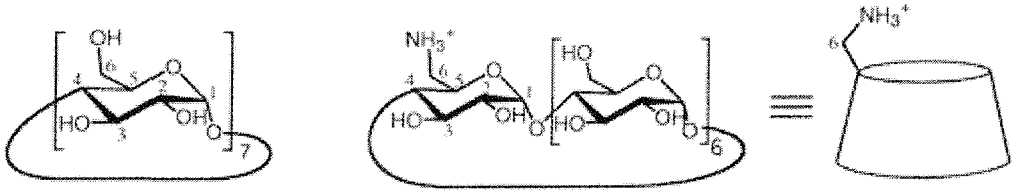

Figure 1-43 Inoue's cyclodextrins

In order to evaluate general rules governing the thermodynamic and chiral behaviour of am-β-CD compared to native β-CD, various negatively charged guests were considered together with neutral and positively charged compounds. Both receptors showed similarities in the mode of penetration, the chiral recognition and in presenting the same enantiomer preference ("chiral memory"). They also showed similar conformational changes upon complexation. As expected, negatively charged guests exhibited larger affinities towards am-β-CD than the unmodified analogue. In general, flexible or less bulky groups showed increased affinities by a factor of 3-5. Bulky or rigid guests showed only a slighter higher affinity for am-β-CD compared to β-CD. The modified cyclodextrins also showed an enhanced chiral discrimination.

Morel-Desrosiers *et al.* studied the binding of dipeptides and tripeptides by water-soluble *p*-sulfonatocalix[*n*]arenes, with n = 4, 6 and 8.[87] ITC and ^{1}H NMR spectroscopy were used to determine the thermodynamic characteristics of complexation of peptides containing lysine and arginine residues. The work concentrated mainly on the complexation of the dipeptides lysil-lysine, **KK**, arginyl-arginine, **RR**, and the mixed dipeptides **KR** and **RK** and two tripeptides, **KKK** and **RRR**. For calix[4]arene sulfonate only a 1:1 stoichiometry was observed, Table 1-5. The binding process was driven by favourable enthalpy, due mainly to the tight inclusion of the apolar part of the guest into the hydrophobic cavity of the host through Van der Waals interactions. Favourable entropy also accompanied the process, as a result of the desolvation of the charged groups upon ionic interaction.

Table 1-5 Thermodynamic parameters of the complexation of guests by p-sulfonatocalix[4]arene in water at pH 8.0 and 298 K (ΔG, ΔH and TΔS in kJ mol^{-1})

	10^{-3} K	ΔG	ΔH	TΔS
Lysine-containing peptides				
K	0.74 ± 0.01	-16.4 ± 0.1	-14.4 ± 0.1	2.0 ± 0.2
KK	3.8 ± 0.3	-20.4 ± 0.2	-29.0 ± 0.3	-8.6 ± 0.5
KKK	30 ± 4	-25.5 ± 0.4	-27.3 ± 0.3	-1.8 ± 0.7
Arginine-containing peptides				
R	1.52 ± 0.09	-18.2 ± 0.1	-20.3 ± 0.3	-2.1 ± 0.4
RR	7.7 ± 0.6	-22.2 ± 0.2	-26.1 ± 0.2	-3.9 ± 0.4
RRR	35 ± 9	-25.9 ± 0.6	-31.2 ± 0.5	-5.3 ± 1.1
Mixed dipeptides				
KR	3.7 ± 0.1	-20.4 ± 0.1	-29.4 ± 0.1	-9.0 ± 0.2
RK	4.3 ± 0.2	-20.8 ± 0.1	-31.0 ± 0.2	-9.7 ± 0.3

The thermodynamic properties of association and the NMR data showed that lysil-lysine, **KK**, adopts a very compact, folded structure upon binding by the tetrameric host. The mixed peptides behave like **KK** with the lysine residue lying preferentially in the receptor cavity. Addition of a third chain perturbed such arrangement causing a more favourable entropic contribution and therefore a more important affinity. Arginyl-arginine, **RR**, which cannot adopt such a structure behaved differently. With

calix[6]arene sulfonate 1:1 and 1:2 (host:guest) complexes were observed. The host bound two lysyl-lysine guests in a non-cooperative manner, probably by adopting a 1,2,3-alternate conformation. The thermodynamic data and the dissymmetry of the NMR spectra showed that only the central side chain of the tripeptides was turned towards the interior of the partial cone, favouring a π-π stacking between the three guanidinium groups of the guest and the phenyl units of the host. A more complex behaviour, associated with higher orders of stoichiometry, and probably aggregation, characterised the binding properties of calix[8]arene sulfonate.

Schmidtchen synthesised a series of bicyclic guanidiniums, **55-58**, and crown compounds, **59-75**, Figure 1-44.[88]

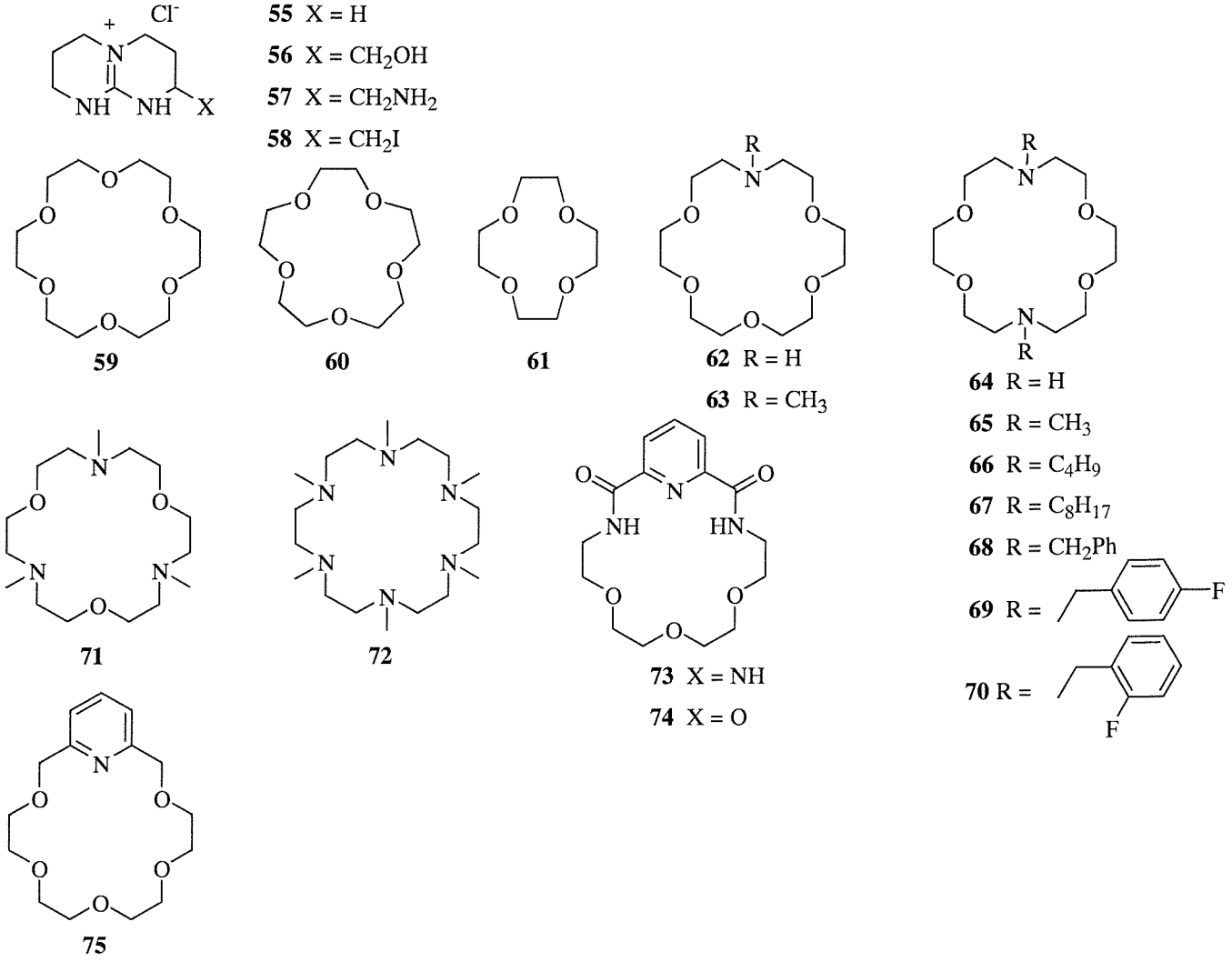

Figure 1-44 Schmidtchen's crown and guanidinium receptors

The influence of ring size, nature and position of the donor atoms of the macrocyclic compounds on the complexation of glycine was investigated. The values of the stability constants and the thermodynamic parameters are summarised in Table 1-6.

Table 1-6 Stability constants and thermodynamic parameters (expressed in kJ mol^{-1}) for complexation of glycine in methanol at 25°C (- = heat produced too small to allow calculations of log K and ΔH)

Host	log K	ΔG	ΔH	TΔS
55-58	-	-	<-2.0	-
59	3.5	-20.0	-49.8	-29.8
60	-	-	-3.0	-
61	-	-	-	-
62	3.4	-19.2	16.3	2.9
63	3.6	-20.7	-17.5	3.2
64	2.9	-16.4	-1.9	14.5
65	2.9	-16.7	6.6	23.3
66	3.6	-20.5	-11.3	9.2
67	3.7	-21.1	-11.1	10.0
68	3.3	-18.6	-13.4	5.2
69	3.8	-21.8	-8.2	13.6
70	3.4	-19.2	-17.3	1.9
71	3.4	-19.7	-21.1	-0.5
72	2.8	-15.8	-8.8	7.0
73	-	-	-1.5	-
74	2.9	-16.8	-5.4	11.4
75	4.2	-24.1	-20.8	3.3

The highest enthalpic contribution was observed for 18-crown-6, **59**. The complexation is disfavoured by entropy, suggesting a high flexibility of the free receptor and almost the same solvation stage of the complexed and uncomplexed form. The ability to complex glycine decreases dramatically with ring size, from 18-crown-6>>15-crown-5>12-crown-4. All nitrogen containing crown compounds presented a

significantly lower ΔH as compared to **59**. In case of hosts **62** and **64**, the lone electron pair of the nitrogen atom is located outside the macrocycle's cavity. The necessary rearrangement of the receptor before complexation causes a decrease in enthalpy. Derivatives of compound **64** (**65-70**), whose bulky groups could shield the host's cavity from solvent molecules, showed more exothermic complexation enthalpies and an increase in complex stability compared to **59**. Compounds **68**, **69** and **70**, which contain benzyl groups to direct the nitrogen lone pair electrons towards the cavity, showed higher stability constants and enthalpies. The reaction entropy for the complexation of glycine with diamidopyridino crown receptor **75** increased remarkably, probably due to the higher degree of preorganisation of **75** compared to 18-crown-6.

De Mendoza, in collaboration with Hamilton, reported the association between tetraguanidinium receptor **76** (Figure 1-45) and a series of peptides in which aspartate had been sequentially replaced by glutamate so that the Asp-Glu ratio spanned from the all aspartate peptide **77** to the all glutamate peptide **81**.[89]

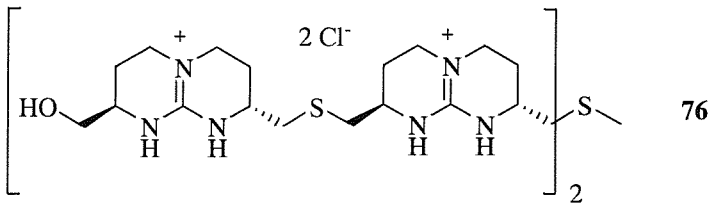

76

Figure 1-45 de Mendoza and Hamilton's tetraguanidinium receptor

The resulting lengthening of the side chain had a dramatic effect on the thermodynamics of binding, which shifted from enthalpically to entropically driven. The helical content of the peptides in solution was assessed by circular dichroism (CD) and showed that the replacement of aspartate by glutamate gradually increased the helical content of the peptide. ITC was used to measure the affinity constants in the cases where there was no change in ellipticity. The data confirmed a 1:1 complexation stoichiometry and are summarised in Table 1-7. Peptide **77** showed an overall negative enthalpy change, while peptide **81** showed a positive enthalpic contribution upon binding. Peptide **79**, with an equal number of aspartate and glutamate residues in its surface showed an enthalpically neutral binding curve. The affinity constants did not vary much between the different peptides, suggesting that it does not depend on the individual nature of the residues involved in the complex formation. Complexation of **77** proved to be enthalpically driven due to the relative rigidity of the aspartate side chains in contact with the receptor, which forces a change in the backbone conformation of the peptide towards a higher helicity. The

complex formation takes place due to the large negative enthalpy of α-helix formation with the entropic contribution of the liberation of counterions and solvent molecules. Complexation of **81** however, proved to be entropically driven. The longer side chain of glutamate allowed the formation of the complex without a major reorganisation of the peptide backbone. This is demonstrated also by the lack of conformation change observed in the CD studies. The complexation is driven by the liberation of solvent molecules bound to the peptide and the host.

*Table 1-7 Thermodynamic and binding data for receptor **76** with tetracarboxylate peptides (ΔG, ΔH and TΔS in kcal mol^{-1}; - no change observed with the noted technique)*

Peptide sequence	Ka (M^{-1})	ΔG	ΔH	TΔS
77 Ac-A-A-A-**D**-Q-L-**D**-A-L-**D**-A-Q-**D**-A-A-Y-NH_2	CD 3.4 ± 1.2 x10^5 ITC 1.2 ± 0.2 x10^5	-7.23	-5.64	1.29
78 Ac-A-A-A-**E**-Q-L-**D**-A-L-**D**-A-Q-**D**-A-A-Y-NH_2	CD 5.6 ± 1.0 x10^4			
79 Ac-A-A-A-**E**-Q-L-**E**-A-L-**D**-A-Q-**D**-A-A-Y-NH_2	CD 5.3 ± 2.2 x10^4 ITC -	-6.44	0	6.44
80 Ac-A-A-A-**E**-Q-L-**E**-A-L-**E**-A-Q-**D**-A-A-Y-NH_2	CD 2.2 ± 1.5 x10^4			
81 Ac-A-A-A-**E**-Q-L-**E**-A-L-**E**-A-Q-**E**-A-A-Y-NH_2	CD - ITC 1.5 ± 0.4 x10^5	-7.06	3.68	10.74

1.7 Aims of the Project

The preceding reviews have highlighted the important areas where progress has been made in the selective binding of carboxylate and carboxylic acid derivatives. One important point to note when comparing the ability of synthetic receptors to selectively bind substrates is that macrocyclic structures tend to be significantly more selective than non-cyclic receptors. The aim of this project was to construct a series of bisthiourea-based macrocyclic receptors and examine their ability to selectively bind amino acid derivatives. Efforts focused on the synthesis of a receptor specifically designed to bind to glutamate. Glutamate has a very important biological role as together with aspartate, it acts as a neurotransmitter. Glutamate receptor ion channels are responsible for most excitatory synaptic

communication in the central nervous system. They play an important role in the regulation of synaptic strength and are involved in a number of neuropathological processes including post-traumatic neuronal damage, epilepsy and neurodegenerative diseases. Glutamate's role in some serious pathologies has been recently discovered: it has been found that some types of brain tumours seem to be triggered by a sudden increase in the concentration of glutamate in the brain. A high concentration of glutamate has been found to be related to some side effects suffered by ischemic patients. Chapter two discusses the synthesis of a bisthiourea-based macrocyclic receptor and its ability to selectively bind to *N*-Boc protected glutamate. Other derivatives were considered, such as aspartate, to fully investigate its binding properties. Traditional NMR titration studies and isothermal calorimetry were employed as tools to study the complexation process in different solvents. Attention was also paid to all the possible conformations the receptor might adopt in solution. In an attempt to enhance the binding strengths of the original macrocycle synthetic variations were prepared containing phenyl groups and a more rigid spacer. The synthesis and binding properties of the new receptors are discussed in chapter three. Chapter four goes on to describe the attempted synthesis of a novel monothiourea-based macrocycle and a novel thiourea-based tweezer receptor. The ultimate aim of this project is to develop a synthetic receptor system, capable of high levels of enantioselective recognition and transport, and therefore with possible applications in separation technology. It should be capable of enantioselectively binding its substrates with sufficient power to draw them across phase boundaries and be able to facilitate transport between separated phases, for example in an aqueous-organic-aqueous system. If the receptor is both non-stoichiometric (*i.e.* catalytic) in action and reasonably versatile, the method could be readily adapted to meet the needs of industry.

2 A Novel Bisthiourea Macrocycle

2.1 Introduction

A large number of tweezer or U-shaped cleft receptors have been synthesised by host-guest chemists. These non-macrocyclic hosts are so named because they contain particular structural features, which give them the appearance and the mode of binding of a pincer. The Kilburn group has synthesised tweezer receptors for peptides with a carboxylic acid terminus. Solid-phase synthesis was employed to construct tweezer receptor **82**, Figure 2-1, which was designed to bind to the carboxy terminus of peptides in organic media.[90] A diamidopyridyl functional group was used as the carboxylic acid binding site. The tweezer arms have the potential to form both hydrophobic and β-sheet-like hydrogen-bonding interactions with the backbone of the peptide substrate.

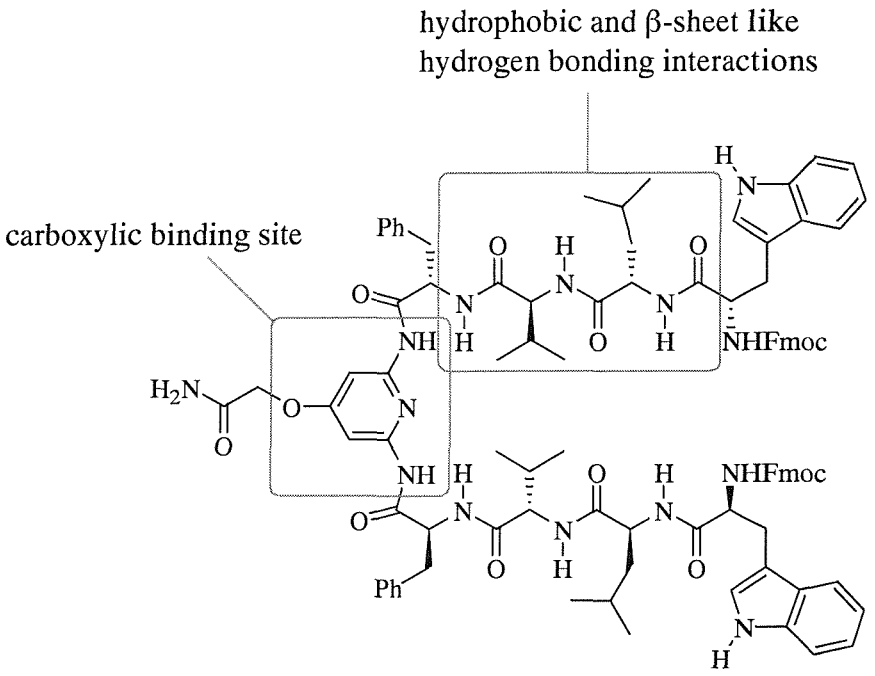

Figure 2-1 Kilburn's tweezer receptor for N-terminal carboxylic acid peptides

UV complexation studies were carried out between tweezer receptor **82** and DNS-L-Glu(O^{t}Bu)-L-Ser(O^{t}Bu)-L-Val-OH in DMSO:$CHCl_3$ (2:98). The data from this experiment showed a good fit for the presumed 1:1 binding and allowed an estimation of the association constant as 2.6 x 10^5 M^{-1}. It was concluded that, as anticipated, the incorporation of a specific binding site for the carboxylic acid terminus of peptide guests into a tweezer structure provided a considerably higher affinity than with a non-specific head group.

Kilburn extended his studies and synthesised a variation of receptor **82**, by substituting two phenylalanine groups by two β-alanine units as the starting point for generation of the peptidic arms, **83**, Figure 2-2.[91]

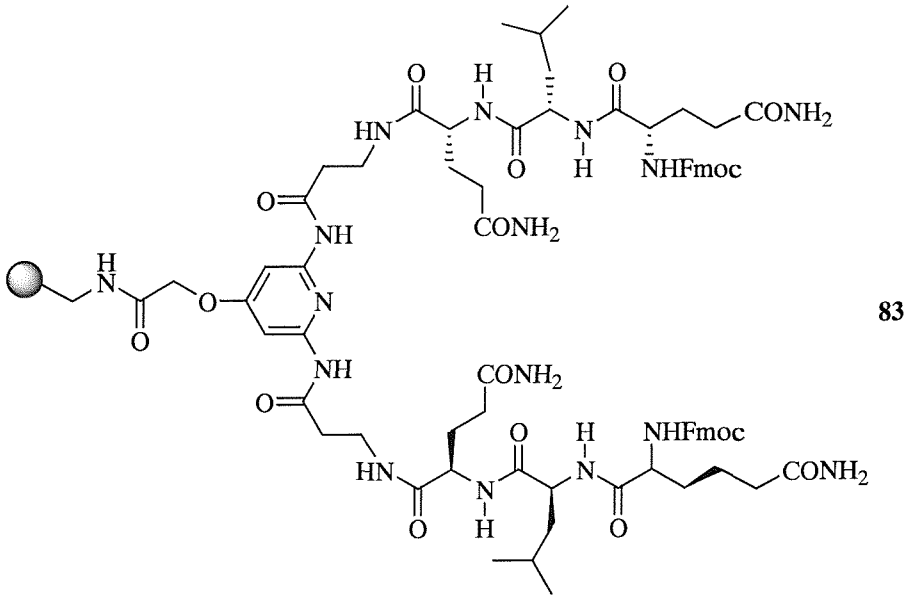

83

Figure 2-2 Kilburn's modified tweezer receptor

HPLC complexation studies were carried out between the resin bound tweezer receptor **83** and DNS-L-Glu-L-Ser-L-Val-OH and the side chain protected analogue DNS-L-Glu(O^{t}Bu)-L-Ser(O^{t}Bu)-L-Val-OH. The addition of **83** to a solution of DNS-L-Glu-L-Ser-L-Val-OH in $CHCl_3$ led to the absorption of 90% of the peptide as adjudged by HPLC after 24 hours incubation. The acetylated red dye was used as internal standard. Addition of the same amount of receptor to the side-chain protected analogue, DNS-L-Glu(O^{t}Bu)-L-Ser(O^{t}Bu)-L-Val-OH, led to an absorption of 20% of the peptide. The association constants for both events were estimated as 3 x 10^5 M^{-1} and 1 x 10^3 M^{-1}, respectively. Therefore it was concluded that the receptor **83** binds the unprotected peptide >100 times more strongly than the side-chain protected analogue. Identical experiments with the enantiomeric peptide DNS-D-Glu-D-Ser-D-Val-OH, led to an estimated binding constant of 9 x 10^3 M^{-1}, suggesting that tweezer receptor **83** binds the L-configured peptide 30 times more strongly than the other enantiomer. Tweezer receptor **84** was synthesised, featuring a guanidinium moiety to bind, *via* a strong interaction, to the carboxylate terminus of the guest peptide, Figure 2-3.[92] UV titration studies, in 15% DMSO/water, of the host with Red dye-L-Glu(O^{t}Bu)-L-Ser(^{t}Bu)-L-Val-OH resulted in a decrease in the absorption at 500 nm, with an isobestic point at 400 nm, with an estimated binding constant of 8.2 x 10^4 M^{-1}. Titration of **84** with the enantiomeric peptide Red dye-D-Glu(O^{t}Bu)-D-Ser(^{t}Bu)-D-Val-OH resulted in a decrease in the absorption at 500 nm, with two isobestic points at 410 and 590 nm and an estimated binding constant of 8.0 x 10^3 M^{-1}. Titration experiments with the side chain deprotected analogue, Red dye-L-Glu-L-Ser-L-Val-OH, resulted in no detectable change to the UV absorption. Tweezer **84**

proved to be highly selective over the side chain deprotected peptide (>100:1) and enantioselective with an approximate ratio L:D of 10:1.

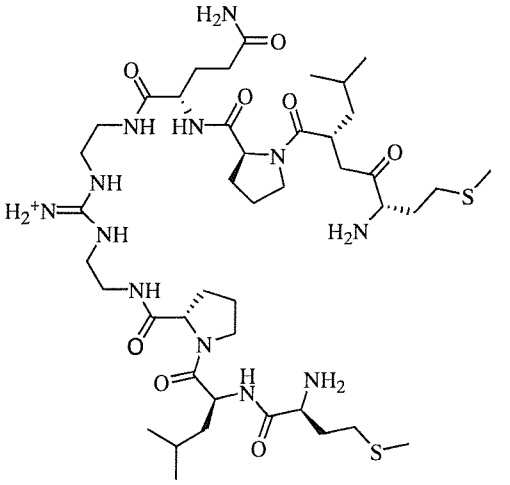

84

Figure 2-3 Kilburn's tweezer receptor for tripeptides

Recent work in the group involved the synthesis of simple acyclic dipyridyl based thiourea tweezers.[93] Tweezer receptor **85** was designed to preorganise into a U-shaped cleft *via* intramolecular hydrogen-bonds from the pyridine nitrogen to the thiourea and amide hydrogens. Evidence of the formation of hydrogen bonds between amide hydrogens and pyridine nitrogens was demonstrated by Hunter, who synthesised a series of receptors for quinones.[94] Cyclic dimers **86** and **87** were synthesised and found to complex *p*-benzoquinone with K_a = 1200 M^{-1} for **86** (X = CH) and K_a = 1800 M^{-1} for **87** (X = N).

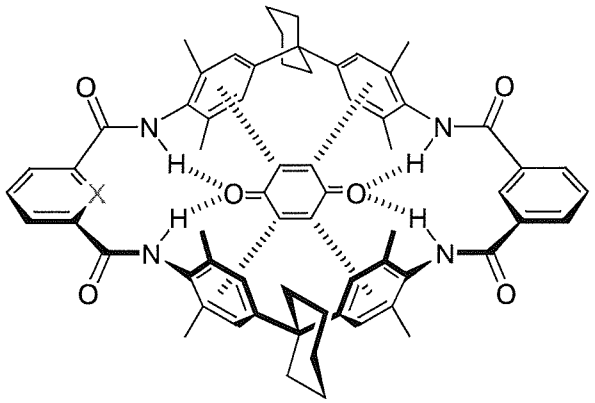

86 X = CH
87 X = N

*Figure 2-4 Complexation of p-benzoquinone by **86** and **87***

Sterically demanding chiral groups were incorporated on the tweezer arms to encourage chiral recognition between the tweezer receptor and carboxylate guest and to interact with the amino acid side chain. Amide groups were also included on the tweezer arms to form hydrogen-bonds to the guest *N*-acetyl group.

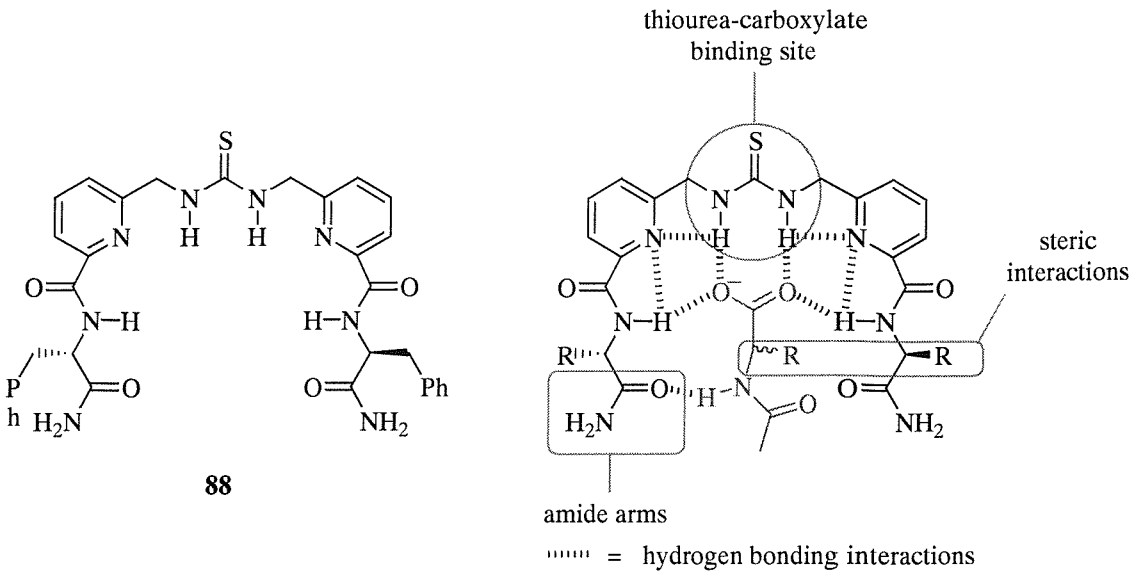

88

Figure **2-5** *Tweezer receptor for enantioselective binding of carboxylates*

Binding studies with the chiral pyridyl receptor **88** and a range of amino acid derivatives, as the tetrabutylammonium salts, were carried out in neat $CDCl_3$ and the results are presented in *Table* 2-1.[95] Phenylalanine and alanine were picked to see the effect of side chain steric bulk upon binding. Amino acids with similar side chain hydrogen-bonding functionality such as asparagine and glutamine were selected to probe the effect of side chain length whilst tryptophan was chosen to probe the effect of the steric bulk of the hydrogen-bond donor on binding selectivity. The receptor proved to be strongly selective for different amino acids, as in the case for *N*-Ac-L-Trp over *N*-Ac-L-Ser (>30:1). In general, tweezer **88** was moderately enantioselective for the L forms of all guests with the highest selectivity for *N*-Ac-L-Gln (L:D 2:1). *N*-Ac-L-Asn was also bound twice as strongly as the corresponding D enantiomer as evidenced by the association constants. In contrast, low selectivity was observed for *N*-Ac-L-Ala and *N*-Ac-L-Phe, presumably a consequence of the lack of side chain hydrogen-bonding functionality in these guests. Binding constants were highest for amino acids with side chains incorporating hydrogen bonding functionality (*N*-Ac-L-Gln) or an electron rich aromatic sidechain (*N*-Ac-L-Trp). *N*-Boc-Gln and *N*-Boc-Trp were studied to ascertain whether the increased steric bulk of the Boc group would enhance the level of enantioselectivity. For *N*-Boc-Gln the association constants were found to be lower than in the *N*-acetyl case as was the level of enantioselectivity. The association constants for *N*-Boc-Trp were similarly lower than the *N*-acetyl case although the enantioselectivity was higher for *N*-Boc-Trp (? ? G = 0.9 kJ mol^{-1} for *N*-Boc-Trp and ? ? G = 0.5 kJ mol^{-1} for *N*-Ac-Trp).

Table *2-1 Screening of a range of guests against pyridyl tweezer* ***88*** *in* $CDCl_3$

Guest	K_a/ M^{-1}	?G/ kJ mol^{-1}	??G/ kJ mol^{-1}
N-Ac-L-Ala	3450	20.3	0.8
N-Ac-D-Ala	2520	19.5	
N-Ac-L-Phe	4770	21.1	1.1
N-Ac-D-Phe	2990	20.0	
N-Ac-L-Asn	1690	18.5	1.8
N-Ac-D-Asn	800	16.7	
N-Ac-L-Gln	9000	22.7	1.7
N-Ac-D-Gln	4520	21.0	
N-Boc-L-Gln	1190	17.7	1.0
N-Boc-D-Gln	810	16.7	
N-Ac-L-Ser	380	14.8	0.6
N-Ac-D-Ser	480	15.4	
N-Ac-L-Trp	12400	23.5	0.5
N-Ac-D-Trp	14800	24.0	
N-Boc-L-Trp	3140	20.1	0.9
N-Boc-D-Trp	2225	19.2	
R-Nap	26200	25.4	0.2
S-Nap	28300	25.6	

For all substrates, binding resulted in significant downfield shifts of the NH signals from the thiourea (1.6 – 2.1 ppm), the secondary amide (0.3 – 0.7 ppm) and for one of the primary amide protons (1.2 – 1.5 ppm) and an upfield shift of the other primary amide proton (0.3 – 0.7 ppm), Figure 2-6. This suggested that binding of the amino acids involves hydrogen bonds to the thiourea, secondary amide and one of the primary amide protons, but also involves the breaking of an intramolecular hydrogen bond to the other primary amide NH. Conversely, binding of the tryptophan derivatives led to a significant upfield shift of the indole signal (>1 ppm) presumably reflecting the breaking of an intramolecular hydrogen bond between the indole NH and the carboxylate on binding. Similarly, binding of the glutamine and asparagines derivatives led to upfield shifts for one of the primary amide NH in each case.

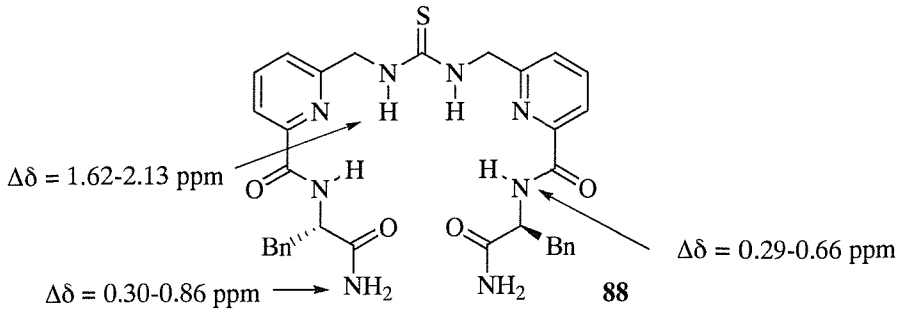

Figure 2-6 Chemical shifts of NH protons during binding studies in $CDCl_3$

To determine if receptor **88** was preorganised, pyridyl tweezer **89** and benzo tweezer **90** were synthesised and the corresponding association constants for these systems with phenylacetic carboxylate measured, Figure 2-7.[93] It was thought that pyridyl thiourea **89** might give a higher association constant than benzo thiourea **90** if **89** was preorganised into a U-shaped cleft, providing there was indeed four hydrogen bonds between the thiourea and amide hydrogens to the pyridyl nitrogen. It was assumed that there would be a smaller entropy loss upon binding if the tweezer arms were in the correct conformation for complexation before the binding event took place. A smaller entropy loss should lead to a higher overall association constant due to the additional energy gained as a result of preorganisation. Benzo thiourea **90** bound the guest with an association constant of 740 M^{-1}, whereas pyridyl thiourea **89** bound the same guest with an association constant of 420 M^{-1} in 10% DMSO-d_6/$CDCl_3$. Although the association constant for **90** was larger than that for **89**, evidence for preorganisation of **89** was achieved by examination of the starting chemical shifts of the amide hydrogens H^1 and H^3. Amide hydrogen H^1 had a starting chemical shift of 8.14 ppm, whereas amide hydrogen H^3 had a starting chemical shift of 7.13 ppm. Thus, H^1 showed a chemical shift 1.01 ppm further downfield than H^3, indicating the possibility of hydrogen-bonds between the pyridyl nitrogens and amide hydrogens. Likewise the thiourea hydrogens H^2 were found to be 0.59 ppm further downfield in **89** than H^4 in **90**, again indicating hydrogen-bonding interactions.

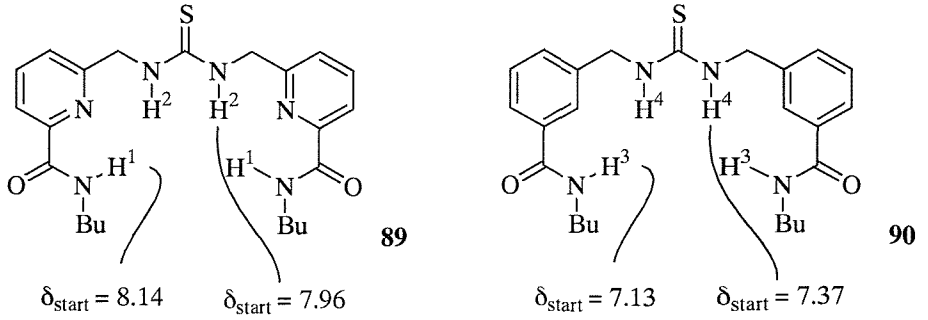

*Figure 2-7 Thioureas **89** and **90***

The stronger association constant observed for benzo thiourea **90** over pyridyl thiourea **89** is consistent with studies by Crabtree who found the nitrogen lone pair in pyridyl amide **88** electrostatically repels negatively charged anions (e.g. carboxylates) more than the C-H in benzo amide **89**.[96] This resulted in the association constant for pyridyl amide **91** being lower than benzo amide **92** for the complexation of acetate in dichloromethane, Figure 2-8.

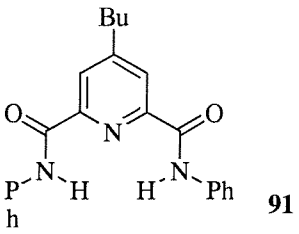

91

$K_a = 525\ M^{-1}$

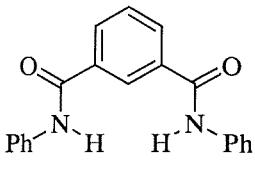

92

$K_a = 1.98 \times 10^4\ M^{-1}$

*Figure 2-8 Binding studies of amides **91** and **92** with acetate in CD_2Cl_2*

2.2 Monothiourea macrocyclic receptor for carboxylates

Building on this work, a macrocyclic analogue was designed, by inserting a rigid linker, **93**. Being a closed structure, macrocycles should present a higher degree of preorganisation and therefore a higher degree of selectivity than U-shaped cleft analogues.

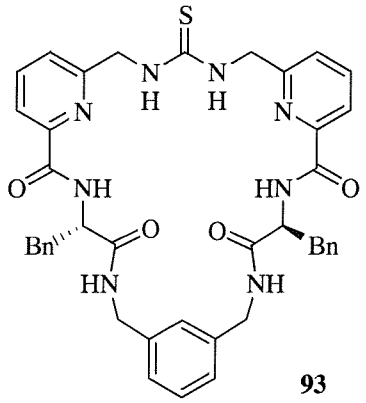

93

Figure **2-9** Design concept of the thiourea macrocyclic receptor

*2.2.1 Synthesis of Thiourea Receptor **93***

The disconnection of the macrocycle illustrates the key intermediates for the synthesis, Scheme 2-1. Initially, the rigid aromatic spacer is coupled to two equivalents of an *N*-protected phenylalanine derivative, which introduces chirality and additional hydrogen bond functionalities to the system. The phenylalanine is then deprotected and coupled with two equivalents of *N*-protected pyridyl carboxylic acid, thus forming the linear, symmetric acyclic precursor bearing the appropriate protecting groups. Ring closure is then achieved by

deprotection of the amine and intramolecular formation of a thiourea subunit to furnish the desired macrocycle. This synthetic strategy allows for alterations to the macrocycle structure to be easily accommodated, for example, different amino acids can be incorporated to provide varying cavity sizes and properties; modification of the aromatic spacer is also a possibility.

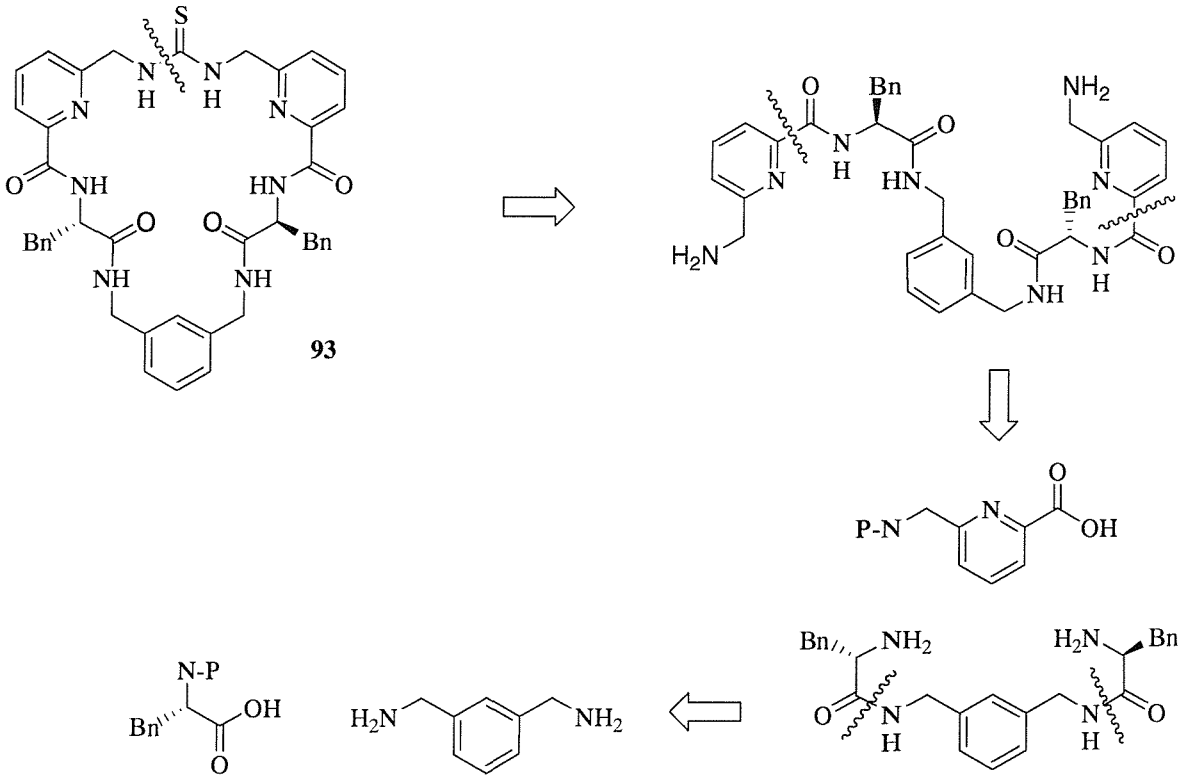

Scheme 2-1 Disconnection approach

The synthesis of carboxylic acid **98** was accomplished by using the procedures by Fife[97] and Scrimin and Tonellato[98], Scheme 2-2. Commercially available pyridine-2,6-dicarboxylic acid was first transformed into the corresponding diacid chloride using thionyl chloride at 0°C. Subsequent reaction with ethanol produced the symmetrical diester **94** in quantitative yield. Diester **94** was partially reduced with $NaBH_4$ to **95**. 6-(1,3-Dioxo-1,3-dihydro-isoindol-2-ylmethyl)-pyridine-2-carboxylic acid ethyl ester **97** was obtained by converting compound **95** to its alkyl halide derivative **93** using neat thionyl chloride and subsequently potassium phtalimide. The ester cleavage to the carboxylic acid **98** was accomplished by modifying a procedure of Olah.[99] The first time the reaction was carried out using NaI. By changing to LiI the reaction yield improved from 35% to 84%, under the same experimental conditions.

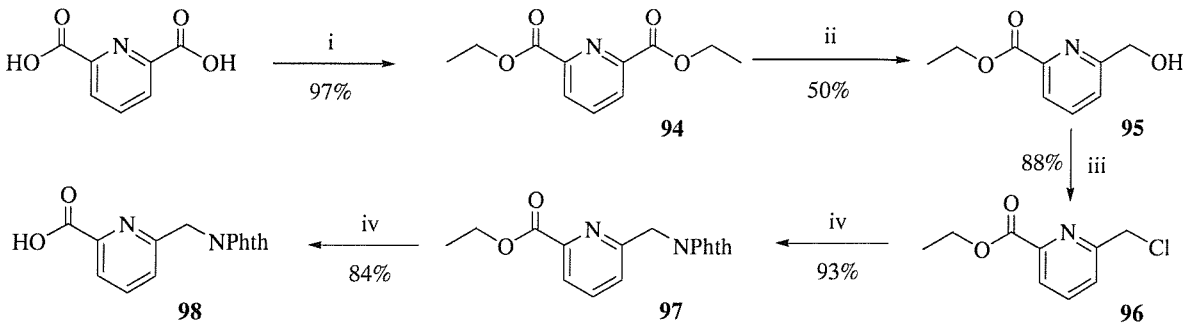

Scheme 2-2 Reagents and conditions: i) $SOCl_2$, EtOH; ii) $NaBH_4$; iii) $SOCl_2$; iv) potassium phtalimide, DMF; iv) Me_3SiCl, LiI

The synthetic strategy proved to be effective and reliable so the preparation of precursor **98** was scaled up to a multigram scale, starting with 100 grams of commercially available dipicolinic acid.

Commercially available *m*-xylylene diamine was coupled to two equivalents of *N*-Boc-L-phenylalanine in presence of HOBt, EDC and DMAP to speed up the coupling process and inhibit possible side reactions.[100] EDC was preferred to DCC as it is water-soluble and can be easily removed. *Bis*amide **99** was obtained in 68% yield. Standard Boc deprotection and basic washing afforded free diamine **100** in 65% yield.

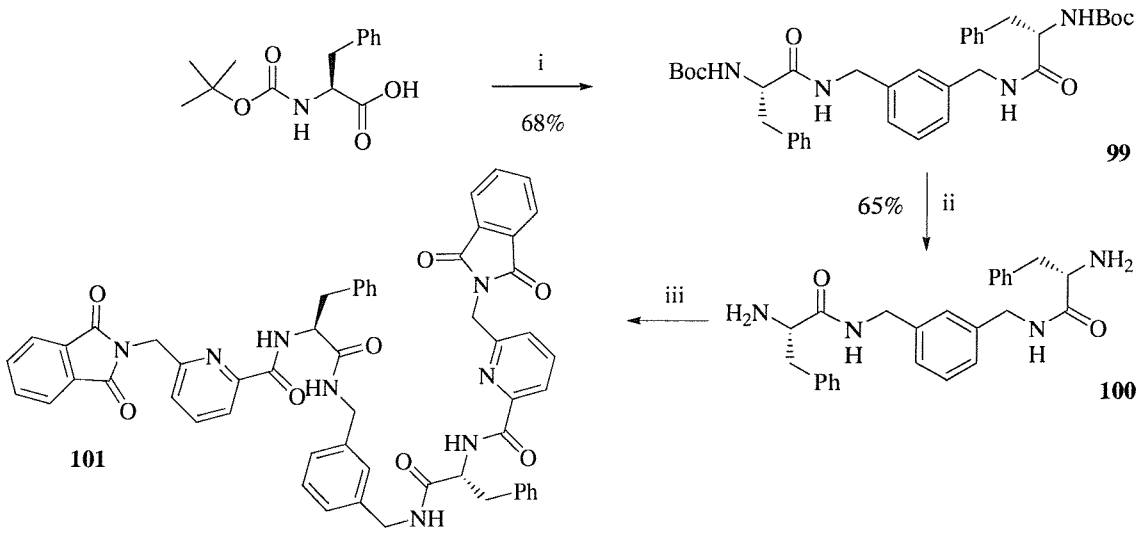

Scheme 2-3 Reagents and conditions: i) m-xylylene diamine, EDC, HOBt, DMAP; ii) TFA/DCM 1:1; NaOH 1M; iii) acid **98**, coupling agents

Final coupling of **98** and **100** to produce the symmetric acyclic precursor **101** proved to be extremely problematic. Initially the coupling reaction was carried out by converting the hydroxy group of pyridyl carboxylic acid **98** to its acyl chloride derivative, **102**, by using $SOCl_2$ in 83% yield. Thionyl chloride is commonly used for the preparation of acyl chlorides since the by-products are gases and the acyl halide can be easily isolated.[101] Addition of

diamine **100** in presence of a stoichiometric amount of DMAP afforded compound **101** after stirring at room temperature few days in 30% crude yield.[102] Purification proved to be complicated by the presence of various side-products. Therefore, alternative strategies were sought and different coupling reagents, normally used in peptide synthesis, were investigated[103]: PyBOP[104], EDC-HOBt in presence of DMAP[100], PyBrop[105] and HATU[106]. The reaction was also carried out in presence of *N-N'*-carbonyldiimidazole, which has been used for peptide synthesis in various cases. In the latter case an alcoholised imidazolide is obtained as an intermediate. The results are summarised in Table 2-2. Excess of coupling reagents and starting material (up to three equivalents) did not result in better yields.

*Table 2-2 Coupling reagents and conditions for product **101** (- no product was isolated)*

Coupling reagent	Temperature	Reaction time	Solvent	Crude yield
i)$SOCl_2$	i) reflux	i) 4 ? 6 hrs	ii) DMF or DCM	30%
ii) DMAP	ii) r. t.	ii) 6 days		
PyBOP, DIPEA	r. t.	1 ? 16 hrs	THF or DCM	4%
PyBrop, DIPEA	r. t.	2 ? 4 hrs	DMF	-
EDC, HOBt, DMAP	r. t.	1 hr ? 2 days	DMF or DCM	30%
Carbonyldiimidazole, Et_3N	r. t.	1 hr ? 3 days	EtOAc or DCM	-
HATU, DIPEA	r. t.	1 hr ? 3 days	DMF	-

Purification of the reaction mixture proved to be very difficult on every occasion. As it was not possible to improve the reaction yield or the purification process, it was decided to change the synthetic strategy. Carboxylic acid **98** was converted to its chloride derivative by reaction with thionyl chloride and coupled with D-phenylalanine methyl ester in presence of DMAP, Scheme 2-4.[107] Cleavage of the methyl ester was accomplished in presence of formic acid and concentrated sulphuric acid[108] to afford acid **103** in 92% yield. The main disadvantage of this reaction is that it did not seem to work as well in a multigram scale. The reaction was also unsuccessfully carried out in presence of LiI and Me_3SiCl.[99]

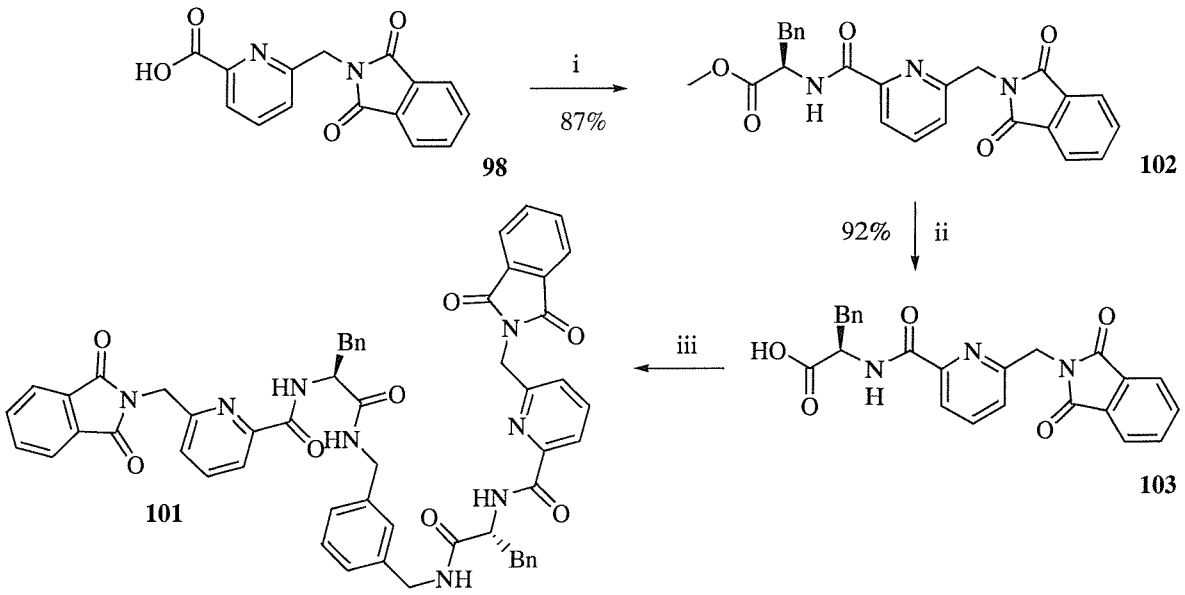

Scheme **2-4** *Reagent and conditions:* i) $SOCl_2$; L-phenylalanine methyl ester, DMAP; ii) HCOOH, H_2SO_4; iii) m-xylylene diamine, coupling agents

Our attempts to couple acid **103** with commercially available *m*-xylylene diamine are summarised in *Table* 2-3. The best coupling reaction was obtained in presence of an excess of EDC and HOBt, an excess of acid **103** and a concentrated solution. It was nevertheless decided to try the reaction using PyBOP because in our hands this proved to be the only coupling reagent that afforded compound **101**, even if in a very poor yield. DIC was also tried in order to see if it was more effective than EDC. Even if the yield could not be improved in this new strategy, in all cases product **101** could be obtained pure by column chromatography.

Table *2-3 Coupling reagents and conditions for product **101** (- no product was isolated)*

Coupling reagent	Temperature	Reaction time	Solvent	Reaction yield
EDC, HOBt, DMAP	r. t.	16 hrs ? 2 days	DCM	28%
DIC, HOBt, DMAP	r. t.	3 days	DMF	22%
PyBOP, DIPEA	r. t.	2 days	DMF	-
PyBOP, HOBt, DIPEA	r. t.	2 ? 5 days	DMF	-
$(CN)_3F_3$, BSA, SKA	-15°C r. t. 60°C	2 hrs	CH_3CN	-
PPh_3, $BrCCl_3$, DABCO	reflux	5 hrs	THF	-

Parallel to the standard coupling agents, alternative strategies were sought. Fmoc and Boc protected amino acid fluorides have been used as a new class of rapid-acting acylating agents.[109] Following Carpino's procedure, acid **103** was converted into its fluoride derivative, **104**, by treatment with cyanuric fluoride.[110] Unfortunately the desired product was not recovered form the reaction mixture. The ES^+ mass spectra showed the presence of a partial coupling of **103** and m-xylylene diamine. Liu obtained good coupling yields by heating an aromatic acid, an appropriate diamine, triphenylphosphine, bromotrichloromethane and 1,4-diazabicyclo-[2.2.2]octane for few hours.[111] A particularly mild procedure, acyl chlorides are produced without the formation of any acidic by-products.[112] The coupling procedure was first attempted on a simple system, Scheme 2-5.

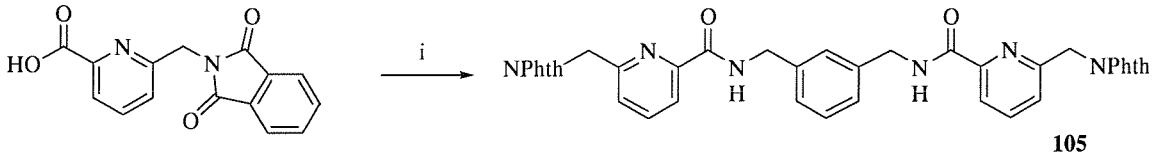

105

Scheme 2-5 Reagents and conditions : i) m-xylylene diamine, PPh_3, $BrCCl_3$, DABCO

The reaction seemed to be promising. Although ^1H NMR showed a marked contamination of Ph_3PO, the MS spectrum showed an intense peak corresponding to the molecular ion of **105**. Therefore it was decided to apply the same reaction conditions to acid **103**, but only partial or no coupling between acid **103** and m-xylylene diamine were noted. The reaction was repeated in presence of an excess of starting materials, but again it failed to give tetraamide **101**.
Thus, despite a large amount of efforts, it was not possible to overcome the problems encountered during the synthesis and the project was abandoned.

2.3 Bisthiourea Receptor for Dicarboxylates

A bisthiourea macrocyclic version of tweezer **88** was also envisaged. As the detection of glutamic acid in biological systems is of considerable interest to biologists, the receptor was specifically designed to bind to *N*-Boc-glutamate through eight hydrogen bonds as shown in Figure 2-10. The thiourea moiety was chosen to provide the primary interaction with the carboxylate guest. The thiourea and amide hydrogens were also intended to act as hydrogen-bonding donors to the *syn* and *anti* lone pairs of the carboxylate guest oxygens. To encourage chiral recognition between the tweezer receptor and carboxylate guest sterically demanding chiral groups were incorporated on the receptor to interact with the amino acid side chain. In addition, receptor **106** was designed to include pyridine moieties to help preorganise the host

via intramolecular hydrogen bonds from the pyridine nitrogen to the thiourea and amide hydrogens.

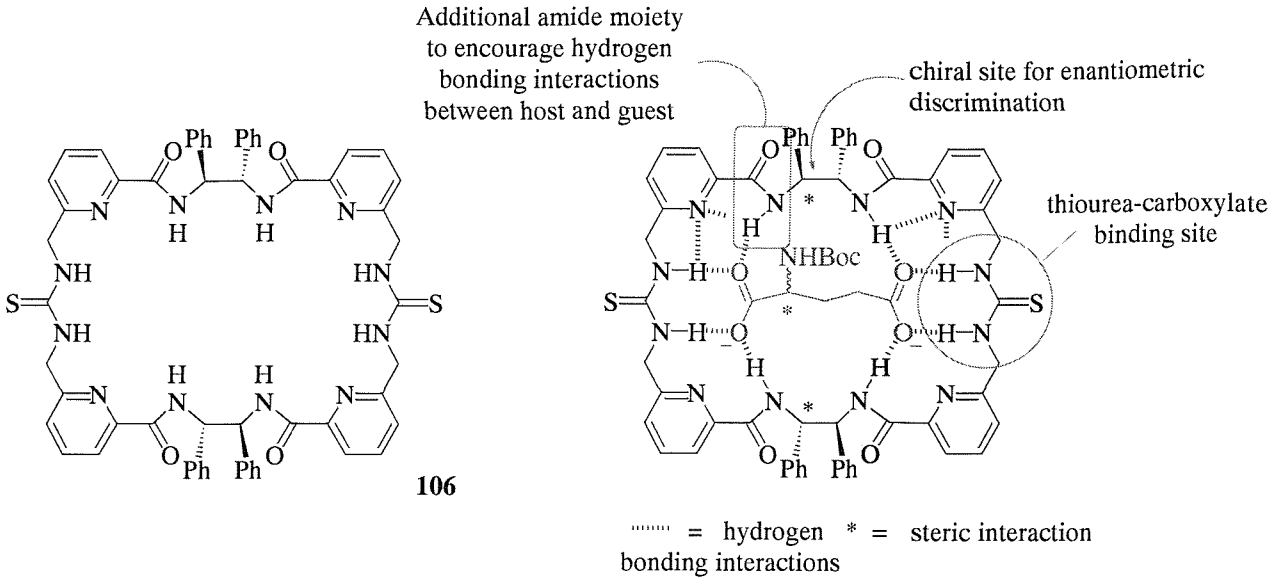

Figure 2-10 Design concept of macrocyclic receptor for glutamate

Initial CPK modelling by G. Kyne of the complex formed between **106** and glutarate showed a tight fit between host and guest. When glutarate was replaced with glutamate the chiral centres in the host and guest were aligned, creating steric interactions, which should favour high levels of enantioselective binding.[92]

Receptor **106** was synthesised and some preliminary studies were undertaken. Binding studies in DMSO suggested that the host bound to N-Boc-Glu not only strongly, but also with some enantioselectivity of the substrate. The data, however, were unreliable. No binding was observed in deuterated chloroform.[92] It is generally known that binding interactions between polar functionalities will lead to strong complexation in a non-polar solvent, such as $CDCl_3$, and weak complexation in more competitive solvents, such as DMSO, with numerous examples present in the literature. Receptor **106** seemed to have anomalous solvent-dependent behaviour. It was therefore decided to re-synthesise the host in order to fully investigate the system.

Some of the results presented here have been published.[113]

*2.3.1 Synthesis of Bisthiourea Receptor **106***

The route followed to produce macrocycle **106** was essentially the same as that developed by G. M. Kyne. However improvements were made in terms of the synthesis strategy and the

yields of the reactions and these alterations are discussed where appropriate. The synthetic pathway is presented as different sections corresponding to the components of the macrocycle.

2.3.1.1 Synthesis of (1*S*,2*S*)-1,2-diphenylethylene Diamine **109**

The synthesis of the chiral diamine was obtained by using the procedure of Corey, Scheme 2-6.[114] Commercially available benzil was converted to the corresponding spirocyclohexane imidazole **107** in nearly quantitative yield. Birch reduction of **107** to **108** was stereospecific and afforded the *trans* product. Resolution was accomplished by using tartaric acid for salt formation and separation of the diasteroisomers by a series of recrystallisations in hot water-ethanol solution. ^{1}H NMR of the tartrate salt **109** showed the presence of only one diastereomer. Its chiral purity as the tartrate salt and as the free diamine was checked by measuring the optical rotation and comparing it to the literature values.

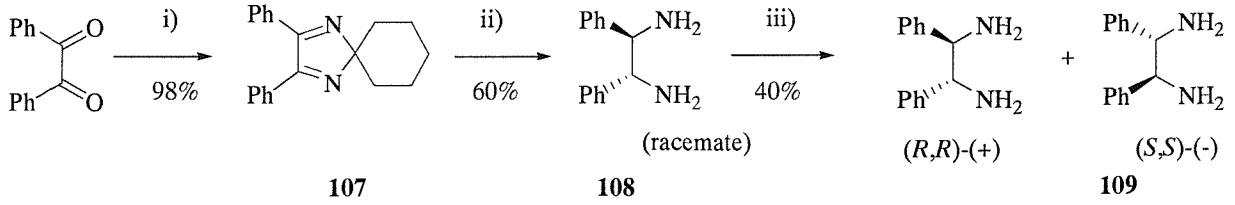

Scheme 2-6 Reagents and conditions: i) NH_4OAc, AcOH, cyclohexanone; ii) Li, THF-NH_3, EtOH, HCl; iii) (L)-(+)-tartaric acid

The preparation of the chiral diamine was carried out on a multigram scale, starting form 90 grams of commercially available benzil.

2.3.1.2 Synthesis of Bisthiourea **106**

Acid **95** was activated with the coupling reagent diphenylchlorophosphate. The mixed anhydride was then coupled with (*S*,*S*)-1,2-diphenylethylene diamine as the tartrate salt. In order to avoid the undesirable process of extracting the chiral diamine from its tartrate salt, a two-phase (water/dichloromethane) reaction was carried out. The diamine salt was basified in water in the presence of potassium carbonate and the aqueous solution was added directly to the mixed anhydride in dichloromethane. Diphthalimide **110** was deprotected using hydrazine hydrate to furnish diamine **111** in 84% yield, Scheme 2-7.

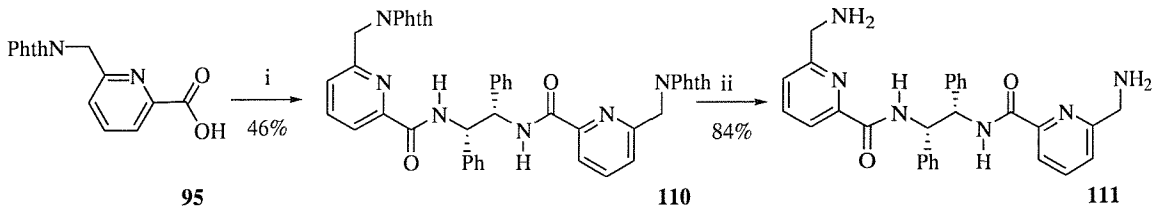

Scheme 2-7 Reagents and conditions: i) diphenylchlorophosphate, DCM, (*S,S*)-diphenylethylene diamine, H_2O, K_2CO_3; ii) NH_2NH_2

After one equivalent of amine **111** and one equivalent of bisthioisocyanate **112** were added to a solution of CH_2Cl_2 and catalytic DMAP *via* syringe pump over three hours, bisthiourea **106** was formed in 20% yield, Scheme 2-8.

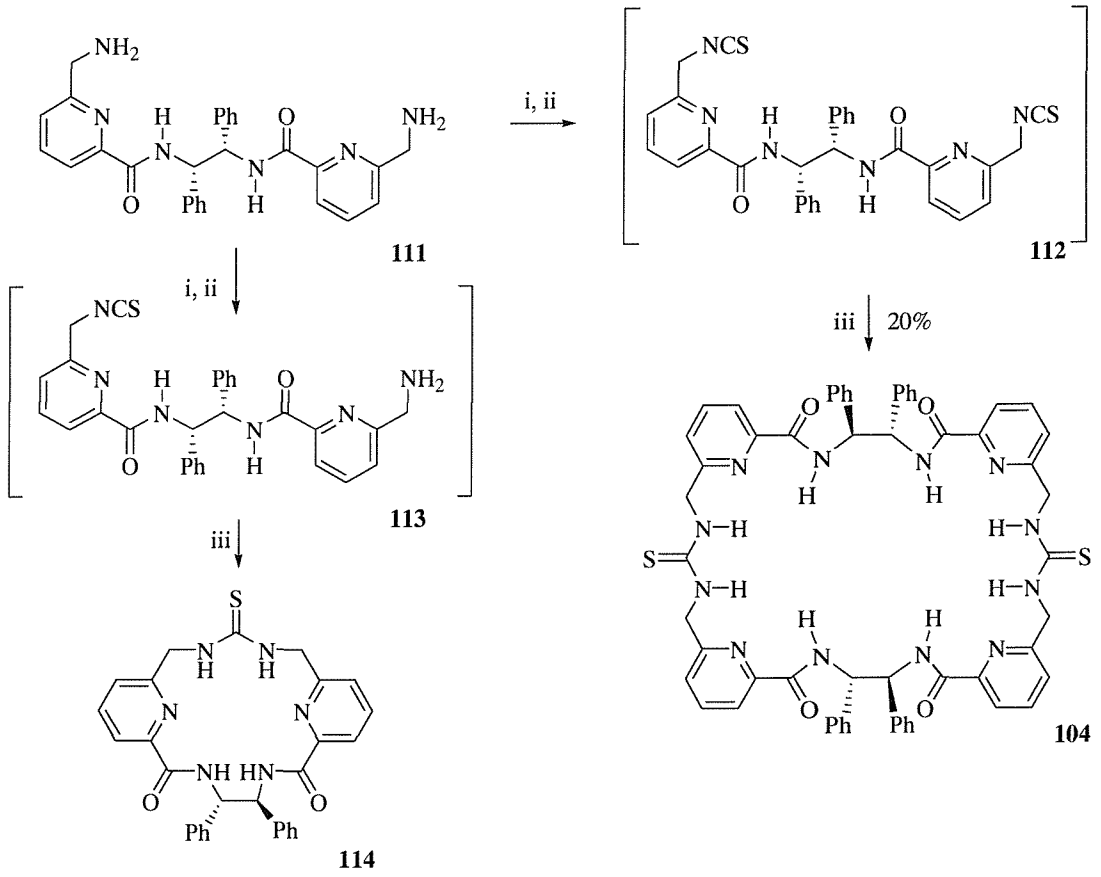

Scheme 2-8 Reagents and conditions: i) CS_2, -10°C; ii) DCC, DMAP, -10°C then warm to r. t.; iii) slow addition of 1 equivalent of **111** and 1 equivalent of **112** to a solution of dry CH_2Cl_2/DMAP at r. t. over 3 hours

Despite lowering the temperature to –10°C, extending the reaction time between carbon disulfide and diamine **111** before adding DCC and the use of slow addition / high dilution techniques it was not possible to avoid the formation of various by-products. In particular the formation of a monothiourea macrocycle **114** was noted, which was probably formed via an intramolecular trapping of the monoisthiocyanate **113** with the second amine. A crystal structure of the monothiourea macrocycle has just been acquired in the group and its binding

properties are being investigated. This methodology gave access to enough material to allow the binding properties to be studied.

In conclusion, macrocycle **106** was synthesised on numerous occasions to afford several hundred milligram quantities of receptor. Binding studies with various guests in different solvents were carried out using both traditional NMR techniques and isothermal calorimetry.

*2.3.2 Conformational Properties of Bisthiourea **106***

To probe the origin of the anomalous behaviour of the receptor, it was decided to investigate the conformation of the receptor in solution.

Bisthiourea **106** was found to be soluble in chloroform, however the peaks in the proton spectra were found to be broad at room temperature. Resolution was not improved at higher temperatures. Changing to deuterated dicholoromethane did not enhance the appearance of the ^{1}H NMR spectrum. A well resolved spectrum was obtained at -40°C in chloroform. The spectrum showed a far more complex structure than would be expected based on the apparently fourfold D_2 symmetry of the host and seemed to indicate a twofold C_2 symmetry. A well resolved spectrum was also obtained by dissolving receptor **106** in DMSO-d_6 or CD_3CN at room temperature. The spectra, however, appeared to be consistent with the expected fourfold D_2 symmetry. The spectra are shown in Figure 2-11.

a)

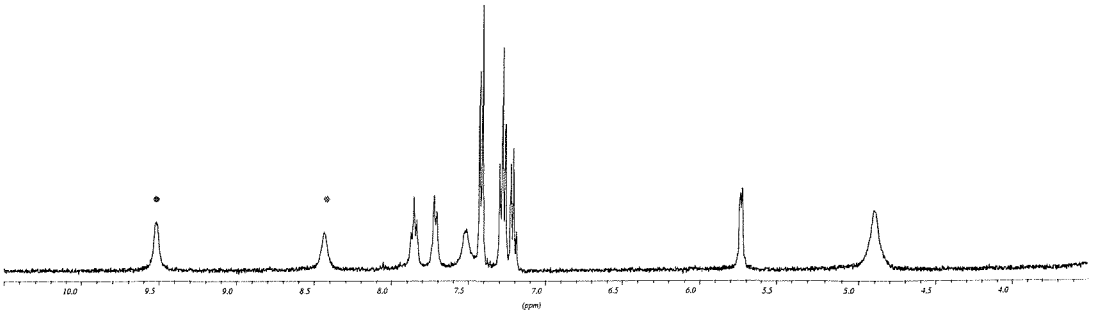

b)

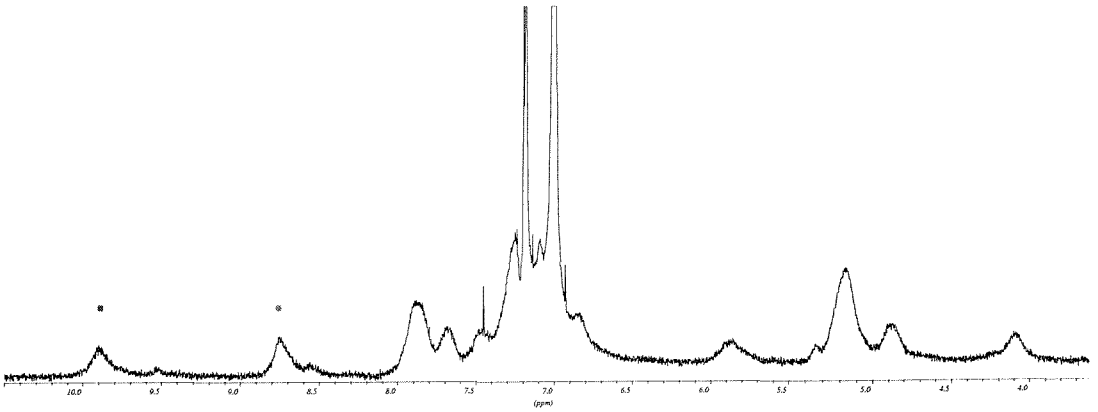

c)

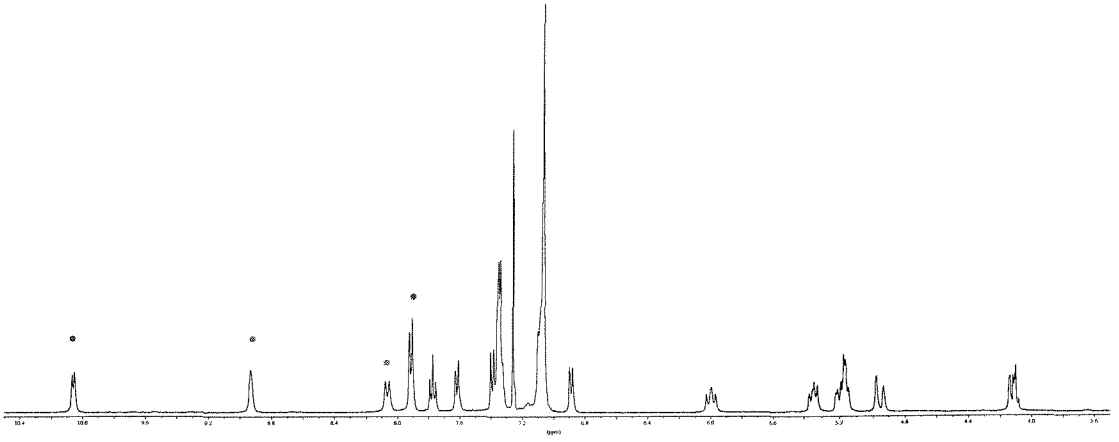

*Figure 2-11 NMR spectrum of macrocycle **106** a) in DMSO at r. t.; b) in $CDCl_3$ at r. t.; c) in $CDCl_3$ at -40 °C (* indicates the thiourea protons, * shows the amide protons)*

Detailed 2D NMR studies were carried out to probe the solution conformation of receptor **106**. COSY and NOESY[115] spectra were run in $CDCl_3$ at -40°C, which allowed for full assignment of all the ^1H NMR signals. These experiments showed that the thiourea NH

protons were not equivalent, with signals at δ=8.96 and 8.08 ppm. Even the amide NH protons showed two different signals, δ=10.10 and 7.88 ppm.

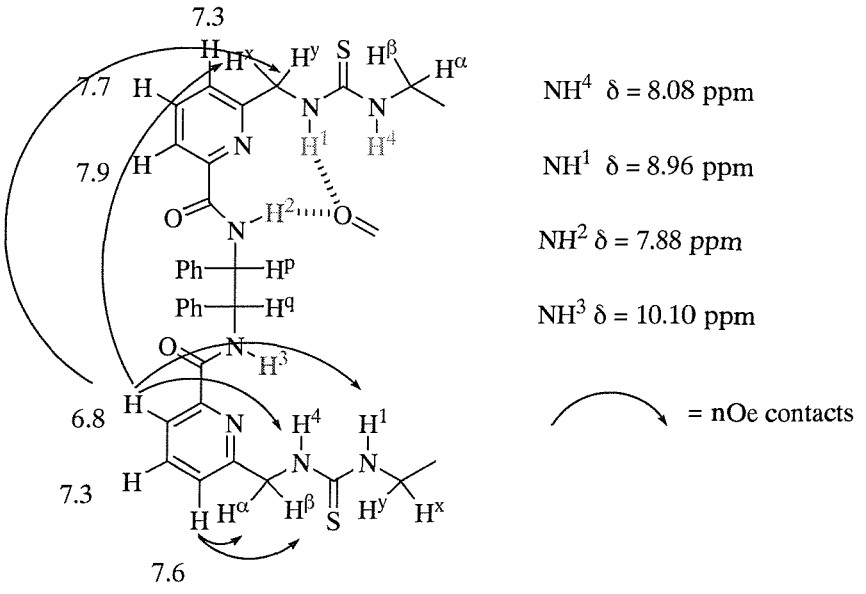

Figure 2-12 Graphic interpretation of n.O.e. results

A possible folded conformation of **106** was suggested, involving hydrogen bonding between a thiourea NH and an amide proton with a carbonyl group in the molecule. Indeed, as these hydrogens are sharing their electrons with two electronegative elements, as is the case with hydrogen bonding, they become deshielded and come into resonance at a lower field. The conformation of the macrocycle in solution in $CDCl_3$ was established using torsion angle dynamics with n.O.e. contacts and scalar coupling constant constraints.[116] The NMR studies showed that the receptor, dissolved in chloroform, adopts a tightly wrapped conformation stabilised by a number of intramolecular hydrogen bonds, in particular those from an amide carbonyl oxygen atom to the thiourea NH and an adjacent amide NH proton, Figure 2-13. Furthermore the model showed the involvement of the pyridyl nitrogen in intramolecular hydrogen bonding with one thiourea NH proton and one amide proton.

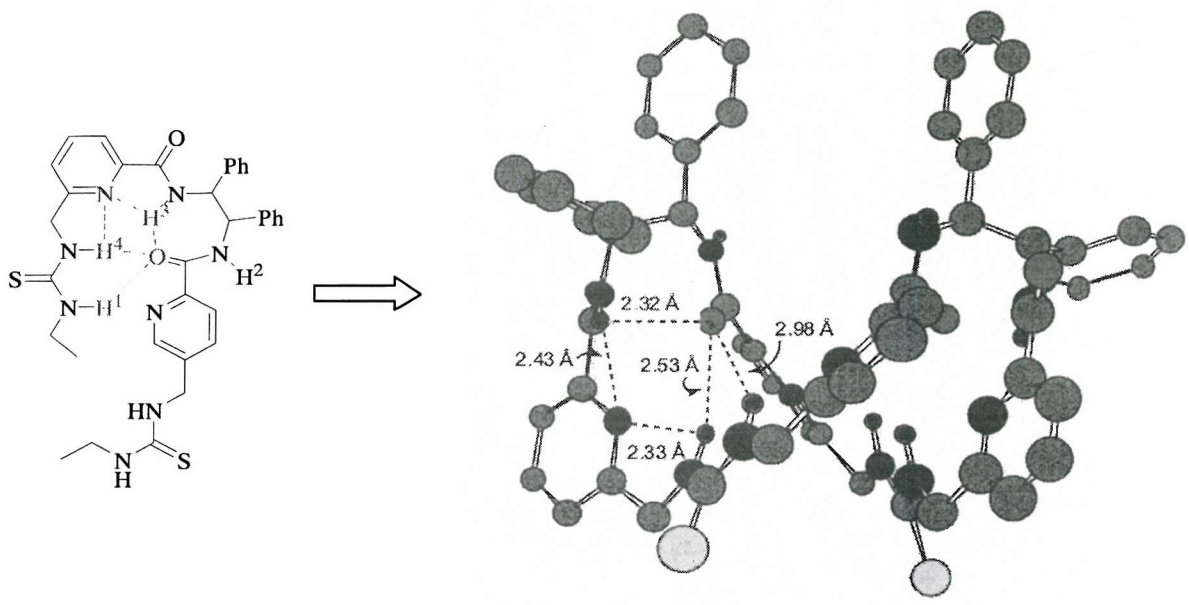

*Figure 2-13 Conformation of macrocycle **106** in $CDCl_3$ as determined by ^1H NMR spectroscopy showing intramolecular H-bonding distances*

This suggests a possible role for the pyridine in preorganising the receptor. These hydrogen bonding motifs have been already observed in the crystal structure of tweezer receptor **115**, Figure 2-14.[95]

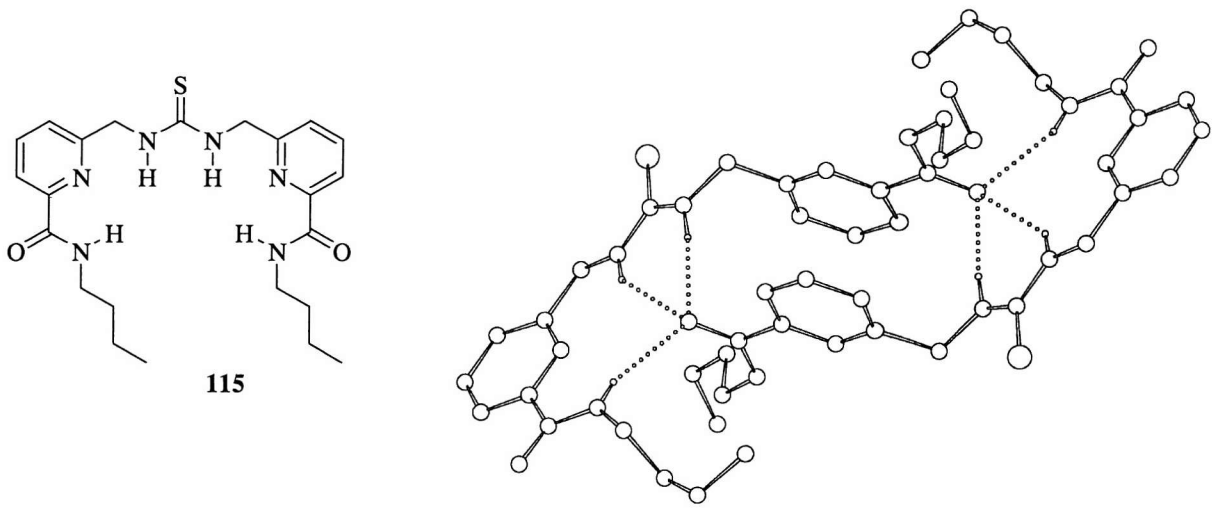

115

*Figure 2-14 Tweezer receptor **115** and its crystal structure*

The achiral pyridyl receptor formed a dimer in the solid-state, with one amide carbonyl forming a triple hydrogen bond motif with both the thiourea NH protons and one amide proton of the other monomer unit. The molecule adopted a folded conformation, with three NH groups pointing inwards to an essentially planar cavity into which the carbonyl of the

second molecule can dock. Weak hydrogen bonding between the pyridyl nitrogen and the thiourea proton and amide NH proved to be positively involved in the preorganisation of the tweezer receptor **115**.

The more polar solvents, such as DMSO and CD_3CN, can solvate the hydrogen bonding functionalities of macrocycle **106** and lead to a less rigidly constrained molecule and therefore give rise to the ^1H NMR spectra which reflects the fourfold D_2 symmetry of the molecule.

As outlined previously, at room temperature in $CDCl_3$ the ^1H NMR spectrum is broad, so it was concluded that the macrocycle is probably in slow chemical exchange between a twisted conformation found at –40°C and a symmetric conformation found in DMSO-d_6.

Unfortunately, albeit despite numerous efforts, it was not possible to grow crystals of the macrocycle in any solvent or solvent mixtures to obtain an X ray structure.

*2.3.3 Binding Studies of Receptor **106***

Binding studies with the chiral bisthiourea receptor **106** and a range of amino acid derivatives, as their tetrabutylammonium salts, were carried out in different solvents, by NMR and isothermal calorimetry, using the procedure outlined in Chapter Five §5.6 and §5.7, Figure 2-15.

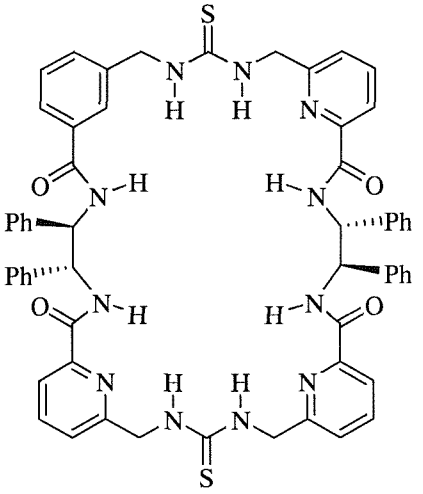

104

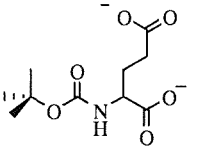

N-Boc-L-Glu **116**
N-Boc-D-Glu **117**

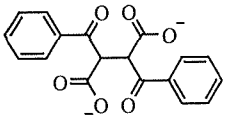

Dibenzoyl-L-tartrate **120**
Dibenzoyl-D-tartrate **121**

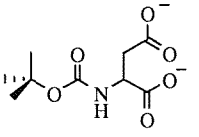

N-Boc-L-Asp **118**
N-Boc-D-Asp **119**

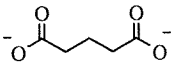

Glutarate **122**

*Figure 2-15 Receptor **106** and substrates*

Particular attention was paid to estimating the selectivity and enantioselectivity of the receptor towards the guests. *N*-Boc-aspartate was investigated in order to probe the possible influence of the chain length between the two carboxylate groups on the binding properties of

the host. Tartrates were also considered as a means of studying the behaviour of the receptor towards different classes of substrates.

2.3.3.1 Binding in Chloroform

^{1}H NMR spectra of 1:1 mixtures of both enantiomers of *N*-Boc-glutamate with macrocycle **106** were performed. Addition of either enantiomer of the glutamate salt did not lead to any discernible change in the ^{1}H NMR spectrum of the macrocycle either at room temperature or at -40°C. No change was observed even after warming the solution for several days in a tightly sealed NMR tube. A 1:1 sample of macrocycle **106** and *N*-Boc-L-glutamate salt was also dissolved in CD_3CN to allow the formation of a complex. The solvent was then removed and the sample re-dissolved in $CDCl_3$. The resulting ^{1}H NMR spectrum again showed no change compared to the parent macrocycle. It was therefore concluded that receptor **106** does not bind glutamate in the apolar solvent. It was also concluded that it was unlikely to be due to slow binding kinetics. The reason lies in the tightly wrapped conformation adopted by the receptor in chloroform, Figure 2-13. Similar results were obtained when 1:1 mixtures of either enantiomer of *N*-Boc-aspartate were considered. Clearly the energy required to reorganise the host into a suitable binding conformation, i.e. to break the intramolecular hydrogen bonds, is not compensated for by the host–guest binding interactions that would be established.

2.3.3.2 Binding in Acetonitrile

*N-Boc-L,D-Glutamate **116, 117***

Addition of *N*-Boc-L-glutamate tetrabutylammonium salt **116** to a solution of **106** in CD_3CN at room temperature led to a dramatic change in the ^{1}H NMR spectrum of the macrocycle. In particular, significant downfield shifts of the thiourea NH ($\Delta\delta_{max}$ = 1.43 ppm), the amide NH ($\Delta\delta_{max}$ = 1.06 ppm) and the benzylic CH signals ($\Delta\delta_{max}$ = 0.59 ppm) were noted after the addition of one equivalent of guest. This is consistent with the formation of strong hydrogen bonds between the host and the substrate. No further shift was registered upon the addition of more guest, suggesting that saturation was reached after the addition of the first equivalent of *N*-Boc-L-glutamate. The binding data could be readily fitted to a 1:1 isotherm and gave a surprisingly high binding constant of 1.5 x 10^5 M^{-1}.[117]

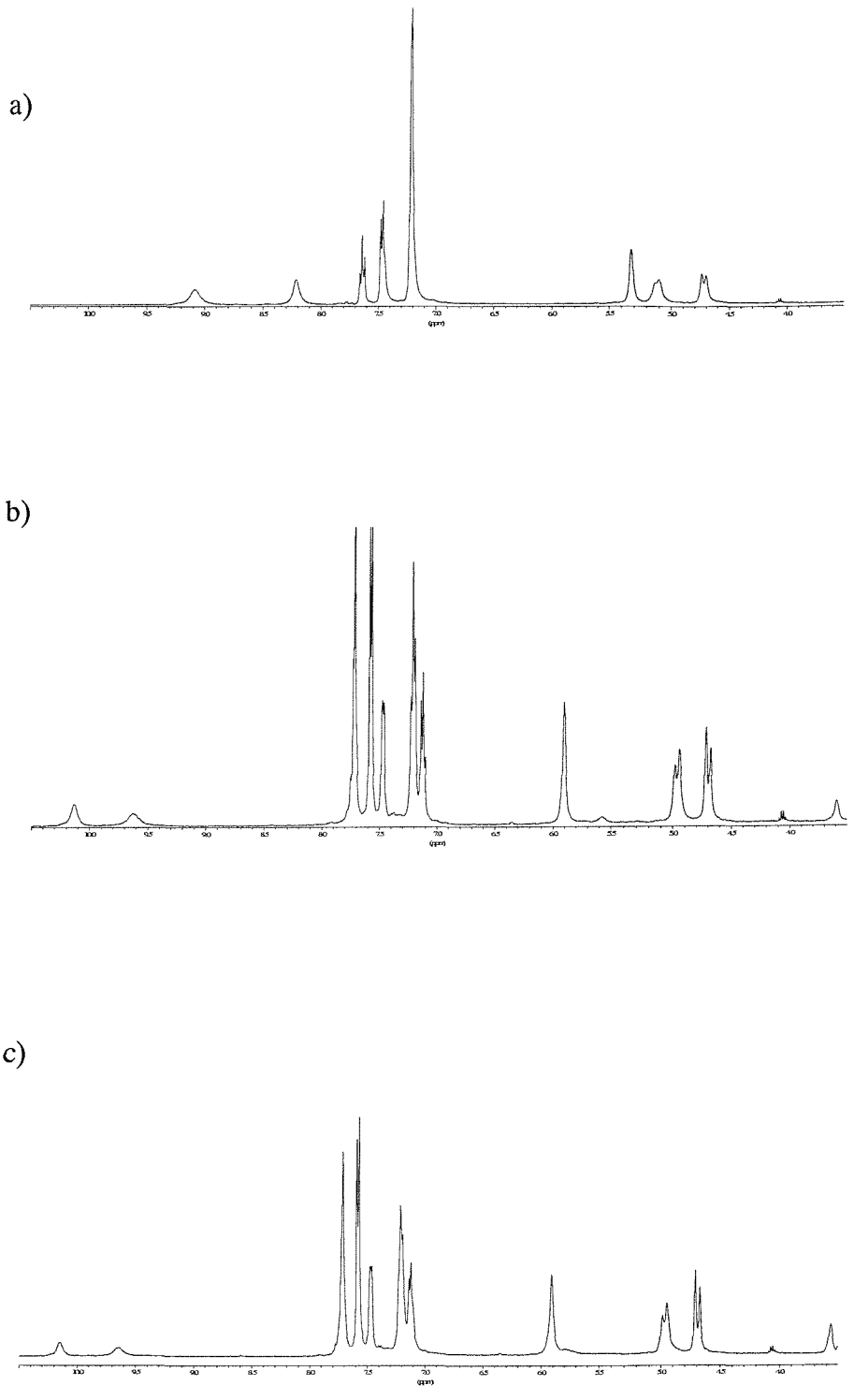

*Figure 2-16 ^{1}H NMR spectra of **106** and N-Boc-L-Glu **116**: a) neat host; b) after addition of 1 equivalent of guest; c) after addition of 2 equivalents of guest*

Addition of the *N*-Boc-D-glutamate tetrabutylammonium salt **117** also led to significant downfield shifts of the thiourea NH ($\Delta\delta_{max}$ = 1.27 ppm), amide NH ($\Delta\delta_{max}$ = 0.95 ppm) and

CH benzylic protons ($\Delta\delta_{max}$ = 0.53 ppm) of the receptor. From the ^{1}H NMR spectra, it seemed that saturation was reached after the addition of two equivalents of guest, Figure 2-17.

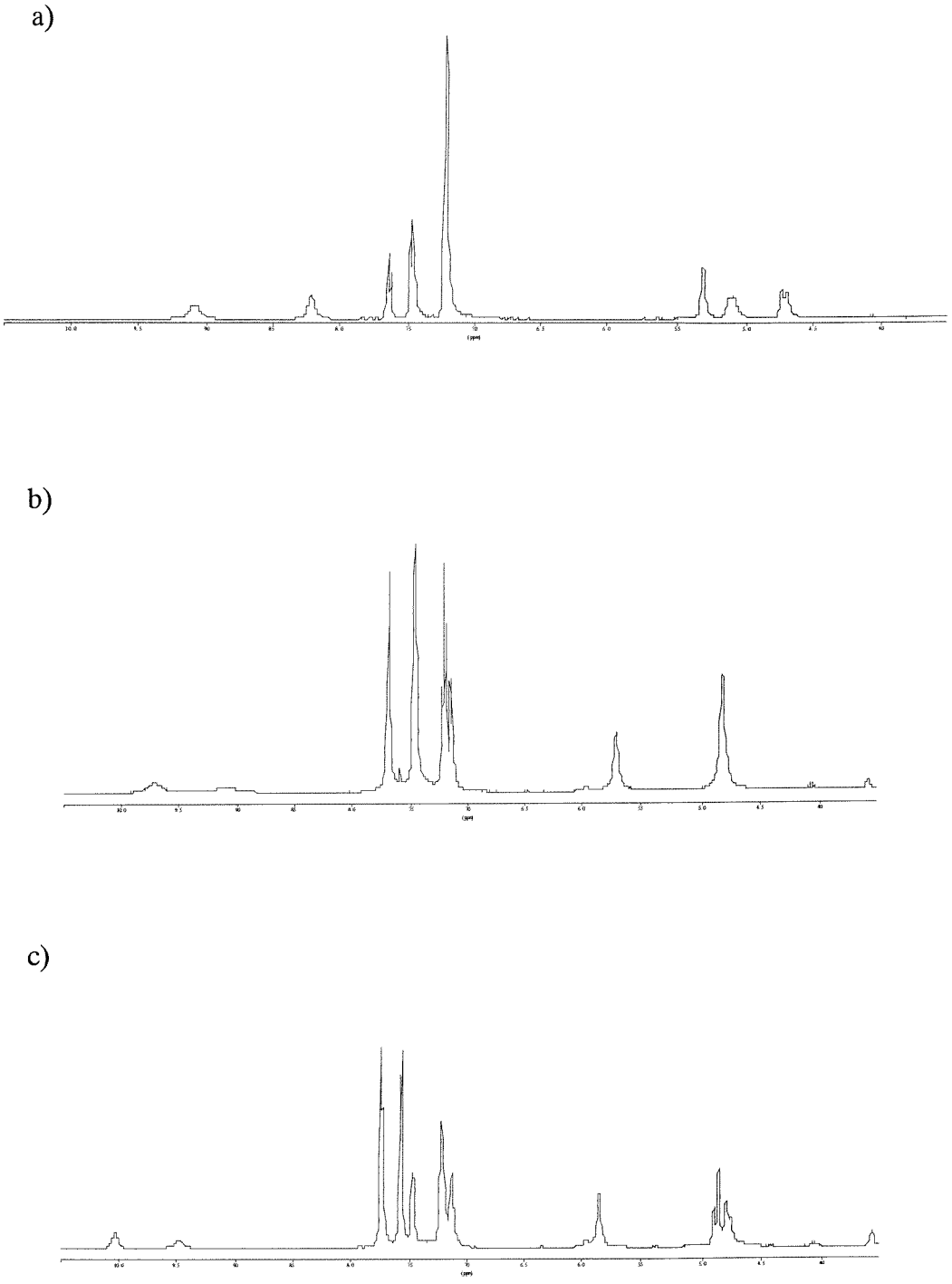

Figure 2-17 ^{1}H NMR spectra of **106** and N-Boc-D-Glu **117**: a) neat host; b) after addition of 1 equivalent of guest; c) after addition of 2 equivalents of guest

Indeed, the binding data could not be fitted to a 1:1 stoichiometry, but instead could be fitted to a 1:2 (host:guest) isotherm and yielded a $K_a^{1:2}$ of 2.2 x 10^4 M^{-1}.

It was evident, through comparison of the ^1H NMR titration curves, that saturation is rapidly reached after the addition of approximately one equivalent of *N*-Boc-L-glutamate salt, whereas saturation is reached only after the addition of two equivalents of the *N*-Boc-D-glutamate salt, Figure 2-18.

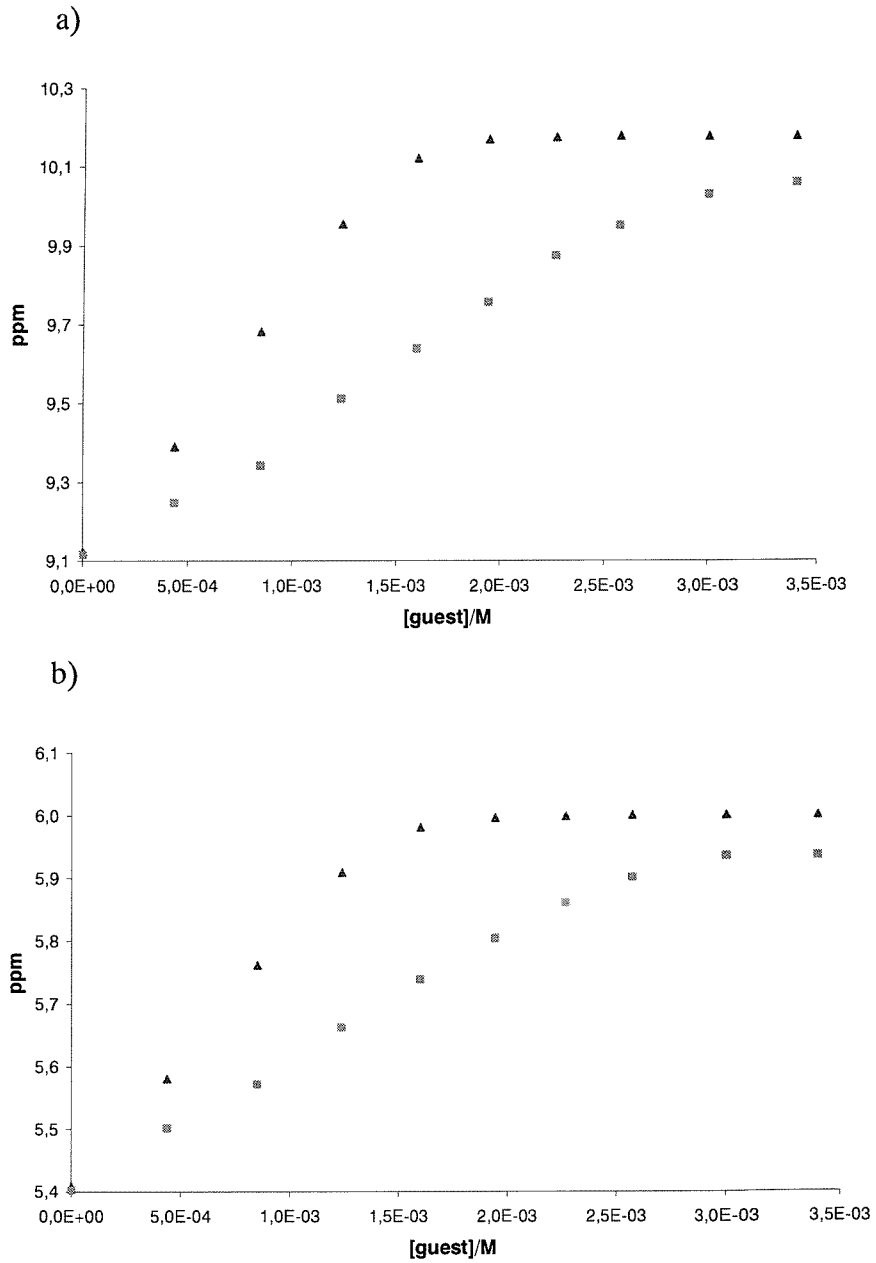

Figure 2-18Binding titration curves for macrocycle ***106*** *showing the shift of a) the amide and b) the benzylic CH protons on the addition of N-Boc-L-glutamate (?) and N-Boc-D-glutamate ( ). The 1:1 [host]:[guest] is reached when [guest] = 1.5 mM*

Furthermore, the relatively smooth titration curve obtained with *N*-Boc-D-glutamate and the lack of a clear transition after the addition of only one equivalent of guest seems to suggest the presence of a positive cooperativity effect: the binding of the second guest molecule is stronger than the binding of the first. Such positive cooperativity would imply that the receptor tends to saturate both binding sites simultaneously, that is, the 1:1 complex is only present in very small amounts relative to the uncomplexed receptor or the 1:2 complex.

The suspected binding stoichiometry, as inferred by the ^{1}H NMR titration curves, was further confirmed by Job plots.[118] The method of continuous variations, or Job plot, is widely used to determine the stoichiometry of a host-guest complex. It involves the preparation of a series of solutions containing both the host and the guest in varying proportions so that a complete range of mole ratios is sampled:

$$0 > \frac{[H]_0}{([H]_0 + [G]_0)} > 1$$

where the total concentration $[H]_0 + [G]_0$ is constant for each solution. The position of the maximum indicates the stoichiometry of the complex.

Job plot of Boc-L-glutamate with **106** produced a maximum at 0.5, showing a 1:1 binding equilibrium, as shown below in Figure 2-19.

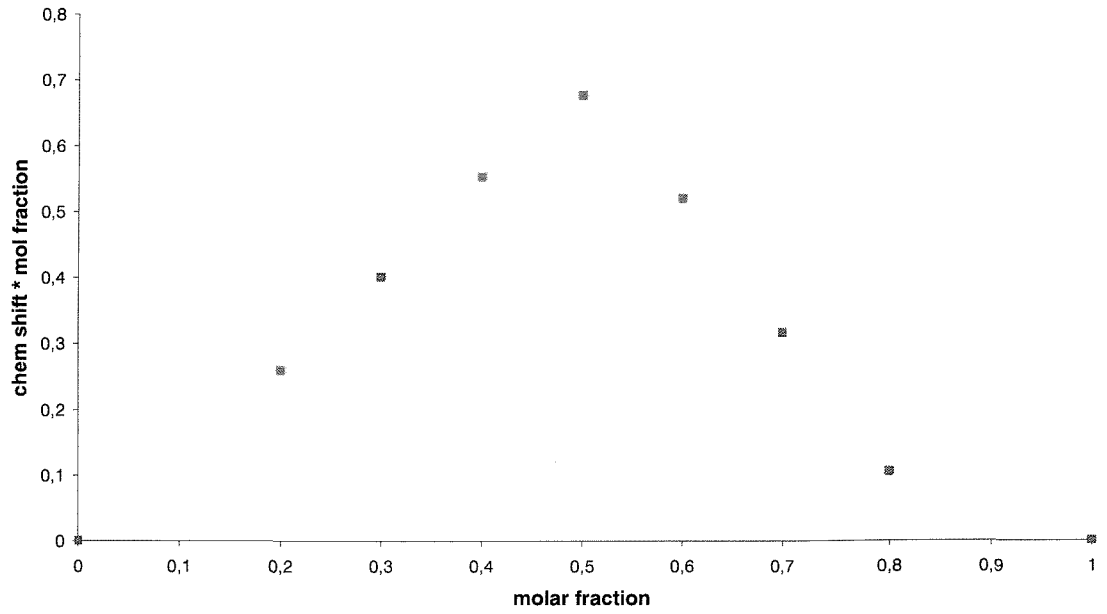

*Figure 2-19 Job plot of Boc-L-glutamate and receptor **106***

Job plot of Boc-D-glutamate with **106**, instead, produced a maximum at 0.3. Such a curve is characteristic of a 1:2 (host:guest) binding equilibrium, Figure 2-20.

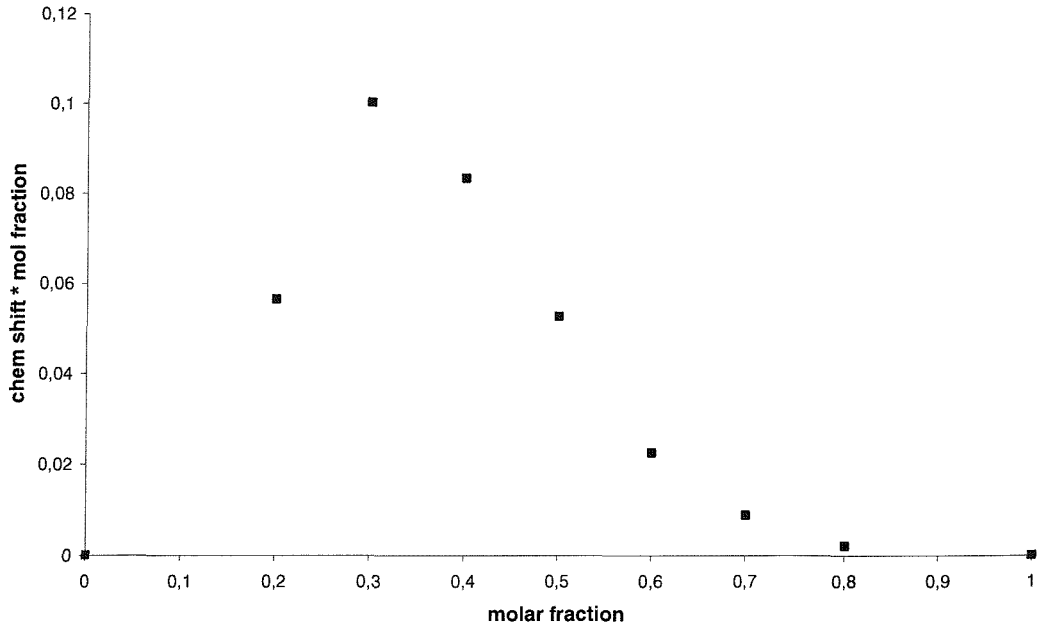

*Figure 2-20 Job plot of Boc-D-glutamate and receptor **106***

It is therefore concluded that dipyridyl bisthiourea receptor **106** is highly enantioselective, binding the two enantiomers in two completely different ways. While complexing *N*-Boc-L-glutamate in a simple 1:1 binding mode, the same cavity is unable to host *N*-Boc-D-glutamate in the same way. The two carboxylate guests, instead, may bind on opposite faces and at opposite ends of the macrocycle to minimise the electrostatic repulsion between them, giving rise to a 1:2 (host:guest) binding stoichiometry, Figure 2-21.

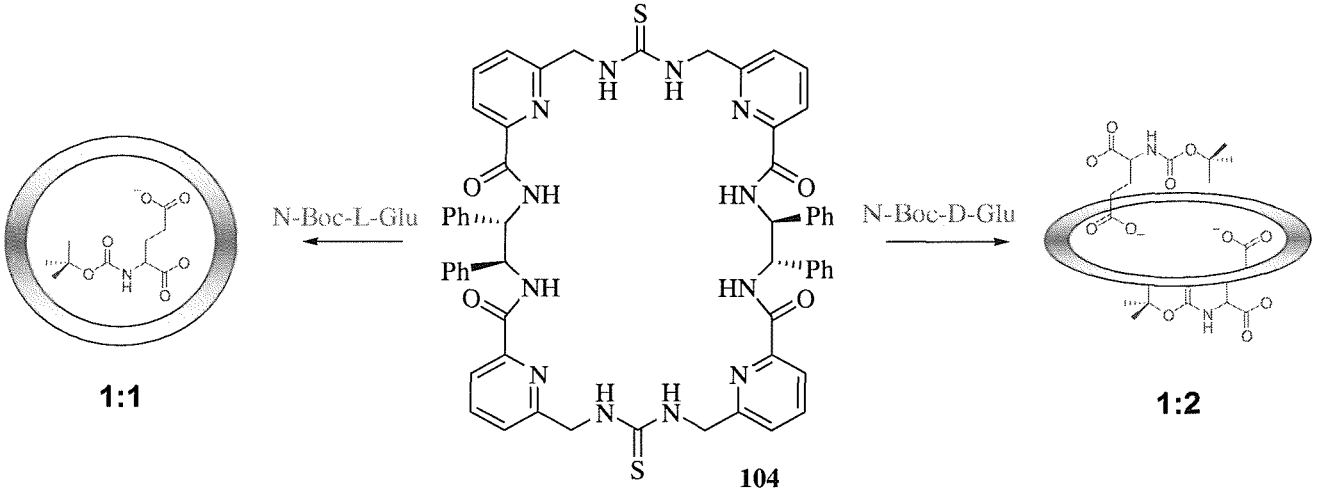

*Figure 2-21 Two modes of binding for the L and D enantiomer of receptor **106***

Isothermal calorimetry (ITC) was employed to study the association and the thermodynamic quantities characterising the complexation process of receptor **106** and *N*-Boc-L,D-glutamate.

ITC allows the measure of association strength, stoichiometry of binding, as well as thermodynamic parameters of association from a single experiment. This method has also a great advantage over NMR: the ability to successfully evaluate the presence of convoluted multiple binding equilibria. NMR titrations, indeed, are limited in the evaluation of multiple binding equilibria. When the first equivalent of guest is added to the host solution, the protons involved in the complexation process display a shift. Complexation of a second equivalent, however, produces little change as the chemical shifts in singly and doubly bound complexes are similar, making distinguishing multiple equilibria difficult. With calorimetry, instead, as long as the two complexation events have different association enthalpies they can be readily observed. Calorimetry, therefore, is able to determine not only the association strength of the host-guest complex, but also the number of bound molecules and the thermodynamics of all the association processes that may be simultaneously present.

Calibration of the VP-ITC equipment was checked prior to use. In particular the y-axis calibration check was performed, by using the default y-axis calibration parameters given by MicroCal. Y-axis calibration is achieved by dissipating a known power through a resistive heater located on the cell wall, and by then adjusting the software coefficient for DP. The reported error in deflection was less than 1%, in agreement with the expected value for a good calibration.[119] Once the calibration check was performed, considerable time and effort were spent in obtaining reliable and reproducible results by performing simple dilution experiments, where the guest was added to neat solvent. Figure 2-22 shows the results of a calorimetric titration of receptor **106** and the tetrabutylammonium salt of *N*-Boc-L-glutamate. Also shown is the non-linear least squares fit of the curve.[120] The binding isotherm displayed in Figure 2-22 is characteristic of a strong, exothermic 1:1 complex. The equimolar stoichiometry is evident from the inflection point in the curve at one equivalent.

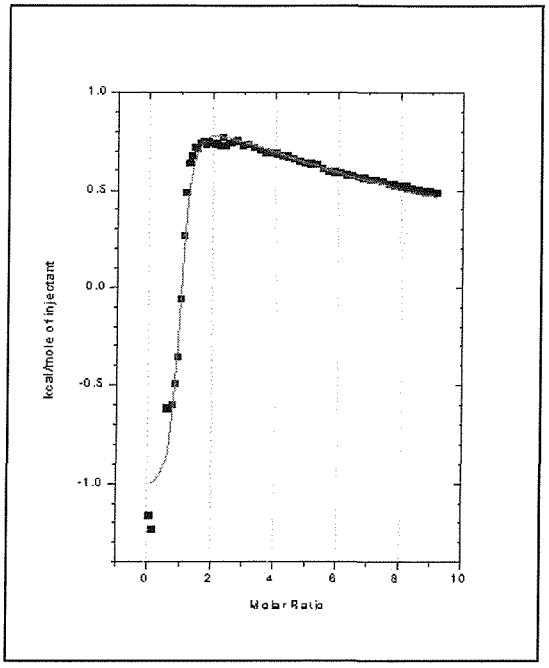

Figure 2-22 Calorimetric curve of N-Boc-L-Glu ***116*** *and* ***106*** *in dry MeCN. The solid line represents the non-linear least-square fit*

Figure 2-23 shows, instead, the results of a calorimetric titration of receptor **106** and the tetrabutylammonium salt of *N*-Boc-D-glutamate.

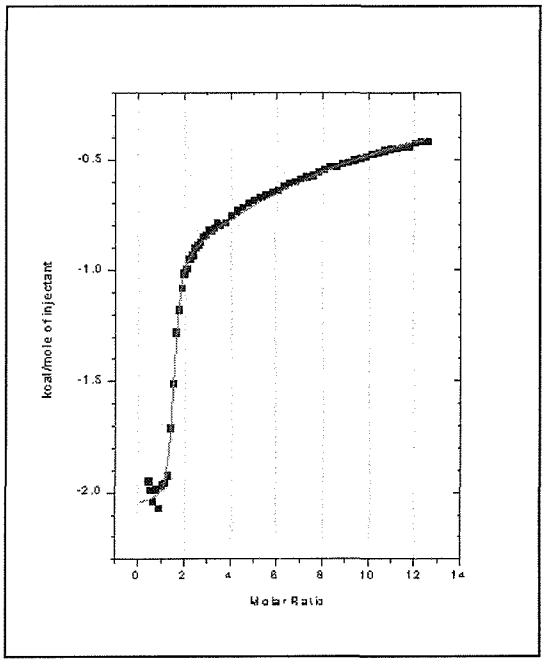

Figure 2-23 Calorimetric curve of N-Boc-D-Glu ***117*** *and* ***106*** *in dry MeCN. The solid line represents the non-linear least-square fit*

The curve shows again a strong exothermic binding. Values for the association constant and association enthalpy were determined by non-linear least squares fit using a two sites binding mode.[120] The calorimetric binding data are summarised in Table 2-4.

*Table 2-4 Binding constants (M^{-1}), association enthalpy and entropy (kJ mol^{-1}) for receptor **106** in MeCN at 25°C*

Guest	$K_a^{1:1}$	$\Delta H^{1:1}$	$T\Delta S^{1:1}$	$K_a^{1:2}$	$\Delta H^{1:2}$	$T\Delta S^{1:2}$
Boc-L-Glu	(2.83±0.48)x10^4	-4.5±0.2	21.0			
Boc-D-Glu	38.4±1.7	*	*	(4.92±0.07)x10^4	-6.7±0.1	20.1

* as the value for the Ka is very low, the uncertainty on the ? H and ? S becomes significant

The calorimetric binding data obtained with *N*-Boc-L-glutamate salt as the guest confirmed the strong 1:1 binding ($\Delta G^{1:1}$ = -25.5 ± 0.5 kJ mol^{-1}), which is dominated by the entropic contribution, indicating a bimolecular association promoted by the release of solvent molecules from the binding sites of the host to bulk solvent. The calorimetric data obtained with the *N*-Boc-D-glutamate salt, using a two sites binding model, yielded a small 1:1 binding constant ($\Delta G^{1:1}$ = -9.0 ± 0.1 kJ mol^{-1}) and a large 1:2 (host:guest) binding constant ($\Delta G^{1:2}$ = -26.8 ± 0.1 kJ mol^{-1}), which again is dominated by the entropic contribution. It has to be stressed that the accuracy of the derived K_a's using isothermal calorimetry is subject to some uncertainty given that the data is fitted with four unknown thermodynamic quantities, but all the titrations have been repeated to produce very similar, and therefore reproducible, results. This data confirms the stronger binding of the second guest relative to the first, as indicated by the NMR titrations. The data seems to suggest that binding of the first *N*-Boc-D-glutamate requires considerable reorganisation of the receptor, and consequent energetic cost. Then, once the first carboxylate is bound, the receptor binds the second carboxylate without significant additional energetic penalty. Conformational changes in the receptor on binding *N*-Boc-D-glutamate are clearly evidenced by the large shifts in many of the CH signals in the ^{1}H NMR spectrum of the receptor on addition of the guest. Furthermore, the data suggests that the enantioselectivity exhibited by receptor **106** for the 1:1 binding of *N*-Boc-glutamate is > 700:1 in favour of the L enantiomer.

To further confirm the thermodynamic data obtained with ITC, it was decided to perform a van't Hoff analysis by running a ^{1}H NMR titration with *N*-Boc-L-glutamate at different temperatures, 60°C, 40°C and 25°C. Van't Hoff analysis of the variable temperature data is widely used to determine the enthalpic and entropic contributions to a host-guest association.[82] Unfortunately, the binding proved to be very strong at high temperatures. Therefore the uncertainty on the association constant proved to be too high to give accurate values.

N-Boc-L,D-Aspartate 118, 119

To investigate further the binding properties of **106**, tetrabutylammonium salts of *N*-Boc-L,D-aspartate were prepared and its ability to enantioselectively bind them studied. *N*-Boc-L,D-aspartate was chosen to probe the effect of the chain length between the two carboxylate groups in the binding properties of the receptor.

Addition of *N*-Boc-L-aspartate tetrabutylammonium salt **118** to a solution of **106** in CD_3CN at room temperature led to dramatic changes in the ^1H NMR spectrum of the macrocycle. In particular, the addition of the guest led to a broadening of the NH signals of the host and a large shift of the CH protons, in particular the benzylic CH signals ($\Delta\delta_{max}$ = 0.57 ppm), which were used to determine the association constant. The binding data could be readily fitted to a 1:1 isotherm and yielded a high binding constant of 2.1x 10^5 M^{-1}.

Addition of *N*-Boc-D-aspartate tetrabutylammonium salt **119** to **106** produced considerable downfield shifts of the thiourea NH ($\Delta\delta_{max}$ = 1.53 ppm), the amide NH ($\Delta\delta_{max}$ = 1.18 ppm) and the benzylic CH signals ($\Delta\delta_{max}$ = 0.55 ppm), consistent with the formation of strong hydrogen bonding between the guest and the host. The binding data, though, could not be fitted to a simple 1:1 or 1:2 binding stoichiometry. Multiple binding equilibria seem to be simultaneously present. Such uncertainty in the stoichiometry was confirmed by a Job plot, Figure 2-24. The maximum is not to be found at 0.5, corresponding to a 1:1 equilibrium, or at 0.3, characteristic of a 1:2 (host:guest) complexation.

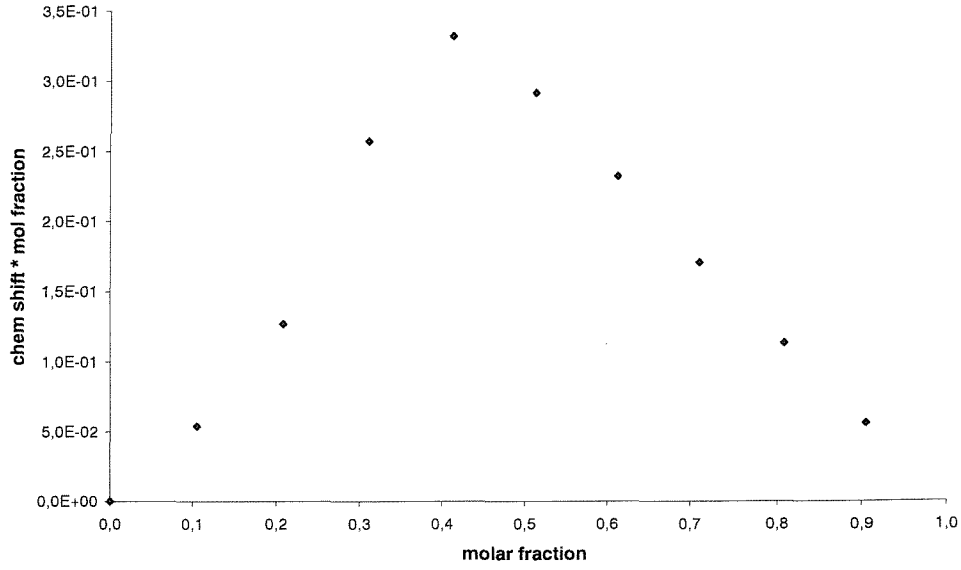

*Figure 2-24 Job plot of Boc-D-aspartate and receptor **106***

Due to time constraints, ITC titrations of receptor **106** and N-Boc-L,D-Aspartate were not performed.

Tetrabutylammonium acetate

Tetrabutylammonium acetate was investigated to ascertain the behaviour of the receptor towards a simple monocarboxylate. Significant changes in the ^{1}H NMR of the parent receptor were noted, after the addition of the guest.

a)

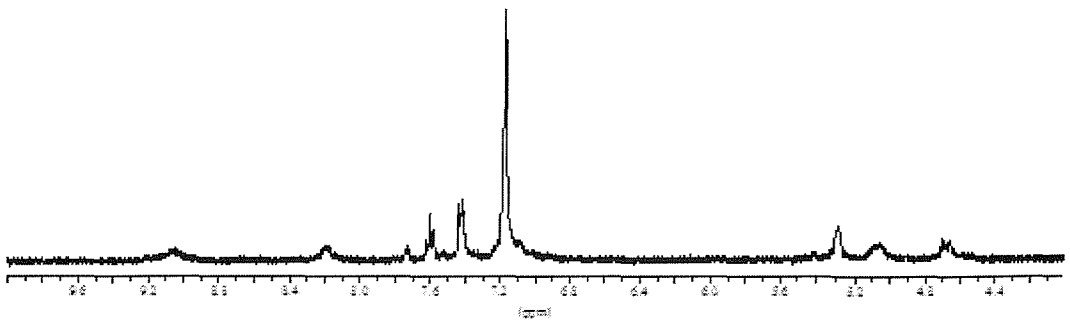

b)

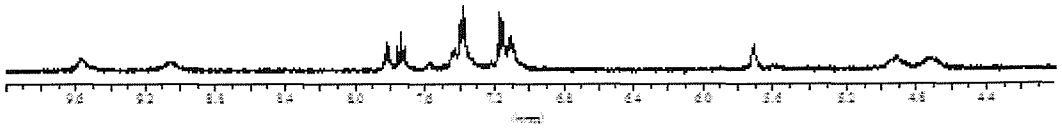

c)

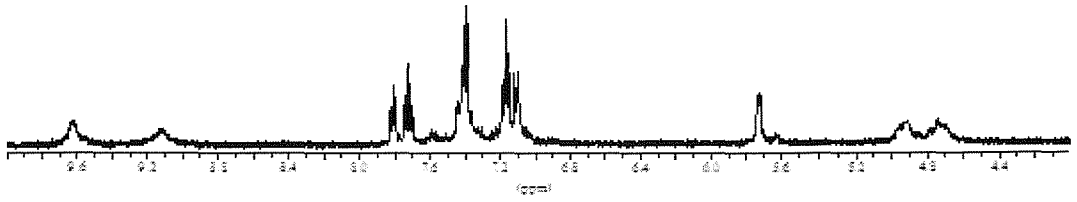

*Figure 2-25 ^{1}H NMR spectra of **106** and TBA acetate: a) neat host; b) after addition of 1 equivalent of guest; c) after addition of 2 equivalents of guest*

Downfield shifts of the thiourea NH ($\Delta\delta_{max}$ = 1.03 ppm), the amide NH ($\Delta\delta_{max}$ = 0.70 ppm) and the benzylic CH signals ($\Delta\delta_{max}$ = 0.47 ppm) were recorded. Saturation is reached after

the addition of two equivalents of acetate, suggesting a strong 1:2 (host:guest) binding equilibrium. The binding data, indeed, could be fitted to a 1:2 stoichiometry, with a $K_a^{1:2}$ of 1.12 x 10^4 M^{-1}. Acetate proved to behave in a similar way to *N*-Boc-D-glutamate.

2.3.3.3 Binding in DMSO-d_6

It was decided to move to a more polar solvent compared to acetonitrile to investigate the effect of the solvent polarity on the binding affinity of receptor **106** towards the guests. Numerous examples of the role of the solvent polarity are present in the literature. Hamilton studied the role of the solvent polarity in the recognition of dicarboxylates by bis-functional hydrogen bonding receptors, Figure 2-26, previously discussed in chapter 1.[82] Hamilton focused his attention on association in increasingly competitive solvents, from DMSO to water, by investigating the enthalpic and entropic contributions to association *via* NMR titrations and isothermal calorimetry. It was found that as the polarity and hydrogen bond ability of the solvent increased, binding affinity for the guests decreased.

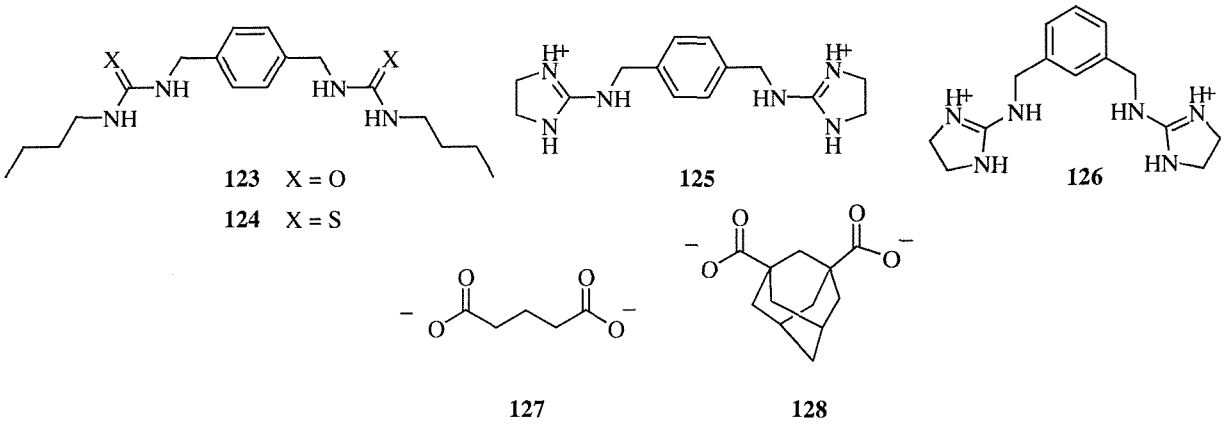

Figure 2-26 Hamilton bis-functional hydrogen receptors

Part of the results obtained, which best exemplify the influence of solvent upon binding, are summarised below, Table 2-5.

Table 2-5 Association constants for dicarboxylates in D_2O / MeOD mixtures

Receptor	Guest	10% D_2O	20% D_2O	25% D_2O	50% D_2O	75% D_2O
125	**127**	2800	850	720	230	
	128	3300	1300	780	300	130
126	**127**	3100	1100	840	290	
	128	5000	1500	1160	440	320

The addition of more competitive solvents reduced the association strength to a measurable level due to favourable solvation of both host and guest. Complementary analysis using NMR and ITC titrations showed also that in less polar solvents the complex formation was enthalpically driven. In methanol and methanol / water mixtures the complex formation was entropically driven, indicating a change from an association promoted primarily by hydrogen bond to an association driven by solvent liberation.

N-Boc-L,D-glutamate ***116, 117***

^{1}H NMR binding studies with the *N*-Boc-L-glutamate **116** in DMSO gave a similar picture compared to the receptor behaviour in CD_3CN. Significant downfield shifts of the thiourea NH ($\Delta\delta_{max}$ = 1.17 ppm) and amide NH ($\Delta\delta_{max}$ = 0.59 ppm) were noted. No appreciable shift of the benzylic CH protons was recorded. The data could be fitted to a strong 1:1 binding isotherm, giving an association constant of 3.7 x 10^3 M^{-1}. The complexation process is characterised by a lower association constant as compared to the $K_a^{1:1}$ obtained in acetonitrile of a factor of 10^2. The more polar DMSO has a higher solvation strength than acetonitrile. A more strongly hydrogen bond donating solvent, DMSO reduces the binding affinity through an increased solvation of both host and guest. Therefore, a higher energetic penalty has to be paid to complex the guest, resulting in a lower association constant.

Although addition of the tetrabutylammonium salt of *N*-Boc-D-glutamate **117** in DMSO led to significant downfield shift of the NH signals, the binding data obtained deviates from the saturation curves expected for simple 1:1 or 1:2 binding. Reliable binding constants could not be obtained. Presumably several binding equilibria, 1:1, 1:2 or even 2:2, are competing when the *N*-Boc-D-glutamate is the guest. However, the NMR titration binding curve approaches saturation after the addition of approximately two equivalents of guest, suggesting a dominant 1:2 (host:guest) binding stoichiometry, Figure 2-27.

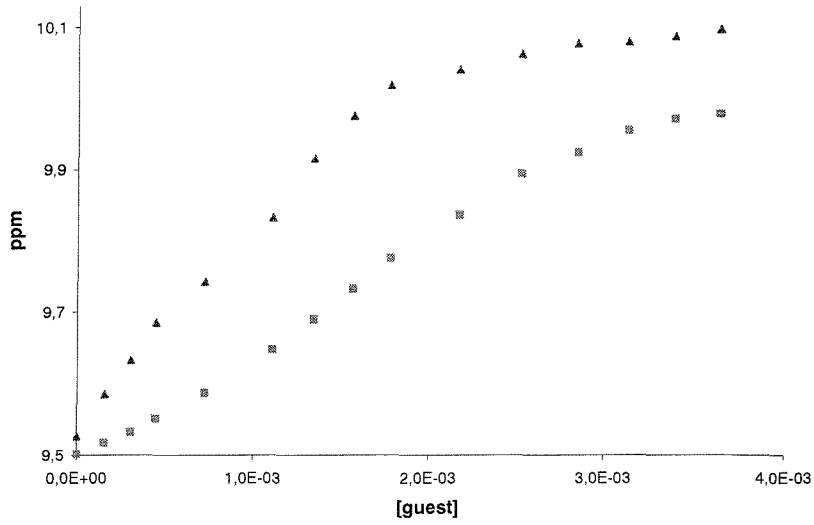

*Figure 2-27 Binding titration curves for macrocycle **106** showing the shift of the amide protons on the addition of N-Boc-L-glutamate (▲) and N-Boc-D-glutamate (■). The 1:1 [host]:[guest] is reached when [guest] ~ 1.7 mM*

Isothermal calorimetry confirmed the results obtained with the ^{1}H NMR binding studies. Complexation of *N*-Boc-L-glutamate by **106** proved to be exothermic and characterised by a large entropic contribution, with a $Ka^{1:1}$ = 2.28 ± 0.26 x 10^3 M^{-1}($\Delta H^{1:1}$ = -10.7 kJ mol^{-}1, $T\Delta S^{1:1}$ = -8.5 kJ mol^{-1}, $\Delta G^{1:1}$ = -19.2 ± 0.3 kJ mol^{-1}). Isothermal calorimetry showed the presence of multiple binding equilibria when the guest is *N*-Boc-D-glutamate, as evidenced by the ^{1}H NMR studies. It was not possible to fit the ITC curve and, therefore, to get meaningful values.

Again, receptor **106** proved to be selective and enantioselective towards *N*-Boc-glutamate in DMSO, In particular, binding of the L enantiomer proved to be a strong 1:1 complexation, while multiple equilibria arise in the association of receptor **106** with the D enantiomer.

*N-Boc-L,D-Aspartate **118, 119***

Addition of the aspartate enantiomers caused a broadening of the thiourea and amide hydrogen peaks in the ^{1}H NMR spectra of **106** in DMSO at room temperature. A decrease in intensity upon addition of successive aliquots of guest was also noted. In addition, a new set of broad signals were found to appear, which became well resolved after the addition of four equivalents of guest, Figure 2-28.

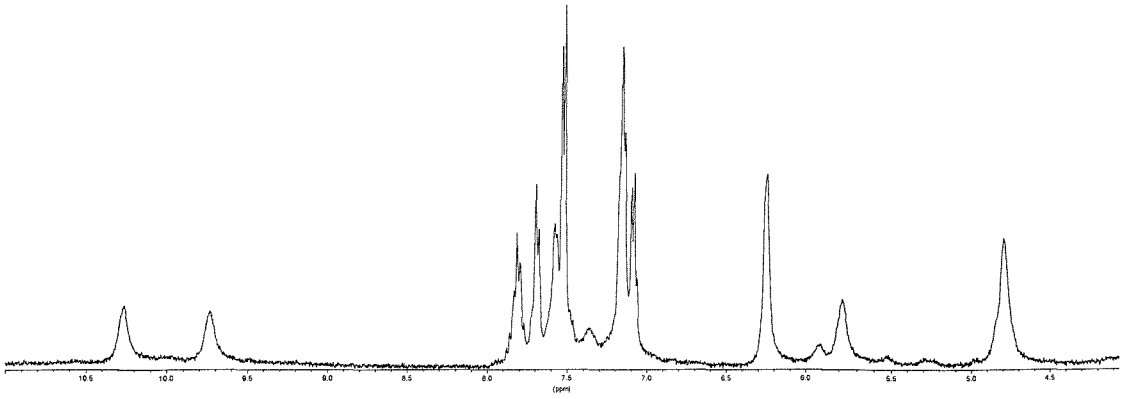

*Figure 2-28 ^1H NMR spectrum of **106** after the addition of four equivalents of Boc-L-Asp*

During the addition of *N*-Boc-L-aspartate to the host solution is was possible to observe one set of peaks for the unbound macrocycle on addition of guest, which decreased in intensity, and a new set of peaks for the bound host-guest complex, which increased in intensity on addition of the guest. It was therefore concluded that macrocycle **106** exhibited changeable binding kinetics, showing slow chemical exchange for aspartate compared to glutamate. It was therefore decided to run ^1H NMR spectra at 90°C to overcome such slow binding kinetics. At 90°C, indeed, the neat macrocycle gave a well-resolved spectrum, Figure 2-29.

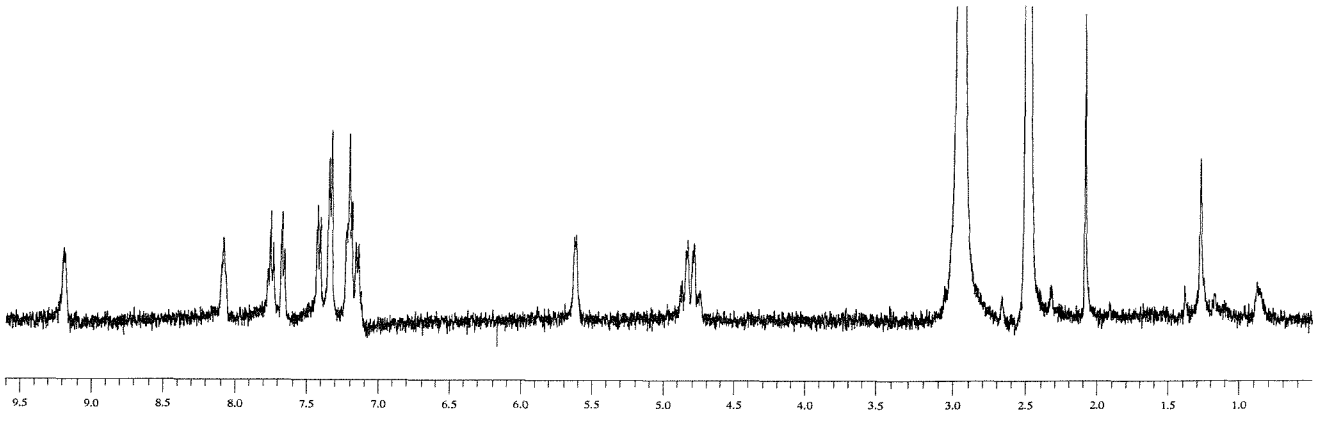

*Figure 2-29 ^1H NMR of **106** in DMSO-d_6 at 90°C*

Preliminary spectra of the 1:1 mixtures of aspartate and macrocycle **106** were also well resolved as a single set of peaks at 90°C, Figure 2-30. It was, then, possible to run some binding studies and obtain the binding constants.

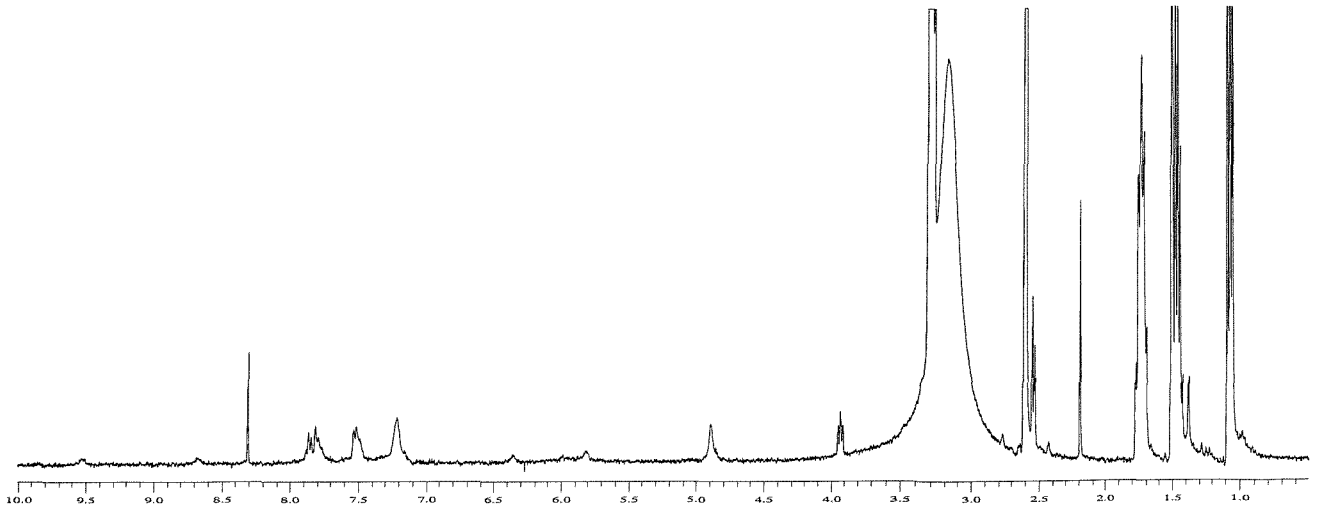

*Figure 2-30 ^1H NMR of a 1:1 solution of **106** and N-Boc-L-asp in DMSO at 90°C*

Addition of *N*-Boc-L-aspartate led to downfield shifts of the thiourea NH ($\Delta\delta_{max}$ = 0.64 ppm) and the amide NH ($\Delta\delta_{max}$ = 0.31 ppm) signals. No shift was noted for the benzylic CH protons. The binding data could be fitted to a 1:1 binding isotherm and the association constant was found to be 1.2 x 10^3 M^{-1}. Addition of *N*-Boc-D-aspartate produced less pronounced downfield shifts of the thiourea NH ($\Delta\delta_{max}$ = 0.42 ppm) and amide NH ($\Delta\delta_{max}$ = 0.21 ppm) protons. Again no appreciable shifts were perceived for the benzylic CH signals. The NMR titrations indicate very weak binding, as only ~25% of saturation is reached after the addition of five equivalents of guest. The data were fitted to a 1:2 (host:guest) binding stoichiometry, with a $K_a^{1:2}$ of 92 M^{-1}. It was not attempted to collect ITC data at these elevated temperatures.

*Dibenzoyl-L,D-tartrate **120, 121***

Addition of the tetrabutylammonium salts of both enantiomers in DMSO led to small downfield shifts in the thiourea NH ($\Delta\delta_{max}$ = 0.27 ppm for dibenzoyl-L-tartrate; $\Delta\delta_{max}$ = 0.31 ppm for the D enantiomer), indicating a weak binding. The binding data could be fitted to a 1:2 (host:guest) isotherm, giving a binding constant of 211 M^{-1} for the L enantiomer and 103 M^{-1} for dibenzoyl-D-tartrate. No or very weak enantioselectivity was noted. Presumably the tartrates substrates are too bulky to allow strong binding with the receptor.

*Glutarate **122***

Addition of the tetrabutylammonium salt of glutarate to a solution of receptor **106** produced a surprising result, as it leads to the formation of a gel. A polymeric complex, n:n, seems to be

formed, made possible by the low steric bulk at both ends of the dicarboxylate. The formation of the gel is being investigated further in the group.

2.3.3.4 Binding in Methanol

It was decided then to move to even more polar solvent. Unfortunately no or very weak binding was observed after the addition of *N*-Boc-L(D)-glutamate. Probably the energy required for the desolvation of both the unbound host and guest is not be compensated for by the formation of the host-guest complex.

2.3.4 Conclusions

A novel bisthiourea macrocyclic receptor specifically designed to bind glutamate has been successfully synthesised and its conformational and binding properties investigated.

Receptor **106** shows the remarkable property of binding the guests in highly competitive solvents (CD_3CN and DMSO-d_6) and not in non-polar ones ($CDCl_3$). Macrocycle **106**, indeed, was found to form alternative conformers in DMSO and chloroform. In DMSO, a symmetric conformation was observed and twisted conformation was seen at –40°C in chloroform. Bisthiourea **106** seems to be in slow chemical exchange between a symmetric and a tightly wrapped conformation in chloroform at room temperature. Consequently it is unsuitable for the complexation of carboxylate salts in the apolar chloroform.

Binding studies with the dipyridyl bisthiourea receptor **106** and a range of guests as tetrabutylammonium salts in different solvents were carried out and the results, obtained with ^1H NMR titrations, are presented in Table 2-6. In an effort to gauge the effect of solvent composition on association, binding titrations were performed in a variety solvents with increasing polarity, from CD_3CN to MeOD. As the polarity and hydrogen bonding ability of the solvent increases, a decline in association strength is noted. In methanol no or very weak binding was observed.

Table 2-6 Association constants (M^{-1}) determined by NMR of different guests with bisthiourea ***106*** *(* multiple equilibria)*

Guests	Solvent	°C	$K_{1:1}$	$K_{1:2}$
N-Boc-L-Glu	CD_3CN	25	1.5×10^5	
N-Boc-D-Glu			38.4	4.9×10^4
N-Boc-L-Glu	DMSO	25	2.2×10^3	
N-Boc-D-Glu			*	*
N-Boc-L-Asp	CD_3CN	25	2.1×10^5	
N-Boc-D-Asp			*	*
N-Boc-L-Asp	DMSO	90	1.2×10^3	
N-Boc-D-Asp				92
Acetate	CD_3CN	25		1.1×10^4
Dibz-L-tartrate	DMSO	25		211
Dibz-D-tartrate				103

Isothermal calorimetric studies showed that binding was driven to a large extent by entropy, presumably produced by releasing bound solvent molecules from the binding sites of the host to bulk solvent. The process remains unaltered in all solvents.

Bisthiourea **106** is highly enantioselective, favouring generally the L enantiomer. The receptor binds the L enantiomer in a 1:1 fashion, while a 1:2 or even multiple equilibria arise when the D enantiomer is added. In particular, the receptor proved to be highly selective for the 1:1 binding of the *N*-protected glutamate dianion, suggesting an enantioselectivity for the 1:1 binding of *N*-Boc-glutamate of > 700:1 in favour of the L enantiomer.

In view of the fact that high levels of enantioselective binding of *N*-Boc-glutamate with macrocycle **106** was observed in CD_3CN, a second generation of receptors were synthesised, to further improve its properties.

3 Second Generation Receptors

3.1 Introduction

In order to further investigate how a small change in the structure of parent receptor **106**, discussed in chapter two, can affect its binding properties it was decided to synthesise macrocyclic analogues of **106**, Figure 3-1. Various alterations were considered:

- an increase in the conformational restraint of the macrocycle (receptor **123**);
- the substitution of the pyridine units by benzylic moieties to investigate to what extent the former groups influence the preorganisation of the system (receptors **129** and **130**);
- conversion of the thiourea carboxylic binding site to guanidinium (receptor **139**).

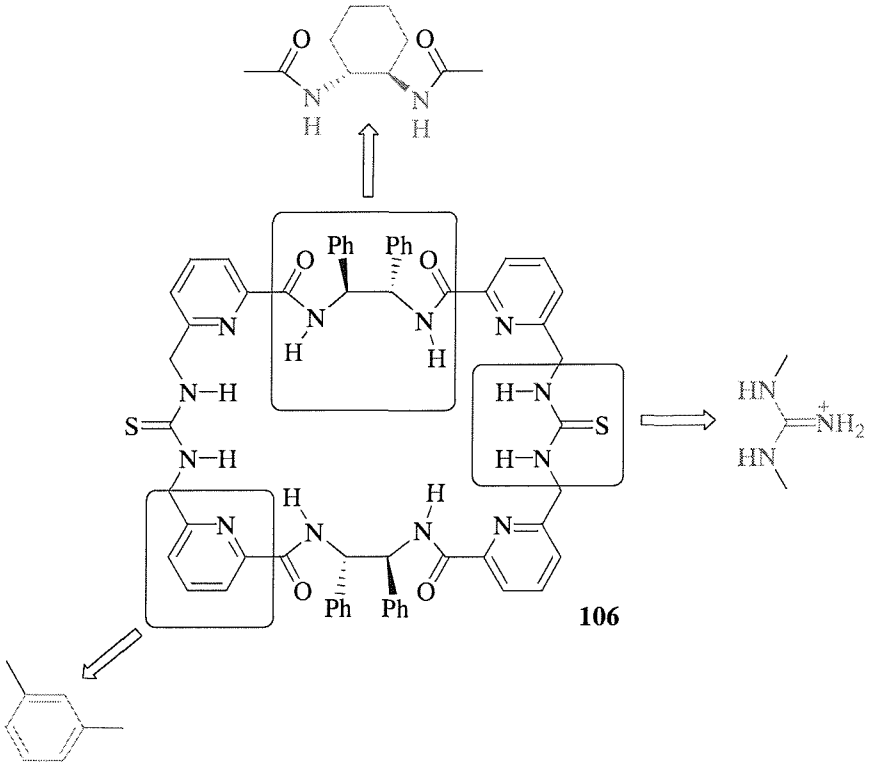

Figure 3-1 Second generation receptors

The modified receptor's binding affinity for glutamate and aspartate were then ascertained by ^{1}H NMR and calorimetric studies in solvents of increasing polarity.

3.2 Bisthiourea Receptor 123

3.2.1 Receptor Design

Chapter two discussed the properties of bisthiourea receptor **106**, which was found to form alternative conformers in DMSO and chloroform. In DMSO, a symmetric conformation was observed and a twisted conformation was seen at –40°C in chloroform. The formation of a tightly

wrapped conformer of the host molecule in chloroform meant that the bisthiourea macrocycle was not able to act as a carboxylate receptor in apolar solvents, like $CDCl_3$. In view of this problem a new host was designed with the purpose of increasing the degree of preorganisation[121] towards the correct conformation to bind carboxylates in apolar solvents. The chiral diphenylethylene diamine was substituted with a cyclic aliphatic diamine, Figure 3-2.

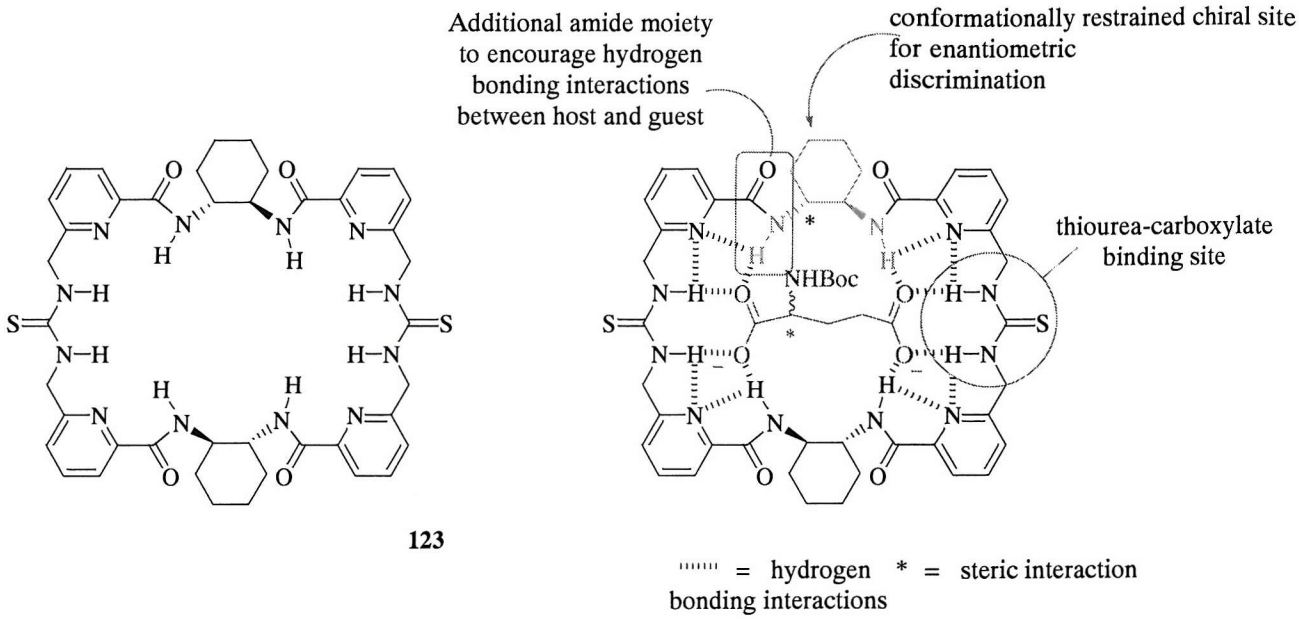

*Figure 3-2 Design concept of macrocyclic receptor **123** for glutamate*

Moreover, the higher conformational rigidity conferred on the macrocycle by the presence of the 1,2-diaminocyclohexane, was intended to give a smaller entropy loss upon binding and therefore a higher overall association constant due to the additional energy gained as a result of the preorganisation of the host.

Chiral 1,2-diaminocyclohexane has been applied to the development of highly enantioselective versions of asymmetric synthetic reactions, such as allylic alkylations.[122] Such a chirality carrier has also been employed in the enantiomeric and diastereomeric recognition of peptides.[123] Lehn *et al.* developed two hexaazamacrocycles incorporating one or two (*R,R*)-1,2-diaminocyclohexane units and studied their protonation and binding properties by means of potentiometry and NMR techniques, Figure 3-3.[124]

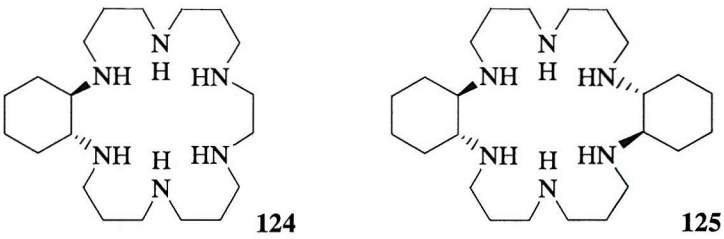

Figure 3-3 Lehn's 22-membered hexaazamacrocycles

Potentiometric titrations showed that **124** is more basic than **125**, the largest difference lying in the fifth protonation step, deriving from the different protonation abilities of the ethylene diamine and cyclohexane diamine moieties. The ethylene fragment has a high flexibility, which is very useful when completely protonated. In contrast, the fifth proton in **125** must be attached to an already monoprotonated *trans*-diequatorial cyclohexane diamine, setting the two positive charges very close and increasing the electrostatic repulsion. No sign of the change to a diaxial conformation, which would have prevented this repulsion, was noted, suggesting a high conformational rigidity for the system.

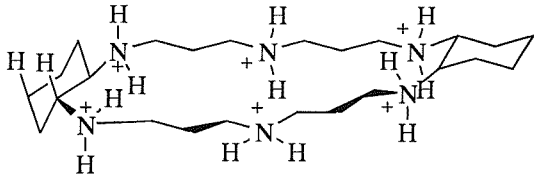

*Figure 3-4. Pentaprotonated receptor **125***

Some binding studies with different dicarboxylates were performed in aqueous solution. Macrocycle **125** proved to form more stable complexes than **124**, probably due to a higher charge density. The presence of the cyclohexane rings increased the hydrophobicity of the receptor, preventing the solvation of the ammonium groups. Moreover, the *trans*-diequatorial conformation of the six-membered ring positioned the ammonium moiety towards the cavity of the host, increasing the charge density. *N*-Ac-glutamate was found to form very stable complexes with both receptors, preferring the D enantiomer. The stoichiometry of the complexes were 1:1 or 1:2 (host:guest) depending on the number of the protons and the enantiomer of the anion.

*3.2.2 Synthesis of Bisthiourea Receptor **123***

The route followed to produce macrocycle **123** was essentially the same as that developed for parent receptor **106**, Scheme 3-1.

All attempts to extract the chiral diaminoyclohexane from its tatrate salts were frustrated by low yields and the high instability of the diamine itself, which seemed to readily absorb CO_2. Therefore, a two-phase (water/dichloromethane) reaction was carried out. The diamine was basified in water in the presence of potassium carbonate. In the meantime, acid **98** was activated with the coupling reagent diphenylchlorophosphate. The aqueous solution was then added directly to the mixed anhydride in dichloromethane to yield bisphtalimide **126** in 52% yield. In order to improve the yield of the reaction, alternative routes were tried. Acid **98** was activated in the presence of EDC, HOBt and DMAP.[104b] Then (*S,S*)-1,2-diaminocyclohexane as tartrate salt was added to the mixture in the

presence of an excess of DIPEA. DIPEA was chosen as a base for its highly hindered structure and its poor nucleophilicity. None of the alternative reactions produced higher yields.

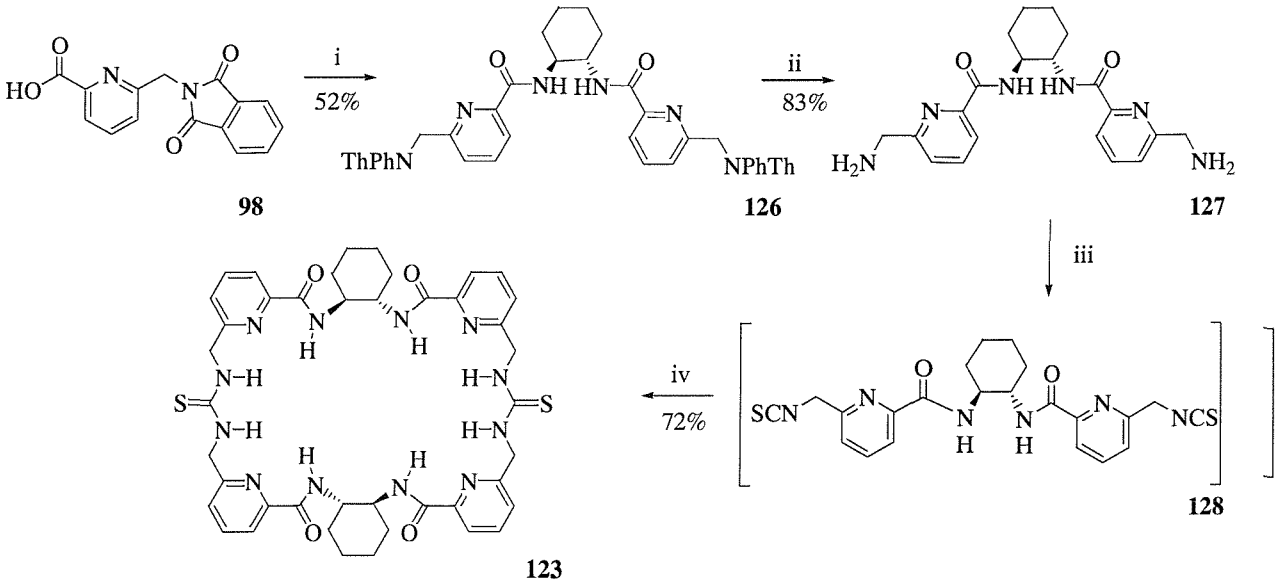

Scheme 3-1 *Reagents and conditions:* i) diphenylchlorophosphate, DCM, (*S*,*S*)-1,2-diaminocyclohexane, H_2O, K_2CO_3; ii) NH_2NH_2; iii) CS_2, -10°C; DCC, DMAP, -10°C then warm to r. t; iv) slow addition of 1 equivalent of **105** and 1 equivalent of **106** to a solution of dry CH_2Cl_2/DMAP at r. t. over 3 hours

Bisphthalimide **126** was deprotected using hydrazine hydrate to furnish diamine **127** in 83% yield. After one equivalent of amine **127** and 1 equivalent of bisthioisocyanate **128** were added to a solution of CH_2Cl_2 and catalytic DMAP *via* syringe pump over three hours, bisthiourea **123** was formed in a 72% yield. The high yield is probably due to the conformational constraint of the diamine, which disfavours the formation of byproducts, such as the monothiourea analogue.

In conclusion, macrocycle **123** was synthesised and binding studies were carried out using both traditional NMR techniques and isothermal calorimetry to compare the results with parent host **106**.

3.2.3 Conformational Properties of Receptor 123

^1H NMR spectra of receptor **123** in $CDCl_3$ and DMSO-d_6 have been run at room temperature. In both solvents it was possible to obtain well resolved spectra. The NMR spectrum in $CDCl_3$ was more complex than the one in DMSO and reflected a twofold C_2 symmetry. In DMSO, instead, the spectrum appeared to be consistent with the expected fourfold D_2 symmetry of the host.

a)

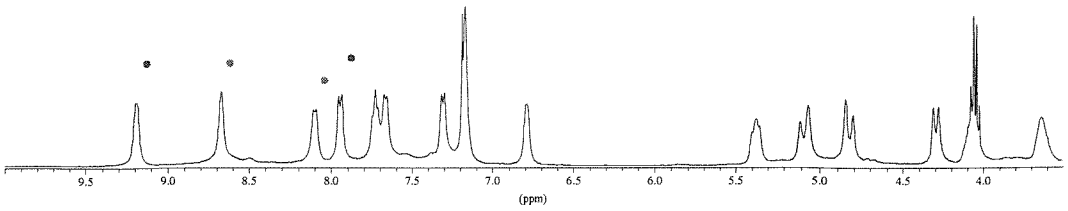

b)

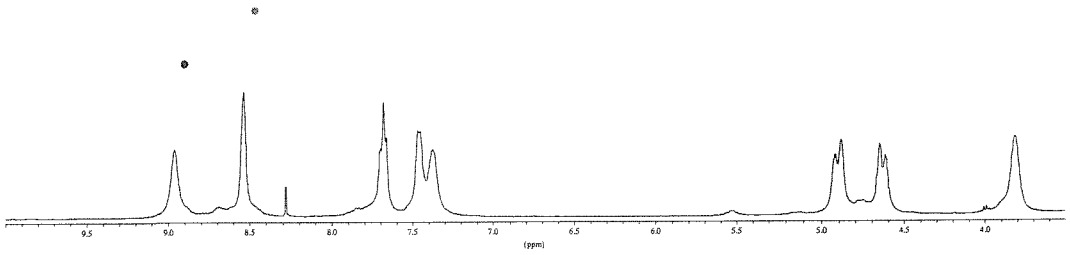

*Figure 3-5 Part of the NMR spectrum of macrocycle **123** a) in $CDCl_3$ and b) in DMSO at r.t. (* indicates the thiourea protons, * shows the amide protons)*

In chloroform, receptor **123** seemed to be tightly locked into a similar twisted conformation as that found at -40°C of the parent receptor **106**. Such a wrapped conformer is present at room temperature suggesting a very stable conformation, which becomes disrupted in the presence of polar solvents.

Detailed 2D NMR studies were carried out. COSY and NOESY ^{1}H NMR experiments were run in deuterated chloroform at room temperature, allowing for full assignment of all the ^{1}H NMR signals. Each proton of the receptor gives a separate signal, indicating that there are no equivalent protons. In particular, the thiourea NH protons have two different signals at δ = 8.7 and 8.1 ppm, while the amide NH protons have signals at δ = 9.2 and 7.7 ppm, Figure 3-6.

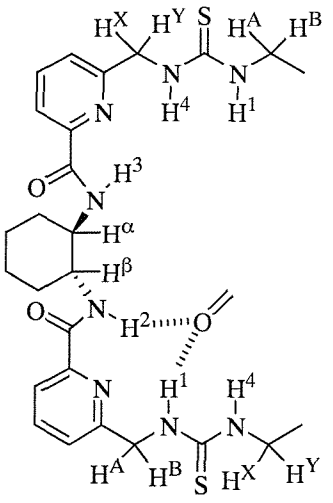

NH^1 δ = 8.7 ppm

NH^4 δ = 8.1 ppm

NH^2 δ = 9.2 ppm

NH^3 δ = 7.7 ppm

Figure 3-6 Graphic interpretation of n.O.e. results

Both NH^1 and NH^2 are significantly more downfield relative to NH^3 and NH^4, which suggest a possible intramolecular bonding between NH^1 and NH^2 and a carbonyl group in the molecule. The NMR studies show that the receptor, dissolved in chloroform, adopts a tightly wrapped conformation stabilised by a number of intramolecular hydrogen bonds, in particular those from an amide carbonyl oxygen atom to the thiourea NH and an adjacent amide NH proton.

*3.2.4 Binding Studies of Receptor **123***

Binding studies with the chiral bisthiourea receptor **123** and *N*-protected glutamate and aspartate, as their tetrabutylammonium salts, were carried out by NMR and isothermal calorimetry.

3.2.4.1 Binding in Chloroform

^{1}H NMR spectra of 1:1 mixtures of both enantiomers of *N*-Boc-glutamate and *N*-Boc-aspartate with macrocycle **123** were performed in chloroform. As expected, addition of either enantiomer of the guests did not lead to any discernible change in the ^{1}H NMR spectrum of the macrocycle. Clearly, switching to a more rigid system did not result in the hoped for outcome. Receptor **123** lies in a conformation unsuitable for binding in apolar solvents and the energy required to reorganise the host into a suitable binding conformation, by breaking the intramolecular hydrogen bonds, is not compensated for by the host–guest binding interactions that would be established.
It was then decided to investigate the binding properties of the host in the more polar solvents DMSO-d_6 and CD_3CN.

3.2.4.2 Binding in Acetonitrile

Initial attempts at obtaining association constants by conventional ^{1}H NMR titration experiments were unsuccessful due to the poor solubility of the receptor in this solvent. The problem was

overcome by running isothermal calorimetric titrations, which due to the higher sensitivity of the technique, allows the use of host solutions at much lower concentrations.

N-Boc-L,D-Glutamate

ITC was employed to study the association and the thermodynamic quantities characterising the complexation process of receptor **123** and *N*-Boc-L,D-glutamate. The curves for both enantiomers show a strong exothermic binding, characterised by negative enthalpy, suggesting a stabilisation by hydrogen bonding[82], Figure 3-7.

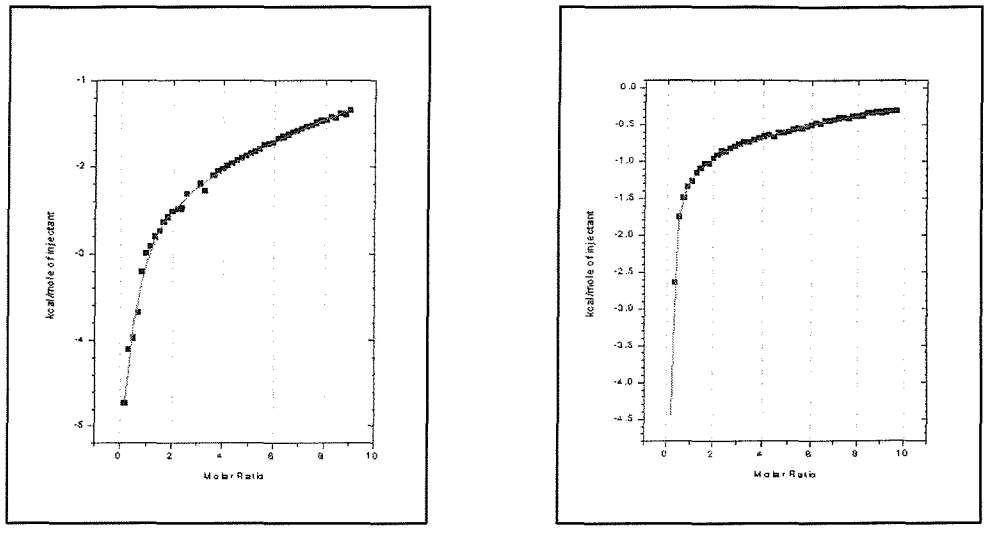

*Figure 3-7 Calorimetric curves of **123** and N-Boc-L-Glu and N-Boc-D-Glu in MeCN at 25°C*

Values for the association constant and association enthalpy were determined by non-linear least squares fit using a one or two sites binding mode.[120] The calorimetric binding data are summarised in Table 3-1.

*Table 3-1 Binding constants (M^{-1}), association enthalpy and entropy (kJ mol^{-1}) for receptor **123** in dry CH_3CN at 25°C*

Guest	$K_a^{1:1}$	$\Delta H^{1:1}$	$T\Delta S^{1:1}$	$K_a^{1:2}$	$\Delta H^{1:2}$	$T\Delta S^{1:2}$
Boc-L-Glu	(1.48±0.88)x10^3	-5.5±0.8	12.4			
Boc-D-Glu	82.9±2.3	*	*	(1.05±0.12)x10^4	-7.4±0.1	16.7

* as the value for the Ka is very low, the uncertainty on the ? H and ? S becomes significant

The calorimetric binding data obtained with *N*-Boc-L-glutamate salt showed a strong 1:1 binding ($\Delta G^{1:1}$ = -17.9 ± 0.5 kJ mol^{-1}), which is dominated by the entropic contribution, indicating a

bimolecular association promoted by the release of solvent molecules from the binding sites of the host to bulk solvent. The association constant proved to be 100-fold smaller that obtained with parent receptor **106** [K_a = (2.83 ± 0.48) x 10^4 M^{-1}], indicating a partial loss of affinity for the guest. The calorimetric data obtained with the *N*-Boc-D-glutamate salt, using a two sites binding model, yielded a small 1:1 binding constant and a large 1:2 (host:guest) binding constant ($\Delta G^{1:2}$ = -24.1 ± 0.1 kJ mol^{-1}), which again is dominated by the entropic contribution. The data seem to suggest that binding of the first *N*-Boc-D-glutamate requires considerable reorganisation of the receptor, and consequent energetic cost. Then, once the first carboxylate is bound, the receptor binds the second carboxylate without significant additional energetic penalty (positive co-operativity). Furthermore, the data show a good enantioselectivity of 18:1 (L:D) exhibited by receptor **123** for the 1:1 binding of *N*-Boc-glutamate.

N-Boc-L,D-Aspartate

Figure 3-8 shows the results of a calorimetric titrations of receptor **123** and the tetrabutylammonium salts of *N*-Boc-L,D-Aspartate. Also shown is the non-linear least squares fit of the curve.

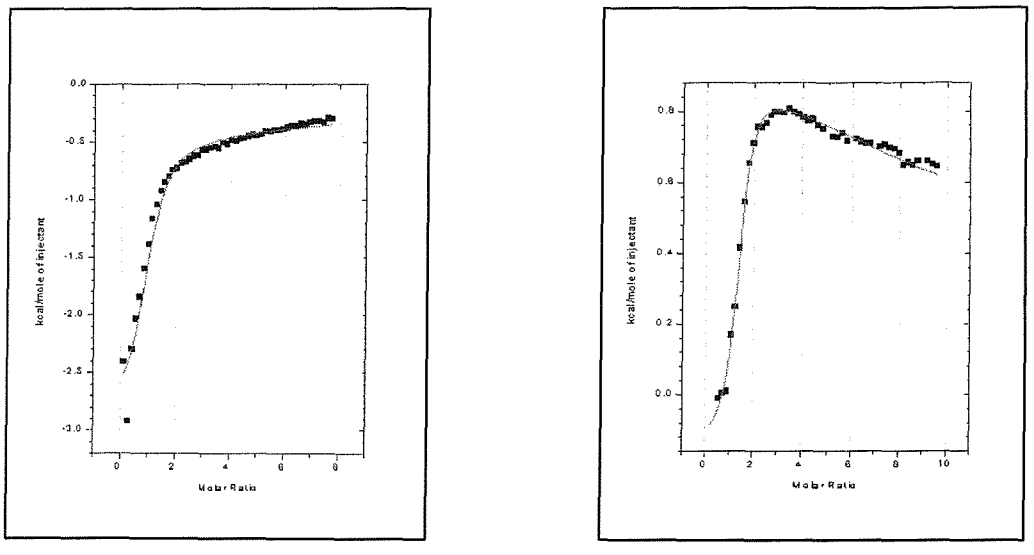

*Figure 3-8 Calorimetric curves of **123** and N-Boc-L-Asp and N-Boc-D-Asp in MeCN at 25°C*

The data derived from the titration curves are shown in Table 3-2.

*Table 3-2 Binding constants (M^{-1}), association enthalpy and entropy (kJ mol^{-1}) for receptor **123** in dry CH_3CN at 25°C*

Guest	$K_a^{1:1}$	$\Delta H^{1:1}$	$T\Delta S^{1:1}$	$K_a^{1:2}$	$\Delta H^{1:2}$	$T\Delta S^{1:2}$
Boc-L-Asp	(3.79±1.5)x10^3	-12.1±0.2	8.3			
Boc-D-Asp	4.5±1.2*			(1.09±0.14)x10^4	-6.1±0.1	2.2

* binding to Boc-D-Asp can be considered a simple 1:2 binding equilibrium

The calorimetric binding data obtained with *N*-Boc-L-aspartate salt as guest showed a 1:1 binding equilibrium ($\Delta G^{1:1}$ = -20.4 ± 0.2 kJ mol^{-1}). The process is mainly enthalpy driven indicative of a bimolecular association promoted by the formation of strong hydrogen bonds between the host and the guest. Furthermore, the exothermic nature of the association suggests that the hydrogen bonds so formed are stronger than those initially formed with the solvent. Although it is not possible to compare directly the behaviour of hosts **123** and **106** towards aspartate, it can be estimated that the association constant for *N*-Boc-L-aspartate is at least 100-fold smaller than the one obtained with parent receptor **106** (K_a=2.1x10^5 M^{-1}, from NMR titrations), indicating a partial loss of affinity for the guest. The calorimetric data obtained with the *N*-Boc-D-aspartate salt, using a two sites binding model, yielded a negligible 1:1 binding constant and a large 1:2 (host:guest) binding constant ($\Delta G^{1:2}$= -8.3 ± 0.1 kJ mol^{-1}) which again is enthalpically driven.

3.2.4.3 Binding in DMSO

N-Boc-L,D-Glutamate

Addition of either enantiomer of *N*-Boc-glutamate to a solution of **123** in DMSO at room temperature showed no change in the ^{1}H NMR spectrum of the free host, suggesting no or very weak binding. To evaluate the possibility of a slow complexation of glutamate by the host, ^{1}H NMR spectra of receptor **123** upon successive aliquots of guest, up to 1 equivalent, were recorded immediately after the additions and after a period of equilibration of 24 hours. Again no changes in the spectra appearance were detected after the equilibration time. The presence of a slow binding process was, therefore, excluded.

N-Boc-L,D-Aspartate

Addition of *N*-Boc-L-aspartate tetrabutylammonium salt to a solution of **123** in DMSO at room temperature showed downfield shifts of the thiourea NH ($\Delta\delta_{max}$ = 0.21 ppm), the amide NH ($\Delta\delta_{max}$ = 0.16 ppm) and the benzylic CH signals ($\Delta\delta_{max}$ = 0.17 ppm) after the addition of the guest. This is consistent with the formation of hydrogen bonds between the host and the substrate. Changes in the NMR spectra of the receptor were registered upon addition of more guest, suggesting that saturation was not reached after the addition of the first equivalent of *N*-Boc-L-aspartate.

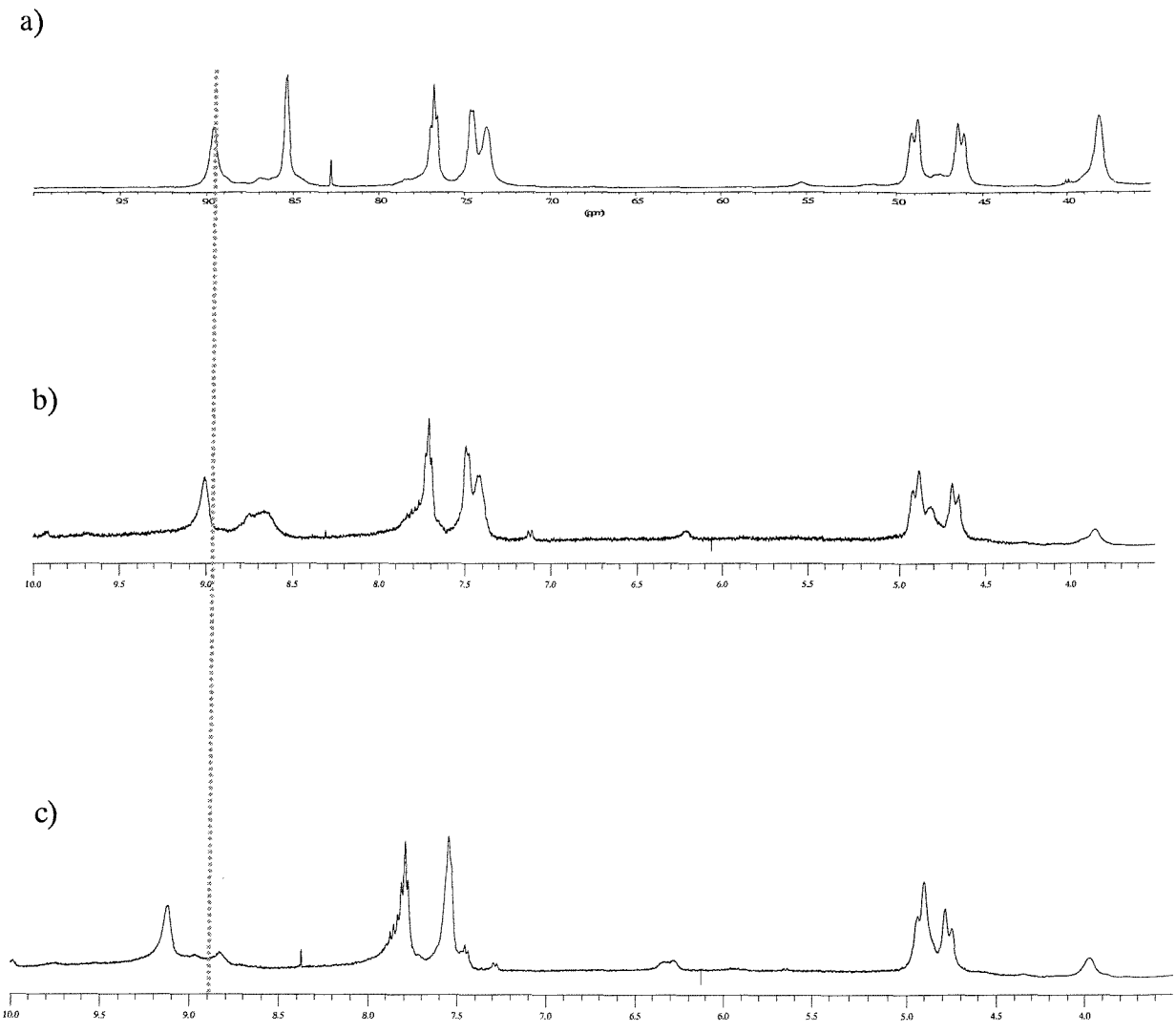

*Figure 3-9 ^1H NMR spectra of **123** and N-Boc-L-Asp: a) neat host; b) after addition of 1 equivalent of guest; c) after addition of 2 equivalents of guest*

The binding data could not be fitted to a 1:1 or a 1:2 (host:guest) stoichiometry, suggesting the presence of multiple binding equilibria.

Addition of the *N*-Boc-D-aspartate tetrabutylammonium salt also led to measurable downfield shifts of the thiourea NH ($\Delta\delta_{max}$ = 0.30 ppm), amide NH ($\Delta\delta_{max}$ = 0.21 ppm) and CH benzylic protons ($\Delta\delta_{max}$ = 0.15 ppm) of the receptor.

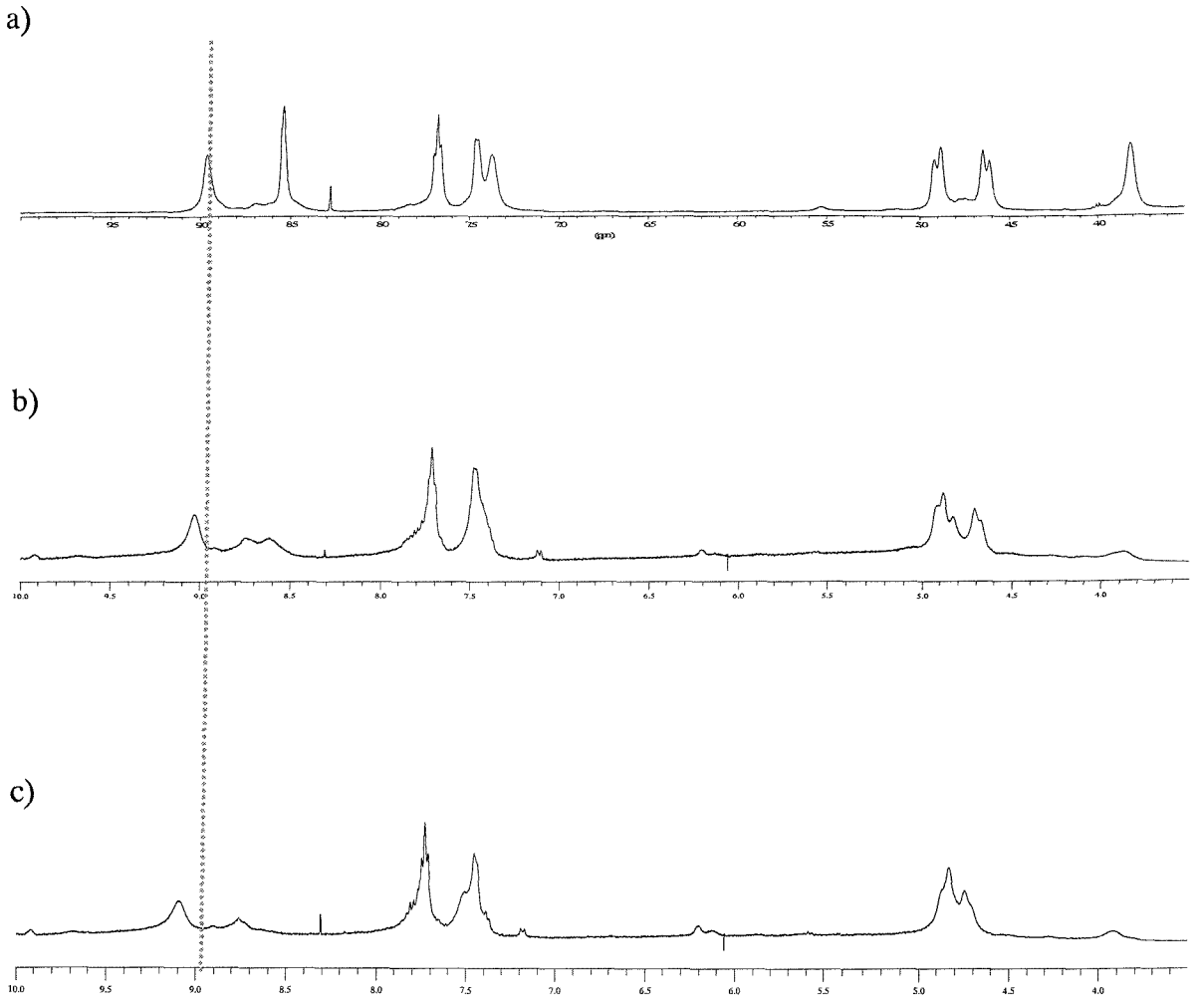

*Figure 3-10 ^{1}H NMR spectra of **123** and N-Boc-D-Asp: a) neat host; b) after addition of 1 equivalent of guest; c) after addition of 2 equivalents of guest*

From the ^{1}H NMR spectra, it seemed that saturation was reached after the addition of two equivalents of guest, Figure 3-10. However, the NMR titration curve of Boc-D-aspartate is not linear. This pronounced sigmoidal shape seems to indicate the presence of a measurable 1:1 complexation process. It was not possible to fit the curve with either 1:1 or 1:2 binding mode.

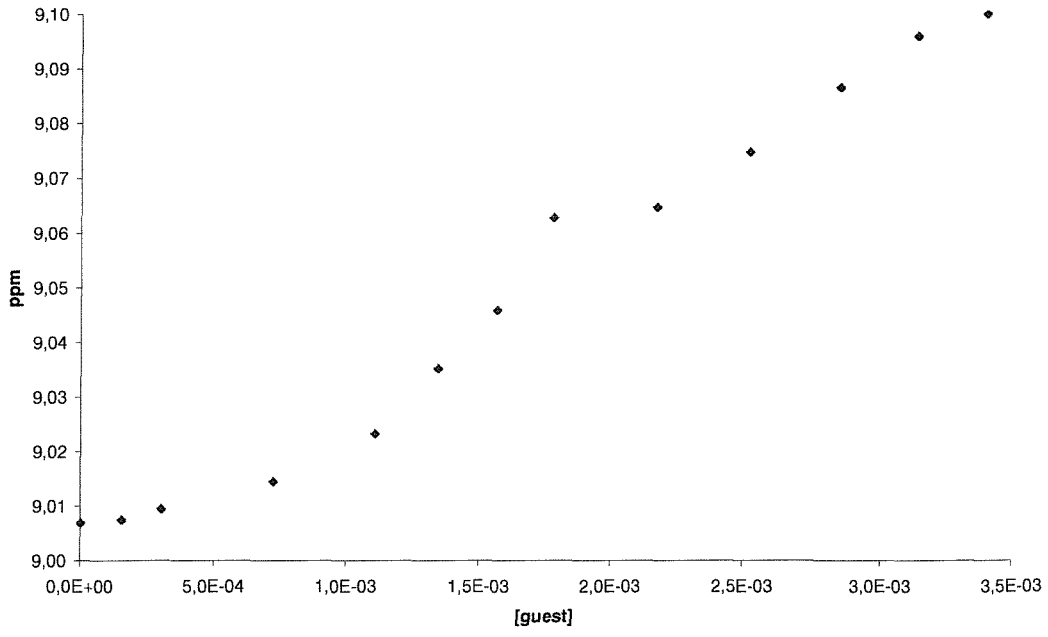

*Figure 3-11 Binding titration curves for macrocycle **123** showing the shift of the amide hydrogens upon addition* N-*Boc-D-aspartate. The 1:1 [host]:[guest] is reached when [guest] ~ 1.5 mM*

Calorimetric titrations were performed with both enantiomers in DMSO at 25°C, Table 3-3. The ITC binding data obtained with *N*-Boc-L-aspartate salt confirmed the simultaneous presence of 1:1 and a dominant 1:2 (host:guest) binding equilibrium ($\Delta G^{1:1}$ = -3.05 ± 0.5 kJ mol^{-1}). Both processes are promoted by the release of solvent molecules from the binding sites of the host to bulk solvent. Addition of *N*-Boc-D-aspartate to host **123** shows the presence of a quantifiable 1:1 and a dominant 1:2 (host:guest) binding complexation, dominated by the enthalpic contribution.

*Table 3-3 Binding constants (M^{-1}), association enthalpy and entropy (kJ mol^{-1}) for receptor **123** in DMSO at 25°C*

Guest	$K_a^{1:1}$	$\Delta H^{1:1}$	$T\Delta S^{1:1}$	$K_a^{1:2}$	$\Delta H^{1:2}$	$T\Delta S^{1:2}$
Boc-L-Asp	(8.72±0.8)x10^2	-19.8±0.6	-3.0	(2.31±0.38)x10^5	-2.15±0.3	5.2
Boc-D-Asp	(1.98±1.7)x10^2	17.8	31	(2.83±1.5)x10^3	-11.9±0.1	7.8

3.2.5 Conclusions

A conformationally restricted bisthiourea macrocyclic receptor has been successfully synthesised. The effects of the insertion of a more rigid subunit were investigated.

Like its parent receptor **106**, macrocycle **123** forms alternative conformers in DMSO and chloroform. A stable twisted conformation in chloroform is present even at room temperature, making the host unsuitable for the complexation of carboxylate salts in this apolar solvent.

In DMSO, the complexation of either enantiomer of both guests is characterised by multiple binding equilibria. As parent macrocycle **106**, in CD_3CN **123** binds the L enantiomer mostly in a 1:1 fashion, while 1:2 or even multiple binding equilibria arise with the D enantiomer. The receptor is selective for the 1:1 binding of the *N*-protected glutamate dianion, suggesting an enantioselectivity for the 1:1 binding of *N*-Boc-glutamate of 18:1 in favour of the L enantiomer, in deuterated acetonitrile.

Isothermal calorimetric studies showed that binding of glutamate is driven to a large extent by entropy, presumably produced by releasing bound solvent molecules from the binding sites of the host to bulk solvent. In the case of aspartate, the binding proved to be dominated by an enthalpic contribution, suggesting that the process is driven by the formation of host-guest hydrogen bonds.

It can be concluded that the conformational restraint had a clear effect in the receptor binding properties, resulting in a general loss of affinity towards both guests and the arising of multiple binding equilibria.

3.3 Benzo Bisthiourea Analogues 129 and 130

3.3.1 Receptors' Design

To determine the role of the pyridyl nitrogen in the preorganisation of the host, two benzo analogues were designed, Figure 3-12. It was thought that pyridyl thioureas **106** and **123** might give higher association constants than benzo thioureas **129** and **130** if the thiourea and amide hydrogens in **106** and **123** are held pointing inside the cavity of the host by weak hydrogen bonding with the pyridyl nitrogen as shown in Figure 2-1. There would be a smaller entropy loss upon binding if the receptor is in the correct conformation for complexation before the binding event took place. A smaller entropy loss should lead to a higher overall association constant due to the additional energy gained as a result of preorganisation.

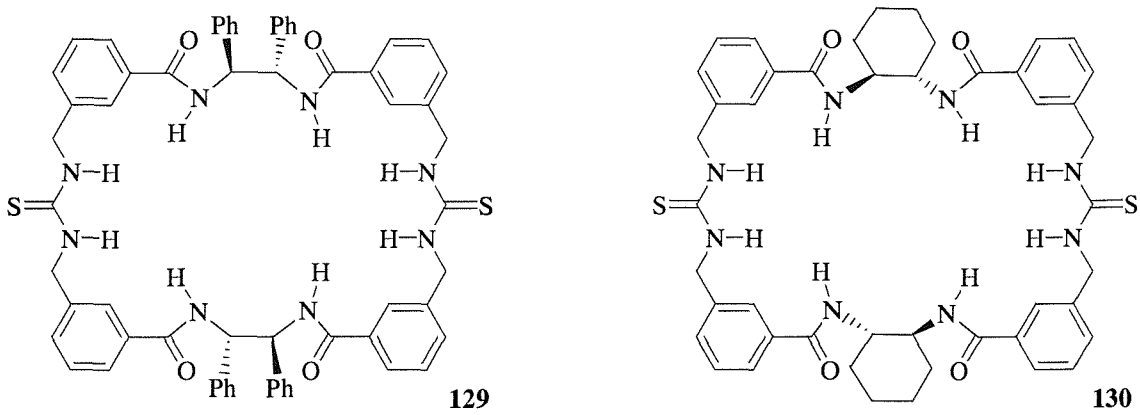

129 130

Figure 3-12 Design concept of benzo macrocyclic receptors

Moreover, changing from pyridyl to benzylic subunits could have a big impact in the receptor's conformation, similar to the case of the cyclic tetramers **131** and **132,** synthesised by Hunter, that were found to adopt two different conformations, Figure 3-13.[94] The two isophthaloyl groups in **132** interacted with each other, leading to a folded conformation, which was stabilised by two hydrogen-bonds and an offset p–stacking interaction.

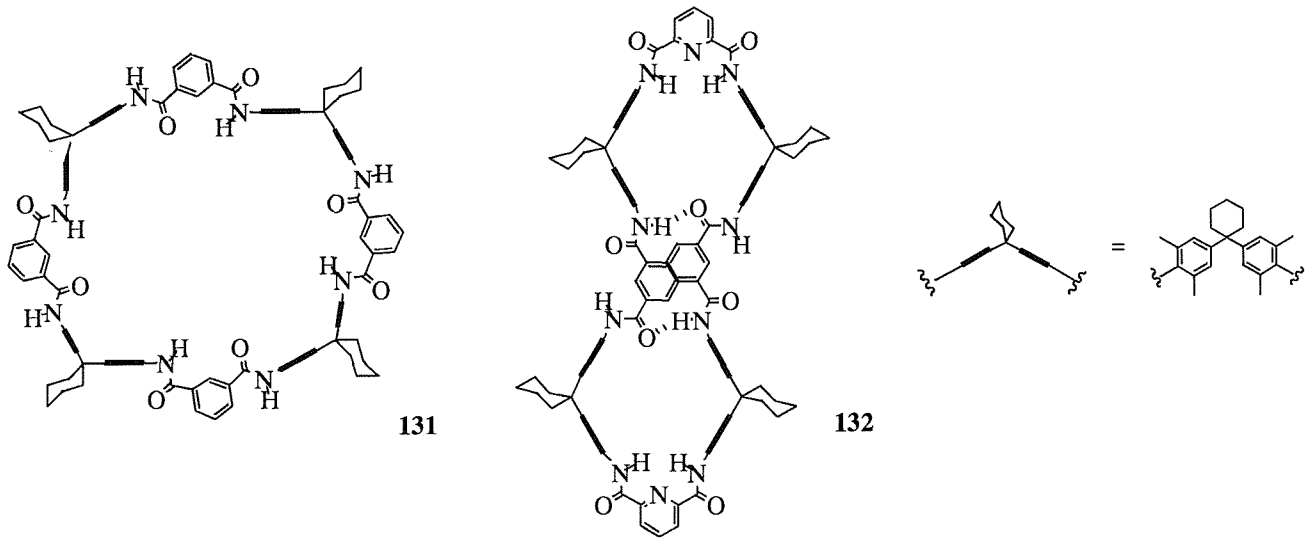

131 **132**

*Figure 3-13. Open and folded conformation adopted by **131** and **132**, respectively*

Molecular mechanics studies on the conformational preferences of the individual subunits provided a clue as to the origin of the difference between **131** and **132**. The 2,6-pyridyl derivative was found to prefer conformation *A*, which is stabilised by attractive electrostatic interactions between the amide protons and the pyridine nitrogen atom. Conformations *B* and *C* have unfavourable electrostatic interactions between the pyridine nitrogen and the carbonyl oxygen atoms. In contrast however, the lowest energy arrangement for the isophthaloyl derivative is conformation B. These conformational preferences would lead to an open conformation for **131** and a folded conformation for **132**.

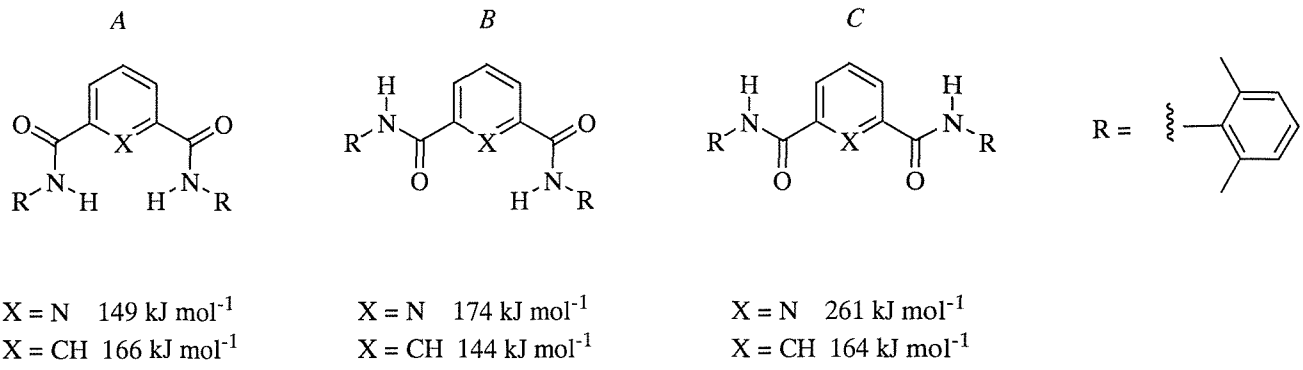

*Figure 3-14 Conformational preferences of the individual subunits of **131** and **132***

Further confirmation of these findings was obtained from the observation that **132** bound two quinone molecules in the two cavities generated by its folded conformation, whereas **131** fails to bind quinone due to its open conformation.

*3.3.2 Synthesis of Benzo Bisthiourea Receptor **129***

Commercially available 3-cyanobenzoic acid was converted into its chloride derivative and coupled with (*S*,*S*)-1,2-diphenylethylene diamine to afford *bis*cyanobenzamide **133** in an overall 48% yield. Following Caddick's procedure, the cyano group was then reduced to amine by using sodium borohydride.[125] To prevent dimerisation by-products, the diamine was trapped *in situ* using di-*tert*-butyl dicarbonate, to provide the Boc-protected diamine **134** in 64% yield. The reaction offered selectivity as the amide group was not affected under the reaction conditions. Palladium catalysed hydrogenolysis[126] was also tried but it proved to be ineffective. Recovery of the free diamine from the reaction mixture was very poor, even after washing the palladium residue with DMSO, probably due to the unwelcome absorption of the product onto the palladium surface. Free diamine **135** was obtained by standard Boc deprotection, by stirring **134** in a 1:1 solution of TFA and CH_2Cl_2.

Attempted cyclisations followed the same procedure as for hosts **106** and **123** failed. Therefore few changes were made. The formation of the *bis*isocyanate was accomplished by reacting diamine **135** with thiophosgene in presence of aqueous K_2CO_3. The formation of the *bis*-isocyanate was checked by TLC. No further purification was done, as the compound proved to be unstable on silica. The *bis*-isocyanate was then added to dry CH_2Cl_2 containing triethylamine along with one equivalent of diamine **135** in dry MeOH under a slow stream of nitrogen over 3 hours *via* syringe pump addition. The receptor precipitated out of solution. Recrystallisation from dimethylformamide and diethyl ether afforded receptor **129** in 17% yield.

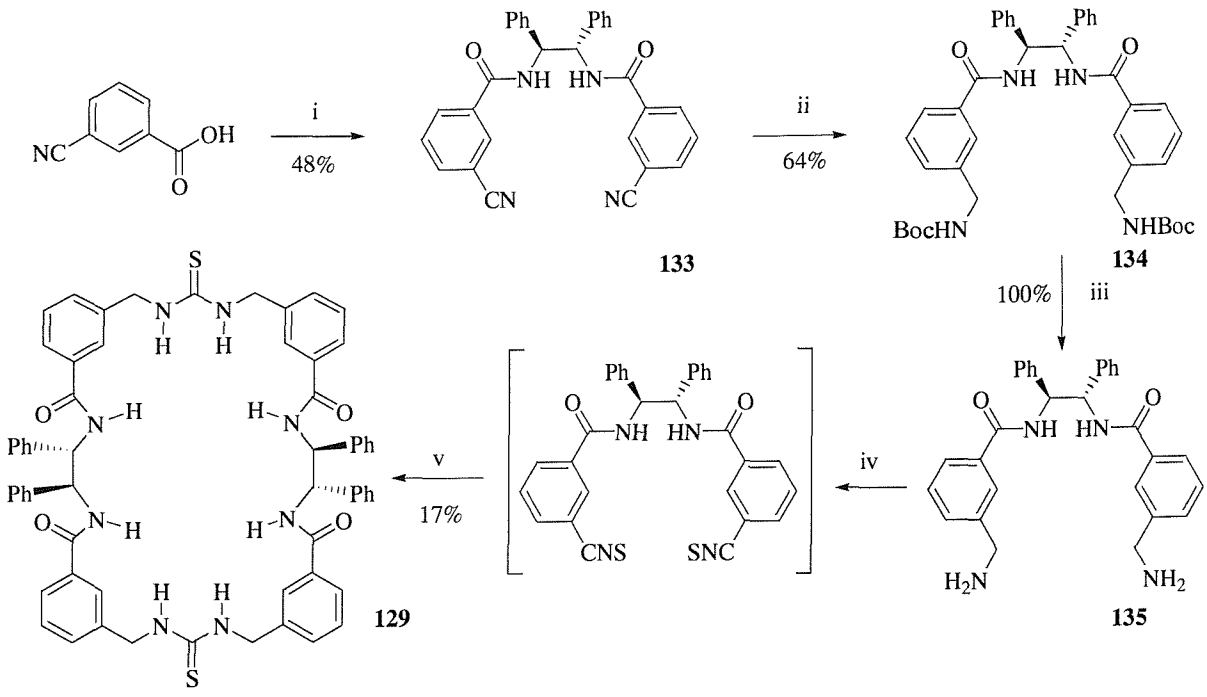

Scheme 3-2 Reagents and conditions: i) $SOCl_2$; (*S,S*)-1,2-diphenylethylene diamine hydrochloride, DMAP; ii) ditertbutyl dicarbonate, $NiCl_2$, $NaBH_4$; iii) TFA/DCM 1:1; iv) thiophosgene, v) slow addition of 1 equivalent of bisisothiocyanate and 1 equivalent of **135** to a solution of dry CH_2Cl_2/Et_3N at r.t. over 3 hours

3.3.3 Synthesis of Benzo Bisthiourea Receptor 130

Benzo receptor **130** was synthesised to compare its binding properties with thiourea receptor **123**. The route followed to produce macrocycle **130** was essentially the same as that developed for previous macrocycle **129**, Scheme 3-3. Commercially available 3-cyanobenzoic acid was activated in presence of diphenylchlorophosphate and coupled with (S,S)-1,2-cyclohexyldiamine as tartrate salt to give *bis*cyanobenzamide **136** in 97% yield. Following Caddick's procedure[125], the cyano group was then reduced to amine with sodium borohydride, in presence of nickel chloride. The free diamine was then trapped *in situ* with di-*tert*-butyl dicarbonate. The Boc-protected diamine **137** was obtained in 64% yield. Free diamine **138** was obtained by standard Boc deprotection, by stirring **137** in a 1:1 solution of TFA and CH_2Cl_2. Formation of the *bis*isocyanate was accomplished by reacting diamine **138** with thiophosgene in presence of aqueous K_2CO_3. The *bis*isocyanate was then added to dry CH_2Cl_2 containing triethylamine along with one equivalent of diamine **138** in dry CH_2Cl_2 under a slow stream of nitrogen over 3 hours *via* syringe pump addition. The receptor precipitated out of solution. Purification by semi-preparative HPLC afforded receptor **130** in 29% yield.

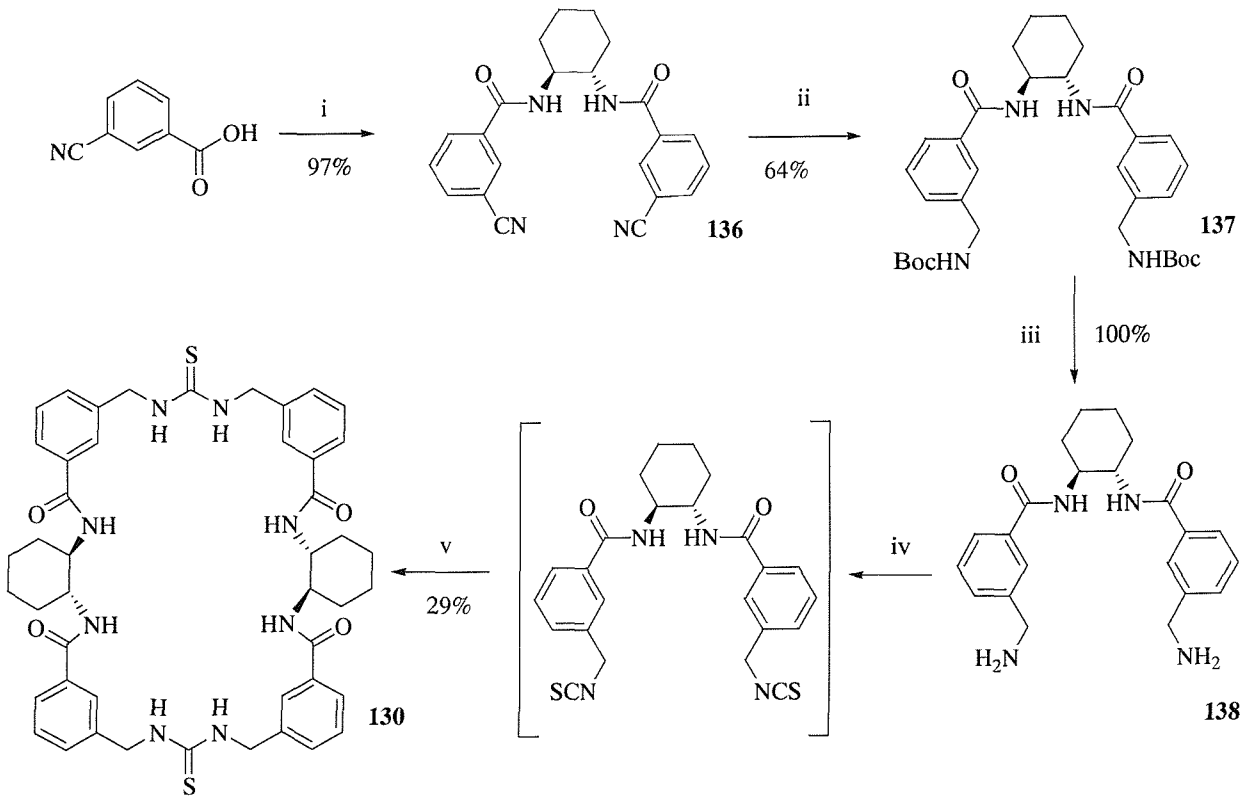

Scheme 3-3 Reagents and conditions: i) diphenylchlorophosphate, DCM; (*S,S*)-1,2-diaminocyclohexane, H_2O, K_2CO_3; ii) di-*tert*-butyl dicarbonate, $NiCl_2$, $NaBH_4$; iii) TFA/DCM 1:1; iv) thiophosgene, v) slow addition of 1 equivalent of bisisothiocyanate and 1 equivalent of **138** to a solution of dry CH_2Cl_2/Et_3N at r. t. over 3 hours

Once macrocycles **129** and **130** were synthesised, binding studies with glutamate were carried out using both traditional NMR techniques and isothermal calorimetry.

*3.3.4 Conformational Properties of Benzo Bisthiourea **129** and **130***

Bisthiourea **129** and **130** were found to be soluble only in DMSO and fluorinated alcohols. A well resolved spectrum was obtained by dissolving both receptors in DMSO-d_6 at room temperature, consistent with the expected fourfold D_2 symmetry, Figure 3-15. Unfortunately, albeit despite numerous efforts, it was not possible to grow crystals of the macrocycles in any solvent or solvent mixtures to obtain an X-ray structure. As it was not possible to have a direct evaluation of the solution conformation of the host, molecular modelling studies on the conformational properties of free receptor **129** were carried out. The molecular modelling package used was MacroModel V5.0[127] along with its implementation of the OPLS* force field. Solvent was included in all the calculations through the use of the GB/SA continuum model for chloroform.[128] The structure was subjected to a minimisation process, using the Polak-Ribiek method, which served to change bond lengths and angles to those which are reasonable. After the first minimisation the structure was subjected to a simulated annealing process, where the temperature was set to 400K and the system cooled over the course of 1ns to 0K. The process of allowing slow cooling should allow the

macrocycle to explore a number of conformations. After the simulated anneal, the structure should be near or at the global energy minimum. The free receptor was found to adopt a tightly wrapped configuration similar to parent receptor **106**. It has to be stressed that these results are purely qualitative as it was not possible to gain direct NOESY data.

a)

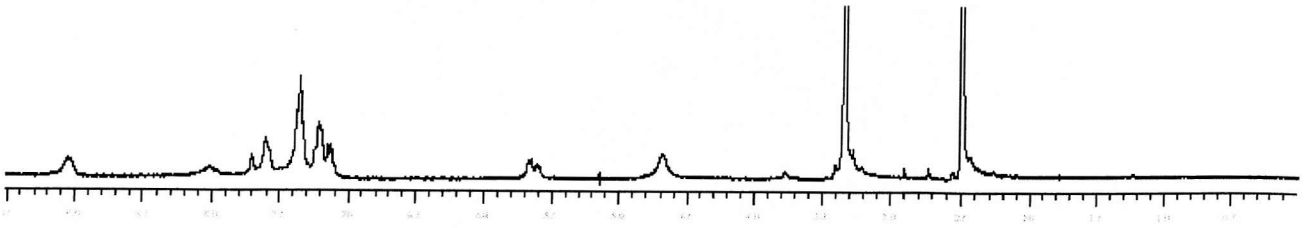

b)

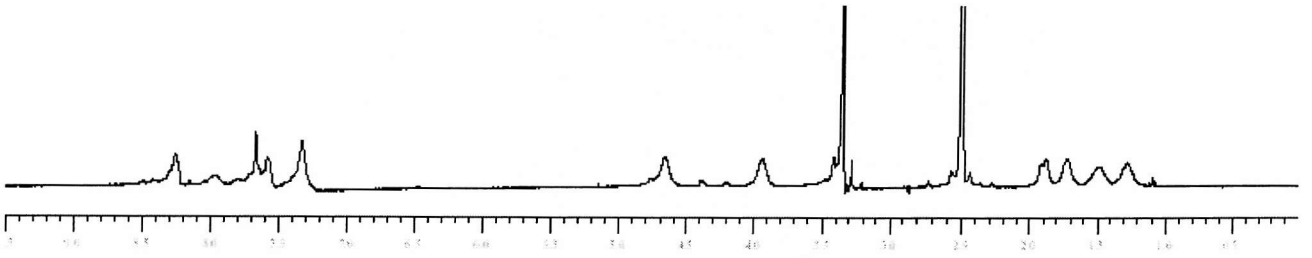

*Figure 3-15 NMR spectra of **129** and **130** in DMSO-d_6 at r. t.*

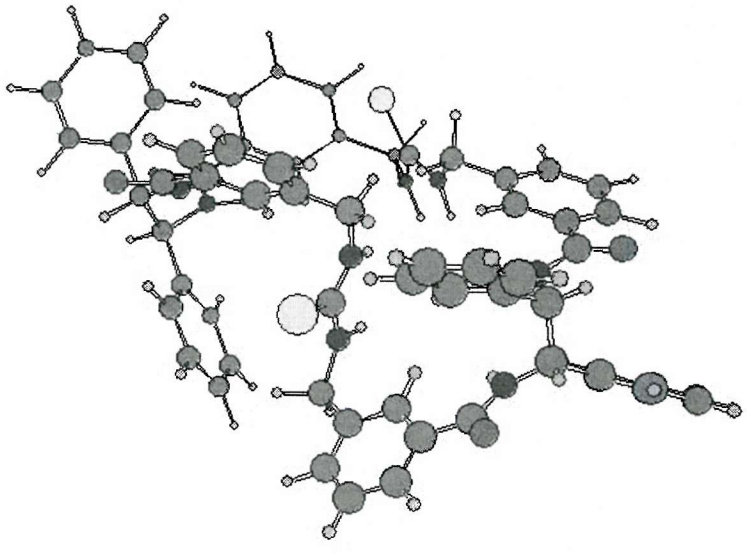

*Figure 3-16 Molecular modelling studies on the methyl derivative of receptor **129***

3.3.5 *Binding Studies of Receptor **129** and **130** - Investigation of the Preorganisation Hypothesis*

With benzo macrocycles **129** and **130** in hand the corresponding association constants for these systems with both enantiomers of *N*-Boc-glutamate were measured using the procedure outlined in chapter five.

Evidence for preorganisation of **106** as compared to **129** was gained by examination of the starting chemical shifts of the amide H^1 and H^3 and the thiourea hydrogens H^2 and H^4 in DMSO. Amide hydrogen H^1 had a starting chemical shift of 9.47 ppm, whereas amide hydrogen H^3 had a starting chemical shift of 9.03 ppm. Thus, H^1 showed a chemical shift 0.44 ppm further downfield than H^3, indicating the possibility of hydrogen-bonds between the pyridyl nitrogens and thiourea hydrogens. Likewise the thiourea hydrogens H^2 were found to be 0.38 ppm further downfield in **106** than H^4 in **129**, again indicating hydrogen-bonding interactions. The free host chemical shifts for Hunter's pyridyl cyclic tetramer **132** were also significantly more downfield that the corresponding free host chemical shifts for benzo cyclic tetramer **131** (Figure 3-13 and Figure 3-14).

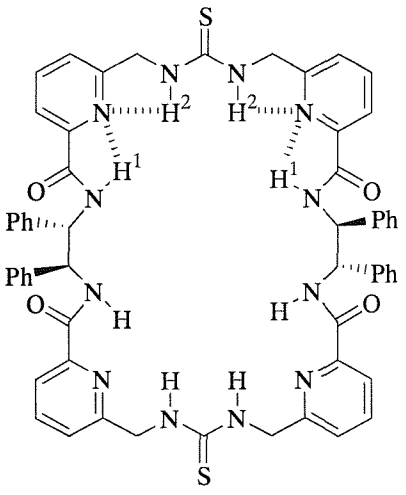

106

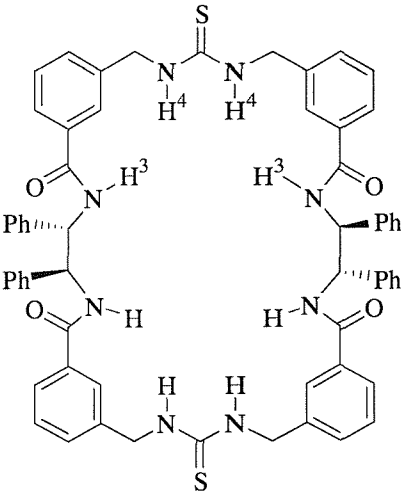

129

H^1 δ_{start} = 9.47
H^2 δ_{start} = 8.39

H^3 δ_{start} = 9.03
H^4 δ_{start} = 8.01

*Figure 3-17 Starting chemical shifts for receptors **106** and **129** in DMSO*

The higher free host chemical shift values for **106** seem to suggest hydrogen-bond formation between the thiourea/amide hydrogens and pyridyl nitrogens and therefore a certain degree of preorganisation. Comparison of the starting chemical shifts of the amide hydrogens H^5 and H^7 and thiourea hydrogens H^6 and H^8 of **123** and **130** confirmed the existence of a certain degree of preorganisation in **123**, given by the presence of pyridine subunits. Amide hydrogen H^5 had a starting chemical shift of 9.02 ppm, whereas amide hydrogen H^7 had a starting chemical shift of 8.31 ppm. Thus, H^5 showed a chemical shift 0.71 ppm further downfield than H^7, indicating the likely presence of hydrogen-bonds between the pyridyl nitrogens and thiourea hydrogens. Like-

wise, the thiourea hydrogens H^6 were found to be 0.35 ppm further downfield in **123** than H^8 in **130**, again indicating hydrogen-bonding interactions.

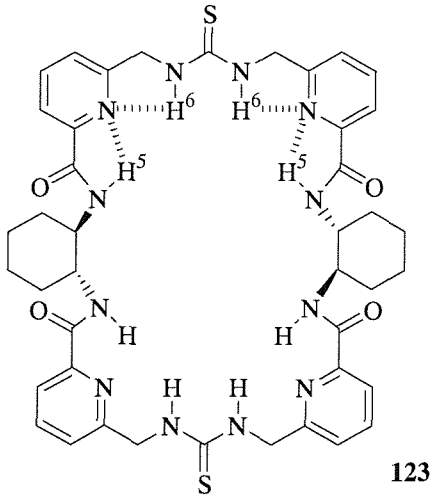

123

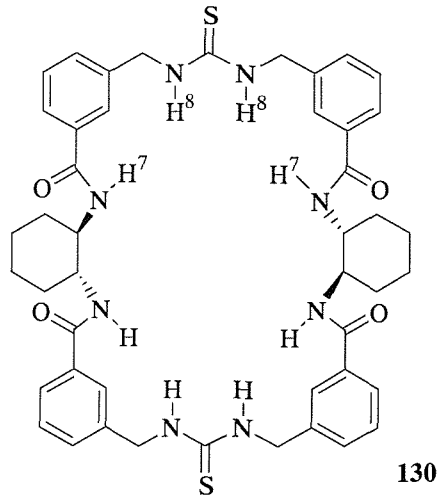

130

H^5 δ_{start} = 9.02
H^6 δ_{start} = 8.59

H^7 δ_{start} = 8.31
H^8 δ_{start} = 8.24

*Figure 3-18 Starting chemical shifts for receptors **123** and **130***

The above results were further confirmed by previous work in the group, pg 55, Figure 2-7.

Binding studies of the macrocyclic receptors **129** and **130** in DMSO were performed. Addition of *N*-Boc-L-glutamate tetrabutylammonium salt to a solution of **129** in DMSO at room temperature led to a dramatic change in the ^{1}H NMR spectrum of the macrocycle. Downfield shifts of the thiourea NH ($\Delta\delta_{max}$ = 0.52 ppm), the amide NH ($\Delta\delta_{max}$ = 0.29 ppm) were noted after the addition of guest. A further shift was registered upon the addition of more guest, suggesting that saturation was not reached after the addition of the first equivalent of *N*-Boc-L-glutamate. The binding data, however, could not be fitted to a 1:1 or 1:2 (host:guest) isotherm. Macrocycle **106** proved to bind *N*-Boc-L-glutamate in a simple 1:1 fashion with an association constant of 3.7 x 10^3 M^{-1}. The difference in the binding affinity of **129** towards *N*-Boc-L-glutamate can be ascribed to the lack of intramolecular hydrogen bonding between the pyridyl nitrogens and thiourea/amide hydrogens, which results in a higher conformational freedom of the receptor. These results seem to imply a higher preorganisation in hosts **106**.

Addition of the *N*-Boc-D-glutamate tetrabutylammonium salt to **129** also led to significant downfield shifts of the thiourea NH ($\Delta\delta_{max}$ = 1.08 ppm), amide NH ($\Delta\delta_{max}$ = 0.37 ppm) protons of the receptor. From the ^{1}H NMR spectra, it seemed that saturation was reached after the addition of two equivalents of guest. Indeed, the binding data could be fitted to a 1:2 (host:guest) isotherm and yielded a $K_a^{1:2}$ of 1.03 x 10^3 M^{-1}.[117] Addition of the same guest to **106** led to multiple binding equilibria competing with each other.

To verify the presence of multiple equilibria, calorimetric measurements were performed in DMSO at 25°C, Table 3-4.

*Table 3-4 Binding constants (M^{-1}), association enthalpy and entropy (kJ mol^{-1}) for receptor **129** in dry DMSO at 25°C*

Guest	$K_a^{1:1}$	$\Delta H^{1:1}$	$T\Delta S^{1:1}$	$K_a^{1:2}$	$\Delta H^{1:2}$	$T\Delta S^{1:2}$
Boc-L-Glu	(4.49±4.2)x10^4	-10.2±0.2	16.4	(4.16±1.4)x10^3	-1.77±0.3	15.7
Boc-D-Glu	262±0.4	-4.4±0.3	9.41	(1.94±0.2)x10^4	-7.9±0.2	16.5

The calorimetric binding data obtained with *N*-Boc-L-glutamate salt showed a strong 1:1 binding ($\Delta G^{1:1}$ = -26.6 ± 0.5 kJ mol^{-1}) and a measurable 1:2 (host:guest) association ($\Delta G^{1:1}$ = -17.5 ± 0.2 kJ mol^{-1}), dominated by the entropic contribution, indicating an association promoted by the release of solvent molecules from the binding sites of the host. Complexation of *N*-Boc-L-glutamate by **106** proved to be exothermic and characterised by a large entropic contribution, with a $Ka^{1:1}$ = (2.28 ± 0.26) x 10^3 M^{-1}. The stronger association constant observed for benzo thiourea **129** over pyridyl thiourea **106** is consistent with studies by Crabtree, pg 56, Figure 2-9.

The calorimetric data obtained with the *N*-Boc-D-glutamate salt and **129** yielded a small 1:1 binding complexation ($\Delta G^{1:1}$ = -13.8 ± 0.2 kJ mol^{-1}) and a large 1:2 (host:guest) binding ($\Delta G^{1:2}$ = -24.5 ± 0.3 kJ mol^{-1}), which again is dominated by the entropic contribution. This data confirms the stronger binding of the second guest relative to the first, as indicated by the NMR titrations and the presence of a possible positive co-operation. Isothermal calorimetry studies on the complexation of *N*-Boc-D-glutamate with **106** showed the presence of multiple binding equilibria, as evidenced by the ^1H NMR studies. It was not possible to fit the ITC curve and, therefore, to get meaningful values.

Addition of either enantiomers of *N*-Boc-glutamate to a solution of benzo bisthiourea **130** in DMSO at room temperature did not lead to any significant shifts in the ^1H NMR spectrum of the neat host, suggesting no or very weak binding.

3.3.6 Conclusions

As a result of the experiments undertaken *vide supra*, it was concluded that, although the association constant for the 1:1 complexation of *N*-Boc-L-glutamate with benzo thiourea **129** is higher than that for the corresponding pyridyl thiourea **106**, the chemical shifts for both the thiourea and amide hydrogens in **106** are significantly more downfield than in benzo thiourea **129**. The higher free host chemical shift values for **106** and the presence of multiple binding equilibria for **129** suggest hydrogen-bond formation between the thiourea/amide hydrogens and pyridyl nitrogens

and therefore a degree of preorganisation. Similar higher free host chemical shifts values were noted for **123** compared to **130**, confirming the hypothesis of a higher degree of preorganisation in the pyridyl receptors.

An alternative approach to further verify the preorganised conformation hypothesis is to compare the difference in enantioselectivities between chiral pyridyl receptors **106** and **123** and chiral benzo hosts **129** and **130** for the enantiomers of a given carboxylate substrate. If the difference in free energies (? ? G) between the enantiomers of a carboxylate guest is larger for pyridyl macrocycles than benzo ones then we could conclude that this difference is due to the increased level of preorganisation in **106**. Unfortunately, the presence of multiple equilibria did not allow us to apply this method.

3.4 Guanidinium Bisthiourea Macrocyclic Analogue

To investigate the role of the carboxylic binding site, it was decided to convert the carboxylic binding moiety from thiourea to guanidinium. The guanidinium group as a carboxylate binding site possesses several useful features. Firstly, it remains protonated over a wide pH range due to its high pK_a, which for guanidinium itself is 13.5. Guanidiniums can also form characteristic pairs of zwitterionic hydrogen bonds, which provide binding strength due to their charge and structural organisation as evidenced from the crystal structure of many guanidinium salts. Various examples exist in literature, as presented in chapter one, § 1.5.4. Due to the availability of receptor **123**, it was decided to start from the synthesis of its guanidinium analogue, **139**, Figure 3-19.

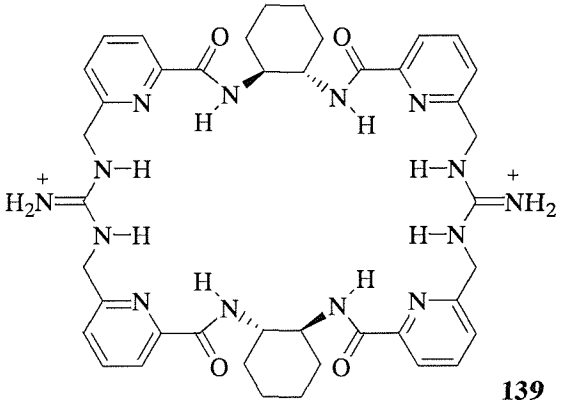

139

Figure 3-19. Design concept of guanidinium macrocyclic receptor

*3.4.1 Attempted Synthesis of Guanidinium Bisthiourea Receptor **139***

The method chosen for converting the thiourea to a guanidinium functionality was to first transform bisthiourea **123** to bisthiouronium iodide **140** followed by reaction with ammonia to produce the

corresponding bisguanidinium iodide **139** and methanethiol, Scheme 3-4. The disappearance of the starting material and the formation of the product were monitored by TLC. The bisthiouronium salt **140** was dissolved in methanol previously saturated with gaseous ammonia. The flask was sealed and the solution stirred at high temperature for a few hours. The crude material was then purified by semi-preparative HPLC. Five main fractions were collected. Three fractions were identified as a mixed guanidine/thiourea macrocycle **141**, starting material, **123**, and an unclean fraction of the bisguanidinium derivative **139**. Two of the main products could not be identified, probably decomposition products. As the presence of iodide ions in the reaction could be responsible for the formation of reversible equilibriums, the synthesis was repeated. Before the reaction with ammonia, the iodide ion was exchanged with hexafluoro phosphate by using silver hexafluoro phosphate. The complete ion exchange was confirmed by mass spectrometry (ES^-). Unfortunately, although the crude yield of the bisguanidinium receptor **139** improved, it was not possible to obtain a pure fraction of the product. Although a peak corresponding to $[M+H]^+$ was detected in the low resolution mass spectrum, no proper NMR characterisation could be obtained. The product proved also to be contaminated with silver, which could not be completely eliminated. Due to time constraints it was not possible to further investigate alternative synthetic approaches. Nevertheless, with few milligrams of **141** in hands, it was decided to perform some binding studies.

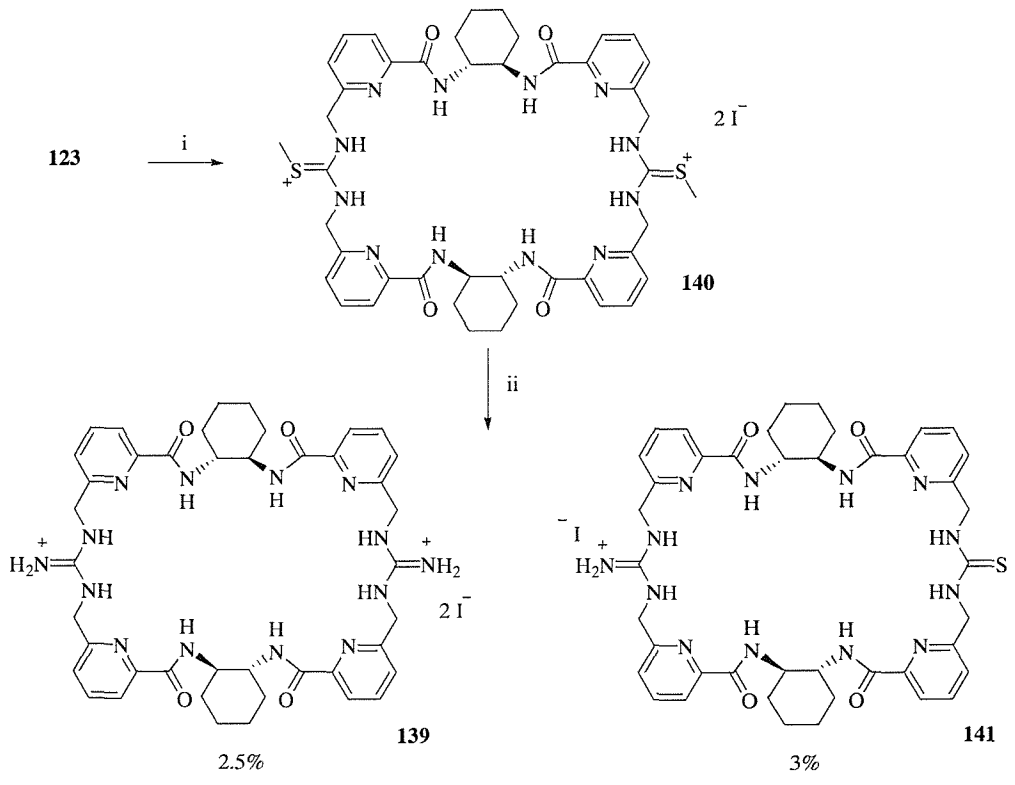

Scheme 3-4 Reagents and conditions: i) methyl iodide, acetone; ii) MeOH saturated with ammonia

*3.4.2 Binding Studies of Receptor **141***

The receptor proved to be insoluble in acetonitrile and only partly soluble in methanol. A well resolved spectrum was obtained in DMSO-d_6 at room temperature, which was the solvent of choice to perform some NMR titrations, Figure 3-20.

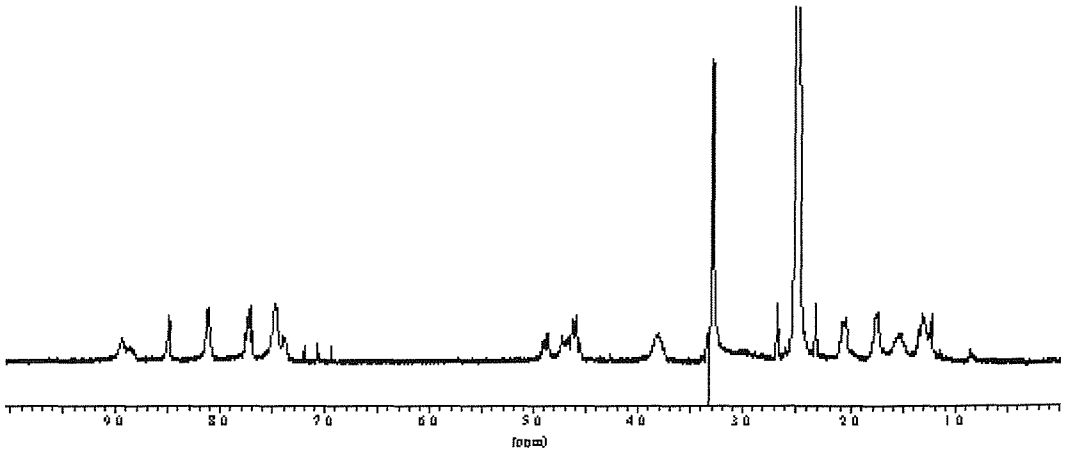

*Figure 3-20 ^1H NMR spectrum of **141** in DMSO at room temperature*

COSY ^1H NMR has been run in deuterated dimethyl sulphoxide at room temperature, allowing for full assignment of all the ^1H NMR signals.
Unfortunately, addition of either enantiomer of N-Boc-glutamate to a solution of macrocycle **128** in DMSO did not lead to any meaningful chemical shifts of the signals of the receptor.

3.5 Conclusions and outlooks

Chapter two discussed the properties of bisthiourea receptor **106**, which was found to be highly selective and enantioselective towards the neurotransmitter glutamate. The receptor proved to be highly selective for the 1:1 binding of the *N*-protected glutamate dianion, suggesting an enantioselectivity for the 1:1 binding of *N*-Boc-glutamate of > 700:1 in favour of the L enantiomer. It was also found to have anomalous solvent-dependent behaviour, due to the formation of alternative conformers in DMSO and chloroform. Different guests were investigated, the receptor proved to bind the L enantiomers in a 1:1 fashion, while a 1:2 or even multiple equilibria arise when the D enantiomer was added.

Starting from these results, analogous receptors were developed in order to investigate and hopefully enhance its binding properties. The experiments, explained in the present chapter, allowed us to get a better understanding of the conformational and binding properties of the original receptor **106**.

Analogous receptors incorporating recognition elements for the ammonium group could be now envisaged to produce enantioselective receptors for zwitterionic glutamate. Incorporation of a fluorescent tag would then produce a sensor for glutamate.

4 Experimental

4.1 General Experimental and Instrumentation

4.1.1 General Experimental

Reactions were carried out in solvents of commercial grade and, where necessary, distilled prior to use (for solvent distilling procedures see Purification of Laboratory Chemical by Perrin and Armarego). THF was distilled under nitrogen from benzophenone and sodium. CH_2Cl_2 was distilled from calcium hydride, as was petroleum ether where the fraction boiling between 40 and 60°C was used. TLC was conducted on foil backed sheets coated with silica gel (0.25 mm) which contained the fluorescent indicator UV_{254}. Column chromatography was performed on Sorbsil C60, 40-60 mesh silica.

4.1.2 Instrumentation

^1H NMR spectra were obtained at 300 MHz on Brüker AC300 and Brüker AM 300 spectrometers and at 400 MHz on a Brüker DPX400 spectrometer. ^{13}C NMR spectra were obtained at 75 MHz on Brüker AC300 and Brüker AM 300 spectrometers and at 100 MHz on a Brüker DPX400 spectrometer. Spectra were referenced with respect to the residual solvent peak for the deuterated solvent. Infrared spectra were obtained on BIORAD Golden Gate FTS 135. Spectra were obtained as neat solids or as oils. All melting points were measured in open capillary tubes using a Gallenkamp Electrothermal Melting Point Apparatus and are uncorrected. Optical rotations were measured on a PolAr2001 polarimeter using the solvent stated, the concentration given is in g/100 mL. Electrospray mass spectra were obtained on a Micromass platform with a quadrupole mass analyser. FAB spectra were obtained on a VG Analytical 70-250-SE normal geometry double focusing mass spectrometer. High-resolution accurate mass measurements were carried out at 10,000 resolution using mixtures of polyethylene glycols and/or polyethylene glycol methyl ethers as mass calibrants for FAB. Analytical HPLC spectra were obtained using a Hewlett Packard HP1100 Chemstation, using a Phenomenex C18 prodigy 5μm (150 mm x 3 mm) column. Water (0.1% TFA) and acetonitrile (0.04% TFA) gradient was employed. Semi-preparative reverse-phase HPLC was carried out using a Hewlett Packard HP1100 Chemstation with an automated fractions collector and a Phenomenex C18 prodigy 5 μm (250 mm x 10 mm) column. Water

(0.1% TFA) and acetonitrile (0.04% TFA) gradient was employed. Calorimetric experiments were performed on an Isothermal Titration Calorimeter from Microcal Inc., Northampton, Massachussetts, USA.

4.2 Experimental for Chapter Two

Diethyl 2,6-pyridine dicarboxylate – 94

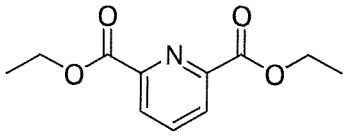

Commercially available 2,6-pyridinedicarboxylic acid (25.1 g, 0.11 mol) was heated at reflux with $SOCl_2$ (88 mL, 0.74 mmol) for 24 hours. After removal of thionyl chloride *in vacuo*, the acyl chloride was suspended in dry CH_2Cl_2 (13 mL) and dry ethanol (125 mL) was added dropwise at 0°C and stirred for 18 hours at room temperature. The solution was then made neutral by dropwise addition of saturated aqueous Na_2CO_3, followed by addition of water (50 mL). The solution was dried over $MgSO_4$, the insoluble material filtered off and the solvent removed *in vacuo* yielding compound **94** as a white solid (24.4 g, 97%): R_f = 0.9 (5% methanol / CH_2Cl_2); m.p. = 47-49°C; IR (neat) ν_{max} = 3061 (m), 1739 (s), 1231 (s) cm^{-1}; ^1H NMR (300MHz, $CDCl_3$) δ 8.25 (2H, d, *J* = 8Hz, Pyr), 7.98 (1H, t, *J* = 8Hz, Pyr), 4.45 (4H, q, *J* = 7Hz, CH_2), 1.42 (6H, t, *J* = 7Hz, CH_3); $^{13}CNMR$ (75MHz, $CDCl_3$) δ 165.0 (0), 148.8 (0), 138.4 (1), 127.9 (1), 62.5 (2), 14.4 (3); *m/z* (ES+) 224 $[M+H]^+$ 246 $[M+Na]^+$, 469 $[2M+Na]^+$ Data consistent with literature [93]

Hydroxymethylpyridine-2-carboxylic acid ethyl ester – 95 [97]

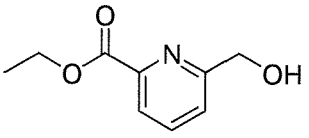

This procedure was modified from that of Fife.[97] To a solution of compound **94** (16.2 g, 89 mmol) in dry ethanol (165 mL), sodium borohydride (1.37 g, 36 mmol) was added. The mixture was refluxed for 2 hours. After allowing cooling to room temperature, water (100 mL) was added and the

solution extracted with chloroform (3 x 100 mL). The organic layers were combined, dried over $MgSO_4$ and the solvent removed *in vacuo* affording a yellow solid. Purification by recrystallisation from chloroform / petrol ether yielded compound **95** as a white solid (7.92 g, 50%): m.p. 93-94°C; IR (neat) ν_{max} = 3263 (br), 1729 (s), 1217 (s) cm^{-1}; ^1H NMR (300MHz, $CDCl_3$) δ 8.01 (1H, d, *J* = 8Hz, PyrH), 7.83 (1H, t, *J* = 8Hz, PyrH), 7.52 (1H, d, *J* = 8Hz, PyrH), 4.86 (2H, s, CH_2OH), 4.46 (2H, q, *J* = 8Hz, CH_2CH_3), 1.43 (3H, t, *J* = 8Hz, CH_2CH_3); ^{13}C NMR (75MHz, $CDCl_3$) δ 165.2 (0), 160.4 (0), 147.4 (0), 137.8 (1), 124.1 (1), 123.8 (1), 64.7 (2), 62.1 (2), 14.4 (3); *m/z* (ES+) 182 $[M+H]^+$ 204 $[M+Na]^+$, 385 $[2M+Na]^+$

Data consistent with that reported by Fife *et al.* [97] and with those previously reported [93]

Ethyl 6-chloromethyl-2-pyridine carboxylate– 96 [98]

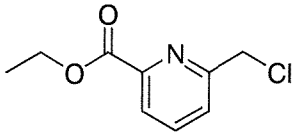

This procedure was modified from that of Scrimin and Tonellato.[98] Compound **95** (7.17 g, 40 mmol) was stirred in neat thionyl chloride (18.5 mL, 0.16 mmol) at 0°C for 1 hour. Thionyl chloride was then removed *in vacuo* to afford a slightly pink oil. Toluene (20 mL) was added to the residue and a 1 M solution of $NaHCO_3$ was added dropwise until the bubbling had subsided. The organic layer was separated, dried over $MgSO_4$ and the solvent removed *in vacuo* to produce compound **96** as a pale orange oil (7.0 g, 88%): IR (neat) ν_{max} = 1713 (s) cm^{-1}; ^1H NMR (400MHz, $CDCl_3$) δ 8.09 (1H, dd, *J* = 8, 1Hz, Pyr H), 7.85 (1H, t, *J* = 8Hz, Pyr H), 7.68 (1H, dd, *J* = 8, 1Hz, Pyr H), 4.82 (2H, s, CH_2Cl), 4.41 (2H, q, *J* = 7Hz, CH_2CH_3), 1.33 (3H, t, *J* = 7Hz, CH_2CH_3); ^{13}C NMR (100MHz, $CDCl_3$) δ 164.7 (0), 157.2 (0), 147.7 (0), 138.0 (1), 125.8 (1), 124.3 (1), 61.9 (2), 45.9 (2), 14.2 (3); *m/z* (ES+) 301 $[M+H]^+$

Data consistent with those reported by Scrimin and Tonellato [98] and previously [93]

Ethyl 6[1,3-dioxo-2,3-dihydro-1*H*-2-isoindolyl)methyl]-2-pyridine carboxylate– 97

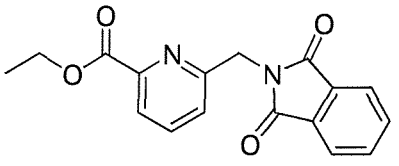

Compound **96** (7.85 g, 35 mmol) was dissolved in anhydrous DMF (8 mL) and slowly added to potassium phtalimide (7.22 g, 39 mmol). After stirring for 1 hour at room temperature and overnight at 60°C, the solvent was removed *in vacuo*. The resultant solid was dissolved in $CHCl_3$ (70 mL) and washed with 0.2 M NaOH (4 x 50 mL), water (50 mL) and dried over $MgSO_4$. The solvent was removed *in vacuo* yielding compound **97** as a white solid (11.6 g, 93%); m.p. 118-120°C; IR (neat) ν_{max} = 1764 (m), 1690 (s), 1586 (w), 1458 (w), 1379 (m) cm^{-1}; ^1H NMR (300MHz, $CDCl_3$) δ 8.01 (1H, d, *J* = 8Hz, Pyr), 7.70-7.90 (5H, m, Pht + Pyr H), 7.35 (1H, d, *J* = 8Hz, Pyr), 5.12 (2H, s, CH_2N), 4.38 (2H, q, *J* = 7Hz, CH_2O), 1.31 (3H, t, *J* = 7Hz, CH_3); ^{13}C NMR (75MHz, $CDCl_3$) δ 173.8 (0), 168.3 (0), 156.1 (0), 149.0 (0), 137.9 (0), 134.5 (1), 134.3 (1), 132.3 (1), 123.9 (1), 123.7 (1), 61.9 (2), 43.2 (2), 14.3 (3); *m/z* (ES+) 333 $[M+Na]^+$, 643 $[2M+Na]^+$

Data consistent with those previously reported [93]

6-[(1,3-dioxo-2,3-dihydro-1*H*-2isoindolyl)methyl]-2-pyridine carboxylic acid – 98 [99]

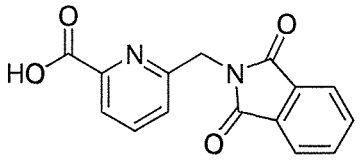

This procedure is modified from that of Olah *et al.* [99] To a solution of compound **97** (8.5 g, 0.027 mol) and LiI (16.5 g, 0.12 mol) in acetonitrile (46 mL) was slowly added chlorotrimethylsilane (14 mL) at 0°C. The reaction was allowed to warm to room temperature and then refluxed for 4 days. After

allowing cooling to room temperature, the solvent was removed *in vacuo* to afford a crude yellow solid. Water (200 mL) and ethyl acetate (100 mL) were added. The organic phase was washed again with water (100 mL) and aqueous sodium thiosulfate (10% wt, 150 mL) to remove inorganic salts and residual iodine. The solvent was then removed *in vacuo* yielding compound **98** as a pale yellow solid (6.52 g, 86%) without any further purification: m.p. 219-221°C; IR (neat) ν_{max} = 3327 (b), 3031 (w), 1752 (s), 1703 (s), 1370 (m) cm^{-1}; ^1H NMR (300MHz, $CDCl_3$ / 10% DMSO) δ 7.96 (1H, d, *J* = 8Hz, Pyr), 7.82-7.71 (5H, m, Phth H + Pyr H), 7.31 (1H, d, *J* = 8Hz, Pyr), 5.02 (2H, s, CH_2); ^{13}C NMR (75MHz $CDCl_3$ / 10% DMSO) δ 167.5 (0), 165.8 (0), 155.5 (0), 147.9 (0), 137.9 (0), 134.1 (1), 131.6 (1), 123.7 (1), 123.3 (1), 123.1 (1), 42.5 (2); *m/z* (ES+) 283 $[M+H]^+$, 305 $[M+Na]^+$
Data consistent with data previously reported [93]

N1-[3-({[(2*R*)-2-Boc-amino-3-phenylpropanoyl]amino} methyl)benzyl]-(2*S*)-2-Boc-amino-3-phenylpropanamide – 99

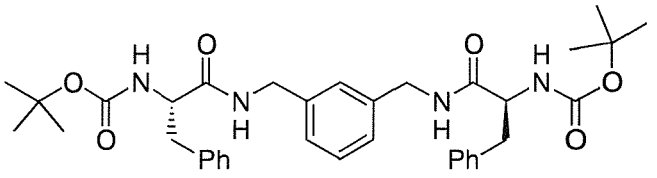

To a solution of *N*-tert-butoxycarbonyl-L-phenylalanine (400 mg, 1.4 mmol) in dry CH_2Cl_2 (20 mL) was added 1-hydroxybenzotriazole hydrate (200 mg, 1.6 mmol) and DMAP (10% wt, 50 mg). 1-[3-(Dimethylamino)propyl]-3-ethylcarbodiimide hydrochloride (300 mg, 1.4 mmol) was added to the suspension and stirred at room temperature for 30 minutes. *m*-Xylylenediamine (180 μL, 1.4 mmol) and triethylamine (140 μL, 1.4 mmol) were added and the mixture stirred at room temperature for 16 hours. The white precipitate was filtered off and the solution washed with 1 M HCl (2 x 20 mL), 1 M NaOH (2 x 20 mL), water (20 mL) and dried over $MgSO_4$. The solvent was then evaporated *in vacuo* to afford compound **99** as a white solid (400 mg, 68%): IR ν_{max} = 3330 (b), 1681 (s), 1654 (s), 1518 (s), 1236 (m) cm^{-1}; ^1H NMR (300MHz, DMSO) δ 7.68 (2H, t, *J* = 6Hz, CH_2NH), 6.90-7.30 (14H, m, ArH), 5.81 (2H, d, *J* = 9Hz, BocNH), 4.10-4.40 (6H, m, CH_2N + CHN), 3.07 (2H, dd, *J* = 14, 9Hz, $PhCH^AH^BNH$), 2.85 (2H, dd, *J* = 14, 9Hz, $PhCH^AH^BNH$), 1.34 (18H, s, CH_3); ^{13}C NMR (75MHz, DMSO) δ 171.3 (0), 168.5

(0), 155.0 (0), 138.3 (0), 136.9 (1), 129.0 (1), 128.3 (1), 127.9 (1), 126.6 (1), 126.1 (1), 78.9 (0), 55.4 (1), 42.6 (2), 38.3 (2), 27.9 (3); *m/z* (ES+) 631 $[M+H]^+$ 653 $[M+Na]^+$, 1283 $[2M+Na]^+$

N1-[3-({[(2*R*)-2- amino-3-phenylpropanoyl]amino} methyl)benzyl]-(2*S*)-2- amino-3-phenyl propanamide – 100

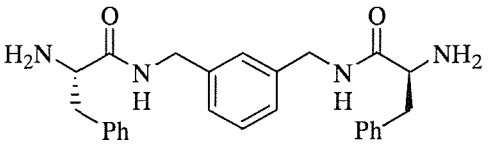

A solution of **99** (2.2 g, 3.5 mmol) was dissolved in a 1:1 solution of TFA and CH_2Cl_2 (58 mL) and stirred at room temperature for 3 hours. Toluene (60 mL) was added and the solution concentrated *in vacuo* to afford a yellowish oil, which was then triturated with diethyl ether to yield a pale yellow solid (2.0 g, 100%). The diamine as TFA salt was partitioned between 1 M aqueous NaOH (10 mL) and $CHCl_3$ (10 mL). The aqueous phase was then washed with $CHCl_3$ (2 x 5 mL). The organic layers were combined, dried over $MgSO_4$ and the solvent evaporated under reduced pressure to afford the free diamine **100** as a white solid (1.3 g, 65%); m.p. = 120-121°C; IR ν_{max} = 3277 (s), 3026 (w), 1637 (s), 1541 (s), 1490 (m) cm^{-1}; ^1H NMR (300MHz, $CDCl_3$) δ 7.65 (2H, bs, N*H*CH_2), 7.40-7.15 (14H, m, Ar H), 4.44 (4H, d, *J* = 7Hz, C*H*$_2$NH), 3.69 (2H, dd, *J* = 9, 4Hz, C*H*NH), 3.30 (2H, dd, *J* = 14, 9Hz, C*H*$_a$H$_b$Ph), 2.76 (2H, dd, *J* = 14, 9 Hz, CH$_a$*H*$_b$Ph), 1.60 (4H, s, NH_2); ^{13}C NMR (75MHz, $CDCl_3$) δ 174.0 (0), 138.9 (0), 137.9 (0), 129.5 (1), 129.1 (1), 128.9 (1), 127.2 (1), 127.0 (1), 126.9 (1), 56.6 (1), 43.1 (2), 41.1 (2); *m/z* (ES+) 431 $[M+H]^+$

Methyl (2*S*)-2-[({{6-[(1,3-dioxo-2,3-dihydro-1*H*-2-isoindolyl)methyl]-2-pyridyl}carbonyl)amino]-3-phenylpropanoate – 102

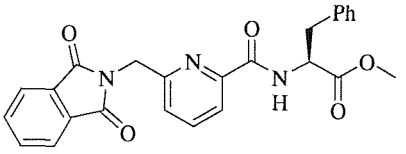

6-[(1,3-dioxo-2,3-dihydro-1*H*-2-isoindolyl)methyl]-2-pyridine carboxylic acid **98** (2.91 g, 10.3 mmol) was heated at reflux in neat thionyl chloride (43 mL) for 6 hours and stirred at room temperature for 14 hours. Excess thionyl chloride was removed *in vacuo* to afford a dark red solid (*). The resulting solid was dissolved in dry CH_2Cl_2 (15 mL). Commercially available phenylalanine methyl ester (1.48 g, 6.9 mmol) and DMAP (2.10 g, 17.2 mmol) were added to the solution. The mixture was stirred at room temperature for 6 days. The solution was washed with 1 M HCl (3 x 15 mL), 1 M NaOH (3 x 15 mL) and water (30 mL). The organic layer was dried over MgSO4 and the solvent removed *in vacuo* to afford compound **102** as a pale yellow foam (2.67 g, 87%): m.p. = 123°C; IR (neat) ν_{max} = 3386 (w), 1737 (m), 1705 (s), 1678 (m) cm^{-1}; ^1H NMR (400MHz, $CDCl_3$) δ 8.21 (1H, d, *J* = 8Hz, NH), 7.96 (1H, dd, *J* = 1, 8Hz, Pyr H), 7.82 (2H, dd, *J* = 3, 5Hz, PhtH), 7.73 (1H, t, *J* = 8Hz, PyrH), 7.67 (2H, dd, *J* = 3, 5Hz, PhtH), 7.35 (1H, dd, *J* = 1, 8Hz, PyrH), 7.01-7.20 (5H, m, ArH), 4.97 (2H, s, NCH_2), 4.86 (1H, m, NHC*H*), 3.58 (3H, s, OCH_3), 3.08 (1H, dd, *J* = 6, 14Hz, CH^AH^B), 2.97 (1H, dd, *J* = 6, 14Hz, CH^AH^B); ^{13}C NMR (100MHz, $CDCl_3$) δ 173.0 (0), 169.5 (0), 165.0 (0), 155.8 (0), 150.6 (0), 139.8 (0), 137.6 (1), 135.7 (1), 133.6 (1), 130.8 (1), 130.1 (1), 128.6 (1), 125.8 (1), 125.1 (1), 122.8 (1), 55.1 (1), 53.8 (2), 44.1 (2), 39.8 (3); *m/z* (ES^+) 444 $[M+H]^+$ 466 $[M+Na]^+$,909 $[2M+Na]^+$; HRMS (ES+) calcd. for $C_{25}H_{21}N_3NaO_5^+$ 466.1373. Found 466.1373

(*) **6-[(1,3-dioxo-2,3-dihydro-1*H*-2isoindolyl)methyl]-2-pyridine carboxylic chloride** – 83%; IR (neat) ν_{max} = 1713 (s), 1621 (m) cm^{-1}; ^1H NMR (300MHz, $CDCl_3$ / 10% DMSO) δ 8.12-7.60 (7H, m, ArH + Pyr H), 5.12 (2H, s, CH_2); ^{13}C NMR (75MHz, $CDCl_3$ / 10% DMSO) δ 168.6 (0), 166.7 (0), 154.6, (0), 146.9 (0), 136.6 (0), 132.7 (1), 130.8 (1), 124.5 (1), 122.6 (1), 122.6 (1), 40.9 (2); *m/z* (ES+) 301 $[M+H]^+$

(2*S*)-2-[({6-[(1,3-dioxo-2,3-dihydro-1*H*-2-isoindolyl)methyl]-2-pyridyl}carbonyl)amino]-3-phenylpropanoic acid –103

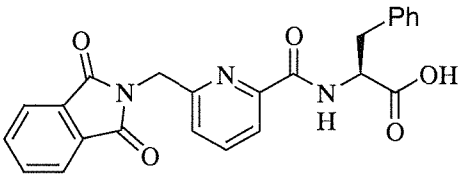

Compound **102** (400 mg, 0.23 mmol) was dissolved in concentrated formic acid (6 ml). Concentrated H_2SO_4 (60 μL) was added and the mixture refluxed for 3 days. Water (10 mL) was added and the precipitate extracted in CH_2Cl_2. The organic layer was dried over magnesium sulphate and the solvent removed *in vacuo*. No further purification proved to be necessary. Compound **103** was obtained as a white solid (357 mg, 92%): R_f = 0.16 (5% MeOH / CH_2Cl_2); m.p. = decomposes at 192°C; IR (neat) ν_{max} = 3236 (w), 1748 (s), 1705 (s), 1351 (s), 953 (m) cm^{-1}; ^1H NMR (400MHz, $CDCl_3$) δ 8.19 (1H, d, *J* = 8Hz, NH), 7.96 (1H, d, *J* = 8Hz, Pyr H), 7.78 (2H, dd, *J* = 3, 5Hz, PhtH), 7.73 (1H, t, *J* = 8Hz, PyrH), 7.63 (2H, dd, *J* = 3, 5Hz, PhtH), 7.36 (1H, d, *J* = 8Hz, PyrH), 7.20-7.05 (5H, m, ArH), 4.96 (2H, s, NCH_2), 4.83 (1H, dd, *J* = 7, 13Hz, NHC*H*), 3.19 (1H, dd, *J* = 6, 14Hz, CH^AH^B), 2.98 (1H, dd, *J* = 6, 14Hz, CH^AH^B); ^{13}C NMR (100MHz, $CDCl_3$) δ 175.0 (0), 168.4 (0), 164.6 (0), 154.7 (0), 149.0 (0), 138.8 (0), 136.3 (0), 134.7 (1), 132.4 (1), 129.7 (1), 129.0 (1), 127.5 (1), 125.0 (1), 124.0 (1), 121.7 (1), 54.2 (1), 42.9 (2), 38.0 (2); *m/z* (ES^+) 430 $[M+H]^+$452 $[M+Na]^+$,858 $[2M^+]$,880 $[2M+Na]^+$; HRMS (ES+) calcd. for $C_{24}H_{19}N_3NaO_5^+$ 452.1217. Found 452.1215

N2-[(1*R*)-2-({3-[({2*S*)-2-[({6-[(1,3-dioxo-2,3-dihydro-1*H*-2-isoindolyl)methyl]-2-pyridyl}carbonyl)amino]-2-phenyl ethanoyl}amino)methyl]benzyl}amino)-2-oxo-1-phenylethyl]-6-[(1,3-dioxo-2,3-dihydro-1*H*-2-isoindolyl)methyl]-2-pyridine carboxamide – 101

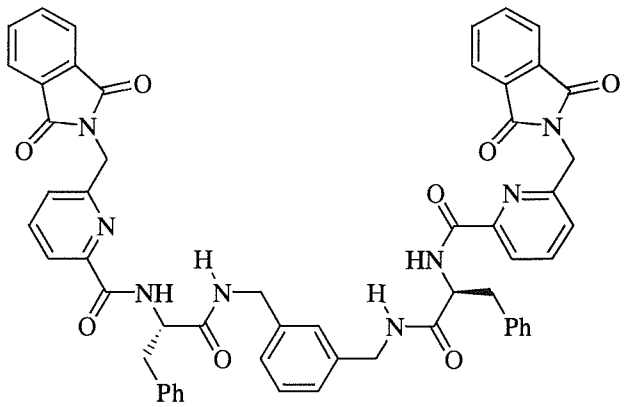

To a solution of compound **103** (330 mg, 0.80 mmol) in dry CH_2Cl_2 (15 mL) was added HOBt (143 mg, 1.06 mmol) and DMAP (33 mg, 10%wt). EDC (202 mg, 1.06 mmol) was added to the suspension. The mixture was stirred at room temperature for 90 minutes. *m*-Xylylene diamine (53 μL,

0.4 mmol) and triethylamine (110 μL, 0.80 mmol) were added and the mixture stirred at room temperature for two days. Purification of the crude brown solid was accomplished by column chromatography (2% MeOH / CH_2Cl_2). Compound **101** was obtained as a white solid (111 mg, 28%): R_f = 0.65 (5% MeOH / CH_2Cl_2); IR (neat) ν_{max} = 3376 (w), 1764 (w), 1705 (s), 1592 (w), 1394 (s), 1308 (m), 953 (m) cm^{-1}; ^1H NMR (400MHz, $CDCl_3$) δ 8.19 (2H, d, *J* = 9Hz, N*H*CH), 7.96 (2H, dd, *J* = 8, 1Hz, Pyr H), 7.82 (4H, dd, *J* = 6, 3 Hz, Pht H), 7.73 (2H, t, *J* = 8Hz, Pyr H), 7.68 (4H, dd, *J* = 6, 3 Hz, Pht H), 7.62 (2 H, bs, CH_2NH), 7.34 (2H, dd, *J* = 8, 1Hz, Pyr H), 7.30-6.90 (14H, m, Ar H), 4.97 (4H, s, CH_2N), 4.90-4.80 (2H, m, C*H*CH_2Ph), 3.58 (4H, s, CH_2NH), 3.09 (2H, dd, *J* = 14, 6Hz, CH^AH^{B}Ph), 2.97 (2H, dd, *J* = 14, 6Hz, CH^A*H*^{B}Ph); ^{13}C NMR (100MHz, $CDCl_3$) 173.6 (0), 170.1 (0), 165.6 (0), 156.4 (0), 151.2 (0), 140.4 (0), 139.9 (0), 138.1 (0), 136.3 (1), 132.3 (1), 134.2 (1), 131.4 (1), 130.7 (1), 129.1 (1), 128.6 (1), 126.4 (1), 125.7 (1), 123.3 (1), 119.1 (1), 55.6 (1), 54.3 (2), 44.7 (2), 40.4 (2); *m/z* (MALDI) 981 $[M+Na]^+$

2-[({5-[1,3-dioxo-2,3-dihydro-1*H*-2-isoindolyl)methyl]-2-pyridyl}-carbonyl)amino]-3-phenylpropanoyl fluoride – 104

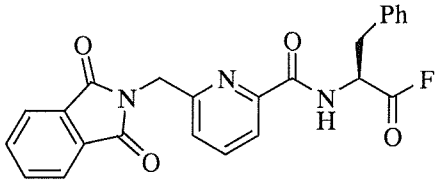

Cyanuric fluoride (24.7 μL, 0.29 mmol) was added to a solution of acid **103** (50 mg, 0.12 mmol) and pyridine (9.7 μL, 0.12 mmol) in dry CH_2Cl_2 at -15°C. The mixture was stirred for 2 hours at -15°C under a gentle stream of nitrogen. The solution was then poured into ice (10 mL) and extracted with CH_2Cl_2 (10 mL). The organic layer was then dried and the solvent evaporated *in vacuo* to give crude acid fluoride **104** as a clear oil (46.4 mg, 90%), which was used directly in the next reaction without purification as highly unstable: IR (neat) ν_{max} = 3401 (m), 1725 (m), 1710 (s), 1650 (m), 1527 (m) cm^{-1}; ^1H NMR 8.07 (1H, d, *J* = 8Hz, NH), 7.97 (1H, d, *J* = 8Hz, PyrH), 7.87 (1H, t, *J* = 8Hz, PyrH), 7.84 (2H, dd, *J* = 6, 3Hz, PhtH), 7.81-7.72 (5H, m, ArH), 7.70 (2H, dd, *J* = 6, 3Hz, PhtH), 7.46 (1H, d, *J* = 8Hz,

PyrH), 5.1 (2H, s, CH_2Pht), 4.95 (1H, m, *CH*NH), 3.17 (1H, dd, J = 14, 6Hz, CH^AH^B), 3.06 (1H, dd, J = 14, 6Hz, CH^AH^B); *m/z* (APCI) 453 $[M+Na]^+$, 430 $[M^+]$

2,2-spirocyclohexane-4,5-diphenyl-2*H*-imidazole – 107 [114]

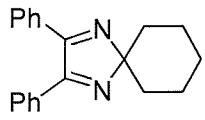

Following a procedure from Corey,[114] a 2-L, three-necked round bottom flask, equipped with a mechanical stirrer and a reflux condenser, was charged with benzil (90.3 g, 0.43 mol), glacial acetic acid (570 mL), ammonium acetate (229 g, 2.97 mol) and cyclohexanone (46 mL). The mixture was refluxed for 90 minutes and then, while hot, poured into 2 L of vigorously stirred water. The mixture was left to cool down to room temperature. The crystals were collected by filtration, washed three times with water (3 x 100 mL), crushed in a mortar and dried to give compound **107** as yellowish-green powder (122.1 g, 98%): m.p. 103-104°C; IR (neat) ν_{max} = 2924 (m), 2844 (w), 1555 (w), 1442 (m), 980 (m), 690 (s) cm^{-1}; ^1H NMR (400MHz, $CDCl_3$) δ, 7.33-7.53 (10H, m, ArH), 1.95-2.00 (4H, m, CH_2C), 1.65-1.92 (6H, m, CH_2CH_2); ^{13}C NMR (400MHz, $CDCl_3$) δ 164.0 (0), 133.3 (0), 130.1 (1), 129.0 (1), 128.3 (1), 104.2 (0), 34.8 (2), 25.8 (2), 24.2 (2); *m/z* (ES+) 289 $[M+H]^+$; Anal. calcd for $C_{20}H_{20}N_2$: C, 83.30; H, 6.99; N, 9.71. Found: C, 82.92; H, 7.04; N, 9.51

Data are consistent with those reported by Corey [138]

(±)-1,2-diphenyl-1,2-ethylenediamine – 108 [114]

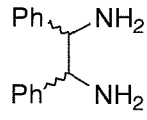

A 2 L, four necked round bottomed flask was equipped with a mechanical stirrer, thermometer, dry ice condenser and compound **90** (70 g, 0.24 mol). The flask was flushed with argon and dry THF (400 mL) was added. The mixture was stirred until all solids dissolved, then cooled to -78°C (dry ice /

acetone bath) and treated with a stream of gaseous NH_3 until the volume increased of 400mL. Lithium (lithium wire in mineral oil, 6.75 g, 0.97 mol) was slowly introduced by cutting the wire with scissors (the mineral oil was wiped off with a paper towel). The rate of lithium addition was such that the temperature didn't rise above -65°C. The mixture was stirred for 30 minutes and EtOH (30 mL) was slowly added. The mixture was then stirred for 20 minutes and ammonium chloride (68 g, 1.24 mol) was added. The cooling bath was removed and the mixture allowed to warm to 0°C. Water (400 mL) was carefully introduced and the phases separated. The aqueous phase was washed with ether (3 x 300 mL) and the combined organic layers washed with brine (100 mL), dried over magnesium sulphate and concentrated to about 200 mL. The solution was then transferred to a 1 L round-bottomed flask with a mechanical stirrer, cooled to 0°C and 2 M HCl added (300 mL). The mixture was stirred at room temperature for 1 hour, water (500 mL) was added and the phases separated. The organic phase was then washed with water (150 mL) and the aqueous layer washed with ether (300 mL). The aqueous phase was then carefully treated with 2 M NaOH (300 mL) and extracted with CH_2Cl_2 (150 mL). The combined organic extracts were washed with brine (100 mL) and dried over magnesium sulphate. The solvent was evaporated *in vacuo* to afford the racemic diamine **108** as a pale yellow solid (29.7 g, 60%): m.p. 81-82°C; IR (neat) ν_{max} = 3386 (w), 3354 (w), 3268 (b) cm^{-1}; ^1H NMR (400MHz, $CDCl_3$) δ 1.59 (s, 4H), 4.10 (s, 2H), 7.2-7.3 (m, 10H); ^{13}C NMR (100MHz, $CDCl_3$) δ 145.0 (0), 127.7 (1), 127.4 (1), 126.3 (1), 62.6 (1); *m/z* (ES+) 213 $[M+H]^+$; HRMS (ES+) Calcd. for $C_{14}H_{17}N_2^+$ 213.1392. Found 213.1378
Data consistent with those reported from Corey [138]

(1*S*,2*S*)-(-)-1,2-diphenyl-1,2-ethylenediamine – 109 [114]

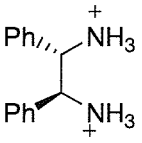

tartrate salt

A 1 L, round-bottomed flask was equipped with a mechanical stirrer and charged with racemic diamine **108** (29.7 g, 0.14 mol), and EtOH (161 mL). The solids were dissolved by heating the mixture to 70°C whereupon a hot solution of (L)-(+)-tartaric acid (20.8 g, 0.14 mol) in EtOH (161 mL) was added. The tartrate salts precipitated while the mixture was cooled to room temperature. The crystals

were collected by filtration, washed with EtOH (30 mL) and dried in oven. The solids were then dissolved in boiling water (161 mL), EtOH (161 mL) was added and the solution allowed cooling slowly to room temperature. The crystals were collected by filtration, washed with EtOH (30 mL) and dried. The recrystallization procedure was repeated twice with the same volumes of solvents to give chiral diamine **109** as a tartrate salt (white solid, 22 g, 40%). ^{1}H NMR shows only one diastereoisomer: $[\alpha]_D^{21}$ = -10° (c = 1, DMSO); ^{1}H NMR (400MHz, DMSO) δ 7.2 (10H, bs, ArH), 6.1 (6H, bs, NH_3^+), 4.3 (2H, s, CHPh), 4.0 (2H, s, *C*HOH); ^{13}C NMR (100MHz, DMSO) δ 174.5 (0), 138.8 (0), 128.2 (1), 127.8 (1), 127.7 91), 71.9 (1), 59.5 (1)
Data consistent with those reported from Corey [138]

(1*S*,2*S*)-(-)-1,2-diphenyl-1,2-ethylenediamine [114]

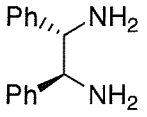

The salt **109** (1g, 2.7 mmol) was suspended in water (13 mL). After the mixture was stirred vigorously and cooled to 0°C, 50% aqueous sodium hydroxide (2 mL) was added dropwise followed by CH_2Cl_2 (10 mL) and stirred for 30 min. The phases were separated and the aqueous phase washed with CH_2Cl_2 (2 x 10 mL). The combined organic phases were washed with brine, dried over magnesium sulphate and filtered. The solvent was removed *in vacuo* to afford a white solid who was recrystallised from hexane to give the chiral diamine as colourless cristals (326 mg, 57%): $[\alpha]_D^{21}$ = -105° (c = 1, DMSO). Spectral properties are the same as that of the racemate **108**.
Data consistent with those reported from Corey [138]

***N*-2-(*1S,2S*)-2-[({6-[(1,3 dioxo-2,3-dihydro-1*H*-2-isoindolyl)methyl]-2-pyridyl}carbonyl) amino]-1,2-diphenylethyl}-6-[(1,3-dioxo-2,3-dihydro-1*H*-2-isoindolyl)methyl]-2-pyridine carboxamide – 110**

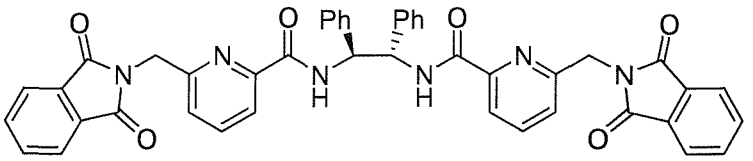

98 (1.84 g, 6.5 mmol) was suspended in CH_2Cl_2 (15 mL) and cooled to 0°C. Triethylamine (1.0 mL, 7.15 mmol) was slowly added. A clear solution was obtained. Diphenylchlorophosphate (1.35 mL, 6.5 mmol) was added and the solution stirred for 1 hour at 0°C. (*1S,2S*)-1,2-diphenyl-1,2-ethylenediamine-L-tartrate salt **109** (1.18 mg, 3.25 mmol) was suspended in water (7 mL) and K_2CO_3 (2.0 g, 10.7 mmol) added. After 30 minutes, the solution of diamine was added to the mixed anhydride solution at 0°C and the resulting mixture stirred for 2 hours at 0°C, and then allowed to warm to room temperature. After 14 hours, the mixture was poured into a separating funnel and CH_2Cl_2 (10 mL) and water (10 mL) added. The organic phase was separated, washed with 2 M HCl (10 mL) and saturated aqueous $NaHCO_3$ (10 mL). The organic layer was dried over magnesium sulphate and the solvent evaporated *in vacuo*. The crude material was purified by column chromatography (30% ethyl acetate / petrol ether up to 50% ethyl acetate / petrol ether) to afford compound **110** as a white solid (1.1 g, 46%): R_f = 0.3 (neat ethyl acetate); m.p. 106-107°C; ^{1}H NMR (300MHz, $CDCl_3$) d 8.79-8.71 (2H, m, CHN*H*Ph), 7.97-7.90 (6H, m, PyrH, PhtH), 7.81-7.77 (4H, m, PhtH), 7.73 (2H, t, *J* = 8Hz, PyrH), 7.32 (2H, d, *J* = 8Hz, PyrH), 7.22 –7.02 (10H, m, ArH), 5.39-5.32 (2H, m, C*H*NHPh), 5.07 (2H, d, *J* = 16 Hz, PhtNCH^AH^B), 5.01 (2H, d, *J* = 16 Hz, PhtNCH^AH^B); ^{13}CNMR (75MHz, $CDCl_3$) d 168.1 (0), 164.1 (0), 154.2 (0), 149.5 (0), 138.7 (0), 138.2 (0), 134.2 (1), 132.4 (1), 128.5 (1), 127.7 (1), 123.7 (1), 121.2 (1), 59.2 (1), 42.6 (2); *m/z* (ES+) 741 $[M+H]^+$, 763 $[M+Na]^+$

Data are consistent with those previously reported [93]

N2-{(*1S,2S*)-2-({[6-(aminomethyl)-2-pyridyl]carbonyl}amino)-1,2-diphenylethyl]-6-(aminomethyl)-2-pyridine carboxamide – 111

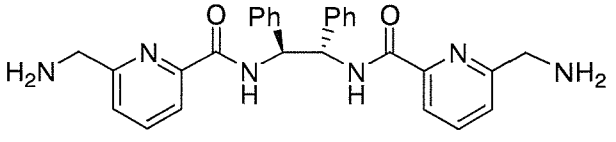

Hydrazine monohydrate (80 μL, 1.64 mmol) was added to a solution of compound **110** (600 mg, 0.82 mmol) in ethanol (5 mL) and the mixture heated at reflux for 8 hours. After allowing cooling to room temperature, the solvent was removed *in vacuo* to afford a white solid to which 2 M HCl (5 mL) was added. The solution was refluxed for 30 minutes, after which the insoluble material was filtered off. The aqueous solution was then basified to pH=9 with 1 M NaOH. The precipitated diamine was extracted with CH_2Cl_2 (5 x 10mL). The organic layer was dried over $MgSO_4$ and the solvent evaporated *in vacuo* to afford compound **111** as white crispy foam (330 mg, 84%): IR (neat) ν_{max} = 2362 (w), 1659 (m), 1590 (w) cm^{-1}; ^1H NMR (400 MHz, $CDCl_3$) d 9.13 (2H, s, N*H*C=O), 7.91 (2H, d, *J* = 7Hz, PyrH), 7.64 (2H, t, *J* = 16Hz, PyrH), 7.24 (2H, d, *J* = 7Hz, PyrH), 7.19-7.12 (10H, m, ArH), 5.48 (4H, dd, *J* = 8, 5Hz, C*H*$_2$NH$_2$), 1.78 (4H, s, NH_2); ^{13}C NMR (100 MHz, $CDCl_3$) d 165.0 (0), 160.9 (0), 149.1 (0), 138.9 (0), 137.9 (0), 128.9 (1), 128.7 (1), 127.8 (1), 124.1 (1), 120.4 (1), 59.7 (1), 47.5 (2)
Data are in agreement with those previously reported [93]

(14*S*,15*S*,35*S*,36*S*)-14,15,35,36-tetraphenyl-4,25-dithioxo-3,5,13,16,24,26,34,37,43, 44,45,46-dodecaazapentacyclo[37.31.1^{7,11}.1^{18,22}.1^{28,32}]hexatetraconta-1(43),7,9,11(46),18,20,22(45),28, 30,32,39,41-dodecaene-12,17,33,38-tetraone – 106

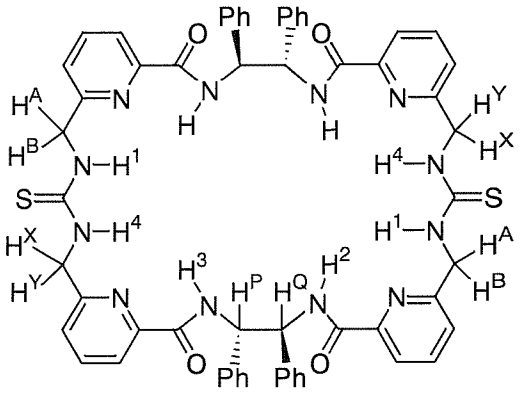

Carbon disulfide (414 μL, 6.86 mmol) was added to a mixture of compound **111** (165 mg, 0.50 mmol) in dry CH_2Cl_2 (10 mL) at -10°C and the mixture stirred for 1 hour. *N-N'*-Dicyclohexlcarbodiimide (200 mg, 0.49 mmol) was added and the mixture stirred for a further 45

minutes at -10°C then 30 minutes at room temperature. The excess carbon disulfide and solvent were removed *in vacuo* yielding a pale yellow solid that was dissolved in dry CH_2Cl_2 (10 mL). This solution was added to dry CH_2Cl_2 (50 mL) containing DMAP (20 mg, 10% by weight) along with a further one equivalent of diamine **111** (165 mg, 0.20 mmol) in dry CH_2Cl_2 (10 mL) under a slow stream of nitrogen over 3 hours *via* syringe pump addition. After stirring at room temperature for 16 hours, the excess solvent was removed *in vacuo*. The resultant yellow residue was purified by column chromatography (30% ethyl acetate / petrol ether up to neat ethyl acetate) yielding macrocycle **106** as a white solid (20.4 mg, 20%): m.p. = 153°C; IR (neat) ν_{max} = 3310 (br), 1670 (s), 1525 (m), 1455 (w) cm^{-1}; ^1H NMR (400 MHz, $CDCl_3$) δ 10.9 (2H, s, CONH^3), 9.0 (2H, s, CH_2NH^4CS), 8.1 (2H, m, CH_2NH^1CS), 7.9 (4H, m, PyrH+CONH^2), 7.7 (2H, d, *J*= 8Hz, PyrH), 7.6 (2H, d, *J*= 8Hz, PyrH), 7.3 (14H, m, PyrH+ArH), 7.2-6.9 (10H, m, ArH), 6.8 (2H, d, *J*= 8Hz, PyrH), 5.9 (2H, m, NHCH^BH^A), 5.3 (2H, m, CH^PPh), 5.1 (4H, m, NHCH^XH^Y+CH^QPh), 4.9 (2H, d, *J*= 18Hz, NHCH$^X H^Y$), 4.1 (2H, m, NHCH$^B H^A$) *; ^{13}C NMR (100 Hz, DMSO-d_6) d 165.1 (0), 157.3 (0), 149.4 (0), 139.8 (0), 138.7 (0), 128.5 (1), 128.0 (1), 127.6 (1), 124.8 (1), 120.8 (1), 60.2 (1), 58.1 (1), 49.2 (2); *m/z* (ES+) 1045 $[M+H]^+$, 1067 $[M+Na]^+$

* Full assignment based on COSY and NOESY spectra at -40°C

Data are coincident with those previously reported [93]

4.3 Experimental for Chapter Three

*N*2-{(*1S,2S*)-2-[({6-[(1,3-dioxo-2,3-dihydro-1*H*-2-isoindolyl)methyl]-2-pyridyl}carbonyl) amino]cyclohexyl}-6-(1,3-dioxo-2,3-dihydro-1H-2-isoindolyl)methyl]-2-pyridinecarboxamide – 126

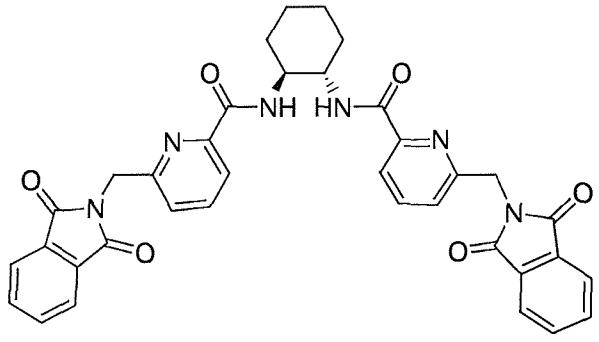

6-[(1,3-dioxo-2,3-dihydro-1*H*-2-isoindolyl)methyl]-2-pyridine carboxylic acid **98** (1.23 g, 4.3 mmol) was suspended in CH_2Cl_2 (10 mL) and cooled to 0°C. Triethylamine (0.66 mL, 4.73 mmol) was slowly added and a clear solution obtained. Diphenylchlorophosphate (0.89 mL, 4.3 mmol) was added and the solution stirred for 1 hour at 0°C. (*1S,2S*)-1,2-diaminocyclohexane-L-tartrate salt (564 mg, 2.15 mmol) was suspended in water (3.3 mL) and K_2CO_3 (980 mg) added. After 30 minutes, the solution of diamine was added to the mixed anhydride solution at 0°C and the resulting mixture stirred for 2 hours at 0°C, then allowed to warm to room temperature. After 14 hours, the mixture was poured into a separating funnel and CH_2Cl_2 (10 mL) and water (5 mL) added. The organic phase was separated, washed with 2 M HCl (5 mL) and saturated aqueous $NaHCO_3$ (5 mL). The organic layer was dried over magnesium sulphate and the solvent evaporated *in vacuo*. The crude material was purified by column chromatography (80% ethyl acetate / petrol ether) to afford compound **126** as a white solid (706 mg, 52%): R_f = 0.49 (neat ethyl acetate); m.p. 122-124°C; $[\alpha]_D^{21}$ = 150.7° (c = 1.08, $CHCl_3$); IR (neat) ν_{max} = 3260 (m), 1730 (s), 1653 (m), 1535 (s) cm^{-1}; ^1H NMR (400MHz, $CDCl_3$) δ 8.09 (2H, d, *J* = 8Hz, NH), 7.93 (2H, d, *J* = 8Hz, PyrH), 7.91 (6H, m, PhtH+PyrH), 7.76 (4H, dd, *J* = 7, 3Hz, PhtH), 7.29 (2H, d, *J* = 8Hz, PyrH), 5.04 (4H, s, NC*H*$_2$), 3.81 (2H, m, NHC*H*), 2.06 (2H, m, C*H*^{A}H^{B}CH$_2$), 1.75 (2H, m, CH^A*H*^{B}CH$_2$), 1.50 (2H, m, CHCH$_2$C*H*$_{eq}$H$_{ax}$), 1.39 (2H, m, CHCH$_2$CH$_{eq}$*H*$_{ax}$); ^{13}C NMR (100MHz,

$CDCl_3$) δ 168.0 (0), 163.9 (0), 157.2 (0), 149.5 (0), 138.0 (0), 134.1 (1), 132.2 (1), 123.6 (1), 123.3 (1), 121.0 (1), 53.1 (1), 42.6 (2), 31.9 (2), 24.5 (2); *m/z* (ES^{+}) 643 $[M+H]^+$, 665 $[M+Na]^+$; HRMS (ES+) Calcd. for $C_{36}H_{30}N_6NaO_6^+$ 655.2125. Found 655.2122

N2-{(1S,2S)-2-({[6-(aminomethyl)-2-pyridyl]carbonyl}amino)cyclohexyl}-6-(aminomethyl)-2-pyridine carboxamide – 127

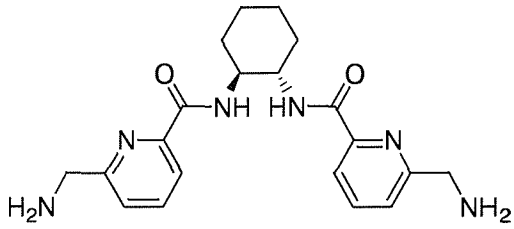

Hydrazine monohydrate (59.2 μL, 1.22 mmol) was added to a solution of phthalimide **126** (392 mg, 0.61 mmol) in ethanol (3 mL) and the mixture heated at reflux for 8 hours. After allowing cooling to room temperature, the solvent was removed *in vacuo* to afford a white solid to which 2 M HCl (3 mL) was added. The solution was refluxed for 30 minutes, after which the insoluble material was filtered off. The filtrate was basified to pH = 9 with 1 M NaOH and the precipitated diamine extracted with CH_2Cl_2 (5 x 10 mL). The combined organic extracts were dried over $MgSO_4$ and the solvent evaporated *in vacuo* to afford compound **127** as a white foam (193 mg, 83%): IR ν_{max} = 3430 (m), 3253 (w), 1703 (s), 1547 (m) cm^{-1}; ^1H NMR (400MHz, $CDCl_3$) δ 8.54 (2H, m, NHCO), 7.96 (2H, d, *J* = 8Hz, PyrH), 7.70 (2H, t, *J*= 8Hz, PyrH), 7.29 (2H, d, *J*= 8Hz, PyrH), 3.90-4.1 (6H, d, m, CH_2NH_2 + CHNH), 2.27 (2H, m, $NHCHCH^AH^B$), 2.13 (6H, m, $NHCHCH^AH^B$ + CH_2NH_2), 1.85 (2H, m, $CHCH_2CH_{eq}H_{ax}$), 1.48 (2H, m, $CHCH_2CH_{eq}H_{ax}$); ^{13}C NMR (100MHz, $CDCl_3$) δ 163.8 (0), 148.2 (0), 136.8 (0), 126.5 (1), 122.8 (1), 119.3 (1), 52.9 (1), 45.9 (2), 31.3 (2), 23.8 (2); *m/z* (ES+) 383 $[M+H]^+$; HRMS (ES+) calcd. for $C_{20}H_{27}N_6O_2^+$ 383.2195. Found 383.2188

(*4S,9S,29S,34S*)-19,44-dithioxo-3,10,18,20,28,35,43,45,51,52,53,54-dodecaazaheptacyclo [45.3.1.1^{12,16}.1^{22,26}.1^{37,41}.0^{4,9}.0^{29,34}]tetrapentaconta-1(51),12(54),13,15,22(53),23,25,37,39, 41(52),47,49-dodecaene-2,11,27,36-tetraone – 123

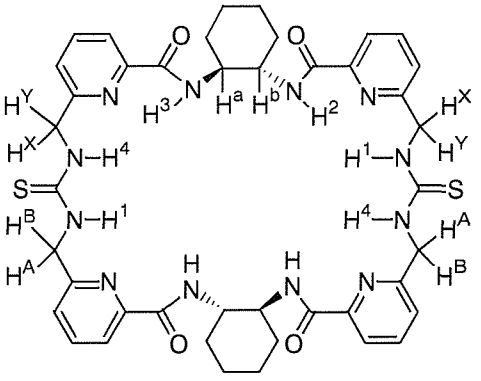

Carbon disulfide (207 μL, 3.7 mmol) was added to a mixture of *bis*amine **127** (100 mg, 0.26 mmol) in dry CH_2Cl_2 (5 mL) at -10°C and the mixture stirred for 1 hour. *N-N'*-Dicyclohexylcarbodiimide (107 mg, 0.50 mmol) was added and the mixture stirred for a further 45 minutes at -10°C then 30 minutes at room temperature. The excess carbon disulfide and solvent were removed *in vacuo* yielding a white solid that was dissolved in dry CH_2Cl_2 (5 mL). This solution was added to dry CH_2Cl_2 (25 mL) in presence of DMAP (10 mg, 10% by weight) along with a further equivalent of **127** (100 mg, 0.26 mmol) in dry CH_2Cl_2 (5 mL) under a slow stream of nitrogen over 3 hours *via* syringe pump. After stirring at room temperature for 16 hours, the excess solvent was removed *in vacuo* and the resultant yellow residue purified by column chromatography eluting in neat ethyl acetate yielding macrocycle **123** as a white solid (156 mg, 72%): R_f = 0.54 (neat ethyl acetate); m.p. = decomposes at 240°C; $[\alpha]_D^{21}$ = 165.5° (c = 1.08, $CHCl_3$); IR ν_{max} = 3310 (br), 2360 (w), 2330 (w), 1670 (m), 1525 (m), 1450 (w), 1360 (w), 1255 (w) cm^{-1}; ^{1}H NMR (400 MHz, $CDCl_3$) d 9.24 (2H, s, N*H*^{2}C=O), 8.73 (2H, s, N*H*^{1}C=S), 8.15 (2H, d, *J* = 8Hz, N*H*^{4}C=O), 8.00 (2H, d, *J* = 7Hz, Pyr*H*), 7.79 (2H, t, *J* = 7Hz, Pyr*H*), 7.72 (2H, d, *J* = 7Hz, N*H*^{3}C=S), 7.36 (2H, d, *J* = 7Hz, Pyr*H*), 7.23 (4H, bs, Pyr*H*), 6.85 (2H, bs, Pyr*H*), 5.42 (2H, m, C*H*^{X}NH), 5.14 (2H, d, *J* = 17Hz, C*H*^{A}H^{B}NH), 4.88 (2H, d, *J* = 17Hz, CH^A*H*^{B}NH), 4.34 (2H, d, *J* = 12Hz, C*H*^{Y}NH), 4.12 (2H, bs, C*H*$^\alpha$NH), 3.69 (2H, bs, C*H*$^\beta$NH), 2.57 (2H, d, *J* = 10Hz, C*H*$_a$H$_b$CH$^\beta$NH), 2.12 (2H, d, *J* = 10Hz, C*H*$_a$H$_b$CH$^\alpha$NH), 1.82 (4H, m, C*H*$_2$CH$_2$CHNH), 1.56 (2H, d, *J* = 10Hz, CH$_a$*H*$_b$CH$^\alpha$NH), 1.53 (2H, d, *J* = 10Hz, CH$_a$*H*$_b$CH$^\beta$NH), 1.31

(4H, m, CH_2CH_2CHNH); ^{13}C NMR (100 MHz, DMSO) d 182.0 (0), 164.1 (0), 154.2 (0), 148.6 (0), 138.5 (1), 120.0 (1), 117.9 (1), 54.5 (2), 49.0 (1), 30.8 (2), 24.0 (2) ; *m/z* (ES^+) 850 $[M+H]^+$; HRMS (ES+) Calcd. for $C_{42}H_{49}N_{12}O_4S_2^+$ 849.3444. Found 849.3448

_N,N'_-(1*S*,2*S*)-diphenyl-ethyl-1,2-diylbis-(3-cyanobenzamide) – 133

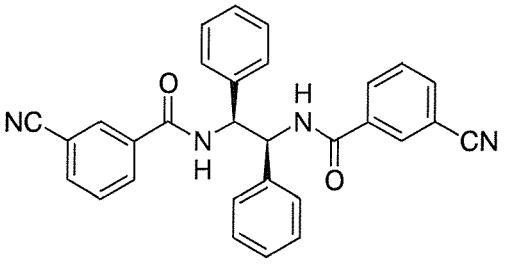

Commercially available 3-cyanobenzoic acid (867 mg, 5.9 mmol) was refluxed in neat thionyl chloride (12 mL) for 4 hours. Excess thionyl chloride was removed *in vacuo* to afford a dark solid, which was then dissolved in dry CH_2Cl_2 (5 mL). (1*S*,2*S*)-(-)-1,2-Diphenylethylenediamine (400 mg, 1.8 mmol) and DMAP (1.15 g, 9.40 mmol) were added and the mixture was stirred at room temperature for 2 days. The crude material was purified by column chromatography (50% ethyl acetate / petrol ether) affording compound **133** as a white solid (420 mg, 48%): R_f = 0.33 (50% ethyl acetate / petrol ether); m.p. 243-244°C; $[\alpha]_D^{23}$ = -102.7° (c = 0.84, DMSO); IR (neat) ν_{max} = 3287 (b), 2981 (w), 2927 (w), 1696 (s), 1631 (s) cm^{-1}; ^1H NMR (DMSO, 400MHz) δ 8.06 (2H, s, ArH), 7.98 (2H, d, *J* = 8Hz, NH), 7.81 (2H, d, *J* = 8Hz, ArH), 7.56 (2H, t, *J* = 8Hz, ArH), 7.32 (2H, *J* = 8Hz, ArH), 7.20-7.10 (10H, m, Ph), 5.58 (2H, m, NHC*H*); ^{13}C NMR (DMSO, 100MHz) δ171.6 (0), 166.5 (0), 140.3 (0), 136.4 (0), 135.9 (1), 132.6 (1), 132.2 (1), 130.6 (1), 129.3 (1), 128.9 (1), 128.6 (1), 119.0 (0), 113.4 (1); *m/z* (ES+) 471 $[M+H]^+$, 963 $[2M+Na]^+$; HRMS (ES+) Calcd. for $C_{60}H_{44}N_8NaO_4^+$ 963.3377. Found 963.3369

(3-{2-[3-(*tert*-butoxycarbonylamino-methyl)-benzoylamino]-1,2-diphenyl-ethylcarbamoyl}-benzyl)-carbamic acid *tert*-butyl ester - 134

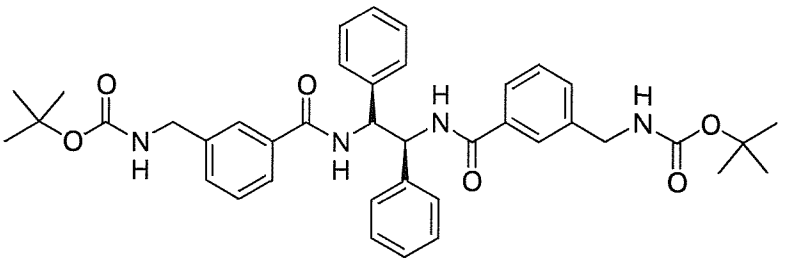

Di-*tert*-butyl dicarbonate (1.25 g, 5.72 mmol) and $NiCl_2$ (371 mg, 2.86 mmol) were added to a solution of **133** (673 mg, 1.43 mmol) in THF (15 mL) and MeOH (10 mL). THF was necessary to dissolve the compound. Sodium borohydride (757 mg, 20.0 mmol) was carefully added to the mixture at 0°C. The mixture was stirred at room temperature for 16 hours. The solvent was removed *in vacuo* and the precipitate dissolved in ethyl acetate (20 mL) and saturated aqueous $NaHCO_3$ (10 mL). The insoluble precipitate was filtered off and washed with ethyl acetate (2 x 15 mL). The combined organic layers were dried over $MgSO_4$ and evaporated *in vacuo* to afford **134** as a white solid. The crude material was then purified by extraction in chloroform (618 mg, 64%): R_f = 0.83 (5% MeOH in CH_2Cl_2); m.p. = 187-188°C; $[\alpha]_D^{23}$ = -40.5° (c = 0.99, DMSO); IR (neat) ν_{max} = 3295 (m), 2973 (w), 1689 (s), 1630 (s), 1528 (s), 1361 (m), 1243 (m) ^{1}H NMR (DMSO, 400MHz) δ 8.97 (2H, d, *J* = 8Hz, N*H*CH), 7.56 (4H, m, ArH), 7.38 (10H, m, ArH), 7.24 (4H, m, ArH), 7.15 (2H, t, *J* = 8Hz, NHCO), 5.67 (2H, d, *J* = 8Hz, C*H*NH), 4.14 (4H, d, *J* = 6Hz, C*H*$_2$NH), 1.37 (18H, s, CH_3); ^{13}C NMR (DMSO, 100MHz) δ 166.5 (0), 155.7 (0), 140.6 (0), 140.4 (0), 134.8 (0), 129.6 (1), 128.1 (1), 127.8 (1), 127.2 (1), 126.7 (1), 125.9 (1), 125.3 (1), 77.8 (0), 57.2 (1), 43.1 (2), 28.2 (3); *m/z* (ES+) 679 $[M+H]^+$, 701 $[M+Na]^+$ (100%), 1379 $[2M+Na]^+$; HRMS (ES+) Calcd. for $C_{40}H_{46}N_4NaO_6^+$ 701.3315. Found 701.3320

N,N'-(1*S*,2*S*)-diphenyl-ethyl-1,2-diylbis-(3-aminomethyl-benzamide) – 135

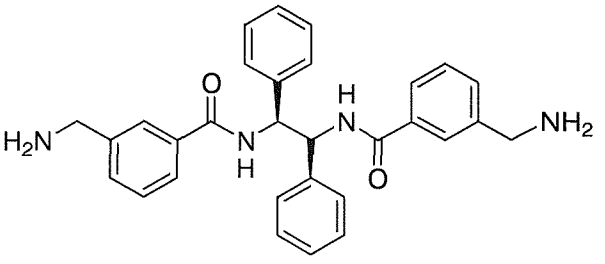

Compound **134** (312 mg, 0.46 mmol) was dissolved in 1:1 solution of TFA and CH_2Cl_2 (10 mL). The solution was stirred at room temperature for 2 hours. Toluene (10 mL) was added and the solvent evaporated in vacuo to give compound **135** as a clear oil (294 mg, quantitative). The oil was extracted with CH_2Cl_2 (10mL) and 10% aqueous K_2CO_3 (10 mL) to afford the free diamine as a white crispy foam (206 mg, 70%): m.p. = 283°C; $[\alpha]_D^{23}$ = -89.1° (c = 0.68, DMSO); IR (neat) ν_{max} = 3298 (w), 1633 (s) cm^{-1}: ^1H NMR (DMSO, 400MHz) δ 9.29 (2H, bs, N*H*CH), 7.8-7.5 (4H, m, ArH), 7.43 (2H, d, *J* = 8Hz, ArH), 7.35-7.10 (12H, m, ArH), 5.69 (2H, d, *J* = 8Hz, C*H*NH), 4.02 (2H, bs, $CH_aH_bNH_2$), 3.71 (2H, bs, $CH_aH_bNH_2$), 1.77 (4H, s, NH_2); ^{13}C NMR (DMSO, 400MHz) δ 166.7 (0), 141.4 (0), 140.6 (0), 134.7 (0), 134.7 (0), 127.7 (1), 127.5 (1), 127.4 (1), 126.7 (1), 126.5 (1), 126.0 (1), 125.2 (1), 57.4 (1), 45.6 (2); *m/z* (ES+) 479 $[M+H]^+$, 501 $[M+Na]^+$, 979 $[2M+Na]^+$; HRMS (ES+) Calcd. for $C_{30}H_{31}N_4O_2^+$ 479.2448. Found 479.2442

(14*S*,15*S*,35*S*,36*S*)-14,15,35,36-tetraphenyl-4,25-dithioxo-3,5,13,16,24,26,34,37-octaazapentacyclo[37.31.1^{7,11}.1^{18,22}.1^{28,32}]hexatetraconta-1,7,9,11,18,20,22,28, 30,32,39,41-dodecaene-12,17,33,38-tetraone – 129

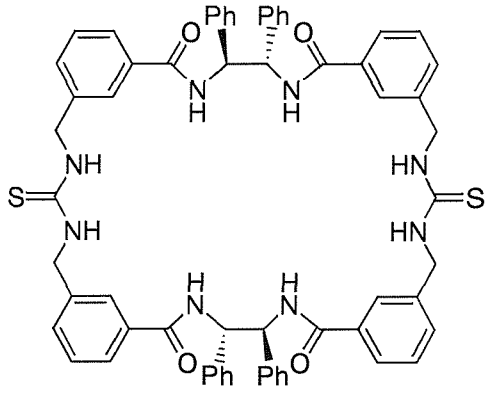

Compound **135** (200 mg, 0.42 mmol) was dissolved in CH_2Cl_2 (5 mL) and 0.5 M aqueous K_2CO_3 was added (5 mL). After stirring for 20 minutes, thiophosgene (127 μL, 1.67 mmol) was added to the bottom layer and stirring restarted. The solution was stirred at room temperature for 16 hours. The phases were separated and the organic layer washed with 2 M aqueous HCl (10 mL), dried over $MgSO_4$

and the solvent evaporated *in vacuo* to give a pale yellow foam. No further purification was done as the compound proved to be unstable on silica. The *bis*isocyanate was then dissolved in dry CH_2Cl_2 (5 mL) and added to dry CH_2Cl_2 (50mL) containing triethylamine (116 μL, 0.84 mmol) along with a further one equivalent of diamine **135** (200 mg, 0.42 mL) in dry MeOH (5mL) under a slow stream of nitrogen over 3 hours *via* syringe pump addition. The mixture was stirred at room temperature for 16 hours. Macrocycle **129** precipitated out of solution as a yellow solid. The compound was filtered off and recrystallised from DMF and diethyl ether to afford a pale yellow solid (68 mg, 17%): m.p = decomposes at 240°C; IR (neat) ν_{max} = 3271 (b), 1637 (s), 1529 (s.) cm^{-1}; ^1H NMR (DMSO, 400MHz) δ 9.00 (4H, bs, NHCO), 7.95 (4H, bs, NHCS), 7.61-7.57 (8H, m, ArH), 7.36 (16H, m, ArH), 7.22-7.20 (8H, m, ArH), 7.14-7.12 (4H, m, ArH), 5.66 (4H, d, *J* = 5Hz, C*H*NH), 4.68 (8H, bs, CH_2NH); ^{13}C NMR (DMSO, 100MHz) δ 168.5 (0), 164.4 (0), 142.7 (0), 136.8 (0), 131.9 (1), 130.2 (1), 129.6 (1), 129.4 (1), 128.9 (1), 128.4 (1), 127.9 (1), 59.4 (1), 50.6 (2); *m/z* (MALDI) 1041 $[M+H]^+$, 1063 $[M+Na]^+$; Anal. Calcd. for $C_{62}H_{56}N_8O_4S_2$: C, 71.54; H, 5.42; N, 10.76; S, 6.16. Found C, 71.11; H, 5.28; 10.36; S, 5.66

N,N'-(1S,2S)-cyclohexane-1,2-diylbis-(3-cyanobenzamide) – 136

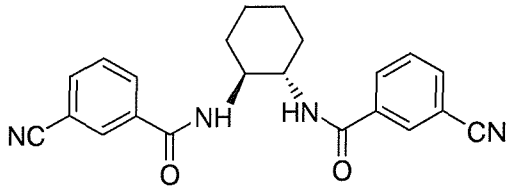

Commercially available 3-cyanobenzoic acid (3 g, 0.02 mol) was suspended in CH_2Cl_2 (15 mL) and cooled to 0°C. Triethylamine (3.1 mL, 0.022 mol) was slowly added to obtain a clear solution. Diphenylchlorophosphate (4.15 mL, 0.02 mol) was added and the solution stirred for 1 hour at 0°C. (1*S*,2*S*)-1,2-Diaminocyclohexane-L-tartrate salt (2.62 g, 0.01 mol) was suspended in water (15 mL) and K_2CO_3 (4.5 g, 0.03 mol) added. A clear solution was obtained. After 30 minutes, the diamine solution was added to the mixed anhydride solution at 0°C. The resulting mixture was stirred for 2 hours at 0°C and then allowed to warm to room temperature. After 14 hours, the mixture was poured into a separating funnel and CH_2Cl_2 (100 mL) and water (50 mL) added. The organic phase was separated, washed with 2 M HCl (50 mL) and saturated aqueous $NaHCO_3$ (50 mL). The organic layer was dried over magnesium

sulphate and the solvent evaporated *in vacuo*. The crude material was purified by flash column chromatography (neat ethyl acetate) to afford compound **136** as a white solid (3.61 g, 97%): R_f = 0.60 (neat EtOAc); m.p. = 236-237°C; $[\alpha]_D^{22}$ = 191° (c = 1, DMSO); IR (neat) ν_{max} = 3273 (m), 1630 (s), 1541 (s); ^{1}H NMR (400MHz, DMSO) δ 8.50 (2H, d, *J* = 8Hz, NH), 8.05 (2H, s, ArH), 7.95 (2H, d, *J* = 8Hz, ArH), 7.88 (2H, d, *J* = 8Hz, ArH), 7.57 (2H, t, *J* = 8Hz, ArH), 3.91 (2H, m, C*H*NH), 1.72 (2H, m, NHCHCH^AH^B), 1.50 (4H, m, NHCHCH^AH^B+ NHCHC$H_{eq}H_{ax}$), 1.26 (2H, m, NHCHCH$_{eq}H_{ax}$); ^{13}C NMR (100MHz, DMSO) δ 164.5 (0), 135.9 (0), 134.4 (0), 131.9 (1), 130.7 (1), 129.6 (1), 118.3 (0), 111.3 (1), 53.1 (1), 31.4 (2), 24.7 (2); *m/z* (ES+) 373 $[M+H]^+$, 410 $[M+Na]^+$; HRMS (ES+) Calcd. for $C_{44}H_{40}N_8NaO_4^+$ 767.3065. Found 767.3065; Anal. Calcd. for $C_{22}H_{20}N_4O_2$: C, 70.95; H, 5.41; N, 15.04. Found C, 70.77; H, 5.41; N, 14.93

(3-{2-[3-(*tert*-butoxycarbonylamino-methyl)-benzoylamino]-cyclohexylcarbamoyl}-benzyl)-carbamic acid *tert*-butyl ester - 137

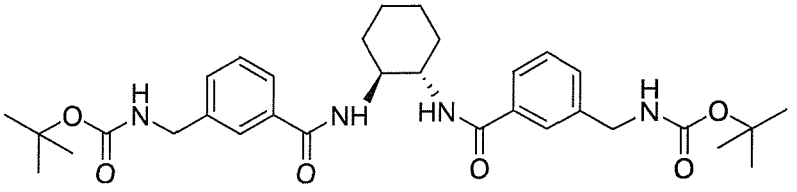

Following a procedure from Caddick,[125] diterbutyl dicarbonate (2.34 g, 10.7 mmol) and $NiCl_2$ (695 mg, 5.36 mmol) were added to a solution of **136** (1.0 g, 2.68 mmol) in THF (10 mL) and MeOH (15 mL). THF was necessary to dissolve the compound. Sodium borohydride (1.42 g, 38.0 mmol) was carefully added to the mixture at 0°C. The mixture was stirred at room temperature for 16 hours. The solvent was removed *in vacuo* and the precipitate dissolved in ethyl acetate (20 mL) and saturated aqueous $NaHCO_3$ (10 mL). The insoluble precipitate was filtered off and washed with EtOAc (2 x 10 mL). The combined organic layers were dried over $MgSO_4$ and evaporated *in vacuo* to afford a white solid. The crude material was then purified by column chromatography (2% MeOH / $CHCl_3$) to yield compound **137** as a white solid (925 mg, 91%): R_f = 0.58 (neat ethyl acetate); m.p. = 101-102°C; $[\alpha]_D^{22}$ = 58.1° (c = 0.5, $CHCl_3$); IR (neat) ν_{max} = 3303 (b), 2981 (w), 2927 (w), 2852 (w), 1696 (s), 1631 (s); ^{1}H NMR (400MHz, $CDCl_3$) δ 7.64 (2H, s, ArH), 7.58 (2H, d, *J* = 8Hz, ArH), 7.41-7.30 (4H, m, ArH), 6.75

(2H, s, NHCO), 5.00 (2H, s, N*H*CH_2), 4.28 (4H, d, *J* = 6Hz, NHC*H*$_2$), 3.99 (2H, m, C*H*NH), 2.21 (2H, d, *J* = 8Hz, NHCHC*H*^{A}H^B), 1.83 (2H, d, *J* = 8Hz, NHCHCH^A*H*^{B}), 1.43 (22H, bs, CH_3 + C*H*$_2$$CH_2$CH); ^{13}C NMR (100MHz, $CDCl_3$) δ 168.1 (0), 167.9 (0), 139.7 (0), 134.6 (0), 130.6 (1), 128.9 (1), 126.1 (1), 125.8 (1), 79.8 (0), 54.7 (1), 44.5 (2), 32.5 (2), 28.5 (2), 24.9 (3); *m/z* (ES+) 581 $[M+H]^+$, 603 $[M+Na]^+$; HRMS (ES+) Calcd. for $C_{32}H_{44}N_4NaO_6$+ 603.3153. Found 603.3148

N,N'-(1S,2S)-cyclohexane-1,2-diylbis-(3-aminomethyl-benzamide) - 138

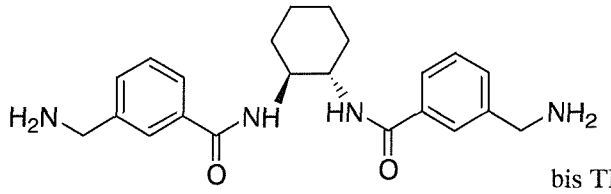

bis TFA salt

Compound **137** (500 mg, 0.86 mmol) was dissolved in 1:1 solution of TFA and CH_2Cl_2 (10 mL). The solution was stirred at room temperature for 2 hours. Toluene (10 mL) was added and the solvent evaporated *in vacuo* to give a clear oil. Trituration of the oil with diethyl ether provided the trifluoroacetate salt of compound **138** as a white solid (450 mg, 86%): m.p. = decomposes at 170°C; $[\alpha]_D^{22}$ = 61° (c = 1, DMSO); IR (neat) ν_{max} = 3290 (m), 2935 (b), 1667 (m), 1635 (s), 1533 (s), 1179 (s), 1120 (s); ^{1}H NMR (400MHz, DMSO) δ 8.26 (2H, bs, NHCO), 7.86 (2H, s, ArH), 7.71 (2H, d, *J* = 8Hz, ArH), 7.54 (2H, d, *J* = 8Hz, ArH), 7.45 (2H, m, ArH), 4.47 (6H, bs, NH_3^+), 4.03 (4H, m, C*H*$_2$$NH_3^+$), 3.95 (2H, m, C*H*NH), 1.90 (2H, d, *J* = 7Hz, NHCHC*H*^{A}H^B), 1.70 (2H, d, *J* = 7Hz, NHCHCH^A*H*^{B}), 1.52 (2H, m, $CHCH_2CH_{eq}H_{ax}$), 1.30 (2H, m, $CHCH_2CH_{eq}H_{ax}$); ^{13}C NMR (100MHz, DMSO) δ 165.6 (0), 157.9 (0, quart., CF_3), 134.8 (0), 133.7 (0), 130.9 (1), 128.1 (1), 127.7 (1), 126.4 (1), 52.6 (1), 41.7 (2), 31.2 (2), 24.2 (2)

(*4S,9S,29S,34S*)-19,44-dithioxo-3,10,18,20,28,35,43,45-octaazaheptacyclo [45.3.1.1^{12,16}.1^{22,26}.1^{37,41}.0^{4,9}.0^{29,34}]tetrapentaconta-1,12,13,15,22,23,25,37,39, 41,47,49-dodecaene-2,11,27,36-tetraone - 130

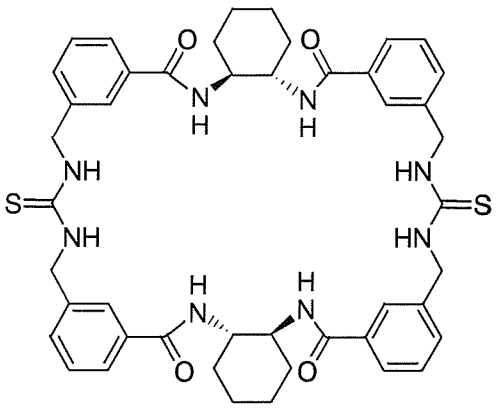

Compound **138** (200 mg, 0.53 mmol) was dissolved in CH_2Cl_2 (10 mL) and 0.5 M K_2CO_3 added (5 mL). After 1 hour, thiophosgene (160 μL, 2.1 mmol) was added to the bottom layer and stirring restarted. The solution was stirred a room temperature for 16 hours. The phases were separated and the organic layer washed with 2 M HCl (10 mL), dried over $MgSO_4$ and the solvent evaporated to give a pale yellow foam. No further purification was done as the compound proved to be unstable on silica. The *bis*isocyanate was then dissolved in dry CH_2Cl_2 (5 mL) and added to dry CH_2Cl_2 (50mL) along with a further equivalent of diamine **138** (200 mg, 0.42 mL) in dry CH_2Cl_2 (5mL) and triethylamine (183 μL, 1.3 mmol) under a slow stream of nitrogen over 3 hours *via* syringe pump addition. The mixture was stirred at room temperature for 16 hours. Macrocycle **130** precipitated out of solution as a pale yellow solid. The compound was filtered off and purified by semi-preparative HPLC (127 mg, 29%, method *40std254*): m.p. = 228-229°C; $[\alpha]_D^{22}$ = 104° (c = 0.5, DMSO); IR (neat) ν_{max} = 3276 (b), 3056 (w), 2983 (w), 2862 (w), 1636 (s), 1534 (s); ^{1}H NMR (400MHz, DMSO) δ 8.20 (4H, d, *J* = 7Hz NHCO), 7.92 (4H, bs, NHCS), 7.66 (4H, m, ArH), 7.33 (8H, bs, ArH), 4.63 (8H, s, CH_2NH), 3.94 (4H, m, $CHCH_2$), 1.91 (4H, d, *J* = 8Hz NHCHCH^AH^B), 1.75 (4H, m, NHCHCH$^A H^B$), 1.53 (4H, m, $CH_{eq}H_{ax}CH_2$), 1.31 (4H, m, $CH_{eq}H_{ax}CH_2$); ^{13}C NMR (100MHz, DMSO) δ 167.0 (0), 162.8 (0), 137.5 (0), 134.8 (0), 128.0 (1), 126.5 (1), 125.4 (1), 120.8 (1), 52.9 (1), 35.7 (2), 30.7 (2), 24.6 (2); *m/z* (MALDI in DMSO) 867 $[M+Na]^+$; Anal. Calcd. for $C_{46}H_{52}N_8O_4S_2$: C, 65.38; H, 6.20; N, 13.25; S, 7.59. Found C, 65.07; H, 5.87; N, 13.02; S, 7.15

(*4S,9S,29S,34S*)-19-guanidino-44-thioxo-3,10,18,20,28,35,43,44,45,51,52,53,54-tridecaazaheptacyclo [45.3.1.1^{12,16}.1^{22,26}.1^{37,41}.0^{4,9}.0^{29,34}]tetrapentaconta-1(51),12(54),13,15,22(53),23,25,37,39, 41(52),47,49-dodecaene-2,11,27,36-tetraone – 141

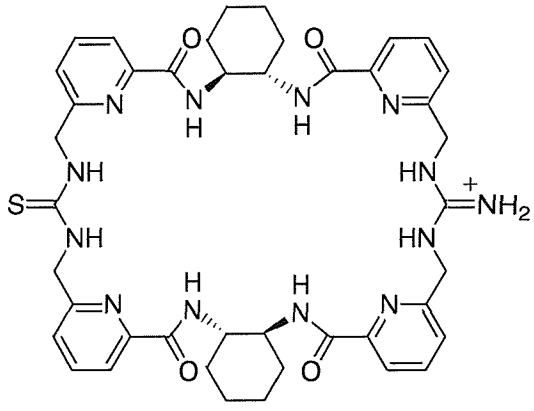

Methyl iodide (15 μL) was added to a solution of macrocycle **123** (40 mg, 0.05 mmol) in acetone and the mixture stirred for 16 hours at room temperature. The solvent was then removed *in vacuo* to afford a pale yellow foam, which was dissolved in methanol (5 mL) previously saturated with gaseous ammonia (saturation checked by pH paper). The flask was sealed and the solution stirred at 70°C for 7 hours. The solvent was then removed in vacuo to afford a pale yellow solid. The crude material was then purified by semi-preparative HPLC. Compound **141** was obtained as a white solid (10 mg, 3%). From the mixture starting material (10 mg) was recovered together with an unclean fraction of the bisguanidinium derivative (9mg, 2.5%) and two unknown compounds: ^{1}H NMR (400MHz, DMSO) δ 8.94 2H, s, NHCS), 8.86 (2H, s, N*H*NH$_2^+$), 8.49 (2H, s, NHCO), (8.12 (4H, s, PyrH), 7.71 (4H, m, PyrH), 7.47 (4H, bs, PyrH), 7.39 (2H, s, NHCO), 4.88 (2H, d, *J* = 14Hz, C*H*NH), 4.73-4.55 (6H, C*H*NH + CH$_2$NHCS), 3.81 (4H, CH$_2$NHNH$_2^+$), 2.06 (4H, m, C*H*^{A}H^{B}CH), 1.76 (4H, m, CH^A*H*^{B}CH), 1.54 (4H, m, C*H*$_{eq}$H$_{ax}$CH$_2$), 1.31 (4H, m, CH$_{eq}$*H*$_{ax}$CH); ^{13}C NMR (100MHz, MeOH-d$_3$) δ 149.4, 139.6, 139.3, 139.1, 125.8, 125.6, 121.6, 120.9, 107.6, 49.8, 46.5, 39.5, 31.9, 25.1; HRMS (ES+) Calcd. for C42H50N13O4S+ 832.3823. Found 832.3813

4.4 Experimental for Appendix 1

N-N'-dypiridyl thiourea (oxidised form) - 146

Thiophosgene (109 μL, 1.44 mmol) was added dropwise to a stirred solution of commercially available 2-aminopyridine (243 mg, 2.58 mmol) in $CHCl_3$ (40 mL) and 0.4 M aqueous potassium carbonate (15 mL). The reaction was refluxed for 5 days. The organic layer was separated and the aqueous layer extracted with $CHCl_3$ (30 mL). The organic fractions were collected, dried over magnesium sulphate and concentrated *in vacuo*. Purification of the crude oil by column chromatography (30% ethyl acetate in petroleum ether) gave as a major product compound **25** as a brown solid (424 mg, 72%): IR ν_{max} = 3057 (w), 1612 (m), 784 (m) cm^{-1}; ^1H NMR (300 MHz, $CDCl_3$), d 8.21 (1H, d, J = 8Hz, PyrH), 7.63 (1H, t, J = 8Hz, PyrH), 7.39 (1H, d, J = 8Hz, PyrH), 6.78 (1H, t, J = 8Hz, PyrH); ^{13}C NMR (75 MHz, $CDCl_3$), d 168.0 (0), 156.3 (0), 137.7 (1), 134.0 (1), 118.9 (1), 113.9 (1); m/z (ES+) 231 $[M+H]^+$.

The structure of **146** was confirmed by X-ray crystallographic analysis as existing in two mesomeric structures.

2[(2'-amino-3'-pyridyl)oxy]tertbutyl acetate - 147

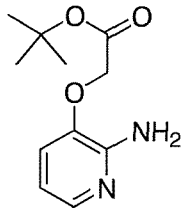

3-Hydroxyaminopyridine (4.4 g, 4.0 mol) in CH_2Cl_2 (40 mL) was added to a solution of 40%wt aqueous NaOH (40 mL) and Adogen 464 (0.235 g). *Tert*-butylbromoacetate (5 mL, 3.4 mol) was added

to the solution. The reaction was stirred for 24 hours. The organic layer was separated and the aqueous extracted in CH_2Cl_2 (120 mL). The combined organic phases were dried over magnesium sulphate and concentrated *in vacuo* to afford a yellow oil. Purification of the crude oil by column chromatography (5% methanol in CH_2Cl_2) gave compound **147** as a brown oil (2.95 g, 67%): R_f = 0.46 (10% methanol in CH_2Cl_2); IR ν_{max} = 3317 (w), 1746 (s), 1152 (m) cm^{-1}; ^1H NMR (300 MHz, $CDCl_3$) δ 7.70 (1H, dd, *J* = 5, 1Hz, PyrH), 6.84 (1H, dd, *J* = 8, 1Hz, PyrH), 6.59 (1H, dd, *J* = 8, 5Hz, PyrH), 4.94 (2H, bs, NH_2), 4.52 (2H, s, CH_2), 1.49 (9H, s, CH_3); ^{13}C NMR (75MHz, $CDCl_3$) δ 167.7 (0), 150.7 (0), 139.8 (0), 131.0 (1), 117.8 (1), 113.5 (1), 82.9 (0), 66.4 (2), 28.2 (3); *m/z* (ES+) 225 $[M+H]^+$; HRMS (ES+) Calcd. for $C_{11}H_{17}N_2O_3^+$ 225.1329. Found 225.1336

O-ethyl-N-(2-oxytertbutylacetate-3-pyridyl) thiourea – 148 and tert-butyl-2-{(3-thioxopyrido[2,1-c][1,2,4]thiadiazol-8-yl)oxy} acetate - 149

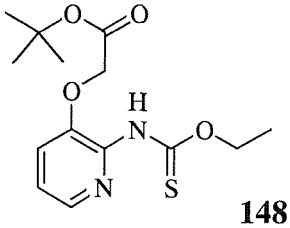

148

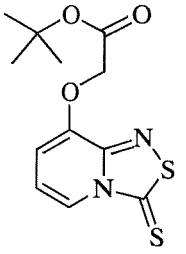

149

Thiophosgene (0.23 mL, 3.0 mmol) was added dropwise to a stirred solution of 2[(2'-amino-3'-pyridyl)oxy]*tert*-butyl acetate (1.34 g, 6.0 mmol) in chloroform (40 mL) and 0.4 M aqueous potassium carbonate (15 mL). The reaction was refluxed for 5 days. After allowing cooling to room temperature, the mixture was transferred to a separating funnel, the organic layer was separated and the aqueous layer extracted with chloroform (30 mL). The organic fractions were collected, dried over magnesium sulphate and concentrated *in vacuo* to afford a brown oil. Purification of the crude oil by column chromatography (30% ethyl acetate in petroleum ether) gave three fractions. Two of the fractions were recrystallised from methanol. The major products proved to be compound **148** (208.4 mg, 16%) and compound **149** (60.4 mg, 5%), both as slightly brown solids: (**148**): R_f = 0.1 (30% ethyl acetate in petrol ether); IR ν_{max} = 3283 (w), 3145 (w), 1727 (s), 1368 (m), 1190 (m) cm^{-1}; ^{1}HNMR (300 MHz, $CDCl_3$) δ 8.88 (1H, s, NH), 8.10 (1H, dd, *J* = 5, 2Hz, PyrH), 7.05 (2H, m, PyrH), 4.63 (2H, q, *J* = 7Hz, CH_2CH_3), 4.60 (2H, s, CH_2CO), 1.49 (9H, s, CCH_3), 1.39 (3H, t, *J* = 7Hz, CH_2CH_3); ^{13}C NMR (75MHz, $CDCl_3$) δ

189.0 (0), 167.2 (0), 144.5 (0), 141.6 (0), 140.9 (1), 120.9 (1), 120.4 (1), 83.4 (0), 68.1 (2), 66.9 (2), 28.2 (3), 14.2 (3); *m/z* (ES+) 647 $[2M+Na]^+$, 313 $[M+H]^+$. (**149**): R_f = 0.28 (30% ethyl acetate in petrol ether); ^1H NMR (400MHz, $CDCl_3$) δ 8.14 (1H, dd, *J* = 7, 1Hz, PyrH), 6.57 (1H, dd, *J* = 7, 7Hz, PyrH), 6.49 (1H, dd, *J* = 7, 1Hz, PyrH), 4.69 (2H, s, CH_2), 1.41 (9H, s, CH_3); ^{13}C NMR (100MHz, $CDCl_3$) δ 192.4 (0), 165.1 (0), 148.4 (0), 147.1 (0), 119.1(1), 112.1 (1), 106.9 (1), 82.3 (0), 65.9 (2), 27.9 (3); *m/z* (ES+) 339 $[M+CH_3CN]^+$, 337 $[M+K]^+$, 299 $[M+H]^+$

The structure of 149 was confirmed by X-ray crystallographic analysis

2-Pyridyl-isocyanate – 150

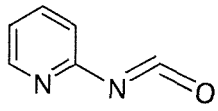

To a solution of commercially available picolinic acid (1.04 g, 8.4 mmol) in dry toluene (100 mL) were added DPPA (2.4 mL, 8.7μmol) and triethylamine (1.6 mL). The mixture was refluxed for 90 minutes. After cooling to room temperature, the solvent was removed *in vacuo* to afford a clear oil. As the oil proved not to be soluble in the eluting system it was absorbed on a small quantity of silica first (silica pad). The silica was then loaded on a column and purified by column chromatography (30% EtOAc in petrol ether) to afford compound **150** as a brownish oil (920 mg, 92%): IR ν_{max} = 2131cm^{-1} (s) cm^{-1}; ^1H NMR (300MHz, $CDCl_3$) δ 8.75 (1H, d, *J* = 5Hz, PyrH), 8.18 (1H, d, *J* = 8Hz, PyrH), 7.89 (1H, dt, *J* = 8, 1Hz, PyrH,), 7.55 (1H, dd, *J* = 8, 5Hz, PyrH)

2-Pyridyl thiourea – 151

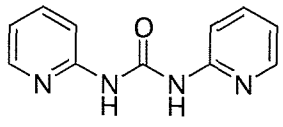

To a solution of 2-pyridyl isocyanate **150** (920 mg, 7.5 mmol) in dry CH_2Cl_2 was added 2-aminopyridine (705 mg, 0.75 mmol) and 0.4 M aqueous solution of potassium carbonate (19 mL). The

mixture was refluxed for 3 days. The organic layer was separated, dried over magnesium sulphate and the solvent removed in vacuo. The crude solid was purified by column chromatography (5% methanol in CH_2Cl_2) to afford compound **151** as a slightly brown solid (53 mg, 5%): R_f = 0.49 (5% methanol in CH_2Cl_2); m.p. = 152-154°C; IR ν_{max} = 3224 (w), 3130 (w), 1690 (s), 1527 (m) cm^{-1}; ^1H NMR (300MHz, $CDCl_3$) δ 8.37 (2H, d, *J* = 6Hz, NH), 7.72 (2H, t, *J* = 8, PyrH), 7.27 (2H, m, PyrH), 6.98 (2H, m, PyrH), 6.90 (2H, d, *J* = 8Hz, PyrH); ^{13}C NMR (75MHz) δ 155.9 (0), 152.3 (0), 148.2 (1), 138.4 (1), 118.2 (1), 113.9 (1); *m/z* (ES+) 215 $[M+H]^+$

4.5 Experimental for guests

N-Boc-D-glutamic acid

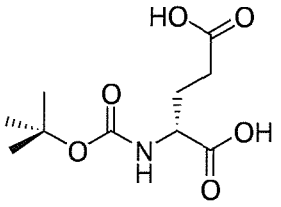

Following the procedure of Einhorn,[139] a mixture of commercially available D-glutamic acid (200 mg, 1.35 mmol), Boc anhydride (354 mg, 1.62 mmol) and solid $NaHCO_3$ (338 mg) was dissolved in methanol and sonicated at room temperature for 4 hours. The solids were filtered off and the solvent evaporated *in vacuo* to afford a white solid. The residue was dissolved in water (10 mL), cooled in an ice bath and acidified to pH=2 with a solution of saturated aqueous $KHSO_4$. The aqueous solution was extracted with diethyl ether (4 x 15 mL). The organic phase was dried over $MgSO_4$ and evaporated *in vacuo* to afford compound **31** as a clear oil (169 mg, 51%): $[\alpha]_D^{21}$ = -14.9° (c = 1, methanol); ^{1}H NMR (400 MHz, $CDCl_3$) d 5.23 (1H, d, *J* = 7Hz, NH), 4.38 (1H, m, *CH*NH), 2.50 (2H, t, *J* = 7Hz, CH_2CO), 2.20 (2H, m, CH_2CH), 1.43 (9H, s, CH_3); m/z (ES^+) 270 $[M+Na]^+$

N-Boc-D-aspartic acid

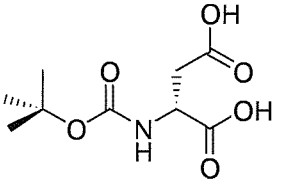

Following the procedure of Einhorn,[139] a mixture of commercially available D-aspartic acid (505 mg, 3.80 mmol), Boc anhydride (984 mg, 4.50 mmol) and solid $NaHCO_3$ (950 mg) was dissolved in methanol and sonicated at room temperature for 4 hours. The solids were filtered off and the solvent

evaporated *in vacuo* to afford a pale yellow foam. The residue was dissolved in water (10 mL), cooled in an ice bath and acidified to pH=2 with a solution of saturated aqueous $KHSO_4$. The aqueous solution was extracted with diethyl ether (3x15 mL). The organic phase was dried over $MgSO_4$ and evaporated *in vacuo* to afford compound as a clear oil (230 mg, 30%): $[\alpha]_D^{21}$ = -5.2° (c = 1, methanol); ^{1}H NMR (300 MHz, $CDCl_3$) d 4.46 (1H, m, C*H*NH), 2.81 (2H, b s, CH_2), 1.50 (9H, s, CH_3); *m/z* (ES^+) 234 $[M+H]^+$, 256 $[M+Na]^+$

Preparation of bis-tetrabutylammonium salts of *N*-Boc-L-(D)-Glutamic acid – 116, 117

A 1 M aqueous solution of tetrabutylammonium hydroxide (TBA, 0.74 mL) was added to a solution of commercially available *N*-Boc-L(D)-glutamic acid (100 mg, 0.39 mmol) in methanol (2.5 mL). The solution was stirred for 2 hours at room temperature. The solvent was then removed *in vacuo*. Residual water was removed by freeze-drying on high vacuum over 16 hours. Compound **116** (**117**) was obtained as a clear oil (456 mg, quantitative).

N-Boc-L-glutamate – **116**: $[\alpha]_D^{21}$ = 35.6° (c = 1, $CHCl_3$) ^{1}H NMR (300 MHz, $CDCl_3$) d 3.91 (1H, m, C*H*NH), 3.25 (16H, t, *J* = 5Hz, $TBACH_2N$), 2.30 (2H, t, *J* = 7Hz, CH_2CO), 1.65 (18H, m, CH_2CHNH + $TBACH_2CH_2CH_3$), 1.38 (25H, m, CH_3 + $TBACH_2CH_3$), 0.98 (24H, t, *J* = 7Hz, $TBACH_3$)

N-Boc-D-glutamate – **117**: $[\alpha]_D^{21}$ = -35.6° (c = 1, $CHCl_3$); ^{1}H NMR same as with the one above

Preparation of bis-tetrabutylammonium salts of *N*-Boc-L-(D)-Aspartic acid – 118, 119

A 1 M aqueous solution of tetrabutylammonium hydroxide (TBA, 0.40 mL) was added to a solution of commercially available *N*-Boc-L(D)-aspartic acid (50 mg, 0.2 mmol) in methanol (2.5 mL). The solution was stirred for 2 hours at room temperature. The solvent was removed *in vacuo*. Residual water was removed by freeze-drying on high vacuum over 16 hours. Compound **118** (**119**) was obtained as a clear oil (210 mg, quantitative).

N-Boc-L-aspartate – **118**: $[\alpha]_D^{21}$ = 16.2° (c = 1, $CHCl_3$); ^{1}H NMR (300 MHz, DMSO) d 3.65 (1H, m, C*H*NH), 3.21 (16H, t, *J* = 5Hz, $TBACH_2N$), 2.30 (2H, t, *J* = 7Hz, CH_2), 1.68 (16H, m, $TBACH_2CH_2CH_3$), 1.45 (25H, m, CH_3 + $TBACH_2CH_3$), 1.0 (24H, t, *J* = 7Hz, $TBACH_3$)

N-Boc-D-aspartate – **119**: $[\alpha]_D^{21}$ = -16.2° (c = 1, $CHCl_3$); ^{1}H NMR same as the one above

Preparation of bis-tetrabutylammonium salts of dybenzoil-L-(D)-Tartaric acid – 120, 121

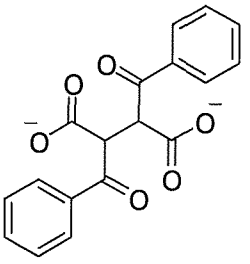

A 1 M aqueous solution of tetrabutylammonium hydroxide (TBA, 0.27 mL) was added to a solution of commercially available dybenzoil-L(D)-tartaric acid (50 mg, 0.14 mmol) in methanol (2.5 mL). The solution was stirred for 2 hours at room temperature. The solvent was removed *in vacuo*. Residual water was removed by freeze-drying on high vacuum over 16 hours. Compound **37** (**38**) was obtained as a white solid (116 mg, quantitative).

Dybenzoyl-L-tartrate – **120**: $[\alpha]_D^{21}$ = 10.9° (c = 1, $CHCl_3$); ^1H NMR (300 MHz, $CDCl_3$) d 8.18 (4H, d, *J* = 7.3Hz, ArH), 7.45 (2H, m, ArH), 7.33 (4H, m, ArH), 5.82 (2H, s, CHCO), 3.25 (16H, m, $TBACH_2N$), 1.58 (16H, m, $TBACH_2CH_2CH_3$), 1.35 (16H, m, $TBACH_2CH_3$), 1.0 (24H, t, *J* = 7Hz, $TBACH_3$)

Dybenzoyl-D-tartrate – **121**: $[\alpha]_D^{21}$ = -10.9° (c = 1, $CHCl_3$); ^1H NMR same as the one above

4.6 Experimental for binding studies

Obtaining association constants by ^{1}H NMR titration experiments involves titration of a solution of host with a specific guest and recording a ^{1}H NMR spectrum after each addition. Upon complexation, protons in the host or guest may undergo a change in chemical shifts. In particular, protons involved in hydrogen bonding undergo a dramatic shift and therefore are used to determine association constants. After the data from the titration experiment have been acquired, curve fitting software is employed to determine the association constant. Free host and guest are in equilibrium with the host-guest complex. As association and dissociation is fast on the NMR time scale, only a time averaged spectrum of the host (or guest) and the host-guest complex is observed. Therefore, any observed chemical shift (δ_{obs}) is the mole fraction weighted average of the shifts observed in the free (δ_{free}) and complexed (δ_{bound}) molecule. During the curve fitting procedure, after an initial estimate for K_a and $\Delta\delta$, the theoretical δ_{obs} is obtained for each point. The theoretical values are then compared with the experimentally observed ones and the sum of the difference between each point is determined by the following equation:

$$\text{Sum of differences} = \Sigma\ (\delta_{obs\ (experimental)} - \delta_{obs(theoretical)})$$

If the sum of differences is positive (or negative), the K_a is increased (or decreased) and the value $\Delta\delta$ recalculated and the whole calculation repeated until the values converge. A detailed explanation of the theoretical basis to the above discussion has been published by Wilcox.[140] A more recent review on the determination of association constants from solution NMR data has been published by Fielding.[118b]

4.6.1 Method Used for obtaining binding constants

All ^{1}H NMR titration experiments were conducted on either a Brüker AM 300 or Brüker DPX 400 spectrometer at 298 K, unless otherwise stated. All $CDCl_3$ was passed over a pad of basic alumina prior to use and collected over molecular sieves (4Å). A sample of host was dissolved in the deuterated solvent. A portion of this solution was used as the host NMR sample and the remainder used to dissolve a sample of the guest, so that the concentration of the host remained constant throughout the titration.

Guest stock solutions were typically prepared such that 10μL of that solution contained 0.1 equivalents of guest with respect to host, unless otherwise stated. Successive aliquots of the guest solution were added to the host NMR sample and ^{1}H NMR sample recorded after each addition. The hydrogens monitored during binding studies were the thiourea or amide protons in the host molecule unless otherwise stated. The changes in chemical shifts of all the hosts signals as a function of guest concentration were analysed with purpose-written software, kindly provided by C.A. Hunter, where a 1:1 binding mode or a 1:2 mode was assumed (see Appendix 2). These programs fit the data to the appropriate binding model to yield the association constant, the bound chemical shift and the free chemical shift. For a greater degree of accuracy, association constants quoted in the results and discussion chapters are taken as average of all the association constants obtained from each proton monitored in the host molecule. All the experiments were repeated at least twice.

*Binding data for N-Boc-L-Glu with macrocycle **112***

Solvent: CD_3CN

Starting volume of host solution: 600μL

Concentration of host solution: 1.5 mM

Concentration of guest solution: 13.6 mM

Association constant: $1.5\times10^5\ M^{-1} \pm 1\%$

Volume added / μL	Amide proton / ppm	Thiourea proton / ppm	CH proton / ppm
0	9.1229	8.2484	5.3583
20	9.3901	8.5985	5.5302
40	9.6823	9.0186	5.7108
60	9.9558	9.4214	5.8587
80	10.1239	9.6020	5.9303
100	10.1728	9.6647	5.9454
120	10.1791	9.6810	5.9478
140	10.1816	9.6798	5.9492
170	10.1829	9.6861	5.9492
200	10.1854	9.6798	5.9492

Binding data for N-Boc-D-Glu with macrocycle ***112***

Solvent: CD_3CN

Starting volume of host solution: 600μL

Concentration of host solution: 1.5 mM

Concentration of guest solution: 13.0 mM

Association constant: $2.2x10^4\ M^{-1} \pm 2\%$

Volume added / μL	Amide proton / ppm	Thiourea proton / ppm	CH proton / ppm
0	9.1153	8.2473	5.3521
20	9.2470	8.4154	5.4512
40	9.3424	8.5809	5.6117
60	9.5117	8.7980	5.6882
80	9.6397	8.9773	5.7535
100	9.7589	9.1216	5.8099
120	9.8768	9.2772	5.8501
140	9.9545	9.3788	5.8802
170	10.0336	9.4779	5.8839
200	10.0662	9.5155	5.8839

Binding data for N-Boc-L-Glu with macrocycle ***112***

Solvent: DMSO

Starting volume of host solution: 600μL

Concentration of host solution: 2.35 mM

Concentration of guest solution: 94.16 mM

Association constant: $3.7\times10^{3}\ M^{-1} \pm 6\%$

Volume added / μL	Amide proton / ppm	Thiourea proton / ppm
0	9.471	8.395
20	9.496	8.447
40	9.555	8.548
60	9.603	8.653
80	9.656	8.754
100	9.713	8.856
140	9.803	9.093
180	9.886	9.251
220	9.946	9.359
260	9.989	9.444
300	10.011	9.483
360	10.033	9.510
420	10.048	9.537
480	10.050	9.556
540	10.058	9.556
600	10.068	9.564

Binding data for N-Boc-D-Glu with macrocycle ***112***

Solvent: DMSO

Starting volume of host solution: 600μL

Concentration of host solution: 2.35 mM

Concentration of guest solution: 94.16 mM

Association constant: multiple binding equilibria competing

Volume added / μL	Amide proton / ppm	Thiourea proton / ppm
0	9.471	8.395
10	9.487	8.430
20	9.502	9.464
30	9.521	8.505
50	9.557	8.586
80	9.618	8.720
100	9.660	8.828
120	9.703	8.911
140	9.746	9.019
180	9.807	9.187
220	9.865	9.296
260	9.895	9.934
300	9.926	9.427
340	9.942	9.460
380	9.949	9.481
400	9.956	9.487

Job plot data for N-Boc-L-Glu with macrocycle ***112***

Solvent:	CD_3CN
Concentration of host stock solution:	4.15 mM
Concentration of guest stock solution:	4.15 mM
Proton monitored:	Thiourea

Host – Guest ratio	Chemical shift /ppm
2:8	8.2484
3:7	8.3808
4:6	8.7007
5:5	9.1146
6:4	9.6302
7:3	9.5851
8:2	9.5449

*Job plot data for N-Boc-D-Glu with macrocycle **112***

Solvent:	CD_3CN
Concentration of host stock solution:	2.56 mM
Concentration of guest stock solution:	2.56 mM
Proton monitored:	Thiourea

Host – Guest ratio	Chemical shift /ppm
2:8	8.2027
3:7	8.2127
4:6	8.2378
5:5	8.3055
6:4	8.4084
7:3	8.5337
8:2	8.4822

*Binding data for N-Boc-L-Asp with macrocycle **112***

Solvent: MeCN

Starting volume of host solution: 600μL

Concentration of host solution: 1.2 mM

Concentration of guest solution: 13.4 mM

Association constant: $2.1 \times 10^5\ M^{-1}$

Volume added / μL	Aromatic protons / ppm	CH proton / ppm
0	7.625	5.325
10	7.638	5.369
20	7.645	5.423
30	7.667	5.479
40	7.678	5.516
50	7.690	5.625
60	7.702	5.817
70	7.710	5.850
80	7.710	5.862
90	7.709	5.872
100	7.708	5.877
110	7.708	5.914
120	7.708	5.901
130	7.707	5.927
140	7.706	5.895
150	7.706	5.887

Binding data for N-Boc-D-Asp with macrocycle ***112***

Solvent:	MeCN
Starting volume of host solution:	600μL
Concentration of host solution:	0.97 mM
Concentration of guest solution:	32.9 mM
Association constant:	multiple binding equilibria present

Volume added / μL	Amide proton / ppm	Thiourea proton / ppm	CH proton / ppm
0	9.0511	8.2291	5.2992
10	9.1387	8.3073	5.3594
20	9.2390*	8.4081*	5.4596
30	9.4561*	8.6283*	5.6723
40	9.6764*	9.0594*	5.8976
50	10.2322	9.7863	5.8976
60	10.2376	9.7738	5.8897
70	10.2267	9.7770	5.8897
80	10.2220	9.7840	5.8850
90	10.2196	9.7676	5.8749
100	10.2095	9.7644	5.8671
110	10.2040	9.7637	5.8600
120	10.1931	9.7558	5.8584
130	10.1985	9.7465	5.8561

1 equivalent added at ~30 μL
* Signal getting very broad

*Binding data for N-Boc-L-Asp with macrocycle **112***

Solvent:	DMSO-d_6
Temperature	90°C
Starting volume of host solution:	600μL
Concentration of host solution:	3.1 mM
Concentration of guest solution:	27.9 mM
Association constant:	$1.2x10^3$ M^{-1} ± 3%

Volume added / μL	Amide proton / ppm	Thiourea proton / ppm
0	8.1808	9.2826
20	8.3035	9.3595
40	8.5045	9.4307
60	8.5931	9.506
80	8.6850	9.5223
100	8.7365	9.5475
120	8.7658	9.5826
140	8.8163	9.5972

Binding data for N-Boc-D-Asp with macrocycle ***112***

Solvent:	DMSO-d_6
Temperature	90°C
Starting volume of host solution:	600μL
Concentration of host solution:	3.1 mM
Concentration of guest solution:	27.9 mM
Association constant:	92 M^{-1} ± 4%

Volume added / μL	Amide proton / ppm	Thiourea proton / ppm
0	9.2670	8.1614
20	9.2844	8.1744
40	9.3013	8.2165
60	9.3344	8.2896
80	9.3554	8.3335
100	9.3795	8.3802
120	9.3924	8.4208
140	9.4113	8.4552
170	9.4378	8.5011
200	9.4517	8.5338
250	9.4778	8.5843

Binding data for TBA Acetate with macrocycle ***112***

Solvent: MeCN

Starting volume of host solution: 600μL

Concentration of host solution: 3.1 mM

Concentration of guest solution: 27.9 mM

Association constant: $1.12 \times 10^4\ M^{-1} \pm 3\%$

Volume added / μL	Amide proton / ppm	Thiourea proton / ppm
0	9.0731	8.2417
10	9.1560	8.3567
20	9.2678	8.5170
30	9.3460	8.6789
40	9.4359	8.8267
50	9.4994	8.9167
60	9.5454	8.9933
70	9.5619	9.0269
80	9.5798	9.0598
90	9.6017	9.0833
100	9.6205	9.1075
110	9.6386	9.1239
120	9.6479	9.1364
130	9.6644	9.1552
140	9.6777	9.1724
150	9.6941	9.1842
160	9.7066	9.1982
170	9.7121	9.2076
180	9.7270	9.2240
190	9.7356	9.2350
200	9.7489	9.2514
220	9.7731	9.2694

*Binding data for Dibenzoyl-L-Tartrate with macrocycle **112***

Solvent: DMSO-d_6

Starting volume of host solution: 600μL

Concentration of host solution: 1.30 mM

Concentration of guest solution: 12.6 mM

Association constant: 211 M^{-1} ± 5%

Volume added / μL	Amide proton / ppm	Thiourea proton / ppm
0	9.4428	8.3590
20	9.4478	8.3766
40	9.4554	8.4292
60	9.4591	8.4793
80	9.4641	8.5221
100	9.4641	8.5446
120	9.4654	8.5760
140	9.4704	8.5998
170	9.4654	8.6248
200	9.4679	8.6325

Binding data for Dibenzoyl-D-Tartrate with macrocycle ***112***

Solvent: DMSO-d_6

Starting volume of host solution: 600μL

Concentration of host solution: 1.30 mM

Concentration of guest solution: 12.6 mM

Association constant: 103 M^{-1} ± 5%

Volume added / μL	Amide proton / ppm	Thiourea proton / ppm
0	9.4428	8.3590
20	9.4491	8.3777
40	9.4529	8.4118
60	9.4641	8.4982
80	9.4641	8.5396
100	9.4654	8.5797
120	9.4679	8.6061
140	9.4717	8.6324
170	9.4704	8.6788
200	9.4729	8.6751

*Binding data for N-Boc-L-Asp with macrocycle **131***

Solvent: DMSO-d_6

Starting volume of host solution: 600μL

Concentration of host solution: 2.13 mM

Concentration of guest solution: 15.1 mM

Association constant: multiple binding equilibria

Volume added / μL	Amide proton / ppm	Thiourea proton / ppm	CH protons / ppm
0	9.0241	8.5875	4.9723
20	9.0229	8.6063	4.9654
40	9.0367	8.6753	4.9504
60	9.0567	8.7945	4.9303
80	9.0781	8.7932	4.8979
100	9.1044	8.8045	4.8897
120	9.1145	8.7882	4.8569
140	9.1295	8.7869	4.8431
170	9.1483	8.7971	4.8193
250	9.1809	8.7945	4.8055

*Binding data for N-Boc-D-Asp with macrocycle **131***

Solvent: DMSO-d_6

Starting volume of host solution: 600μL

Concentration of host solution: 2.13 mM

Concentration of guest solution: 16.3 mM

Association constant: multiple binding equilibria

Volume added / μL	Amide proton / ppm	Thiourea proton / ppm
0	9.0069	8.5641
20	9.0074	8.5635
40	9.0094	8.5672
60	9.0144	85785
80	9.0232	8.6024
100	9.0351	8.6231
120	9.0458	8.6325
140	9.0627	8.6438
160	9.0646	8.6463
180	9.0746	8.7085
200	9.0866	8.7585
220	9.0960	8.7541
240	9.1000	8.7667

*Binding data for N-Boc-L-Glu with macrocycle **137***

Solvent: DMSO

Starting volume of host solution: 600μL

Concentration of host solution: 2.89 mM

Concentration of guest solution: 24.5 mM

Association constant: multiple binding equilibria

Volume added / μL	Amide proton / ppm	Thiourea proton / ppm	CH proton / ppm
0	9.0379	8.0172	5.5988
10	9.0402	8.0172	5.6106
20	9.0402	8.0430	5.6300
30	9.0590	8.0782	5.6497
40	9.0715	8.1064	5.6544
50	9.1059	8.1494	5.6551
60	9.1255	8.2080	5.6653
70	9.1404	8.2691	5.6770
80	9.1693	8.3144	5.6794
90	9.1912	8.4114	5.6778
100	9.2170	8.4568	5.6794
110	9.2608	84834	5.6849
120	9.2937	8.5300	5.6817
130	9.2921	8.5358	5.6825

*Binding data for N-Boc-D-Glu with macrocycle **137***

Solvent: DMSO

Starting volume of host solution: 600μL

Concentration of host solution: 3.49 mM

Concentration of guest solution: 24.4 mM

Association constant: $1.03 \times 10^3\ M^{-1} \pm 3\%$

Volume added / μL	Amide proton / ppm	CH proton / ppm
0	9.0363	5.6289
10	9.0395	5.6328
20	9.0434	5.6602
30	9.0637	5.6653
40	9.0684	5.6657
50	9.1122	5.6664
60	9.1419	5.6688
70	9.1615	5.6673
80	9.1709	5.6817
90	9.1990	5.6810
100	9.2319	5.6817
110	9.2718	5.6849
120	9.2937	5.6856
130	9.2983	5.6864
140	9.3116	5.872
150	9.3296	5.864
160	9.3367	5.6888
170	9.3609	5.6896
180	9.3969	5.6919
190	9.4012	5.6919
200	9.4000	5.6919
220	9.4024	5.6966

4.7 Experimental for calorimetric studies (ITC)

By directly measuring the heat evolved or absorbed as a function of time ITC can determine, in one stroke, all the thermodynamic parameters involved in a chemical process. In a single experiment the binding constant (K_a), the stoichiometry (n) and the enthalpy (ΔH) of the process investigated are determined. From the association constant, it is possible to determine the free energy and entropy of binding for the interaction. A typical ITC titration begins with a known concentration of macrocycle dissolved in solution to which controlled aliquots of the guest species under test are added through a syringe. As the complexation takes place, an endothermic or exothermic signal, depending on the nature of the complexation, is observed. As the guest concentration increases and the supply of macrocycle available for binding is exhausted, we reach a plateau in terms of the amount of heat evolved or absorbed on further addition of guest.

4.7.1 Method for obtaining calorimetric data

All binding experiments were performed on an isothermal titration calorimeter from Microcal Inc. (Northampton, MA). In a typical experiment a 1 - 2 mM receptor solution is added to the calorimetric cell. A 64 mM solution of tetrabutylammonium salts of N-Boc-Glu and N-Boc-Asp is introduced in 65 injections (30 of 2.5 μL and 35 of 5 μL), for a total of 250μL of added guest. Such high concentrations of guests are important to generate sharp curves, necessary for acceptable curve fitting. The solution is continuously stirred to ensure rapid mixing and kept at 25°C, through the combination of an external cooling bath and an internal heater. Dilution effects are determined by performing a blank experiment by adding the same guest solution into the pure solvent and subtracting this from the raw titration to produce the final binding curve. Association parameters are found by applying either one-site or two-sites models, using the Origin software provided. These methods rely on standard non-linear least-squares regression (Levenberg-Marquard method) to fit the curves, taking into account the change in volume that occurs during the calorimetric titration (see Appendix 3). All experiments were repeated twice.

*Calorimetric data for N-Boc-L-Glu with macrocycle **1***

Solvent: CD_3CN

Concentration of host solution: 1.29 mM

Concentration of guest solution: 63.8 mM

$K_{1:1}$: $(2.83 \pm 0.48) \times 10^4\ M^{-1}$

ΔG: $-25.5 \pm 0.5\ kJmol^{-1}$

ΔH: $-4.5 \pm 0.2\ kJmol^{-1}$

$T\Delta S$: $21.0\ kJmol^{-1}$

Area (μcal)	Injection (μL)	[guest] (mM) (before inj.)	[host] (mM) (before inj.)	[host] / [guest] (after inj.)	Cal / mol of injected guest
-189.249	2.5	0	1.29	0.08481	-1006.41
-153.764	2.5	0.10922	1.2878	0.16977	-994.711
-48.8784	2.5	0.21825	1.28559	0.25487	-979.505
-38.8221	2.5	0.3271	1.2834	0.34011	-959.343
-39.0044	2.5	0.43576	1.2812	0.42551	-932.017
-37.446	2.5	0.54423	1.27901	0.51104	-894.113
-28.8245	2.5	0.65251	1.27683	0.59672	-840.351
-27.3975	2.5	0.76061	1.27464	0.68255	-762.769
-19.1454	2.5	0.86852	1.27247	0.76852	-650.441
-3.40689	2.5	0.97624	1.27029	0.85464	-491.936
23.05663	2.5	1.08378	1.26812	0.9409	-284.261
68.71635	2.5	1.19113	1.26595	1.0273	-45.9641
123.3233	2.5	1.29829	1.26379	1.11385	184.2439
155.6574	2.5	1.40527	1.26163	1.20055	372.7141
182.2862	2.5	1.51206	1.25947	1.28739	509.6974
185.8849	2.5	1.61866	1.25732	1.37438	603.046
195.1904	2.5	1.72507	1.25517	1.46151	665.0635
195.5603	2.5	1.8313	1.25302	1.54878	706.0239
198.4545	2.5	1.93734	1.25088	1.6362	733.0598
200.9079	2.5	2.04319	1.24874	1.72377	750.8193

197.6934	2.5	2.14886	1.24661	1.81148	762.2913
201.0834	2.5	2.25434	1.24448	1.89933	769.4118
199.4598	2.5	2.35963	1.24235	1.98733	773.4588
199.4112	2.5	2.46474	1.24022	2.07548	775.2908
199.9179	2.5	2.56966	1.2381	2.16377	775.4984
197.5559	2.5	2.67439	1.23599	2.2522	774.4956
204.3711	2.5	2.77893	1.23387	2.34078	772.5789
197.0166	2.5	2.88329	1.23176	2.42951	769.9635
198.3899	2.5	2.98746	1.22966	2.51838	766.8094
199.3671	2.5	3.09144	1.22755	2.6074	763.2363
408.6134	5	3.19524	1.22545	2.78586	757.2538
397.7125	5	3.40227	1.22126	2.96491	748.5533
397.2287	5	3.60856	1.21709	3.14453	739.2767
392.9763	5	3.81409	1.21293	3.32473	729.651
387.8707	5	4.01888	1.20878	3.50552	719.8238
383.2565	5	4.22292	1.20465	3.68688	709.8975
380.2648	5	4.42621	1.20053	3.86883	699.9397
378.5055	5	4.62876	1.19642	4.05135	689.9992
373.7875	5	4.83055	1.19233	4.23446	680.1104
371.6359	5	5.0316	1.18825	4.41814	670.2981
368.181	5	5.2319	1.18419	4.6024	660.5799
362.3546	5	5.43145	1.18013	4.78725	650.9688
358.7509	5	5.63025	1.17609	4.97267	641.4738
355.7086	5	5.82831	1.17207	5.15867	632.1017
353.4957	5	6.02562	1.16806	5.34526	622.8568
345.1381	5	6.22218	1.16406	5.53242	613.7422
341.4609	5	6.41799	1.16007	5.72016	604.7598
337.9775	5	6.61305	1.1561	5.90848	595.9105
336.817	5	6.80737	1.15213	6.09739	587.1947
330.3869	5	7.00094	1.14819	6.28687	578.6119
328.342	5	7.19376	1.14425	6.47693	570.1617
325.628	5	7.38583	1.14033	6.66757	561.843
324.4354	5	7.57715	1.13642	6.85879	553.6546
319.7499	5	7.76773	1.13252	7.0506	545.595

317.4505	5	7.95756	1.12864	7.24298	537.6627
313.8304	5	8.14664	1.12476	7.43594	529.856
308.8789	5	8.33497	1.1209	7.62948	522.173
306.1113	5	8.52255	1.11706	7.8236	514.612
304.1368	5	8.70939	1.11322	8.0183	507.171
302.4893	5	8.89548	1.1094	8.21358	499.8481
297.8454	5	9.08082	1.10559	8.40944	492.6414
295.0179	5	9.26541	1.10179	8.60588	485.5489
292.5818	5	9.44925	1.098	8.8029	478.5686
291.6189	5	9.63235	1.09422	9.0005	471.6987
287.6484	5	9.8147	1.09046	9.19868	464.9372

Calorimetric data for N-Boc-L-Glu with macrocycle 1

Solvent: DMSO

Concentration of host solution: 1.70 mM

Concentration of guest solution: 63.8 mM

$K_{1:1}$: $(2.28 \pm 0.26) \times 10^3\ M^{-1}$

ΔG: $-19.2 \pm 0.3\ kJmol^{-1}$

ΔH: $-10.7 \pm 0.3\ kJmol^{-1}$

$T\Delta S$: $8.5\ kJmol^{-1}$

Area (µcal)	In*J*ection (µL)	[guest] (mM) (before in*J*.)	[host] (mM) (before in*J*.)	[host] / [guest] (after in*J*.)	Cal / mol of in*J*ected guest
-161.886	2.5	0	1.1	0.0993	-1337.65
-90.2475	2.5	0.10905	1.09812	0.19878	-1375.09
11.27755	2.5	0.21791	1.09624	0.29842	-703.811
39.90831	2.5	0.32659	1.09437	0.39824	-496.342
38.48032	2.5	0.43507	1.0925	0.49822	-421.463
37.12389	2.5	0.54338	1.09063	0.59837	-461.924
34.64639	2.5	0.65149	1.08877	0.6987	-436.947
39.17605	2.5	0.75942	1.08691	0.79919	-410.543
44.05991	2.5	0.86716	1.08505	0.89985	-392.674
45.30751	2.5	0.97472	1.08319	1.00069	-385.668
50.10141	2.5	1.08208	1.08134	1.10169	-334.315
49.97473	2.5	1.18927	1.07949	1.20286	-335.466
54.46843	2.5	1.29626	1.07765	1.3042	-321.788
51.83733	2.5	1.40307	1.07581	1.40571	-325.658
55.12957	2.5	1.50969	1.07397	1.50739	-311.95
57.1755	2.5	1.61612	1.07213	1.60924	-287.235
58.55822	2.5	1.72237	1.0703	1.71127	-282.892
61.45247	2.5	1.82843	1.06847	1.81346	-248.663
59.96674	2.5	1.93431	1.06664	1.91582	-263.674
64.83653	2.5	2.04	1.06482	2.01835	-253.113
65.06789	2.5	2.1455	1.063	2.12104	-222.724

67.32089	2.5	2.25081	1.06118	2.22391	-207.731
66.03197	2.5	2.35594	1.05937	2.32695	-210.502
66.42182	2.5	2.46088	1.05755	2.43016	-204.351
68.53337	2.5	2.56563	1.05575	2.53354	-184.38
65.1799	2.5	2.6702	1.05394	2.63709	-198.573
69.1444	2.5	2.77458	1.05214	2.74081	-183.189
71.21907	2.5	2.87878	1.05034	2.84469	-140.362
71.91211	2.5	2.98278	1.04854	2.94875	-160.102
72.54432	2.5	3.08661	1.04675	3.05298	-145.411
142.559	5	3.19024	1.04496	3.26194	-134.39
143.9514	5	3.39695	1.04139	3.47158	-124.404
144.0609	5	3.60291	1.03783	3.68191	-119.432
145.1212	5	3.80812	1.03428	3.89291	-114.274
144.5124	5	4.01259	1.03074	4.10458	-111.096
145.3643	5	4.21631	1.02722	4.31694	-100.176
148.5058	5	4.41928	1.02371	4.52998	-80.438
149.9882	5	4.62151	1.02021	4.7437	-71.3016
150.9199	5	4.82299	1.01672	4.95809	-65.0885
146.0983	5	5.02372	1.01324	5.17316	-82.63
148.2582	5	5.22371	1.00977	5.38892	--
148.4458	5	5.42295	1.00632	5.60535	-70.4224
147.901	5	5.62144	1.00287	5.82246	-65.3843
146.5182	5	5.81919	0.99944	6.04025	-64.0796
144.6853	5	6.01619	0.99602	6.25872	-68.4385
144.654	5	6.21244	0.99261	6.47786	-55.5948
143.5786	5	6.40795	0.98921	6.69769	-59.6914
142.709	5	6.60271	0.98582	6.9182	-50.3022
142.2546	5	6.79672	0.98244	7.13938	-59.2032
144.7085	5	6.98998	0.97907	7.36124	-30.7934
143.647	5	7.1825	0.97572	7.58379	-44.7431
141.9071	5	7.37427	0.97237	7.80701	-46.0725
142.2937	5	7.5653	0.96904	8.03091	-47.0604
141.0659	5	7.75557	0.96572	8.25549	-36.5681
140.4693	5	7.9451	0.9624	8.48074	-39.5955

136.228	5	8.13389	0.9591	8.70668	-46.0735
135.4401	5	8.32193	0.95581	8.9333	-40.4926
129.5075	5	8.50922	0.95253	9.16059	-73.6058
128.4891	5	8.69576	0.94926	9.38856	-65.8069
127.3033	5	8.88156	0.946	9.61722	-68.0248
127.6564	5	9.06661	0.94275	9.84655	-58.9859
126.8861	5	9.25091	0.93951	10.07656	-58.9804
128.8799	5	9.43447	0.93628	10.30725	-48.7928
124.5153	5	9.61727	0.93306	10.53862	-49.9541
126.2051	5	9.79934	0.92985	10.77066	-53.7917

Calorimetric data for N-Boc-D-Glu with macrocycle 1

Solvent: CD_3CN

Concentration of host solution: 0.96 mM

Concentration of guest solution: 65.1 mM

$K_{1:1}$: 38.4 ± 1.7 M^{-1} $K_{1:2}$: (4.92 ± 0.07) x10^4 M^{-1}

ΔG: -26.8 ± 0.1 k*J*mol^{-1}

ΔH: -6.7 ± 0.1 k*J*mol^{-1}

TΔS: 20.1 k*J*mol^{-1}

Area (μcal)	**In*J*ection (μL)**	**[guest] (mM) (before in*J*.)**	**[host] (mM) (before in*J*.)**	**[host] / [guest] (after in*J*.)**	**Cal / mol of in*J*ected guest**
-163.719	2.5	0	0.94	0.11621	-2041.35
-196.252	2.5	0.10905	0.93839	0.23261	-2039.39
-188.462	2.5	0.21791	0.93679	0.34922	-2036.85
-183.107	2.5	0.32659	0.93519	0.46602	-2033.48
-186.473	2.5	0.43507	0.93359	0.58302	-2028.92
-185.276	2.5	0.54338	0.93199	0.70023	-2022.52
-178.878	2.5	0.65149	0.9304	0.81763	-2013.19
-186.245	2.5	0.75942	0.92881	0.93522	-1998.97
-173.145	2.5	0.86716	0.92722	1.05302	-1976.03
-171.419	2.5	0.97472	0.92564	1.17102	-1936.71
-162.417	2.5	1.08208	0.92406	1.28921	-1865.6
-131.26	2.5	1.18927	0.92248	1.4076	-1737.26
-94.9491	2.5	1.29626	0.9209	1.52619	-1538.3
-61.1531	2.5	1.40307	0.91933	1.64498	-1320.06
-42.0515	2.5	1.50969	0.91775	1.76397	-1157.13
-28.0974	2.5	1.61612	0.91618	1.88316	-1058.73

-20.2937	2.5	1.72237	0.91462	2.00254	-1000.25
-13.1429	2.5	1.82843	0.91306	2.12213	-962.691
-8.54055	2.5	1.93431	0.91149	2.24191	-936.147
-4.22314	2.5	2.04	0.90994	2.36189	-915.726
-0.45496	2.5	2.1455	0.90838	2.48207	-898.93
1.15022	2.5	2.25081	0.90683	2.60245	-884.414
2.37363	2.5	2.35594	0.90528	2.72303	-871.412
4.78172	2.5	2.46088	0.90373	2.84381	-859.465
7.65869	2.5	2.56563	0.90218	2.96478	-848.287
8.14733	2.5	2.6702	0.90064	3.08595	-837.692
9.06747	2.5	2.77458	0.8991	3.20733	-827.554
9.9707	2.5	2.87878	0.89756	3.3289	-817.787
12.13907	2.5	2.98278	0.89603	3.45067	-808.329
13.29957	2.5	3.08661	0.8945	3.57263	-799.134
29.02517	5	3.19024	0.89297	3.81717	-785.787
31.09795	5	3.39695	0.88991	4.06249	-768.63
34.02882	5	3.60291	0.88687	4.30861	-752.129
36.58593	5	3.80812	0.88384	4.55553	-736.197
38.94935	5	4.01259	0.88082	4.80324	-720.777
40.09813	5	4.21631	0.87781	5.05174	-705.825
40.88099	5	4.41928	0.8748	5.30104	-691.309
42.01826	5	4.62151	0.87181	5.55113	-677.202
43.33526	5	4.82299	0.86883	5.80202	-663.482
43.74343	5	5.02372	0.86586	6.0537	-650.132
45.50059	5	5.22371	0.8629	6.30618	-637.133
45.81537	5	5.42295	0.85994	6.55945	-624.472

46.65492	5	5.62144	0.857	6.81352	-612.136
47.17971	5	5.81919	0.85407	7.06838	-600.112
47.51448	5	6.01619	0.85114	7.32403	-588.39
47.64501	5	6.21244	0.84823	7.58048	-576.957
48.34218	5	6.40795	0.84532	7.83772	-565.806
49.1942	5	6.60271	0.84243	8.09576	-554.926
49.67137	5	6.79672	0.83954	8.35459	-544.308
48.73941	5	6.98998	0.83666	8.61422	-533.944
49.47997	5	7.1825	0.8338	8.87464	-523.827
49.06059	5	7.37427	0.83094	9.13586	-513.948
49.83424	5	7.5653	0.82809	9.39787	-504.3
50.39214	5	7.75557	0.82525	9.66068	-494.876
50.46469	5	7.9451	0.82242	9.92427	-485.669
50.54157	5	8.13389	0.8196	10.18867	-476.673
50.91086	5	8.32193	0.81678	10.45386	-467.882
51.19185	5	8.50922	0.81398	10.71984	-459.29
50.30102	5	8.69576	0.81118	10.98662	-450.891
50.31416	5	8.88156	0.8084	11.25419	-442.679
50.05067	5	9.06661	0.80562	11.52256	-434.649
49.99682	5	9.25091	0.80285	11.79172	-426.795
50.63248	5	9.43447	0.80009	12.06167	-419.114
50.94008	5	9.61727	0.79734	12.33242	-411.6
50.28977	5	9.79934	0.7946	12.60397	-404.248

Calorimetric data for N-Boc-D-Glu with macrocycle 1

Solvent: DMSO

Concentration of host solution: 1.10 mM

Concentration of guest solution: 63.8 mM

Multiple binding equilibria

Area (μcal)	**Injection (μL)**	**[guest] (mM) (before inj.)**	**[host] (mM) (before inj.)**	**[host] / [guest] (after inj.)**	**Cal / mol of injected guest**
-161.886	2.5	0	1.1	0.0993	-1337.65
-90.2475	2.5	0.10905	1.09812	0.19878	-1375.09
11.27755	2.5	0.21791	1.09624	0.29842	-703.811
39.90831	2.5	0.32659	1.09437	0.39824	-496.342
38.48032	2.5	0.43507	1.0925	0.49822	-421.463
37.12389	2.5	0.54338	1.09063	0.59837	-461.924
34.64639	2.5	0.65149	1.08877	0.6987	-436.947
39.17605	2.5	0.75942	1.08691	0.79919	-410.543
44.05991	2.5	0.86716	1.08505	0.89985	-392.674
45.30751	2.5	0.97472	1.08319	1.00069	-385.668
50.10141	2.5	1.08208	1.08134	1.10169	-334.315
49.97473	2.5	1.18927	1.07949	1.20286	-335.466
54.46843	2.5	1.29626	1.07765	1.3042	-321.788
51.83733	2.5	1.40307	1.07581	1.40571	-325.658
55.12957	2.5	1.50969	1.07397	1.50739	-311.95
57.1755	2.5	1.61612	1.07213	1.60924	-287.235
58.55822	2.5	1.72237	1.0703	1.71127	-282.892
61.45247	2.5	1.82843	1.06847	1.81346	-248.663
59.96674	2.5	1.93431	1.06664	1.91582	-263.674

64.83653	2.5	2.04	1.06482	2.01835	-253.113
65.06789	2.5	2.1455	1.063	2.12104	-222.724
67.32089	2.5	2.25081	1.06118	2.22391	-207.731
66.03197	2.5	2.35594	1.05937	2.32695	-210.502
66.42182	2.5	2.46088	1.05755	2.43016	-204.351
68.53337	2.5	2.56563	1.05575	2.53354	-184.38
65.1799	2.5	2.6702	1.05394	2.63709	-198.573
69.1444	2.5	2.77458	1.05214	2.74081	-183.189
71.21907	2.5	2.87878	1.05034	2.84469	-140.362
71.91211	2.5	2.98278	1.04854	2.94875	-160.102
72.54432	2.5	3.08661	1.04675	3.05298	-145.411
142.559	5	3.19024	1.04496	3.26194	-134.39
143.9514	5	3.39695	1.04139	3.47158	-124.404
144.0609	5	3.60291	1.03783	3.68191	-119.432
145.1212	5	3.80812	1.03428	3.89291	-114.274
144.5124	5	4.01259	1.03074	4.10458	-111.096
145.3643	5	4.21631	1.02722	4.31694	-100.176
148.5058	5	4.41928	1.02371	4.52998	-80.438
149.9882	5	4.62151	1.02021	4.7437	-71.3016
150.9199	5	4.82299	1.01672	4.95809	-65.0885
146.0983	5	5.02372	1.01324	5.17316	-82.63
148.2582	5	5.22371	1.00977	5.38892	--
148.4458	5	5.42295	1.00632	5.60535	-70.4224
147.901	5	5.62144	1.00287	5.82246	-65.3843
146.5182	5	5.81919	0.99944	6.04025	-64.0796
144.6853	5	6.01619	0.99602	6.25872	-68.4385

144.654	5	6.21244	0.99261	6.47786	-55.5948
143.5786	5	6.40795	0.98921	6.69769	-59.6914
142.709	5	6.60271	0.98582	6.9182	-50.3022
142.2546	5	6.79672	0.98244	7.13938	-59.2032
144.7085	5	6.98998	0.97907	7.36124	-30.7934
143.647	5	7.1825	0.97572	7.58379	-44.7431
141.9071	5	7.37427	0.97237	7.80701	-46.0725
142.2937	5	7.5653	0.96904	8.03091	-47.0604
141.0659	5	7.75557	0.96572	8.25549	-36.5681
140.4693	5	7.9451	0.9624	8.48074	-39.5955
136.228	5	8.13389	0.9591	8.70668	-46.0735
135.4401	5	8.32193	0.95581	8.9333	-40.4926
129.5075	5	8.50922	0.95253	9.16059	-73.6058
128.4891	5	8.69576	0.94926	9.38856	-65.8069
127.3033	5	8.88156	0.946	9.61722	-68.0248
127.6564	5	9.06661	0.94275	9.84655	-58.9859
126.8861	5	9.25091	0.93951	10.07656	-58.9804
128.8799	5	9.43447	0.93628	10.30725	-48.7928
124.5153	5	9.61727	0.93306	10.53862	-49.9541
126.2051	5	9.79934	0.92985	10.77066	-53.7917

Calorimetric data for N-Boc-L-Glu with macrocycle 2

Solvent: CD_3CN

Concentration of host solution: 1.31 mM

Concentration of guest solution: 63.8 mM

$K_{1:1}$: $(1.48 \pm 0.8) \times 10^3\ M^{-1}$

ΔG: $-17.9 \pm 0.5\ kJmol^{-1}$

ΔH: $-5.5 \pm 0.8\ kJmol^{-1}$

$T\Delta S$: $12.4\ kJmol^{-1}$

Area (μcal)	**In*J*. (μL)**	**[guest] (mM) (before in*J*.)**	**[host] (mM) (before in*J*.)**	**[host] / [guest] (after in*J*.)**	**Cal / mol of in*J*ected guest**
-92.49136	5	0	1.53	0.14291	-2406.52205
107.30367	5	0.21791	1.52477	0.28631	-2925.87422
305.7526	5	0.43507	1.51957	0.4302	-2299.02741
382.14744	5	0.65149	1.51438	0.57458	-2037.0338
427.93249	5	0.86716	1.5092	0.71945	-1843.32993
488.18946	5	1.08208	1.50405	0.8648	-1601.71109
539.75566	5	1.29626	1.49891	1.01064	-1385.49784
589.39671	5	1.50969	1.49379	1.15697	-1162.97225
615.89157	5	1.72237	1.48869	1.30379	-1040.74764
636.78784	5	1.93431	1.4836	1.4511	-923.61697
643.04246	5	2.1455	1.47853	1.59889	-851.7749
643.3811	5	2.35594	1.47348	1.74718	-802.31654
644.09968	5	2.56563	1.46845	1.89595	-740.002
638.61319	5	2.77458	1.46343	2.0452	-728.17472
634.29042	5	2.98278	1.45843	2.19495	-683.97513
624.88081	5	3.19024	1.45344	2.34519	-673.91855
617.60891	5	3.39695	1.44848	2.49591	-652.62243
614.15984	5	3.60291	1.44352	2.64712	-622.94885
599.23806	5	3.80812	1.43859	2.79882	-621.77855
599.23302	5	4.01259	1.43367	2.95101	-571.33487

586.57223	5	4.21631	1.42877	3.10368	-568.17739
575.54864	5	4.41928	1.42388	3.25685	-554.76202
567.60315	5	4.62151	1.41901	3.4105	-542.91352
550.88514	5	4.82299	1.41416	3.56464	-557.42749
557.90346	5	5.02372	1.40932	3.71927	-508.17755
540.26426	5	5.22371	1.4045	3.87438	-518.66753
541.10762	5	5.42295	1.39969	4.02999	-484.70364
527.69152	5	5.62144	1.3949	4.18608	-491.64789
519.03911	5	5.81919	1.39013	4.34266	-478.6081
511.97422	5	6.01619	1.38537	4.49973	-462.63511
503.49879	5	6.21244	1.38062	4.65729	-450.96734
495.58383	5	6.40795	1.3759	4.81533	-442.68574
484.94399	5	6.60271	1.37118	4.97387	-449.79823
480.30998	5	6.79672	1.36649	5.13289	-437.18707
476.77743	5	6.98998	1.3618	5.2924	-412.42792
466.30101	5	7.1825	1.35714	5.4524	-412.45413
459.14985	5	7.37427	1.35248	5.61288	-398.58457
452.80829	5	7.5653	1.34785	5.77385	-397.39272
447.07525	5	7.75557	1.34322	5.93532	-388.31246
440.84591	5	7.9451	1.33862	6.09727	-375.05595
437.6931	5	8.13389	1.33402	6.25971	-357.89337
428.07722	5	8.32193	1.32944	6.42263	-361.66388
423.9577	5	8.50922	1.32488	6.58605	-346.53819
414.47442	5	8.69576	1.32033	6.74995	-347.16262
409.76552	5	8.88156	1.3158	6.91434	-332.50308
403.95852	5	9.06661	1.31128	7.07922	-324.91631
396.40623	5	9.25091	1.30677	7.24459	-325.852
390.05446	5	9.43447	1.30228	7.41044	-328.49383
390.08231	5	9.61727	1.2978	7.57678	-297.32689
382.64458	5	9.79934	1.29334	7.74361	-305.15463

Calorimetric data for N-Boc-D-Glu with macrocycle 2

Solvent: CD_3CN

Concentration of host solution: 1.31 mM

Concentration of guest solution: 63.8 mM

$K_{1:1}$: 82.9 ± 2.3 M^{-1} $K_{1:2}$: (1.05 ± 0.1) x 10^4 M^{-1}

ΔG: -24.1 ± 0.3 k*J*mol^{-1}

ΔH: -7.4 ± 0.1 k*J*mol^{-1}

TΔS: 16.7 k*J*mol^{-1}

Area (μcal)	**In*J*ection (μL)**	**[guest] (mM) (before in*J*.)**	**[host] (mM) (before in*J*.)**	**[host] / [guest] (after in*J*.)**	**Cal / mol of in*J*ected guest**
-95.1721	5	0	1.25	0.17849	--
-178.098	5	0.22235	1.24573	0.35759	-2644.15
105.351	5	0.44394	1.24148	0.5373	-1762.82
193.9395	5	0.66477	1.23724	0.71762	-1497.53
233.9105	5	0.88483	1.23301	0.89855	-1350.73
257.3857	5	1.10413	1.2288	1.08009	-1268.58
284.3982	5	1.32267	1.2246	1.26223	-1161.79
299.4787	5	1.54045	1.22042	1.44499	-1093.66
305.9875	5	1.75747	1.21625	1.62836	-1037.23
297.7314	5	1.97372	1.21209	1.81233	-1038.24
307.8205	5	2.18921	1.20795	1.99692	-969.666
317.3467	5	2.40394	1.20382	2.18212	-915.321
320.6082	5	2.61791	1.19971	2.36792	-870.234
309.3379	5	2.83112	1.19561	2.55434	-881.594
317.4429	5	3.04356	1.19153	2.74136	-836.684
317.6478	5	3.25524	1.18745	2.929	-804.291

317.6342	5	3.46616	1.1834	3.11724	-775.894
318.3204	5	3.67632	1.17935	3.3061	-742.89
310.0876	5	3.88572	1.17532	3.49556	-743.057
312.2355	5	4.09435	1.1713	3.68563	-714.017
308.4497	5	4.30222	1.1673	3.87632	-686.694
310.6111	5	4.50933	1.1633	4.06761	-666.212
305.2017	5	4.71568	1.15932	4.25951	-640.607
293.0352	5	4.92127	1.15536	4.45202	-677.271
298.8794	5	5.12609	1.15141	4.64514	-616.282
299.5859	5	5.33015	1.14747	4.83888	-608.516
295.8911	5	5.53345	1.14354	5.03322	-594.949
299.2872	5	5.73599	1.13963	5.22817	-564.103
293.7691	5	5.93776	1.13573	5.42373	-557.338
289.7578	5	6.13878	1.13184	5.6199	-549.435
287.7317	5	6.33903	1.12796	5.81668	-530.913
283.8299	5	6.53852	1.1241	6.01406	-516.642
288.7942	5	6.73724	1.12025	6.21206	-480.116
280.8526	5	6.93521	1.11641	6.41067	-490.786
284.7717	5	7.13241	1.11258	6.60989	-456.533
280.4919	5	7.32885	1.10877	6.80972	-448.627
281.7936	5	7.52453	1.10497	7.01015	-437.801
281.7778	5	7.71945	1.10118	7.2112	-414.914
274.9901	5	7.9136	1.0974	7.41286	-409.693
268.7288	5	8.107	1.09364	7.61512	-423.917
272.9118	5	8.29963	1.08989	7.818	-399.117
263.376	5	8.49149	1.08615	8.02148	-398.862

264.1807	5	8.6826	1.08242	8.22558	-387.223
267.5108	5	8.87295	1.0787	8.43028	-354.269
266.1047	5	9.06253	1.075	8.6356	-344.118
263.7852	5	9.25135	1.0713	8.84152	-337.559
258.847	5	9.43941	1.06762	9.04806	-341.548
257.3103	5	9.6267	1.06395	9.2552	-327.827
256.6965	5	9.81324	1.06029	9.46295	-319.989
252.5119	5	9.99901	1.05665	9.67131	-318.538

Calorimetric data for N-Boc-L-Asp with macrocycle 2

Solvent: CD_3CN

Concentration of host solution: 1.53 mM

Concentration of guest solution: 63.8 mM

$K_{1:1}$: $(3.79 \pm 1.5) \times 10^3\ M^{-1}$

ΔG: $-20.4 \pm 0.2\ kJmol^{-1}$

ΔH: $-12.1 \pm 0.2\ kJmol^{-1}$

$T\Delta S$: $8.3\ kJmol^{-1}$

Area (μcal)	Injection (μL)	[guest] (mM) (before inj.)	[host] (mM) (before inj.)	[host] / [guest] (after inj.)	Cal / mol of injected guest
-92.4914	5	0	1.53	0.14291	-2406.52
107.3037	5	0.21791	1.52477	0.28631	-2925.87
305.7526	5	0.43507	1.51957	0.4302	-2299.03
382.1474	5	0.65149	1.51438	0.57458	-2037.03
427.9325	5	0.86716	1.5092	0.71945	-1843.33
488.1895	5	1.08208	1.50405	0.8648	-1601.71
539.7557	5	1.29626	1.49891	1.01064	-1385.5
589.3967	5	1.50969	1.49379	1.15697	-1162.97
615.8916	5	1.72237	1.48869	1.30379	-1040.75
636.7878	5	1.93431	1.4836	1.4511	-923.617
643.0425	5	2.1455	1.47853	1.59889	-851.775
643.3811	5	2.35594	1.47348	1.74718	-802.317
644.0997	5	2.56563	1.46845	1.89595	-740.002
638.6132	5	2.77458	1.46343	2.0452	-728.175
634.2904	5	2.98278	1.45843	2.19495	-683.975
624.8808	5	3.19024	1.45344	2.34519	-673.919

617.6089	5	3.39695	1.44848	2.49591	-652.622
614.1598	5	3.60291	1.44352	2.64712	-622.949
599.2381	5	3.80812	1.43859	2.79882	-621.779
599.233	5	4.01259	1.43367	2.95101	-571.335
586.5722	5	4.21631	1.42877	3.10368	-568.177
575.5486	5	4.41928	1.42388	3.25685	-554.762
567.6032	5	4.62151	1.41901	3.4105	-542.914
550.8851	5	4.82299	1.41416	3.56464	-557.427
557.9035	5	5.02372	1.40932	3.71927	-508.178
540.2643	5	5.22371	1.4045	3.87438	-518.668
541.1076	5	5.42295	1.39969	4.02999	-484.704
527.6915	5	5.62144	1.3949	4.18608	-491.648
519.0391	5	5.81919	1.39013	4.34266	-478.608
511.9742	5	6.01619	1.38537	4.49973	-462.635
503.4988	5	6.21244	1.38062	4.65729	-450.967
495.5838	5	6.40795	1.3759	4.81533	-442.686
484.944	5	6.60271	1.37118	4.97387	-449.798
480.31	5	6.79672	1.36649	5.13289	-437.187
476.7774	5	6.98998	1.3618	5.2924	-412.428
466.301	5	7.1825	1.35714	5.4524	-412.454
459.1499	5	7.37427	1.35248	5.61288	-398.585
452.8083	5	7.5653	1.34785	5.77385	-397.393
447.0753	5	7.75557	1.34322	5.93532	-388.312
440.8459	5	7.9451	1.33862	6.09727	-375.056
437.6931	5	8.13389	1.33402	6.25971	-357.893
428.0772	5	8.32193	1.32944	6.42263	-361.664

423.9577	5	8.50922	1.32488	6.58605	-346.538
414.4744	5	8.69576	1.32033	6.74995	-347.163
409.7655	5	8.88156	1.3158	6.91434	-332.503
403.9585	5	9.06661	1.31128	7.07922	-324.916
396.4062	5	9.25091	1.30677	7.24459	-325.852
390.0545	5	9.43447	1.30228	7.41044	-328.494
390.0823	5	9.61727	1.2978	7.57678	-297.327
382.6446	5	9.79934	1.29334	7.74361	-305.155

Calorimetric data for N-Boc-L-Asp with macrocycle 2

Solvent: DMSO

Concentration of host solution: 1.40 mM

Concentration of guest solution: 62.7 mM

$K_{1:1}$: $(8.72 \pm 0.8) \times 10^2\ M^{-1}$ $K_{1:2}$: $(2.31 \pm 0.3) \times 10^5\ M^{-1}$

ΔG: $-3.1 \pm 0.1\ kJmol^{-1}$

ΔH: $2.15 \pm 0.3\ kJmol^{-1}$

$T\Delta S$: $-5.21\ kJmol^{-1}$

Area (μcal)	Injection (μL)	[guest] (mM) (before inj.)	[host] (mM) (before inj.)	[host] / [guest] (after inj.)	Cal / mol of injected guest
19.57986	5	0	1.4	0.15349	4859.473
-25.3126	5	0.21415	1.39522	0.30751	--
-31.1503	5	0.42757	1.39045	0.46205	4203.735
28.69318	5	0.64026	1.3857	0.61711	470.4325
-69.642	5	0.85221	1.38097	0.7727	-1188.79
-274.647	5	1.06343	1.37625	0.92881	-2122.01
-226.095	5	1.27391	1.37155	1.08545	-2069.61
-163.747	5	1.48366	1.36687	1.24261	-1713.01
-87.2094	5	1.69268	1.3622	1.40029	-1519.66
-32.129	5	1.90096	1.35754	1.5585	-1355.78
5.5186	5	2.10851	1.35291	1.71723	-1174.84
30.95018	5	2.31532	1.34828	1.87649	-1044.15
52.52969	5	2.5214	1.34368	2.03627	-936.033
69.00599	5	2.72675	1.33909	2.19658	-853.838
84.5777	5	2.93136	1.33451	2.35741	-789.644
99.21238	5	3.13523	1.32995	2.51877	-716.778

112.1537	5	3.33838	1.3254	2.68064	-647.495
123.052	5	3.54079	1.32087	2.84305	-597.484
134.5412	5	3.74247	1.31636	3.00597	-545.829
141.5382	5	3.94341	1.31186	3.16943	-498.792
147.7945	5	4.14362	1.30737	3.3334	-455.147
156.5529	5	4.34309	1.3029	3.4979	-413.868
160.6846	5	4.54183	1.29844	3.66293	-376.338
168.3402	5	4.73984	1.294	3.82848	-354.88
173.57	5	4.93711	1.28958	3.99455	-306.731
176.0243	5	5.13365	1.28516	4.16115	-273.278
175.737	5	5.32945	1.28077	4.32827	-257.111
179.513	5	5.52452	1.27638	4.49591	-234.218
179.4765	5	5.71886	1.27201	4.66408	-215.798
182.1658	5	5.91246	1.26766	4.83278	-195.08
182.9023	5	6.10533	1.26332	5.002	-182.129
182.4359	5	6.29746	1.25899	5.17174	-162.635
182.2669	5	6.48887	1.25468	5.34201	-142.643
181.2915	5	6.67953	1.25038	5.5128	-138.767
182.6703	5	6.86947	1.24609	5.68411	-126.496
180.7899	5	7.05866	1.24182	5.85595	-117.055
180.311	5	7.24713	1.23757	6.02832	-109.666
179.676	5	7.43486	1.23332	6.20121	-106.59
179.8755	5	7.62186	1.22909	6.37462	-103.999
177.4881	5	7.80812	1.22488	6.54855	-96.6454
176.2429	5	7.99365	1.22067	6.72302	-87.762
174.8874	5	8.17844	1.21648	6.898	-84.3818

174.2055	5	8.36251	1.21231	7.07351	-67.2684
173.2867	5	8.54583	1.20815	7.24954	-63.9011
171.692	5	8.72843	1.204	7.4261	-58.4405
170.0657	5	8.91029	1.19986	7.60319	-57.5496
167.8168	5	9.09141	1.19574	7.78079	-59.0377
167.3328	5	9.2718	1.19163	7.95892	-54.0292
165.17	5	9.45146	1.18753	8.13758	-51.6236
164.6553	5	9.63038	1.18345	8.31676	-45.5578

Calorimetric data for N-Boc-D-Asp with macrocycle 2

Solvent: MeCN

Concentration of host solution: 1.24 mM

Concentration of guest solution: 64.2 mM

$K_{1:1}$: 4.5 ± 1.2 M^{-1}

$K_{1:2}$: (1.09 ± 0.1) x10^4 M^{-1}

ΔG: -8.3 ± 0.1 kJmol^{-1}

ΔH: -6.1 ± 0.2 kJmol^{-1}

TΔS: 2.2 kJmol^{-1}

Area (μcal)	Injection (μL)	[guest] (mM) (before inj.)	[host] (mM) (before inj.)	[host] / [guest] (after inj.)	Cal / mol of injected guest
1727.611	5	0	1.24	0.17744	-96.6439
1774.855	5	0.21928	1.23576	0.35549	-75.5326
1784.452	5	0.4378	1.23154	0.53414	-45.4269
1772.393	5	0.65558	1.22734	0.7134	-1.70758
1749.548	5	0.8726	1.22315	0.89327	62.01032
1776.496	5	1.08887	1.21897	1.07374	152.3554
1781.112	5	1.30439	1.2148	1.25482	270.6306
1804.072	5	1.51915	1.21065	1.43651	404.888
1823.299	5	1.73317	1.20652	1.6188	531.7046
1835.088	5	1.94644	1.2024	1.80169	632.2431
1837.472	5	2.15895	1.19829	1.9852	702.454
1832.122	5	2.37071	1.19419	2.1693	747.9569
1818.242	5	2.58172	1.19011	2.35402	776.1833
1810.272	5	2.79198	1.18605	2.53934	793.0088
1794.855	5	3.00149	1.18199	2.72527	802.3948
1781.873	5	3.21024	1.17795	2.9118	806.8773

1753.841	5	3.41824	1.17393	3.09894	808.0681
1734.489	5	3.6255	1.16992	3.28668	807.004
1714.629	5	3.832	1.16592	3.47504	804.3642
1699.205	5	4.03775	1.16193	3.66399	800.6043
1681.575	5	4.24275	1.15796	3.85356	796.0362
1662.684	5	4.44699	1.154	4.04372	790.878
1649.271	5	4.65049	1.15005	4.2345	785.2855
1634.683	5	4.85323	1.14612	4.42588	779.371
1615.328	5	5.05522	1.1422	4.61787	773.2191
1601.738	5	5.25646	1.13829	4.81046	766.8915
1580.689	5	5.45695	1.13439	5.00366	760.4356
1567.068	5	5.65669	1.13051	5.19747	753.888
1551.534	5	5.85567	1.12664	5.39188	747.277
1539.26	5	6.05391	1.12278	5.5869	740.6246
1520.831	5	6.25139	1.11894	5.78252	733.9484
1500.055	5	6.44812	1.11511	5.97875	727.2623
1491.178	5	6.6441	1.11129	6.17559	720.5776
1479.314	5	6.83933	1.10748	6.37303	713.9032
1462.409	5	7.03381	1.10368	6.57108	707.2466
1450.789	5	7.22753	1.0999	6.76973	700.6135
1443.856	5	7.42051	1.09613	6.96899	694.009
1427.553	5	7.61273	1.09237	7.16886	687.4368
1415.443	5	7.8042	1.08863	7.36933	680.9004
1401.768	5	7.99492	1.08489	7.57041	674.4024
1389.129	5	8.18488	1.08117	7.77209	667.9449
1372.148	5	8.3741	1.07746	7.97438	661.5296

1353.013	5	8.56257	1.07376	8.17728	655.1582
1341.485	5	8.75028	1.07007	8.38078	648.8316
1329.359	5	8.93724	1.0664	8.58489	642.5509
1323.152	5	9.12345	1.06273	8.78961	636.3168
1306.038	5	9.30891	1.05908	8.99493	630.1297
1303.291	5	9.49362	1.05544	9.20085	623.9902
1289.66	5	9.67757	1.05181	9.40739	617.8986
1279.571	5	9.86077	1.04819	9.61453	611.855

Calorimetric data for N-Boc-D-Asp with macrocycle 2

Solvent: DMSO

Concentration of host solution: 1.4 mM

Concentration of guest solution: 63.8 mM

$K_{1:1}$: $(1.98 \pm 1.7) \times 10^2\ M^{-1}$ $K_{1:2}$: $(2.83 \pm 1.5) \times 10^3\ M^{-1}$

ΔG: $-17.9 \pm 0.2\ kJmol^{-1}$

ΔH: $-11.9 \pm 0.1\ kJmol^{-1}$

$T\Delta S$: $7.8\ kJmol^{-1}$

Area (μcal)	Injection (μL)	[guest] (mM) (before inj.)	[host] (mM) (before inj.)	[host] / [guest] (after inj.)	Cal / mol of injected guest
331.6769	2.5	0	1.4	0.07803	-2306.26
73.82266	2.5	0.10905	1.39761	0.15618	-2273.73
-144.007	2.5	0.21791	1.39522	0.23448	-2238.79
-123.016	2.5	0.32659	1.39283	0.3129	-2201.28
-96.3294	2.5	0.43507	1.39045	0.39146	-2161.04
-84.317	2.5	0.54338	1.38808	0.47015	-2117.9
-65.9627	2.5	0.65149	1.3857	0.54898	-2071.7
-57.7405	2.5	0.75942	1.38334	0.62794	-2022.3
-49.6291	2.5	0.86716	1.38097	0.70703	-1969.56
-38.1821	2.5	0.97472	1.37861	0.78625	-1913.4
-34.3197	2.5	1.08208	1.37625	0.86561	-1853.75
-26.1279	2.5	1.18927	1.3739	0.9451	-1790.59
-18.5949	2.5	1.29626	1.37155	1.02473	-1723.95
-8.37452	2.5	1.40307	1.36921	1.10449	-1653.95
1.78595	2.5	1.50969	1.36687	1.18438	-1580.75
9.96184	2.5	1.61612	1.36453	1.26441	-1504.61

23.32804	2.5	1.72237	1.3622	1.34457	-1425.88
34.7635	2.5	1.82843	1.35987	1.42486	-1344.99
45.37907	2.5	1.93431	1.35754	1.50528	-1262.42
59.48185	2.5	2.04	1.35522	1.58584	-1178.77
71.17588	2.5	2.1455	1.35291	1.66654	-1094.64
82.34278	2.5	2.25081	1.35059	1.74736	-1010.71
98.16509	2.5	2.35594	1.34828	1.82832	-927.617
106.943	2.5	2.46088	1.34598	1.90941	-846.025
118.5258	2.5	2.56563	1.34368	1.99064	-766.538
129.8965	2.5	2.6702	1.34138	2.072	-689.706
142.9678	2.5	2.77458	1.33909	2.15349	-616.003
155.8672	2.5	2.87878	1.3368	2.23512	-545.814
159.4285	2.5	2.98278	1.33451	2.31688	-479.434
172.0028	2.5	3.08661	1.33223	2.39877	-417.066
362.7622	5	3.19024	1.32995	2.56295	-331.758
380.166	5	3.39695	1.3254	2.72767	-231.8
396.3759	5	3.60291	1.32087	2.89293	-147.654
407.1927	5	3.80812	1.31636	3.05871	-77.9726
418.252	5	4.01259	1.31186	3.22503	-21.0754
425.4498	5	4.21631	1.30737	3.39188	24.80583
427.6537	5	4.41928	1.3029	3.55927	61.3727
431.7582	5	4.62151	1.29844	3.72719	90.17277
432.0796	5	4.82299	1.294	3.89564	112.5625
433.7505	5	5.02372	1.28958	4.06463	129.7017
431.9191	5	5.22371	1.28516	4.23415	142.5648
431.7452	5	5.42295	1.28077	4.4042	151.9611

427.5396	5	5.62144	1.27638	4.57479	158.5572
424.413	5	5.81919	1.27201	4.74591	162.8993
422.1842	5	6.01619	1.26766	4.91756	165.4334
419.6252	5	6.21244	1.26332	5.08975	166.5224
416.04	5	6.40795	1.25899	5.26247	166.4622
412.7318	5	6.60271	1.25468	5.43573	165.4926
408.9629	5	6.79672	1.25038	5.60951	163.8088
405.6645	5	6.98998	1.24609	5.78383	161.5691
401.0232	5	7.1825	1.24182	5.95869	158.9021
396.9242	5	7.37427	1.23757	6.13408	155.9122
394.4404	5	7.5653	1.23332	6.31	152.6841
389.4798	5	7.75557	1.22909	6.48645	149.286
385.81	5	7.9451	1.22488	6.66344	145.7738
383.366	5	8.13389	1.22067	6.84096	142.192
378.8998	5	8.32193	1.21648	7.01902	138.5766
374.9873	5	8.50922	1.21231	7.19761	134.9564
369.8641	5	8.69576	1.20815	7.37673	131.3545
365.3658	5	8.88156	1.204	7.55639	127.789
361.9582	5	9.06661	1.19986	7.73657	124.2743
357.9443	5	9.25091	1.19574	7.9173	120.8215
354.0893	5	9.43447	1.19163	8.09855	117.439
349.4024	5	9.61727	1.18753	8.28034	114.1328
346.5817	5	9.79934	1.18345	8.46266	110.9081

Calorimetric data for N-Boc-L-Glu with macrocycle 3

Solvent:	DMSO
Concentration of host solution:	0.96 mM
Concentration of guest solution:	63.8 mM

$K_{1:1}$:	$(4.49 \pm 4.2) \times 10^4$ M^{-1}	$K_{1:2}$:	$(1.16 \pm 1.4) \times 10^3$ M^{-1}
ΔG:	-26.6 ± 0.1 kJmol^{-1}	ΔG:	-17.5 ± 0.1 kJmol^{-1}
ΔH:	-10.2 ± 0.1 kJmol^{-1}	ΔH:	-1.8 ± 0.1 kJmol^{-1}
$T\Delta S$:	16.4 kJmol^{-1}	$T\Delta S$:	15.7 kJmol^{-1}

Area (μcal)	Injection (μL)	[guest] (mM) (before inj.)	[host] (mM) (before inj.)	[host] / [guest] (after inj.)	Cal / mol of injected guest
74.50041	2.5	0	0.96	0.11379	-1859.61
97.52066	2.5	0.10905	0.95836	0.22777	-1787.04
-29.821	2.5	0.21791	0.95672	0.34194	-1707.25
-70.8563	2.5	0.32659	0.95509	0.45631	-1621.07
-65.0043	2.5	0.43507	0.95345	0.57088	-1529.93
-59.6385	2.5	0.54338	0.95182	0.68564	-1435.79
-53.3412	2.5	0.65149	0.9502	0.80059	-1340.95
-44.5306	2.5	0.75942	0.94857	0.91574	-1247.83
-33.7178	2.5	0.86716	0.94695	1.03108	-1158.6
-16.6089	2.5	0.97472	0.94533	1.14662	-1075.01
0.39347	2.5	1.08208	0.94372	1.26235	-998.237
17.38409	2.5	1.18927	0.9421	1.37828	-928.863
26.74415	2.5	1.29626	0.94049	1.4944	-866.98
32.39921	2.5	1.40307	0.93889	1.61071	-812.306
41.73516	2.5	1.50969	0.93728	1.72722	-764.323
45.87701	2.5	1.61612	0.93568	1.84393	-722.384

52.99478	2.5	1.72237	0.93408	1.96082	-685.802
55.71731	2.5	1.82843	0.93248	2.07792	-653.905
57.81987	2.5	1.93431	0.93089	2.19521	-626.066
60.84859	2.5	2.04	0.9293	2.31269	-601.722
60.13929	2.5	2.1455	0.92771	2.43036	-580.377
65.0282	2.5	2.25081	0.92612	2.54823	-561.601
65.15118	2.5	2.35594	0.92454	2.6663	-545.024
65.50691	2.5	2.46088	0.92296	2.78456	-530.332
67.2987	2.5	2.56563	0.92138	2.90301	-517.256
65.78315	2.5	2.6702	0.9198	3.02166	-505.568
68.09184	2.5	2.77458	0.91823	3.14051	-495.077
66.02349	2.5	2.87878	0.91666	3.25954	-485.618
67.38673	2.5	2.98278	0.91509	3.37878	-477.053
68.78892	2.5	3.08661	0.91353	3.4982	-469.262
134.0012	5	3.19024	0.91196	3.73764	-458.877
130.8076	5	3.39695	0.90885	3.97786	-446.811
131.3317	5	3.60291	0.90574	4.21885	-436.437
129.2559	5	3.80812	0.90264	4.46062	-427.366
129.3438	5	4.01259	0.89956	4.70317	-419.303
128.4375	5	4.21631	0.89648	4.9465	-412.024
127.2875	5	4.41928	0.89342	5.1906	-405.351
127.3219	5	4.62151	0.89036	5.43548	-399.147
129.2325	5	4.82299	0.88732	5.68115	-393.299
131.1952	5	5.02372	0.88428	5.92758	-387.717
130.9191	5	5.22371	0.88125	6.1748	-382.328
130.8043	5	5.42295	0.87824	6.4228	-377.071

130.1433	5	5.62144	0.87523	6.67157	-371.894
129.0193	5	5.81919	0.87224	6.92112	-366.753
128.8926	5	6.01619	0.86925	7.17145	-361.609
127.217	5	6.21244	0.86627	7.42255	-356.432
126.6934	5	6.40795	0.86331	7.67444	-351.192
124.353	5	6.60271	0.86035	7.9271	-345.864
123.5786	5	6.79672	0.8574	8.18054	-340.426
122.6288	5	6.98998	0.85446	8.43476	-334.86
122.3841	5	7.1825	0.85154	8.68975	-329.148
122.5149	5	7.37427	0.84862	8.94553	-323.278
122.3417	5	7.5653	0.84571	9.20208	-317.237
120.6825	5	7.75557	0.84281	9.45941	-311.017
120.2104	5	7.9451	0.83992	9.71752	-304.611
119.2698	5	8.13389	0.83703	9.97641	-298.017
117.7176	5	8.32193	0.83416	10.23607	-291.233
117.1429	5	8.50922	0.8313	10.49651	-284.263
116.067	5	8.69576	0.82844	10.75773	-277.111
116.3074	5	8.88156	0.8256	11.01973	-269.786
114.2157	5	9.06661	0.82276	11.2825	-262.301
113.4571	5	9.25091	0.81993	11.54606	-254.67
112.6626	5	9.43447	0.81712	11.81039	-246.912
112.2565	5	9.61727	0.81431	12.0755	-239.049
111.2721	5	9.79934	0.81151	12.34139	-231.102

*Calorimetric data for N-Boc-D-Glu with macrocycle **3***

Solvent: DMSO

Concentration of host solution: 0.96 mM

Concentration of guest solution: 63.8 mM

$K_{1:1}$: $(2.62 \pm 0.4) \times 10^2\ M^{-1}$ $K_{1:2}$: $(1.94 \pm 0.2) \times 10^4\ M^{-1}$

ΔG: $-24.5 \pm 0.2\ kJmol^{-1}$

ΔH: $-8.0 \pm 0.2\ kJmol^{-1}$

$T\Delta S$: $16.5\ kJmol^{-1}$

Area (μcal)	Injection (μL)	[guest] (mM) (before inj.)	[host] (mM) (before inj.)	[host] / [guest] (after inj.)	Cal / mol of injected guest
62.91751	2.5	0	0.96	0.11379	-1795.61
51.89695	2.5	0.10905	0.95836	0.22777	-1770.51
-81.1643	2.5	0.21791	0.95672	0.34194	-1736.94
-118.208	2.5	0.32659	0.95509	0.45631	-1691.37
-123.3	2.5	0.43507	0.95345	0.57088	-1628.86
-113.732	2.5	0.54338	0.95182	0.68564	-1543.12
-92.9804	2.5	0.65149	0.9502	0.80059	-1427.75
-77.6178	2.5	0.75942	0.94857	0.91574	-1279.93
-51.2993	2.5	0.86716	0.94695	1.03108	-1106.01
-26.3541	2.5	0.97472	0.94533	1.14662	-923.817
-3.06833	2.5	1.08208	0.94372	1.26235	-755.293
21.84286	2.5	1.18927	0.9421	1.37828	-614.968
46.14084	2.5	1.29626	0.94049	1.4944	-505.913
52.79022	2.5	1.40307	0.93889	1.61071	-423.88
60.69648	2.5	1.50969	0.93728	1.72722	-362.53
63.13243	2.5	1.61612	0.93568	1.84393	-316.169

70.30955	2.5	1.72237	0.93408	1.96082	-280.482
79.02114	2.5	1.82843	0.93248	2.07792	-252.409
77.30496	2.5	1.93431	0.93089	2.19521	-229.834
84.52519	2.5	2.04	0.9293	2.31269	-211.296
83.26833	2.5	2.1455	0.92771	2.43036	-195.781
89.45713	2.5	2.25081	0.92612	2.54823	-182.571
88.53462	2.5	2.35594	0.92454	2.6663	-171.152
85.01858	2.5	2.46088	0.92296	2.78456	-161.152
86.70741	2.5	2.56563	0.92138	2.90301	-152.293
89.02892	2.5	2.6702	0.9198	3.02166	-144.367
93.22999	2.5	2.77458	0.91823	3.14051	-137.216
88.2301	2.5	2.87878	0.91666	3.25954	-130.715
94.04049	2.5	2.98278	0.91509	3.37878	-124.768
93.30024	2.5	3.08661	0.91353	3.4982	-119.296
184.2897	5	3.19024	0.91196	3.73764	-111.889
178.8933	5	3.39695	0.90885	3.97786	-103.122
179.6489	5	3.60291	0.90574	4.21885	-95.4428
181.234	5	3.80812	0.90264	4.46062	-88.6456
178.9776	5	4.01259	0.89956	4.70317	-82.5794
176.2317	5	4.21631	0.89648	4.9465	-77.1289
175.3992	5	4.41928	0.89342	5.1906	-72.2043
175.6947	5	4.62151	0.89036	5.43548	-67.7337
173.7684	5	4.82299	0.88732	5.68115	-63.6591
174.2266	5	5.02372	0.88428	5.92758	-59.9321
170.9364	5	5.22371	0.88125	6.1748	-56.5124
168.7411	5	5.42295	0.87824	6.4228	-53.3659

169.737	5	5.62144	0.87523	6.67157	-50.4637
170.5513	5	5.81919	0.87224	6.92112	-47.7804
168.1541	5	6.01619	0.86925	7.17145	-45.2943
168.948	5	6.21244	0.86627	7.42255	-42.9865
167.0643	5	6.40795	0.86331	7.67444	-40.8402
164.4968	5	6.60271	0.86035	7.9271	-38.8407
164.3187	5	6.79672	0.8574	8.18054	-36.975
162.3624	5	6.98998	0.85446	8.43476	-35.2314
161.6916	5	7.1825	0.85154	8.68975	-33.5995
162.5269	5	7.37427	0.84862	8.94553	-32.0701
159.2604	5	7.5653	0.84571	9.20208	-30.6349
158.9997	5	7.75557	0.84281	9.45941	-29.2864
159.5651	5	7.9451	0.83992	9.71752	-28.0178
157.4398	5	8.13389	0.83703	9.97641	-26.8229
156.0154	5	8.32193	0.83416	10.23607	-25.6963
155.7766	5	8.50922	0.8313	10.49651	-24.6329
155.0909	5	8.69576	0.82844	10.75773	-23.628
153.4241	5	8.88156	0.8256	11.01973	-22.6776
153.1888	5	9.06661	0.82276	11.2825	-21.7778
152.5356	5	9.25091	0.81993	11.54606	-20.925
151.4852	5	9.43447	0.81712	11.81039	-20.1162
148.949	5	9.61727	0.81431	12.0755	-19.3483
148.6201	5	9.79934	0.81151	12.34139	-18.6187

References

1. F. Wöhler, *Poggendorf Ann. Physik*, **1828**, *12*, 253
2. E. Fischer, *Ber. Deutsch. Chem. Ges.*, **1894**, *27*, 2985
3. A. Werner, *Zeitschr. Anorg. Chem.*, **1893**, *3*, 267
4. P. Ehrlich, Studies on Immunity; Wiley: New York, **1906**
5. J-M Lehn, *Pure Appl. Chem.*, **1978**, *50*, 871
6. J-M Lehn, *Ang. Chem. Int. Ed.*, **1988**, *27*, 89
7. P. D. Beer, P. A. Gale, D. K. Smith, Supramolecular Chemistry, Oxford University Press, Oxford, **1999**
8. J-M Lehn, *Ang. Chem. Int. Ed.*, **1988**, *27*, 89
9. M. M. spence, S. M. Rubin, I. E. Dimitrov, E. J. Ruiz, D. E. Wemmer, A. Pines, S. Q. Yao, F. Tian, P. G. Schultz, *PNAS*, **2001**, *98*, 10654
10. J-M. Lehn, C. Sirlin, *New J. Chem.*, **1987**, *11*, 693
11. J-P Behr, J-M Lehn, *J. Chem. Soc. Chem. Commun.*, **1978**, 143
12. F.P. Schmidtchen, *Tetrahedron lett.*, **1989**, *30*, 4493
13. M.W Hosseini, J.-M Lehn, A.J. Blacker, *J. of the Am. Chem. Soc.*, **1990**, *112*, 3896
14. G. Deslongchamps, A. Galán, J. de Mendoza, J. Rebek, , *Ang. Chem. Int. Ed.*, **1992**,*31*, 61
15. R.P. Bonar-Law, A.P. Davies, B.A. Murray, *Ang. Chem. Int. Ed.*, **1990**, *29*, 1407
16. R.P. Bonar-Law, A.P. Davies, K.M. Bhattarai, B.A. Murray, *J. Chem Soc., Chem. Commun.*, **1993**, 752
17. W.H. Pirkle, T.C. Pochawski, *J. Am. Chem. Soc.*, **1987**, *109*, 5975
18. J-I Hong, S.K. Namgoong, A. Bernardi, W.C. Still, *J. Am. Chem. Soc.*, **1991**, *113*, 5111
19. P. Dauber, A. Hagler, *Acc. Chem. Res.*, **1980**, *13*, 105
20. A. D. Hamilton; S. K. Chang, *J. Am. Chem. Soc.*, **1988**, *110*, 1318
21. T. J. Murray, S. C. Zimmerman, *J. Am. Chem. Soc.*, **1992**, *114*, 4010
22. J. Pranata, S. G. Wierschke, W. L. Jorgensen, *J. Am. Chem. Soc.*, **1991**, 113, 2810

23. W. L. Jorgensen, J. Pranata, *J. Am. Chem. Soc.*, **1990**, *112*, 2008
24. G. R. Desijaru, T. Steiner, The weak hydrogen bonds in structural chemistry and biology, Oxford University Press, Oxford, **1999**
25. T. Steiner, *Chem. Commun.*, **1997**, 727
26. C. Schmuck, J. Lex, *Eur. J. Org. Chem.*, **2001**, 1519
27. E. Kimura, A. sakonaka, T. Yatsunami, M. Kodama, *J. Am. Chem. Soc.*, **1981**, *103*, 3041
28. E. Kimura, Y. Kuramoto, T. Koike, H. Fujioka, M. Kodama, *J. Org. Chem.*, **1990**, *55*, 42
29. M .W. Hosseini, J-M Lehn, *J. Am. Chem. Soc.*, **1982**, *104*, 3525
30. M .W. Hosseini, J-M Lehn, *Helv. Chim. Acta.*, **1988**, *71*, 749
31. P. Cudic, J. P. Vigneron, J-M Lehn, M. Cesario, T. Prange, *Eur. J. Org. Chem.*, **1999**, 2479
32. G. Karlstrom; P. Linse; A. Wallquist; B. Jonsson, *J. Am. Chem. Soc.*, **1983**, *105*, 3777
33. W. L. Jorgensen, D. L. Severance, *J. Am. Chem. Soc.*, **1990**, 112, 4768
34. G. Karlstrom, P. Linse, A. Wallqvist, N. Jonsson, *J. Am. Chem. Soc.*, **1983**, 105, 3777
35. S. Pkival, S. Geils, C. S. Wilcox, *J. Am. Chem. Soc.*, **1994**, 116, 4487
36. H. Adams, F. J. Carver, C. A. Hunter, J. C. Morales, E. M. Seward, *Angew.Chem. Int. Ed.*, **1996**, 35, 1542
37. H. Schneider, *Angew.Chem. Int. Ed.*, **1997**, 36, 1072
38. C. A. Hunter, J. Mcquillan, P. Brooksby, D. Purvis, A. Rowan, R. Walsh, *Ang. Chem. Int. Ed.*, **1995**, 33, 2489
39. S.C. Zimmerman, W. Wu, Z.J. Zeng, *J. Am. Chem. Soc.*, **1991**, *113*, 196
40. S.R. Labrenz, J.W. Kelly, *J. Am. Chem. Soc.*, **1995**, *117*, 1655
41. D. B. Smithrud, F. Diederich, *J. Am. Chem. Soc.*, **1990**, 112, 339
42. J. Dunitz, M. Dobler, P. Seiler, R. J. Phizacherly, *Adv. Crystallogr. Sect.B.*, **1974**, 30, 2733
43. M. S. westwell, M. S. Searle, D. H. Williams, *J. Mol. Rec.*, **1996**, *9*, 88
44. A. K. Sum, S. I. Sandler, *J. Phys. Chem A*, **2000**, *104*, 1121
45. A. P. Bisson, C. A. Hunter, *Chem. Commun.*, **1996**, 1723
46. D. A. Bell, S. G. Diaz, V. M. Lynch, E. V. Anslyn, *Tet. Lett.*, **1995**, *36*, 4155
47. N. Colocci, P. B. Dervan, *J. Am. Chem. Soc.*, **1995**, *117*, 4781

48. A. P. Bisson, C. A. Hunter, J. C. Morales, K. Young, *Chem. Eur. J.*, **1998**, 4, 845

49. J. P. Mackay, U. Gerhard, D. A. Beuregard, M. S. Westwell, M. S. Searle, D. H. Williams, *J. Am. Chem. Soc.*, **1994,** *116*, 4581

50. C. Compari, E. Fisicaro, A. Braibanti, *Polyhedron*, **2002**, *21*, 1503

51. C. Tanford, The Hydrophobic Effect, Wiley, New York, **1990**

52. C. Steal, F. Vogtle, *Angew.Chem. Int. Ed.*, **1992**, 31, 528

53. J. Rebek, B. Askew, D. Nermeth, K. Paris, *J. Am. Chem. Soc.*, **1987**, 109, 2432

54. A. Galan, D. Andreu, A. M. Echavarren, P. Prades, J. de Mendoza, *J. Am. Chem. Soc.*, **1992**, 114, 1511

55. E. Kimura, A. Sakonaka, T. Yatsunami and M. Kodama, *J. Am. Chem. Soc.*, **1981**, *103*, 3041

56. E. Kimura, Y. Kuramoto, T. Koike, H. Fujioka, M. Kodama, *J. Org. Chem.*, **1990**, *55*, 42

57. B. Dietrich, M. W. Hosseini, J. M. Lehn and R. B. Sessions, *J. Am. Chem. Soc.*, **1981**, *103*, 1282

58. P. Cudic, J-P Vigneron, J-M Lehn, M. Cesario, T. Prangé, *Eur. J. Org. Chem.*, **1999**, 2479

59. B. Hinzen, P. Seiler, F. Diederich, *Helv. Chim. Acta.*, **1996**, 79, 942

60. H. Patel, J. D. Kilburn, G. J. Langley, P. D. Edwards, T. Mitchell and R. Southgate, *Tetrahedron Lett.*, **1994**, *35*, 481

61. M. Pietraszkiewicz, M. Kozbial, O. Pietraszkiewicz, *J. Membrane Science*, **1998**, *138*, 109

62. V. Král, A. Andrievsky, J. L. Sessler, *J. Am. Chem. Soc.*, **1995**, *117*, 2953

63. J. S. Albert, A. D. Hamilton, *Tetrahedron Lett.*, **1993**, *34*, 7363

64. E. Fan, A. van Arman, S. Kincaid and A.D. Hamilton, *J. Am. Chem. Soc.*, **1993**, *115*, 369

65. S. Nishizawa, P. Buhlmann, M. Iwao and Y. Umezawa, *Tetrahedron Lett.*, **1995**, *36*, 6483

66. G.J. Pernia, J.D. Kilburn, J.W. Essex, R.J. Mortishire-Smith, M. Rowley, *J. Am. Chem. Soc.*, **1996**, *118*, 10220

67. C. P. Waymark, J. D. Kilburn, I. Gillies, *Tetrahedron Lett.*, **1995**, *36*, 3051

68. P. D. Henley, C. P. Waymark, I. Gillies, J. D. Kilburn, *J. Chem. Soc., Perkin Trans 1*, **2000**, 1021

69. P. D. Henley, J. D. Kilburn, *J. Chem. Soc., Chem. Commun.*, **1999**, 1335

70. H. Miyaji, M. Dudic, J. H. R. Tucker, I. Prokes, M. E. Light, M. B. Hursthouse, I. Stibor, P. Lhoták, *Tetrahedron Lett.*, **2002**, *43*, 873

71. A. Echavarren, A. Galán, J-M Lehn, J de Mendoza, *J. Am. Chem. Soc.*, **1989**, *111*, 4994

72. A. Metzger, K. Gloe, H. Stephan, F. P. Schmidtchen, *J. Org. Chem.*, **1996**, *61*, 2051

73. C. Schmuck, *Chem. Eur. J.*, **2000**, *6*, 709

74. L. J. Lawless, A. G. Blackburn, A. J. Ayling, M. N. Pérez-Payán, A. P. Davis, *J. Chem. Soc., Perkin Trans. 1*, **2001**, 1329

75. L. A. Cabell, M. D. Best, J. J. Lavigne, S. E. Schneider, D. M. Perreault, M-K Monahan, E. V. Anslyn, *J. Chem. Soc, Perkin Trans. 2*, **2001**, 315

76. I. Prévot-Halter, T. J. Smith, J. Weiss, *Tetrahedron Lett.*, **1996**, *37*, 1201

77. H-J Kim, C. W. Lim, J-I Hong, *Materials Science and Engineering C*, **2001**, *18*, 265

78. a) J. D. Carr, L. Lambert, D. E. Hibbs, M. B. Hursthouse, K. M. A. Malik, J. H. R. Tucker, *J. Chem. Soc., Chem. Commun.*, **1997**, 1649; b) J. D. Carr, S. J. Coles, M. B. Hursthouse, M. E. Light, J. H. R. Tucker, J. Westwood, *Angew. Chem. Int. Ed.*, **2000**, *39*, 3296

79. P. D. Beer, D. Hesek, K. C. Nam, M. G. Drew, *Organometallics*, **1999**, *18*, 3933

80. S. Rossi, *Int. Lab. News*, **2003**, *June*, 18

81. B. Linton, A. D. Hamilton, *Tetrahedron*, **1999**, 6027

82. B. Linton, M. S. Goodman, E. Fan, S. A. van Arman, A. D. Hamilton, *J. Org. Chem.*, **2001**, *66*, 7313

83. For an example of hydrophobic binding see E. Fan, S. A. VanArman, S. Kincaid, A. D. Hamilton, *J. Am. Chem. Soc.*, **1993**, *115*, 369

84. M. Davies, M. Bonnat, F. Guillier, J. D. Kilburn, M. Bradley, *J. Org. Chem.*, **1998**, *63*, 8696

85. M. Rekharsky, Y. Inoue, *J. Am. Chem. Soc.*, **2000**, *122*, 4418

86. M. Rekharsky, Y. Inoue, *J. Am. Chem. Soc.*, **2002**, *124*, 813

87. N. Douteau-Guével, F. Perret, A. W. Coleman, J-P Morel, N. Morel-Desrosiers, *J. Chem. Soc., Perkin Trans. 2*, **2002**, 524

88. M. Czekalla, H: Stephan, B. Habermann, J. Trepte, K. Gloe, F. P. Smidtchen, *Thermochimica Acta*, **1998**, 137

89. X. Salvatella, M. W. Peczuh, M. Gairí, R. K. Jain, J. Sánchez-Quesada, J. de Mendoza, A. D. Hamilton, E. Giralt, *J. Chem. Soc., Chem. Commun.*, **2000**, 1399

90. T. Braxmeier, M. Demarcus, T. Fessman, S. McAteer, J. D. Kilburn, *Chem. Eur. J.*, **2001**, *7*, 1889

91. R. Arienzo, J. D. Kilburn, *Tetrahedron*, **2002**, *58*, 711

92. K. B. Jensen, T. M. Braxmeier, M. Demarcus, J. G. Frey, J. D. Kilburn, *Chem. Eur. J.*, **2002**, *8*, 1300

93. G. M. Kline, PhD Thesis, **2000**, University of Southampton

94. C. A. Hunter and D. H. Purvis, *Angew. Chem., Int. Ed.*, **1992**, *31*, 792

95. G. M: Kline, M. E. Light, M. B. Hursthouse, J. de Mendoza, J. D. Kilburn, *J. Chem. Soc., Perkin Trans. 1,* **2001**, 1258

96. K. Kavallieratos, C. M. Bertao and R. H. Crabtree, *J. Org. Chem.,* **1999**, *64*, 1675

97. T. H. Fife and T.J. Przystas, *J. Am. Chem. Soc.*, **1982**, *104*, 2251

98. P. Scrimin, U. Tonellato, D. Milani and R. Fornasier, *J. Chem. Soc., Perkin Trans. 2*, **1986**, 233

99. G. A. Olah, S. C. Naramg, B. G. Balaram Gupta, R. Malhotra, *J. Org. Chem.*, **1979**, *44*, 1247

100. E. I. Al-Afaleq, S. A. Abubshait, *Synth. Commun.*, **1999**, *29*, 1965

101. J. S. Pizey, "Synthetic Reagents", vol. 1, pp. 321-357, Wiley, New York, **1974**

102. X. Y. Wu, X. H. Li, Q. L. Zhou, *Tetrahedron: Asymmetry*, **1998**, *9*, 4143

103. M. A. Bailen, R. Chinchilla, D. J. Dodsworth, C. Najera, *J. Org. Chem.*, **1999**, 64, 8936

104. a) N. Aguilar, A. Moyano, M. A. Pericas, A. Riera, *Synthesis*, **1998**, 313; b) M. H. Kim, D. V. Patel, *Tetrahedron Lett.*, **1994**, *35*, 5603

105. J. Coste, M-N Dufour, A. Pantaloni, B. Castro, *Tetrahedron Lett.*, **1990**, *31*, 669

106. K. C. Nicolau, T. Ohshima, F. Murphy, S. Barluenga, J. Xu, N. Winssinger, *Chem. Commun.*, **1999**, 809

107. C. N. Cow, P. H. M. Harrison, *J. Org. Chem.*, **1997**, *62*, 8834

108. J. Bornstein, S. F. Bedell, P. E. Drummond, C. L. Kosloski, *J. Am. Chem. Soc.*, **1956**, *78*, 83

109. a) H. Wenschuh, M. Beyermann, E. Krause, M. Brudel, R. Winter, M. Schuman, L. A. Carpino, M. Bienert, *J. Org. Chem.*, **1994**, *59*, 3275; b) H. Wenschuh, M. Beyermann, E. Krause, L. A. Carpino, M. Bienert, *Tetrahedron Lett.*, **1993**, *34*, 3733

110. L. A. Carpino, E. M. E. Mansour, D. Sadataalaee, *J. Org. Chem.*, **1991**, *56*, 2611

111. L. K. Liu, T-P Hsieh, S-M Kuo, *Synthesis*, **1994**, 309

112. J. B. Lee, *J. Am. Chem. Soc.*, **1966**, *88*, 3440

113. S. Rossi, G. M. Kyne, D. L. Turner, N. J. Wells, J. D. Kilburn, *Angew. Chem. Int. Ed.*, **2002**, *41*, 4233

114. E. J. Corey, D-H Lee, S. Sarshar, *Tetrahedron: Asymmetry*, **1995**, *6*, 3

115. M. Rance, O. W. Sorensen, G. Bodenhausen, E. R. R. Wagner, K. Wüthrich, *Biochem. Biophys. Res. Commun.*, **1983**, *117*, 479

116. Model provided by Dr. D. L. Turner, University of Southampton

117. The binding constants were calculated by fitting the data using NMRTit HG software for 1:1 isotherms and NMRTit HGG for 1:2 binding stoichiometries, provided by Prof. C. A. Hunter, University of Sheffield: A. P. Bisson, C. A. Hunter, J. C. Morales, K. Young, *Chem. Eur. J.*, **1998**, *4*, 845. See appendix 2 for full description of calculations

118. (a) K. A. Connors, *Binding Constants*, Wiley, New York, **1987**; (b) L. Fielding, *Tetrahedron*, **2000**, *56*, 6151

119. ITC User manual, version 5.0, MicroCal, 1998

120. Data was analysed by non linear least-squares fitting using the Origin software supplied by MicroCal: T. Wiseman, S. Williston, J. F. Brandts, L-N Lin, *Anal. Biochem.*,**1989**, *179*, 131. Data was modelled using the one site binding model, or the model with two independent binding sites in cases where data could not be fitted with the one binding site model. See appendix 3 for a more detailed description of the models

121. D. J. Cram, *Angew. Chem., Int. Ed.*, **1988**, *27*, 1009

122. For some examples see: a) Y. K. Kim, S. J. Lee, K. H. Ahn, *J. Org. Chem.*, **2000**, *65*, 7807; M. Palucki, N. S: Finney, P. J. Pospisil, M. L. Güler, T. Ishida, E. N. Jacobsen, *J. Am. Chem. Soc.*, **1998**, *120*, 948

123. a) Z. Pan, W. C. Still, *Tetrahedron Lett.*, **1996**, *37*, 8699; b) F. Gasparrini, D. Misiti, W. C: Still, C. Villani, H. Wennemers, *J. Org. Chem.*, **1997**, *62*, 8221

124. I. Alfonso, B. Dietrich, F. Rebolledo, V. Gotor, J-M Lehn, *Helvetica Chimica Acta*, **2001**, *84*, 280

125. S. Caddick, A. K. de K. Haynes, D. B. Judd, M. R. V. Williams, *Tetrahedron Lett.*, **2000**, *41*, 3513

126. I. Ernest, J. Kalvoda, G. Rihs, M. Mutter, *Tetrahedron Lett.*, **1990**, *31*, 4011

127. F. Mohamadi, N. G. J. Richards, W. C. Guida, R. Liskamp, M. Lipton, C. Caufield, G. Chang, T. Hendrickson and W. C. Still, *J. Comp. Chem.*, **1990**, *11*, 440

128. W. C. Still, A. Tempczyk and R. C. Hawley, *J. Am. Chem. Soc.*, **1990**, *112*, 6127

129. G. L'abbe, *Synthesis*, **1987**, 525

130. a) O-E Schultz, K.K Gauri, *Arch. Pharm.*, **1962**, *295*, 146; b) D. J. Le Count, D. J. Dewsbury, W. Grundy, *Synthesis*, **1977**, 582

131. R. L. N. Harris, *Aust. J. Chem*, **1972**, *25*, 993

132. S. Coles, D. Douhéret, M. Hursthouse, J. D. Kilburn, S. Rossi, *Acta Crys.*, **2000**, *C56*, e224

133. M. Yamada, T. yura, M. Morimoto, T. Harada, K. Yamada, Y. Honma, M. Kinoshita, M. Sugiura, *J. Med. Chem.*, **1996**, *39*, 596

134. J. A. Joule, G. F. Smith, "Heterocyclic Chemistry", Chapt. 3, Van Nostrand Reinhold Company Ltd., **1978**

135. M. P. Cava, M. I. Levinson, *Tetrahedron*, **1985**, *41*, 5061

136. T. Choshi, A. Tonari, H. Yoshioka, K. Harada, E. Sugino, S. Hibino, *J. Org. Chem.*, **1993**, *58*, 7952

137. W. H. Press, S. A. Teukolsky, W. T. Vetterling, B. P. Flannery, Numerical recipes in C, Cambridge University Press, Cambridge, 2nd edn., 1988

138. S. Pikul, E. J. Corey, *J. Org. Synth.*, **1992**, *71*, 22

139. J. Einhorn, C. Einhorn, J-L Luche, *Synlett*, **1991**, 37

Appendices

Appendix 1

Thiourea U-cleft receptor for carboxylates

Introduction

Sideways to the main project, it was decided to prepare tweezer receptors bearing a dipyridyl thiourea, **142**, or dipyridyl guanidinium group, **143**, as carboxylic binding site using conventional solution phase chemistry. Chiral recognition would be provided by the insertion of sterically demanding chiral groups, which would interact with the amino acid's side chain. As the receptors previously reported, each arm would consist of a series of amino acids to form both hydrophobic and *β*-sheet-like hydrogen-bonding interactions with the backbone of the substrate.

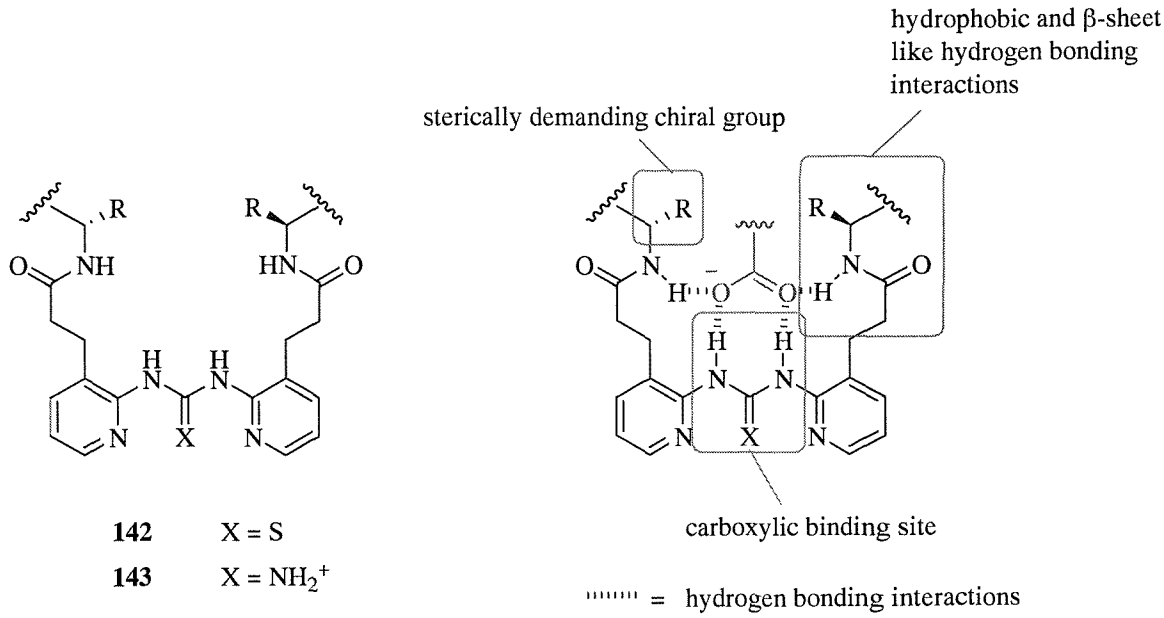

142 X = S

143 X = NH_2^+

*Figure 1 Design concept of tweezer receptors **142** and **143***

The tweezers were designed to incorporate two pyridine rings, which in our experience have a noteworthy role in the preorganisation of a receptor. Both receptors, indeed, can exist in two different conformational equilibria, Figure 2. The presence of a guanidinium group should effect the preorganisation of the tweezer and increase the acidity of the nitrogen protons. Indeed, for the guanidinium derivative ($X=NH_2^+$) we expect a different conformation than for the thiourea derivative (X=S). Because of a higher degree of internal hydrogen bonding, the guanidinium

derivative should be much less flexible than the thiourea analogue. A decrease in flexibility or spatial freedom should result in a higher degree of preorganisation and a tighter binding of the substrate.

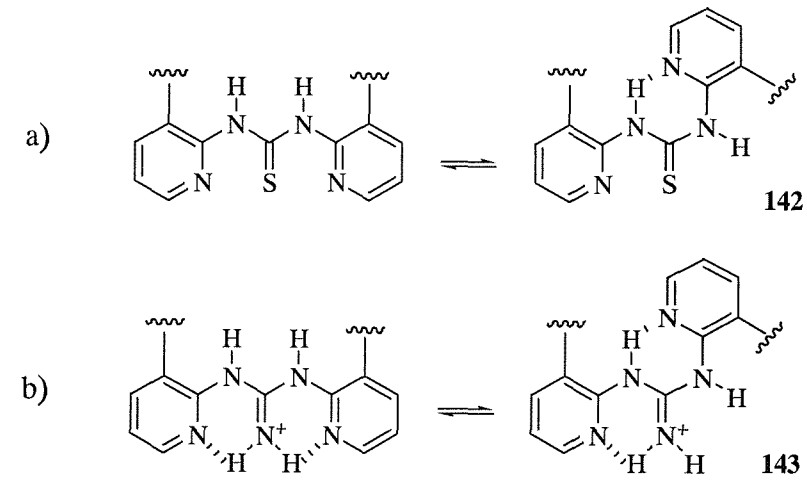

Figure 2 Conformational equilibria for a) thiourea and b) guanidinium systems

Internal hydrogen bonding of receptor **142** would lead to a conformation not suitable for binding of a guest, Figure 2a. However, protonation of the pyridine nitrogens would favour the right conformation with both arms extending parallel from the carboxylic binding site.

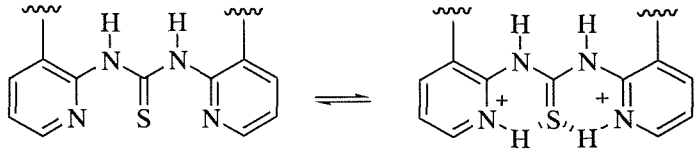

Figure 3 Effect of protonation upon conformational equilibrium of thiourea

All these effects have to be considered as they may have important consequences on the binding events that will take place afterwards.

*Synthesis of thioureas **144** and **145***

The first aim of the project was to synthesise a *N,N'*-dipyridyl thiourea as shown below, via the formation of isothiocyanate *in situ*.

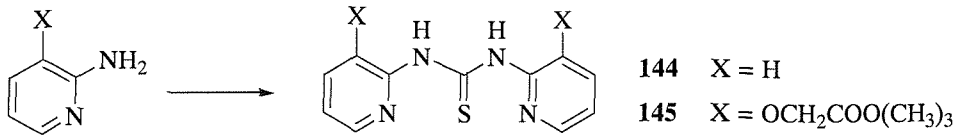

Figure 4 Schematic synthetic route for the preparation of dipyridyl thiourea

Preparation of alkyl and aryl isothiocyanates is well documented in literature, but less effort has been given to the preparation of heterocyclic derivatives.[129] Thiophosgene or carbon disulphide resulted to be widely employed in the preparation of *N,N'*-dipyridyl thiourea.[130] In a preliminary attempt to synthesise thiourea **144**, commercially available 2-aminopyridine was reacted with thiophosgene. The reaction however gave an unexpected result. A crystalline product was obtained in 72% yield. The crystal structure showed an oxidation product of *N-N'*-di-2-pyridyl thiourea **144**.

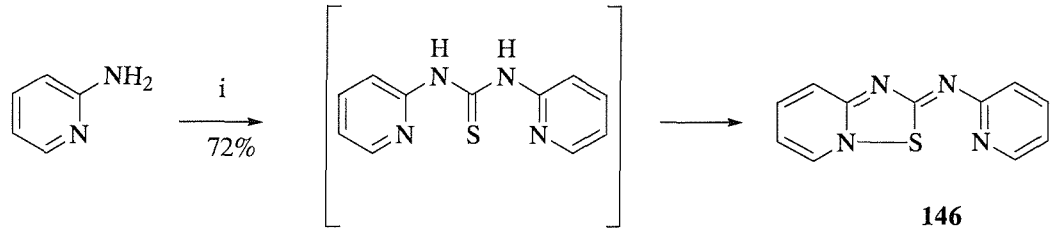

Scheme 1 Reagents and conditions: i) $SCCl_2$, K_2CO_3

Probably thiourea **144** is oxidised *in situ* to cause the loss of the amine protons in the thiourea product to produce the final product **146**, which exists in two resonance forms.

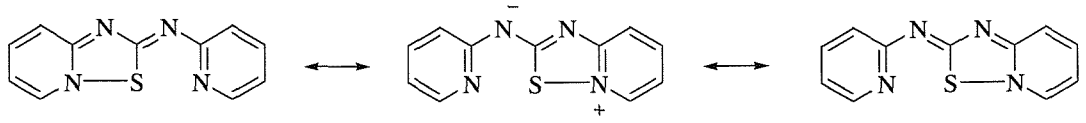

*Figure 5 Resonance structures of **146***

The unusual stability of this compound can be explained in terms of a possible involvement of the d-orbitals of the sulphur atom. Crystallographic analysis showed an essentially planar structure, with the distances between the sulphur and the two nitrogen atoms significantly less than the sum of the van der Waals radii. Moreover, the C-S bond proved to be much longer than the double bond normally observed in thiourea derivatives and may be considered a formal single bond. Few cases of sulphur in a similar coordination environment have been found in literature and none with aromatic moieties. Our finding is confirmed by Harris' work that

established the existence of this resonance hybrid by NMR spectra, chemical properties and by mass spectroscopy.[131]

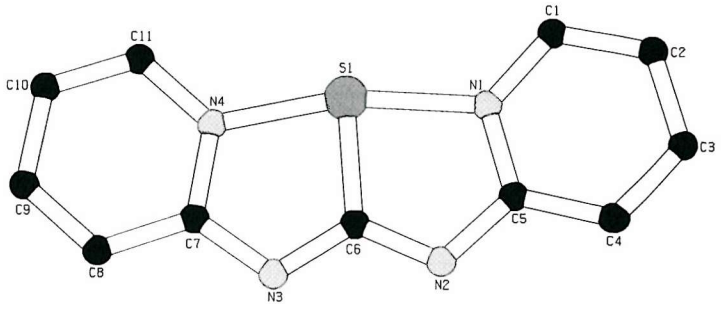

Figure 6 Crystal structure of ***146***

Although the desired product was not obtained, the procedure seemed to be promising. Therefore it was applied to obtain the substituted thiourea **145**. Conversion of the hydroxyl group into ester was achieved by reacting commercially available 3-hydroxyaminopyridine with ^{tert}butyl bromoacetate. ^{tert}Butyl ester **147** was obtained in 67% yield. It was anticipated that treatment with an acid would easily deprotect the ester and afford a suitable group for subsequent insertion of amino acids. Thiophosgene was added to a solution of **147** in excess in chloroform and aqueous potassium carbonate. Three main fractions were recovered. Two fractions were successfully recrystallised from methanol.[132] The results obtained were unexpected.

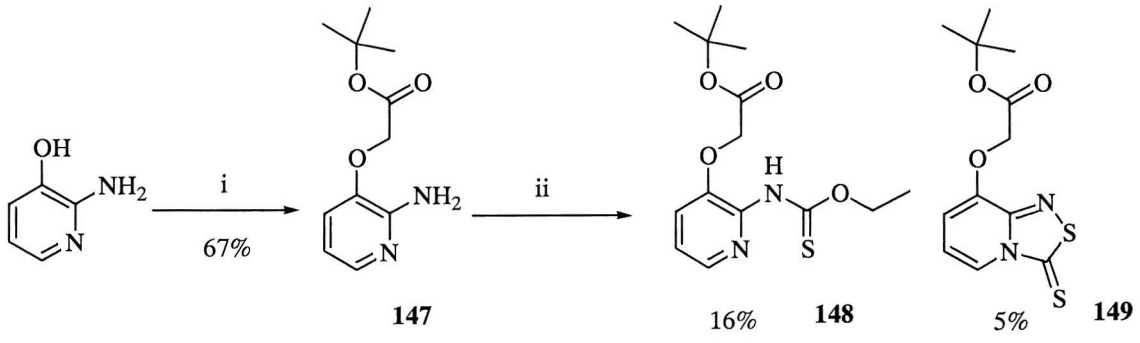

Scheme 2 Reagents and conditions: i) tert-butyl bromoacetate, Adogen 464, NaOH; ii) $SCCl_2$, K_2CO_3

148 contain an ethoxycarbothioylamine moiety. Chloroform was used as solvent. As ethanol is present as a stabilising agent in chloroform (0.5-1%) it may have trapped the isothiocyanate *in situ* or it may have reacted directly with thiophosgene. Product **149**, instead, possesses a novel exocyclic thione system fused with a pyridine ring. Although the mechanism is not completely

understood, it is though that it may go via addition of thiophosgene to the pyridyl nitrogen and subsequent intramolecular ring closure.

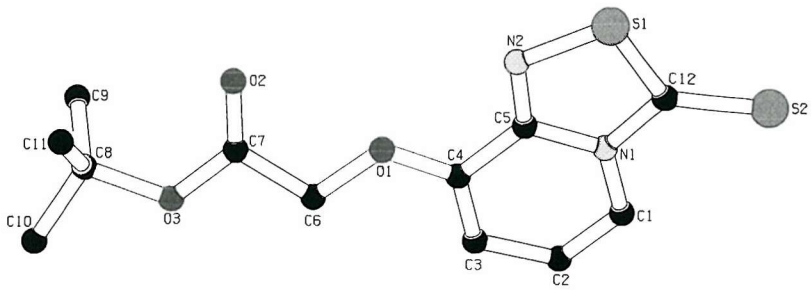

Figure 7 Crystal structure of ***149***

It was then decided to seek different approaches to obtain simple *N,N'*-dipyridyl thiourea **144.** Both carbon disulfide and thiophosgene were used under different experimental conditions. All different parameters were considered and changed. The number of reagents' equivalents was changed from stoichiometric to excess.

Table 1 Experimental conditions applied

Reagent	Base	Solvent	Temperature
CS_2, DCC	DMAP	DCM	-10°C and then r. t.
exs CS_2, DCC		THF	-10°C and then r. t.
Cl_2CS	$NaHCO_3$	$CHCl_3$	-10°C and then r. t.
Cl_2CS	$NaHCO_3$	$CHCl_3$	0°C and then reflux[133]

All reactions were tried twice. Some of them were split into two steps: preparation of isothiocyanate and subsequent reaction with 2-aminopyridine. None of them proved to be successful.

The major problem encountered in the reactivity of pyridyl systems is their very low nucleophilicity.[134] Two factors are responsible for its inertia. The first is that a pyridine ring is intrensically less nucleophilic than benzene. This effect is due to inductive and mesomeric electron withdrawal by the nitrogen atom, Figure 8.

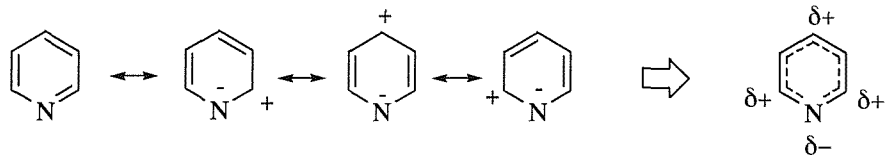

Figure 8 Mesomeric resonance structures in pyridine

Aminopyridines exist as amino tautomers, which causes the lone pair electrons on the amino group to be much less available to react with an electrophile, Figure 9.

Figure 9 a-aminopyridine resonance structures

The synthetic strategy was then changed to get first the urea **150** and subsequently transform into the thiourea analogue in an attempt to overcome the very low nucleophilicity of 2-aminopyridines. The suggested synthesis is shown below. Commercially available picolinic acid would be converted into its isocyanate **150**, then reacted with 2-aminopyridine to afford urea **151**, which would be converted to its thiourea analogue by using the Lawesson's reagent[135]. Following Choshi's procedure, picolinic acid was heated in toluene in the presence of diphenyl phosphorazidate (DPPA) under Curtius conditions to give the relatively stable isocyanate **150** in 92%.[136] The reaction's yield of urea proved to be very poor and 2-aminopyridine was always recovered from the reaction mixture (15-20%).

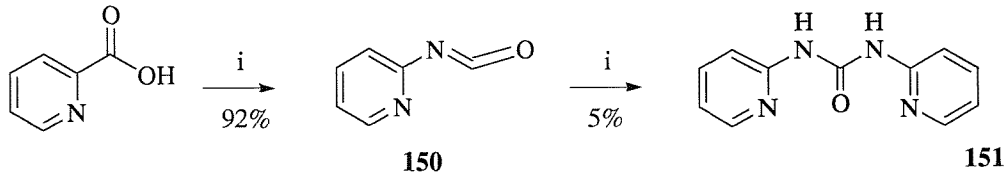

Scheme 3 Reagents and conditions: i) DPPA, Et_3N, toluene; ii) 2-aminopyridine, K_2CO_3

In conclusion, although we found some interesting compounds, it was decided to put aside the project, due to its synthetic difficulties.

Appendix 2

Software for the determination of association constants from MRN binding studies [117]

1. NMRTit HG

NMRTit HG fits the data to a 1:1 binding isotherm by solving the equations (1) – (3) in which $[H]_0$ is the total concentration of host; $[G]_0$ is the total concentration of guest; [H] is the concentration of unbound free host; [HG] is the concentration of host + guest complex; K is the association constant for the formation of the host·guest complex; d_f is the free chemical shift of the host; d_b is the limiting bound chemical shift of the host·guest complex.

$$[HG] = \frac{1 + K[H]_0[G]_0 - \sqrt{\{(1 + [H]_0[G]_0)^2 - 4K^2[H]_0[G]_0\}}}{2K} \quad (1)$$

$$[H] = [H]_0 - [HG] \quad (2)$$

$$\delta_{obs} = \frac{[HG]}{[H]_0}\delta_b + \frac{[H]}{[H]_0}\delta_t \quad (3)$$

2. NMRTit HGG

NMRTit HGG fits the data to a 1:2 binding isotherm by an iterative procedure to solve the following simultaneous equations. The method starts by assuming the [HGG]=0, so that Equation (4) can be solved exactly for [HG]. This value of [HG] is the used to solve Equation (5) for [HGG]. Equation (6) gives the concentration of free host [H]. At this point, [H]+[HG]+[HGG]?$[H]_0$ so the value of [HGG] from equation (5) is used in equation (4) to re-evaluate [HG].

$$[HG] = \frac{1 + 2K_1[G]_0([H]_0 - [HGG]) - \sqrt{\{(1 + 2K_1[G]_0([H]_0 - [HGG]))^2 - 16K_1^2[G]_0([H]_0 - [HGG])\}}}{4K_1} \quad (4)$$

$$[HGG] = \frac{1 + 0.5K_2[G]_0([H]_0 - [HG]) - \sqrt{\{(1 + 0.5K_2[G]_0([H]_0 - [HG]))^2 - K_2[G]_0([H]_0 - [HG])\}}}{K_2} \quad (5)$$

$$[H] = [H]_0 - [HG] - [HGG] \quad (6)$$

$$\delta_{obs} = \frac{[HGG]}{[H]_0}\delta_{b2} + \frac{[HG]}{[H]_0}\delta_{b1} + \frac{[H]}{[H]_0}\delta_f \quad (7)$$

This procedure is reiterated until [H]+[HG]+[HGG]=$[H]_0$. This allows the set of simultaneous equations [Eq. (4)-(7)] to be solved for the concentrations of all species present where [HGG] is the concentration of host·$(guest)_2$ complex; K_1 is the microscopic association constant for formation of the host·guest complex; K_2 is the microscopic association constant for formation of the host·$(guest)_2$ complex; d_{b2} is the limiting bound chemical shift of the host·$(guest)_2$ complex.

Appendix 3

1 Marquadt-Levenberg method

The Levenberg-Marquad method is a widely used method of fitting a non-linear model function to experimental data.[137] A brief outline is presented.

The problem is to model a set of N experimental data points (x_i, y_i) to a function y, using a set of non-linear fitting functions, with M parameters a_i:

$$y = y(x_i, a_1 \ldots a_M) \tag{1}$$

The set of parameters a_i may be represented by a vector quantity **a**. To find the set of parameters which provide the best agreement between experimental and model, a solution is needed which minimises the χ^2 function:

$$\chi^2 = \sum_{i=1}^{N} \left(\frac{y_1 - y(x_i, a)}{\sigma_i} \right)^2 \tag{2}$$

where σ_i is the variance of the individual value y_i. This is carried out by defining a vector quantity β, which contains M elements such that:

$$\beta_k = \sum_{i=1}^{N} \left(\frac{y_i - y(x_i, a)}{\sigma_i} \right)^2 \frac{\partial y(x_i, a)}{\partial a_k} \tag{3}$$

and defining a matrix [α], where the coefficients are defined by:

$$\alpha_{kl} = \sum_{i=1}^{N} \frac{1}{\sigma_i^2} \left[\frac{\partial y(x_i, a)}{\partial a_k} \frac{\partial y(x_i, a)}{\partial a_l} \right] \tag{4}$$

The solution which minimizes χ_2 is thus given by

$$[\alpha]\mathbf{a} = \beta \tag{5}$$

which may be solve by finding the covariance matrix [C], such that

$$[C] = [\alpha]^{-1} \tag{6}$$

and hence

$$\mathbf{a} = [C]\beta \tag{7}$$

within the computational scheme described by Press, a routine *mrqmin* is defined which returns the values of the parameters **a**, which are the best fit of the data of the model function, together with the covariance matrix C and the χ^2 parameter.

1.2 χ^2 minimization

The aim of the fitting procedure is to find those values of the parameters which best describe the data. The most common way to achieve it is to choose the parameters so that the sum of the squares of the deviations of the theoretical curve from the experimental points for a range of independent variables is at a minimum. For the ITC models, the theoretical models can be represented by

$$y = f(x; p_1, p_2, p_3, \ldots) \tag{8}$$

where p_i are the fitting parameters.

The expression for χ^2 is

$$\chi^2 = \frac{1}{n^{eff} - p} \sum [y_i - f(x_i; p_1, p_2, p_3, \ldots)]^2 \tag{9}$$

where n^{eff} is the total number of experimental points used in the fitting; p is the total number of adjustable parameters; y_i are the experimental data points and $f(x;p_1,p_2,\ldots.)$ is the fitting function. As the difference (n^{eff}-p) represents the number of degrees of freedom, the χ^2 of the fit is equal tot eh sum of the squares of the deviations of the theoretical curve from the experimental points divided by the number of degrees of freedom.

2 Equations used for fitting ITC binding studies [119]

2.1 Dilution correction

The calorimetric cell can be schematically represented as below:

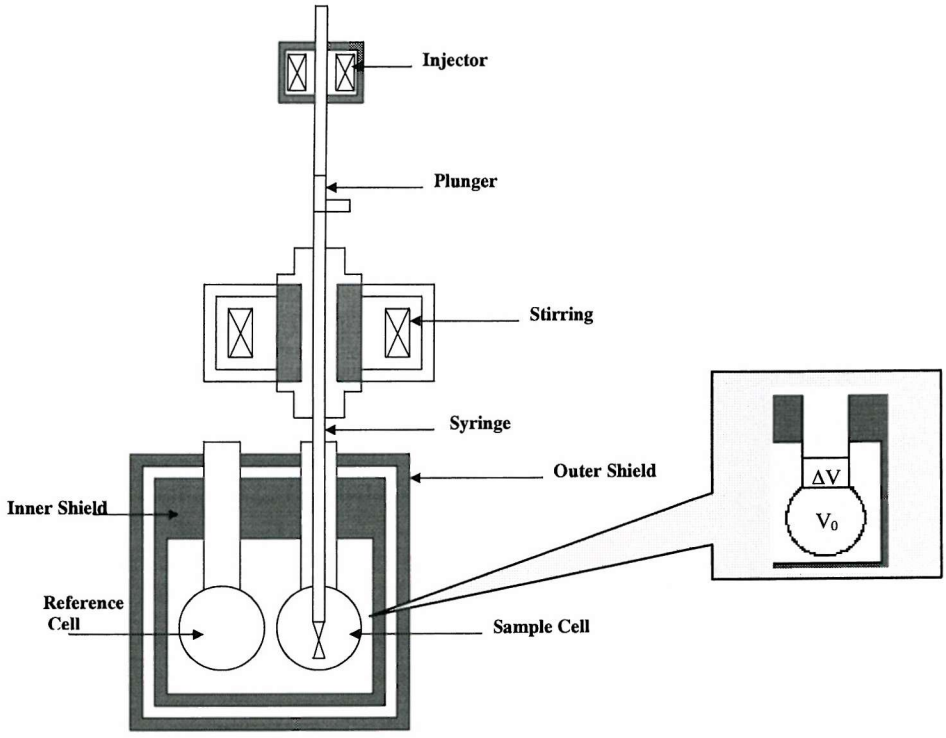

The solution contained within V_0 is sensed calorimetrically. Because of the total-fill nature of the cell, each injection drives some liquid (ΔV) out of the working volume and up to the reservoir. Therefore the concentration of the host changes by being distributed in a larger volume, V_0 + ΔV. Since the average bulk concentration of host in ΔV is the mean of the beginning concentration M_t^0, the conservation of mass requires that

$$M_t^0 = M_t V_0 + \frac{1}{2}(M_t + M_t^0)\Delta V \tag{10}$$

Thus, M_t, the present concentration of host in the active volume, is given as

$$M_t = M_t^0 \frac{1 - \frac{\Delta V}{2V_0}}{1 + \frac{\Delta V}{2V_0}} \tag{11}$$

Analogously, assuming all the injected ligand remains in V_0, X_t, the actual bulk concentration of ligand in V_0 is related to the hypothetical bulk concentration X_t^0 as follows:

$$X_t^0 V_0 = X_t V_0 + \frac{1}{2} X_t^0 \Delta V \tag{12}$$

And

$$X_t = X_t^0 \left(1 - \frac{\Delta V}{2V_0}\right) \tag{13}$$

Equation 11 and equation 13 are used by the software Origin to correct for the displaced volume effects occurring with each injection.

2.2 Single set of identical sites

The model for one set of sites is used for a molecule containing any number of equivalent sites n, characterised by the same K and ΔH.

The binding constant K is expressed as

$$K = \frac{\Theta}{(1-\Theta)[X]} \tag{14}$$

Where Θ is the fraction of sites occupied by the ligand X and [X] is the free concentration of ligand in V_0. The bulk concentration of the ligand X_t is

$$X_t = [X] + n\Theta M_t \tag{15}$$

Combining equation 14 and equation 15 gives

$$\Theta^2 - \Theta\left[1 + \frac{Xt}{nM_t} + \frac{1}{nKM_t}\right] + \frac{X_t}{nM_t} = 0 \tag{16}$$

At fractional saturation Θ, the total heat content Q of the solution contained in V_0 is

$$Q = n\Theta M_t \Delta H V_0 \tag{17}$$

Where ΔH is the molar heat of ligand binding. Solving the equation 16 for Θ and substituting this into equation 17 gives

$$Q = \left[\frac{nM_t \Delta H V_0}{2}\right]\left[1 + \left(\frac{X_t}{nM_t}\right) + \left(\frac{1}{nKM_t}\right) - \sqrt{\left(1 + \frac{X_t}{nM_t} + \frac{1}{nKM_t}\right)^2 - \frac{4X_t}{nM_t}}\right] \tag{18}$$

The parameter of interest is, however, the change in heat from the i-1 injection to the i injection, ΔQ_i. The equation 18 only applies to the liquid contained in V_0. After correction for the displaced volume ΔV_1, ΔQ_i is given by

$$\Delta Q(i) = Q(i) + \frac{dV}{V_0}\left[\frac{Q(i)+Q(i-1)}{2}\right] - Q(i-1) \tag{19}$$

The process of fitting the parameters involves 1) initial guesses of n, K and ΔH; 2) calculation of ΔQ_i. for each injection and comparison of these values with the measured heat for the corresponding experimental injection; 3) improvement in the initial values of n, K and ΔH by standard Marquadt methods; 4) iteration of the above procedure until no further significant improvement in fit occurs with continued iteration.

2.3 Two sets of Independent sites

Using the same definitions as above, we have

$$K_1 = \frac{\Theta_1}{(1-\Theta_1)[X]} \quad K_2 = \frac{\Theta_2}{(1-\Theta_{21})[X]} \tag{20}$$

$$X_t = [X] + M_t(n_1\Theta_1 + n_2\Theta_2) \tag{21}$$

Solving equation 10 for Θ_1 and Θ_2 and substituting into equation 21,

$$X_t = [X] + \frac{n_1 M_t [X] K_1}{1+[X]K_1} + \frac{n_2 M_t [X] K_2}{1+[X]K_2} \tag{22}$$

Clearing equation 12 of fraction and collecting like terms leads to a cubic equation of the form

$$[X]^3 + p[X]^2 + q[X] + r = 0 \tag{23}$$

Where

$$p = \frac{1}{K_1} + \frac{1}{K_2} + (n_1 + n_2)M_t - X_t$$

$$q = \left(\frac{n_1}{K_2} + \frac{n_2}{K_1}\right)M_t - \left(\frac{1}{K_1} + \frac{1}{K_2}\right)X_t + \frac{1}{K_1 K_2}$$

$$r = \frac{-X_t}{K_1 K_2} \tag{24}$$

Equations 14 and 15 can be solved numerically by using Newton's method when n_1, n_2, K_1 and K_2 are assigned, while Θ_1 and Θ_2 can be obtained from equation 20.

As discussed before the heat content Q after any injection i is;

$$Q = M_t V_0 (n_1 \Theta_1 \Delta H_1 + n_2 \Theta_2 \Delta H_2) \tag{25}$$

After correcting for the displaced volume, the calculated heat effect for the injection i is

$$\Delta Q(i) = Q(i) + \frac{dV_i}{V_0}\left[\frac{Q(i) + Q(i-1)}{2}\right] - Q(i-1) \tag{26}$$

which is used in the Marquadt algorithm to get a better fit of the experimental curve.

Table 1. Crystal data and structure refinement.

Identification code	**99sot022 (compound 146)**	
Empirical formula	$C_{11}H_{10}N_4S$	
Formula weight	230.29	
Temperature	150(2) K	
Wavelength	0.71073 Å	
Crystal system	Monoclinic	
Space group	*C2/c*	
Unit cell dimensions	a = 10.970(2) Å	α = 90°
	b = 8.986(2) Å	β = 103.66(3)°
	c = 20.881(4) Å	γ = 90°
Volume	2000.2(7) Å^3	
Z	8	
Density (calculated)	1.530 Mg / m^3	
Absorption coefficient	0.297 mm^{-1}	
F(000)	960	
Crystal	Plate; pale yellow	
Crystal size	0.1 × 0.1 × 0.025 mm^3	
θ range for data collection	2.96 – 27.46°	
Index ranges	$-14 \le h \le 14$, $-11 \le k \le 11$, $-27 \le l \le 26$	
Reflections collected	9713	
Independent reflections	2287 [R_{int} = 0.0522]	
Completeness to θ = 27.46°	93.8 %	
Absorption correction	Semi-empirical from equivalents	
Max. and min. transmission	0.994 and 0.957	
Refinement method	Full-matrix least-squares on F^2	
Data / restraints / parameters	2287 / 0 / 145	
Goodness-of-fit on F^2	0.972	
Final R indices [$F^2 > 2\sigma(F^2)$]	*R1* = 0.0479, *wR2* = 0.1315	
R indices (all data)	*R1* = 0.0692, *wR2* = 0.1454	
Largest diff. peak and hole	0.325 and –0.674 e Å^{-3}	

Diffractometer: *Enraf Nonius KappaCCD* area detector (ϕ scans and ω scans to fill *Ewald* sphere). **Data collection and cell refinement**: *Denzo* (Z. Otwinowski & W. Minor, *Methods in Enzymology* (1997) Vol. **276**: *Macromolecular Crystallography*, part A, pp. 307–326; C. W. Carter, Jr. & R. M. Sweet, Eds., Academic Press). **Absorption correction**: *SORTAV* (R. H. Blessing, Acta Cryst. A**51** (1995) 33–37; R. H. Blessing, J. Appl. Cryst. **30** (1997) 421–426). **Program used to solve structure**: *SHELXS97* (G. M. Sheldrick, Acta Cryst. (1990) A**46** 467–473). **Program used to refine structure**: *SHELXL97* (G. M. Sheldrick (1997), University of Göttingen, Germany).

Further information: http://www.soton.ac.uk/~xservice/strat.htm

Special details:

Table 2. Atomic coordinates [$\times 10^4$], equivalent isotropic displacement parameters [$Å^2 \times 10^3$] and site occupancy factors. U_{eq} is defined as one third of the trace of the orthogonalized U^{ij} tensor.

Atom	*x*	*y*	*z*	U_{eq}	*S.o.f.*
S1	1894(1)	230(1)	5219(1)	26(1)	1
N1	1138(2)	1567(2)	4488(1)	26(1)	1
N2	364(2)	2502(2)	5336(1)	27(1)	1
N3	1106(2)	1060(2)	6282(1)	26(1)	1
N4	2409(2)	−738(2)	6042(1)	24(1)	1
C1	1307(2)	1576(3)	3870(1)	30(1)	1
C2	733(2)	2621(3)	3422(1)	35(1)	1
C3	−41(2)	3679(3)	3619(1)	34(1)	1
C4	−202(2)	3682(3)	4251(1)	32(1)	1
C5	418(2)	2587(2)	4693(1)	27(1)	1
C6	1030(2)	1387(2)	5654(1)	25(1)	1
C7	1884(2)	−92(2)	6499(1)	25(1)	1
C8	2199(2)	−643(3)	7148(1)	30(1)	1
C9	3052(2)	−1769(3)	7305(1)	30(1)	1
C10	3595(2)	−2391(3)	6822(1)	32(1)	1
C11	3256(2)	−1859(2)	6197(1)	29(1)	1

Table 3. Bond lengths [Å] and angles [°].

S1–C6	1.791(2)
S1–N4	1.8902(19)
S1–N1	1.9657(19)
N1–C1	1.345(3)
N1–C5	1.345(3)
N2–C6	1.322(3)
N2–C5	1.359(3)
N3–C6	1.328(3)
N3–C7	1.351(3)
N4–C7	1.355(3)
N4–C11	1.357(3)
C1–C2	1.370(3)
C2–C3	1.400(4)
C3–C4	1.372(4)
C4–C5	1.410(3)
C7–C8	1.407(3)
C8–C9	1.364(3)
C9–C10	1.403(3)
C10–C11	1.357(3)
C6–S1–N4	83.46(9)
C6–S1–N1	82.10(9)
N4–S1–N1	165.55(8)
C1–N1–C5	121.8(2)
C1–N1–S1	128.31(16)
C5–N1–S1	109.89(15)
C6–N2–C5	112.99(19)
C6–N3–C7	112.84(18)
C7–N4–C11	122.1(2)
C7–N4–S1	110.98(15)
C11–N4–S1	126.77(15)
N1–C1–C2	120.9(2)
C1–C2–C3	118.5(2)
C4–C3–C2	120.5(2)
C3–C4–C5	118.5(2)
N1–C5–N2	116.3(2)
N1–C5–C4	119.7(2)
N2–C5–C4	124.1(2)
N2–C6–N3	124.2(2)
N2–C6–S1	118.75(17)
N3–C6–S1	117.09(16)
N3–C7–N4	115.6(2)
N3–C7–C8	125.8(2)
N4–C7–C8	118.6(2)
C9–C8–C7	119.4(2)
C8–C9–C10	120.4(2)
C11–C10–C9	119.0(2)
N4–C11–C10	120.4(2)

Symmetry transformations used to generate equivalent atoms:

Table 4. Anisotropic displacement parameters [$Å^2 \times 10^3$]. The anisotropic displacement factor exponent takes the form: $-2\pi^2[h^2a^{*2}U^{11} + \cdots + 2\,h\,k\,a^*\,b^*\,U^{12}]$.

Atom	U^{11}	U^{22}	U^{33}	U^{23}	U^{13}	U^{12}
S1	26(1)	26(1)	26(1)	−3(1)	7(1)	−2(1)
N1	23(1)	26(1)	27(1)	−1(1)	3(1)	−5(1)
N2	25(1)	26(1)	31(1)	−2(1)	8(1)	0(1)
N3	28(1)	28(1)	26(1)	−4(1)	10(1)	0(1)
N4	23(1)	26(1)	25(1)	−1(1)	6(1)	−2(1)
C1	29(1)	34(1)	27(1)	−2(1)	5(1)	−6(1)
C2	34(1)	43(1)	27(1)	0(1)	3(1)	−10(1)
C3	30(1)	36(1)	32(1)	8(1)	−4(1)	−7(1)
C4	28(1)	29(1)	37(1)	1(1)	1(1)	−4(1)
C5	24(1)	26(1)	30(1)	−2(1)	4(1)	−7(1)
C6	21(1)	25(1)	27(1)	−4(1)	5(1)	−5(1)
C7	23(1)	26(1)	27(1)	−4(1)	8(1)	−6(1)
C8	33(1)	32(1)	27(1)	−2(1)	10(1)	−5(1)
C9	31(1)	32(1)	25(1)	4(1)	3(1)	−5(1)
C10	27(1)	27(1)	39(1)	3(1)	3(1)	1(1)
C11	28(1)	28(1)	34(1)	−2(1)	11(1)	−2(1)

Table 5. Hydrogen coordinates [$\times 10^4$] and isotropic displacement parameters [$Å^2 \times 10^3$].

Atom	*x*	*y*	*z*	U_{eq}	*S.o.f.*
H2	−60	3109	5517	33	1
H3	702	1532	6525	32	1
H1	1822	864	3746	36	1
H2A	855	2627	2996	42	1
H3A	−450	4387	3319	41	1
H4	−709	4390	4384	39	1
H8	1830	−243	7467	36	1
H9	3274	−2127	7735	36	1
H10	4178	−3156	6929	38	1
H11	3607	−2265	5872	35	1

University of Southampton · Department of Chemistry

EPSRC National Crystallography Service

Table 1. Crystal data and structure refinement.

Identification code	**99sot048 (compound 149)**	
Empirical formula	$C_{12}H_{14}N_2O_3S_2$	
Formula weight	298.37	
Temperature	150(2) K	
Wavelength	0.71073 Å	
Crystal system	Monoclinic	
Space group	$P2_1/c$	
Unit cell dimensions	a = 15.521(3) Å	α = 90°
	b = 6.8270(10) Å	β = 100.06(3)°
	c = 13.574(3) Å	γ = 90°
Volume	1416.2(5) Å^3	
Z	4	
Density (calculated)	1.399 Mg / m^3	
Absorption coefficient	0.381 mm^{-1}	
F(000)	624	
Crystal	Plate; light brown	
Crystal size	0.175 × 0.15 × 0.025 mm^3	
θ range for data collection	2.67 – 27.43°	
Index ranges	$-19 \le h \le 19$, $-8 \le k \le 8$, $-17 \le l \le 17$	
Reflections collected	12963	
Independent reflections	3159 [R_{int} = 0.0583]	
Completeness to θ = 27.43°	98.0 %	
Absorption correction	Semi-empirical from equivalents	
Max. and min. transmission	0.998 and 0.888	
Refinement method	Full-matrix least-squares on F^2	
Data / restraints / parameters	3159 / 0 / 175	
Goodness-of-fit on F^2	0.807	
Final R indices [$F^2 > 2\sigma(F^2)$]	*R1* = 0.0393, *wR2* = 0.1033	
R indices (all data)	*R1* = 0.0679, *wR2* = 0.1218	
Largest diff. peak and hole	0.278 and –0.292 e Å^{-3}	

Diffractometer: *Enraf Nonius KappaCCD* area detector (ϕ scans and ω scans to fill *Ewald* sphere). **Data collection and cell refinement**: *Denzo* (Z. Otwinowski & W. Minor, *Methods in Enzymology* (1997) Vol. **276**: *Macromolecular Crystallography*, part A, pp. 307–326; C. W. Carter, Jr. & R. M. Sweet, Eds., Academic Press). **Absorption correction**: *SORTAV* (R. H. Blessing, Acta Cryst. A**51** (1995) 33–37; R. H. Blessing, J. Appl. Cryst. **30** (1997) 421–426). **Program used to solve structure**: *SHELXS97* (G. M. Sheldrick, Acta Cryst. (1990) A**46** 467–473). **Program used to refine structure**: *SHELXL97* (G. M. Sheldrick (1997), University of Göttingen, Germany).

Further information: http://www.soton.ac.uk/~xservice/strat.htm

Special details:

Table 2. Atomic coordinates [$\times 10^4$], equivalent isotropic displacement parameters [$Å^2 \times 10^3$] and site occupancy factors. U_{eq} is defined as one third of the trace of the orthogonalized U^{ij} tensor.

Atom	*x*	*y*	*z*	U_{eq}	*S.o.f.*
S1	1797(1)	1646(1)	3813(1)	27(1)	1
S2	2678(1)	2169(1)	5971(1)	31(1)	1
O1	−1041(1)	2369(2)	3333(1)	24(1)	1
O2	−2085(1)	1316(2)	1632(1)	33(1)	1
O3	−3255(1)	2608(2)	2181(1)	33(1)	1
N1	945(1)	2276(2)	5158(1)	19(1)	1
N2	724(1)	1847(2)	3449(1)	24(1)	1
C1	658(1)	2565(3)	6060(2)	23(1)	1
C2	−198(1)	2841(3)	6053(1)	23(1)	1
C3	−814(1)	2824(3)	5133(2)	23(1)	1
C4	−539(1)	2480(3)	4255(1)	21(1)	1
C5	375(1)	2175(2)	4244(1)	20(1)	1
C6	−1956(1)	2667(3)	3287(2)	24(1)	1
C7	−2421(1)	2105(3)	2255(2)	24(1)	1
C8	−3916(1)	2016(3)	1309(2)	34(1)	1
C9	−3943(1)	−180(3)	1242(2)	45(1)	1
C10	−4755(2)	2806(5)	1576(3)	65(1)	1
C11	−3714(2)	2968(5)	371(2)	69(1)	1
C12	1818(1)	2046(3)	5063(2)	23(1)	1

Table 3. Bond lengths [Å] and angles [°].

S1–N2	1.6593(17)
S1–C12	1.712(2)
S2–C12	1.653(2)
O1–C4	1.355(2)
O1–C6	1.426(2)
O2–C7	1.196(2)
O3–C7	1.326(3)
O3–C8	1.481(3)
N1–C1	1.388(3)
N1–C5	1.394(3)
N1–C12	1.393(3)
N2–C5	1.308(3)
C1–C2	1.341(3)
C2–C3	1.434(3)
C3–C4	1.355(3)
C4–C5	1.437(3)
C6–C7	1.509(3)
C8–C9	1.502(3)
C8–C11	1.510(4)
C8–C10	1.511(4)
N2–S1–C12	97.23(9)
C4–O1–C6	116.05(15)
C7–O3–C8	121.40(17)
C1–N1–C5	122.74(17)
C1–N1–C12	124.42(17)
C5–N1–C12	112.84(16)
C5–N2–S1	107.91(14)
C2–C1–N1	118.88(18)
C1–C2–C3	120.99(19)
C4–C3–C2	120.21(19)
C3–C4–O1	127.14(18)
C3–C4–C5	119.79(18)
O1–C4–C5	113.06(17)
N2–C5–N1	116.92(17)
N2–C5–C4	125.76(18)
N1–C5–C4	117.30(17)
O1–C6–C7	108.36(16)
O2–C7–O3	127.09(19)
O2–C7–C6	125.05(19)
O3–C7–C6	107.85(17)
O3–C8–C9	109.19(18)
O3–C8–C11	109.85(19)
C9–C8–C11	112.7(2)
O3–C8–C10	102.50(19)
C9–C8–C10	110.7(2)
C11–C8–C10	111.3(2)
N1–C12–S2	126.63(16)
N1–C12–S1	105.06(14)
S2–C12–S1	128.30(13)

Symmetry transformations used to generate equivalent atoms:

Table 4. Anisotropic displacement parameters [$Å^2 \times 10^3$]. The anisotropic displacement factor exponent takes the form: $-2\pi^2[h^2a^{*2}U^{11} + \cdots + 2\,h\,k\,a^*\,b^*\,U^{12}]$.

Atom	U^{11}	U^{22}	U^{33}	U^{23}	U^{13}	U^{12}
S1	21(1)	38(1)	23(1)	−1(1)	5(1)	2(1)
S2	22(1)	38(1)	30(1)	−2(1)	−4(1)	1(1)
O1	16(1)	38(1)	19(1)	−2(1)	1(1)	−1(1)
O2	21(1)	51(1)	27(1)	−8(1)	6(1)	−5(1)
O3	18(1)	44(1)	35(1)	−9(1)	−3(1)	4(1)
N1	18(1)	20(1)	18(1)	0(1)	1(1)	−1(1)
N2	21(1)	32(1)	19(1)	0(1)	4(1)	0(1)
C1	27(1)	24(1)	17(1)	0(1)	2(1)	−1(1)
C2	30(1)	25(1)	16(1)	−1(1)	6(1)	−2(1)
C3	19(1)	25(1)	24(1)	0(1)	5(1)	−2(1)
C4	21(1)	20(1)	19(1)	2(1)	1(1)	−2(1)
C5	22(1)	18(1)	17(1)	1(1)	0(1)	−1(1)
C6	19(1)	30(1)	24(1)	0(1)	4(1)	0(1)
C7	18(1)	27(1)	27(1)	3(1)	2(1)	−4(1)
C8	15(1)	49(1)	34(1)	−2(1)	−5(1)	−3(1)
C9	26(1)	53(2)	52(2)	−6(1)	−4(1)	−7(1)
C10	26(2)	85(2)	77(2)	−21(2)	−10(1)	14(1)
C11	43(2)	106(2)	50(2)	37(2)	−18(1)	−27(2)
C12	22(1)	22(1)	26(1)	2(1)	4(1)	1(1)

Table 5. Hydrogen coordinates [$\times 10^4$] and isotropic displacement parameters [$Å^2 \times 10^3$].

Atom	*x*	*y*	*z*	U_{eq}	*S.o.f.*
H1	1054	2567	6660	27	1
H2A	−396	3048	6653	28	1
H3	−1404	3049	5139	27	1
H6A	−2071	4030	3419	29	1
H6B	−2165	1868	3787	29	1
H9A	−3415	−649	1046	67	1
H9B	−4438	−576	755	67	1
H9C	−3994	−718	1883	67	1
H10A	−4851	2225	2192	97	1
H10B	−5236	2492	1053	97	1
H10C	−4711	4202	1654	97	1
H11A	−3626	4348	483	104	1
H11B	−4194	2764	−169	104	1
H11C	−3193	2397	203	104	1